Exploring the Effects of Dietary Interventions on Gut Microbiota Dynamics in Obesity and Its Health Implications in C57Bl/6 Male Mice

Salma Mahmoodianfard, M.Sc.

Supervisor: Dr. Krista A. Power
Co-Supervisor: Dr. Éric Doucet

This thesis is submitted to the University of Ottawa in partial fulfillment of the requirements for the Doctorate in Philosophy Degree in Human Kinetics

School of Human Kinetics
Faculty of Health Sciences
University of Ottawa

Thesis Abstract

Gut microbiota is increasingly recognized as a promising target for therapeutic interventions aimed at preventing and managing obesity and associated dysfunctions. Recently, there has been a growing interest in the consumption of functional foods, like dietary pulses with a unique nutrient-dense profile, linked to enhanced intestinal health by interacting closely with the gut microbiota, weight management, cognitive function, and significant improvement in overall health. This thesis explored the intricate interplay of diet, gut microbiota, and metabolic health in the context of obesity through three linked projects. In Project 1, the impact of incorporating white and dark red kidney beans into a low-fat diet (LFD) was explored, focusing on fecal gut microbiota composition and function, inflammatory state, and metabolic health in high-fat diet (HFD)-induced obese male mice. Project 2 broadened the scope to explore the influence of common beans on the gut-brain axis. This included an assessment of cecal microbiota, colon histomorphology, and anxiety behaviors and well-being. The findings from these two projects highlighted that, compared to the HFD fed obese control group, transitioning to an LFD supplemented with beans led to reduced weight gain, enhanced body composition (increased FFM and decreased FM), caused distinctive fecal and cecal microbiota changes at both phyla and genus levels with notable shifts in the abundance of specific beneficial bacterial genera, particularly those associated with short-chain fatty acids (SCFAs) production. While both bean varieties enhanced the gut microbiota microenvironment, they revealed unique effects on certain bacterial taxa, attributed to their distinct phenolic contents. On the other hand, beans did not promote additional improvements in fasting serum metabolic outcomes, beyond those induced from transitioning to an LFD, except for reduced inflammatory adipokine resistin by dark beans. The study found no improvements in nest-building behavior, indicative of well-being, but did observe some evidence of anxiolytic effects in the Elevated Plus Maze (EPM) test, particularly with white bean supplementation. Project 3 explored the intricate interplay among diet, inflammation, and gut microbiota in the development of obesity phenotypes. This project elucidated the potential contributions of *Akkermansia* genus abundance in generating phenotypes resistance to obesity and associated inflammatory and metabolic dysfunctions, even under an HFD with *ad libitum* food access. Overall, the findings of this thesis contribute to our understanding of factors contributing to diet-induced obesity phenotypes and emphasize the potential health implications of specific bean varieties, providing insights into both physiological and mental health outcomes in C57Bl/6 male mice models.

Figure 1-Thesis Graphical Abstract

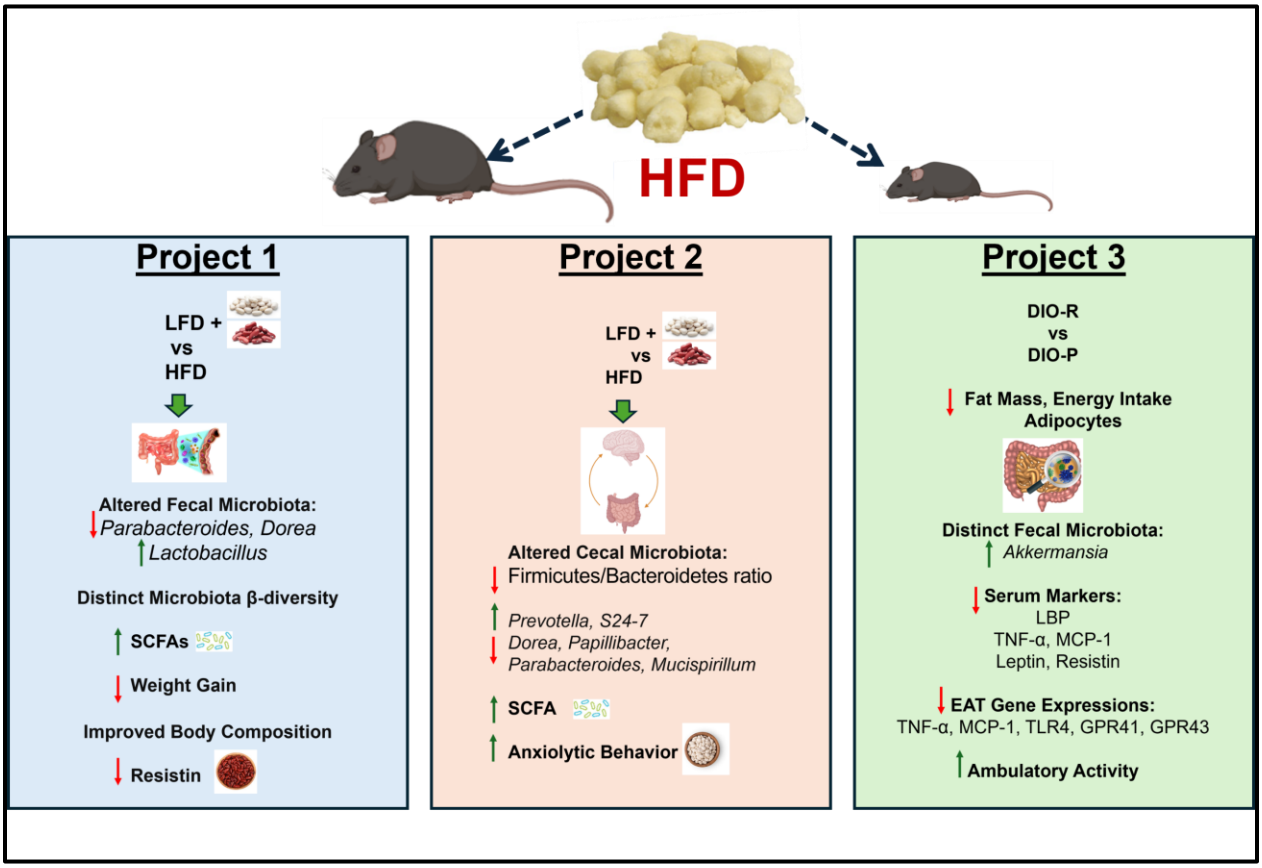

For definitions of abbreviations, please refer to the list of abbreviations on pages ix-xi.

Preface to the Thesis

I am pleased to present this thesis, representing a significant milestone in my PhD journey. Before moving into the contents, I would like to briefly explain the circumstances that shaped the evolution of this project. Initially, my research proposal focused on conducting a human clinical trial under the supervision of Dr. Éric Doucet at the school of Human Kinetics, aimed at investigating the combined impacts of synbiotics supplementation and energy restriction on gut microbiota composition and metabolic health in individuals living with obesity. This trial was planned to commence in September 2019. After meeting Dr. Krista Power and getting familiar with research projects in her lab at the School of Nutrition Sciences focused on utilizing whole foods and their impact on gut health, I became interested in exploring the potential use of dietary pulses, specifically common beans, to target gut microbiota, instead of utilizing commercial synbiotic supplements. Subsequently, I obtained the REB approval and began preparation for the human trial, including preparation of beans powder required for the clinical intervention, at the School of Nutrition Sciences experimental and sensory kitchen. At the same time, in September 2019, I started planning to conduct an animal study investigating gut health aspects utilizing dietary pulses under supervision of Dr. Power, in order to get some preliminary data before starting the human trial.

Unfortunately, the onset of the COVID-19 pandemic in March 2020 resulted in the suspension of the human trial, as the target participants, including individuals with obesity, were at increased risk. However, by that time, I had already developed an obesity mouse model at the University of Ottawa Animal Care and Veterinary Service Facility, and I was prepared to initiate the intervention arm of the pre-clinical trial including the incorporating common beans. Despite the need to ramp down non-essential research activities, I was fortunate to receive approval to

continue conducting animal work under granting a derogation from the University of Ottawa with the support of Dr. Power's, enabling me to finish the animal part of the pre-clinical project. However, to comply with the University of Ottawa Animal Facility guidelines and restrictions on campus access, certain pre-planned study outcomes were either excluded or deferred until the end of the intervention period. Given the indefinite timeline for the reopening of human facilities post-pandemic, with the agreement of Dr. Doucet and Dr. Power, the human trial component was removed from my PhD thesis plan, and this decision was communicated to the respective thesis advisory committee members. Consequently, I shifted my entire focus within the animal trial, expanding its scope and conducting a more in-depth analysis of the planned outcomes. This involved acquiring proficiency in biochemical and molecular biology techniques, as well as bioinformatics analysis. Additionally, I underwent training in behavioral testing methods to comprehensively investigate the impact of dietary intervention on mental well-being, alongside with the assessment of intestinal health, inflammation state, metabolic outcomes. The experimental protocol was approved by the University of Ottawa Animal Care Committee (Protocol number HSe-2857-R3).

I am deeply grateful to all those who have supported me throughout this journey specially during the unprecedented circumstances. In terms of contributions to the projects outlined in Chapters 2-4, I was primarily responsible for all aspects of the animal work, including data collection and behavior testing, laboratory experiments, data analysis, drafting and preparation of manuscripts. The co-authors who played significant roles in the conceptualization and execution of the projects are listed below:

Dr. Power and Dr. Doucet contributed to conceptualization, Dr. Power provided guidance in study design, Lalit Kishore, post-doctoral fellow, assisted with sample collection and animal testing

behavior, Alexane Rodrigue, PhD Candidate, contributed to sample collection and provided training and mentorship for sample analysis, Valérie Roumelis and Giorgio Freije, undergraduate students, contributed to data entry and collection. Their expertise, guidance, and support were instrumental in the successful completion of this work, and I extend my sincerest gratitude to each of them.

Acknowledgements

I started my PhD journey as an international student at the University of Ottawa. I am deeply grateful to Dr. Doucet for accepting me as a PhD student into the Human Kinetics program, bringing me closer to pursuing my goals and changing my life in so many ways. His support and guidance over the past years have been invaluable. His encouragement ignited my passion for gut microbiota research, and for that, I am deeply thankful.

I extend my heartfelt thanks to my supervisor Dr. Power for welcoming me into her lab and for her exceptional leadership and supervision provided throughout every aspect of my PhD research. I am deeply appreciative of the guidance and hands-on experience gained while working in Dr. Power lab, where I had the opportunity to learn a wide range of biological techniques and bioinformatic analyses. For this, I am truly grateful. I am immensely thankful for the countless hours Dr. Power dedicated to supporting and guiding me through the completion of my thesis. Her unwavering commitment and invaluable feedback have been instrumental in shaping the outcome of my research. I am especially grateful for her encouragement in pursuing opportunities such as the Nutrition & Mental Health doctoral scholarship, made possible by the generous funding I received from the School of Nutrition Sciences. This support allowed me to dedicate more focus to my thesis, for which I am profoundly grateful.

I express my gratitude to Dr. Isabelle Giroux and Dr. Garry Goldfield for their support and guidance as members of my comprehensive examination committee and thesis advisory team.

I extend my gratitude to all current and former members of Dr. Power lab team for their invaluable contributions. Specifically, I would like to thank my fellow PhD Candidate, Alex Rodrigues, for her continuous support throughout the experimental process and patient guidance in training me on various lab procedures. I am also thankful to Dr. Lalit Kishore for his consistent

presence and assistance in various stages of my thesis. His support and companionship were invaluable. I extend my appreciation to former undergraduate students Valérie Roumelis and Giorgio Freije for their assistance in data collection, Laili Mahmoudian for her support in conducting literature reviews and preparing materials for starting the thesis projects, and Dawson Livingston for generously providing guidance in bioinformatic data analysis.

I am thankful to Dr. Mahmoud Ally and Dr. Ahmed Gomaa for their mentorship and support in facilitating microbiota sequencing analysis and gas chromatography procedures. Their expertise ensured the smooth operation of those experimental procedures.

I extend my sincere gratitude to Applied Bean Genomics and NSERC for generously funding this research, and the University of Guelph for their generous donation of the kidney beans utilized in this thesis. I would like to acknowledge the valuable assistance provided by the University of Ottawa, animal care and veterinary services (ACVS) team in animal care aspect of this research, and the Animal Behaviour and Physiology Core Facility team for supporting the behavior tests training and provision of essential equipment.

Special thanks to former PhD Candidate Dr. Shuhiba Mohammad for her support during my time in the graduate student office. Her willingness to listen to me throughout my challenging PhD journey was invaluable. I am immensely grateful to my parents, my spouse, my siblings, and friends for their continuous love, understanding, and encouragement. Their unwavering support sustained me through the ups and downs of my PhD journey. Lastly, to my double blessings, my two-year-old twins. Their presence in my life has been a constant source of strength and inspiration.

Dedication

To my parents, who supported me to continue my education and encouraged me to pursue my dreams.

List Of Abbreviations

- **16S rRNA**: 16S Ribosomal Ribonucleic Acid
- **AB**: Alcian Blue
- **α- Diversity**: Alpha Diversity
- **ANOVA**: Analysis of Variance
- **β- Diversity**: Beta Diversity
- **BBB**: Blood-Brain Barrier
- **BBK**: Beam Break Test
- **BCFAs**: Branched-Chain Fatty Acids
- **BMI**: Body Mass Index
- **CNS**: Central Nervous System
- **CRP**: C-Reactive Protein
- **DB**: Dark-Red Kidney Beans
- **DIO**: Diet-Induced Obesity
- **DIO-P**: Diet-Induced Obesity Prone
- **DIO-R**: Diet-Induced Obesity Resistant
- **DNA**: Genomic Deoxyribonucleic Acid
- **EAT**: Epididymal Adipose Tissue
- **EPM**: Elevated Plus-Maze
- **F/B ratio**: Firmicutes/Bacteroidetes ratio
- **FDR**: False Discovery Rate
- **FFA**: Free Fatty Acid
- **FITC**: Fluorescein Isothiocyanate–Dextran
- **g**: Genus
- **GBA**: Gut-Brain Axis
- **GC**: Gas Chromatography
- **GIP**: Gastric Inhibitory Polypeptide

- **GLP-1**: Glucagon-Like Peptide-1
- **GIT**: Gastrointestinal Tract
- **GPR**: G-Protein Coupled Receptor
- **H&E:** Hematoxylin and Eosin
- **HF:** High-Fat Diet Fed Group
- **HF→LF:** High-Fat to Low-Fat Diet Transition Group
- **HF→WB:** High-Fat to Low-Fat + White Kidney Beans Diet Transition Group
- **HF→DB:** High-Fat to Low-Fat + Dark-Red Kidney Beans Diet Transition Group
- **HFD**: High-Fat Diet
- **HOMA-IR**: Homeostatic Model Assessment of Insulin Resistance
- **HPA**: Hypothalamic-Pituitary-Adrenal
- **IBD**: Inflammatory Bowel Disease
- **IFN-γ**: Interferon-Gamma
- **IL**: Interleukin
- **KEGG**: Kyoto Encyclopedia of Genes and Genomes
- **KW**: Kruskal-Wallis Test
- **LBP**: Lipopolysaccharide-Binding Protein
- **LF**: Low-Fat Diet Fed Group
- **LFD**: Low-Fat Diet
- **LPS**: Lipopolysaccharide
- **MCP-1**: Monocyte Chemoattractant Protein-1
- **MUC2**: Mucin 2
- **NDCs**: Non-Digestible Carbohydrates
- **NF-κB**: Nuclear Factor Kappa B
- **p:** Phylum
- **PAI-1**: Plasminogen Activator Inhibitor-1
- **PCoA**: Principal Coordinate Analysis

- **PICRUSt2**: Phylogenetic Investigation of Communities by Reconstruction of Unobserved States 2
- **PPAR-γ**: Peroxisome Proliferator-Activated Receptor-Gamma
- **RS**: Resistant Starch
- **SCFAs**: Short-Chain Fatty Acids
- **sp**: Species
- **TJ**: Tight-Junction
- **TLR4**: Toll-Like Receptor 4
- **TNF-α**: Tumor Necrosis Factor-Alpha
- **WB**: White Kidney Beans

Contents

List of Tables

List of Figures

1 CHAPTER 1. INTRODUCTION

1.1 Obesity

According to the World Health Organization (WHO) [1], obesity is defined as abnormal or excessive fat accumulation that presents a risk to health. Individuals with a body mass index (BMI) equal to or exceeding 30 kg/m^2 are classified as obese. Obesity is an alarming public health concern worldwide and a predictor of early death [2]. According to WHO estimates in 2022, 2.5 billion adults (18 years and older) were overweight. Of these, 890 million were living with obesity [3]. Obesity extends its impact across nearly every organ system, from the cardiovascular system to the endocrine system, gastrointestinal, and central nervous systems (CNS) [4], therefore it is not only associated with a higher prevalence of chronic diseases, but also with psychological issues that affect quality of life [2]. Recent evidence highlights a significant rise in obesity rates in Canada over the last two decades. According to a Health Survey, nearly one in three Canadian adults were living with obesity in 2022, with a sharp increase from just over one in five in 2003 [5]. WHO also reports that in 2019, one in every eight people or 970 million people worldwide were living with one of the mental health related issues mainly anxiety and depressive disorders which surged significantly amid the COVID-19 pandemic crisis with a 26% and 28% increase, respectively, within just one year [6]. Importantly, a bidirectional convergent correlation between obesity and mood disorders has been reported [7]. Individuals with obesity are more likely to develop mental health problems including depression and anxiety disorders or neurodegenerative diseases [8].

While the intake of energy beyond energy expenditure is the primary factor involved in storing excess energy as fat, it is crucial to understand that obesity is characterized as a heterogeneous chronic disease. This complexity arises from the interaction of various biological, environmental, and behavioral factors, all contributing to producing of a state of positive energy balance and

subsequent weight gain **(Figure 1-1)** [9,10]. Biological factors, mainly genetics, prenatal influences, neuroendocrine conditions, medications, gut microbiome and the gut-brain axis play pivotal roles in the development of obesity [10]. These biological elements interact with environmental factors, such as food supply, built environments (such as physical structures, infrastructure, and amenities), socioeconomic status, cultural influences, social bias, and exposure to environmental chemicals. Behavioral influences, comprising excessive energy intake, eating patterns, sedentary lifestyles, inadequate sleep, and smoking cessation, further contribute to the complexity of obesity etiology. Recognizing the specific determinants of adiposity in individuals with obesity is crucial for tailoring prevention and treatment strategies effectively in the ongoing effort to combat this public health challenge [10].

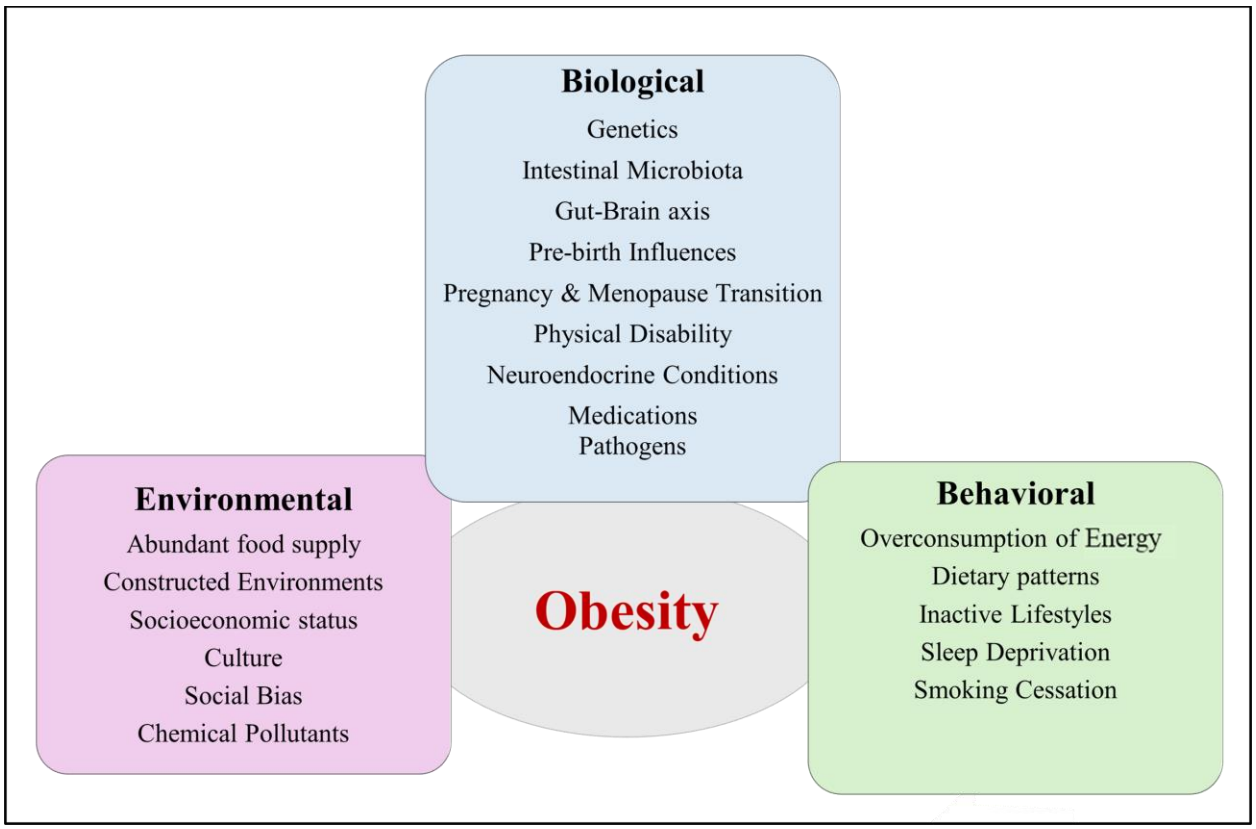

Figure 1-1. Factors Contributing to Obesity (adapted from [10])

As the prevalence of obesity continues to rise worldwide, there is a growing need to address this global health challenge. The utilization of mice as models for diet-induced obesity (DIO) has become progressively widespread due to their higher reliability in replicating human obesity, as compared to mice that have been genetically modified to develop obesity [11,12], including monogenic mutations in the leptin pathway (such as leptin-deficient (ob/ob) mice, leptin receptor-deficient (db/db) mice) or obesity models with a deficit downstream of the brain leptin receptor (such as POMC knockout mice or POMC/AgRP double knockout mice). Evidence has shown that only an increased dietary fat content was associated with elevated energy intake and adiposity in various studied mouse strains compared to diets with increased carbohydrates (particularly sugars), or reduced protein [13]. Mice fed a high-fat diet (HFD) develop an obesity syndrome that features metabolic complications similar to those observed in humans including hyperleptinemia, hyperinsulinemia, and impaired glucose tolerance, mirroring human obesity-associated metabolic dysfunctions [14,15]. However, previous studies have highlighted variations in the physiological phenotypes among different mouse strains [16–18]. While the C57BL/6 strain is considered a suitable model for investigating metabolic diseases like obesity and type 2 diabetes [19,20], it exhibits significant individual variations in weight gain when subjected to an HFD, [21] emphasizing the intricate and multifaceted nature of obesity [22]. However, the precise factors contributing to these non-genetic-related variations in weight gain responses are currently unknown and warrant further research. Notably, studies have demonstrated differences in gut microbiota composition between obesity-prone and obesity-resistant phenotypes [23,24]. However, comprehensive exploration is needed to unravel the precise contribution of host-microbial interactions and obesity-resistant phenotype, as prior studies have only partially delved into this matter, offering conflicting findings on alterations in metabolic profiles and gut

microbiota composition between the obesity-prone (DIO-P) and obesity-resistant (DIO-R) phenotypes [23–28]. Therefore, an aim of this thesis **(Chapter 4, Project 3)** was to investigate the role of the gut microbiota in the susceptibility to HFD in sub-groups of C57BL/6 mice either resistant or prone to HFD-induced obesity.

1.2 Gut Health Implications in Obesity

A healthy gut is characterized by the selective permeability of nutrients, water, and bacterial products[29]. The gut barrier is a dynamic system influenced by the composition of the intestinal microbiome and the function of intercellular connections, and is regulated by hormones, dietary components, inflammatory mediators, and the enteric nervous system [30]. There exists a close interaction between nutrients (such as dietary fiber, protein, and fat), the gut microbiota, and the intestinal barrier under health or disease conditions [29]. Evidence has shown that obesity may be associated with alterations in gut microbiota composition, potentially leading to impairment in intestinal barrier function which could significantly impact both immunological and metabolic functions in the host [31–33]. DIO in animal models have been linked to a substantial reduction in colonic mucus thickness, defective mucosal growth rate, and higher penetrability of the mucus and epithelial layer, defective tight junction protein expressions, and increased colonic and systemic inflammation [34,35]. The integrated components crucial for maintaining the physiological integrity of the intestinal barrier include: (1) the gut microbiota, forming the microbial barrier; (2) mucus, creating a protective layer at the interface between the intestinal lumen and the brush border of enterocytes and colonocytes; (3) the coordination between gastrointestinal motility and secretions, establishing the functional barrier; (4) the epithelial barrier featuring tight junctions; (5) immune-competent cells contributing to the immunological barrier [29,36]; (6) the gut–vascular interface comprised of endothelial cells tightly integrated with pericytes and enteric glial cells to form a vascular unit, facilitates the translocation of substances from the intestinal lumen to the systemic circulation while preventing migration of bacteria and their byproducts from the gut lumen into the bloodstream [37]. The following sections introduce the gut microbiota,

highlighting its key functions as the first line of barrier defense, and then explore its connections to obesity.

1.2.1 The Links Between Gut Microbiota and Obesity

1.2.1.1 Gut Microbiota

In comparison to other body regions, the human gastrointestinal tract (GIT) harbors a substantial microbial community, comprising approximately 100 trillion microorganisms [38].The gut microbiome, as defined by molecular biologist Joshua Lederberg, encompasses all microorganisms—bacteria, viruses, protozoa, and fungi—along with their collective genetic material found in the GIT. The gut bacteria, a subset of the microbiome, consists of both commensal and pathogenic species residing in the GIT [39]. The gut microenvironment primarily supports the growth of bacteria from seven major divisions. The predominant bacterial phyla in the human gut microbiota are Firmicutes and Bacteroidetes, collectively constituting more than 90% of the total community. Additionally, there are subdominant phyla, such as Actinobacteria, Proteobacteria, Verrucomicrobia, Cyanobacteria and Fusobacteria, [40,41].

This microbial balance plays a crucial role in human health and disease. In a healthy state, gut microbiota exhibits stability, resilience, and symbiotic interaction with the host. Extensive research is dedicated to defining a "healthy" gut microbiota and its correlation with host physiological functions. The gut microbiota in a healthy community typically exhibits high taxonomic diversity, substantial microbial gene richness, and a stable core microbiota [38].

The gut microbiota is distributed along the GIT, with its abundance and diversity generally increasing from the proximal to distal intestine [42]. For instance, the stomach harbors only 10^1 bacteria per gram content, while increasing densities and bacterial diversities are found in the

duodenum (10^3/g), jejunum (10^4/g), ileum (10^7/g), and colon (10^{12} bacteria/gram) [43]. The establishment and modulation of the gut microbiome are influenced by numerous factors, including birthing and infant feeding methods, exposure to stress, environmental factors, dietary choices, medication usage, stage of the lifecycle, and the presence of comorbid diseases **(Figure 1-2)** [39]. The gut microbiota significantly contributes to nutrient and micronutrient absorption, synthesizes enzymes, vitamins, and amino acids, facilitates food fermentation, and produces short-chain fatty acids (SCFAs). Additionally, the gut microbiota not only produces antimicrobial substances to protect the host from external pathogens but also plays a vital role in shaping the development of intestinal mucosa and the immune system [38–40].

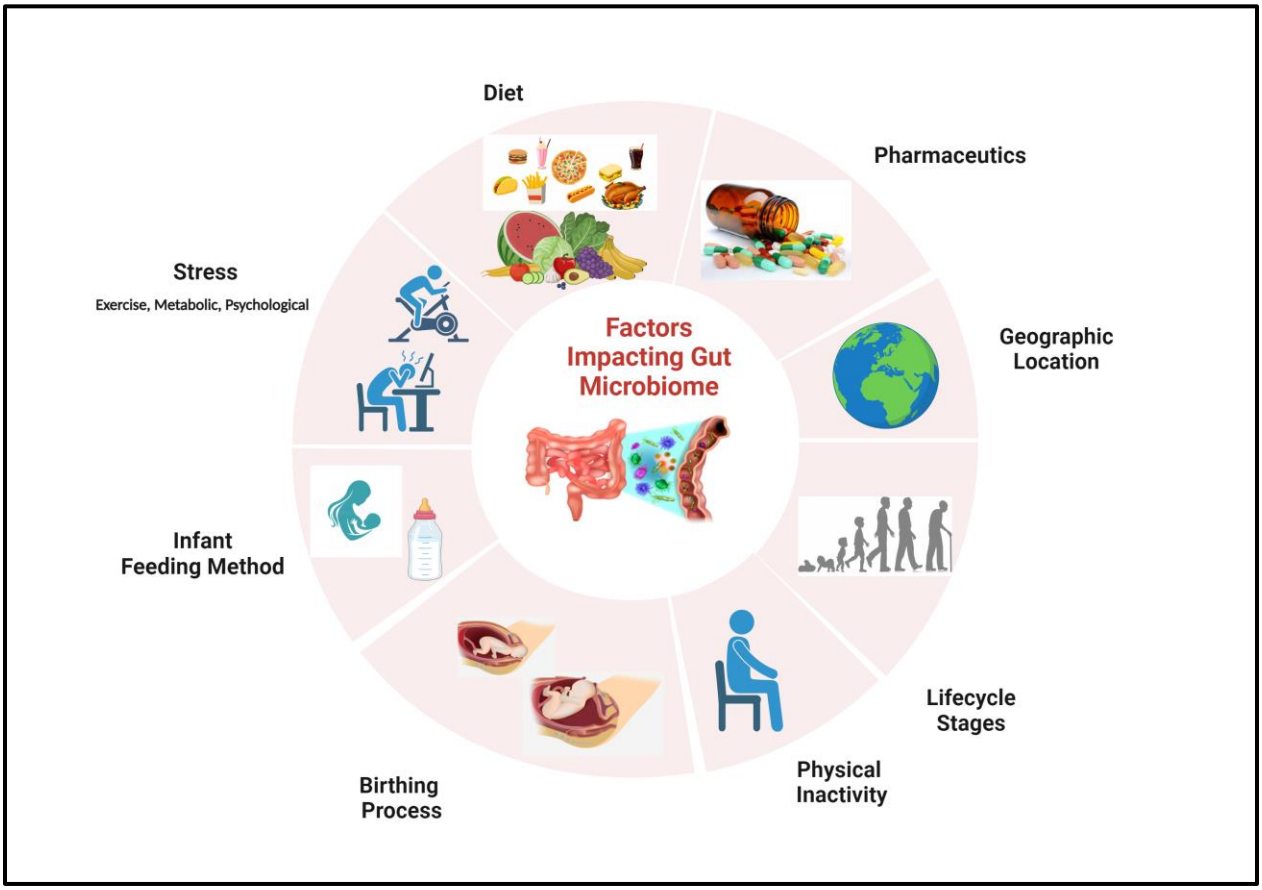

Figure 1-2. Factors Affecting the Gut Microbiome

(Created using Biorender.com, adapted from [39]).

Over the past decade, extensive research has delved into potential interactions between the gut microbiota and the host, including impacts on metabolism, immune responses, and neuroendocrine functions [39]. As the microbiota significantly contributes to human well-being and actively participates in various biological processes and disease development, research on human gut microbiota is expanding beyond compositional studies and member associations. There is a growing focus on elucidating the causality of microbiota functions, particularly with the advent of new techniques such as high-throughput sequencing, microbiota interactive modeling, and simulation. However, additional research is crucial to unravel the diverse roles of the human microbiota, ultimately supporting the advancement of microbiome-based diagnostics and personalized medicine [38].

It is important to note that the relative distribution of microorganisms is unique between individuals and may undergo variations within the same individual [38]. Furthermore, gut microbiota exhibit variations across different anatomical regions of the intestine, responding to diverse physiological conditions such as pH and oxygen tension, varying digesta flow rates (rapid from the mouth to the caecum, slower afterward), substrate availability, and host secretions [44]. The small intestine poses a more challenging environment for microbial colonizers due to relatively short transit times (3–5 hours) and high bile acid concentrations. In contrast, the large intestine, characterized by slow digesta flow rates and a neutral to mildly acidic pH, hosts the largest microbial community, predominantly composed of obligate anaerobic bacteria [44]. The majority of bacterial activity is concentrated in the proximal colon, where substrate availability is most abundant. As moving towards the distal colon, substrate availability decreases, and the extraction of free water diminishes the diffusion of both substrates and microbial products. Consequently, the proximal colon stands out as the primary site of fermentation. Notably,

saccharolytic bacteria, primarily represented by Bacteroidetes, play a pivotal role in fermenting nondigestible carbohydrates (NDCs) in the proximal colon. This fermentation process yields SCFAs along with the production of gases (such as CO_2 and H_2) [45]. The fermentation of bacterial proteins and amino acids, originating from primary fermenters like Bacteroidetes, takes place in the more distal portion of the colon, facilitated by secondary fermenters known as proteolytic bacteria. The breakdown of proteins and amino acids leads to the production of branched-chain fatty acids, along with the generation of potentially toxic metabolites such as amines, phenolic compounds, and volatile sulfur compounds [46]. The study of the human intestinal microbiota along different locations presents challenges due to invasive sampling methods, ethical considerations, and scalability issues. These limitations have prompted researchers to explore alternative approaches with rodent models, especially mice, as effective alternatives [47]. **Considering the potential differences in microbiota composition and function throughout the GIT, this thesis investigated the gut microbiota composition and function of both the distal (Chapter 2, Project 1) and proximal (Chapter 3, Project 2) colon regions of the GIT in C57BL/6 mice. As transitioning to the general discussion section, the qualitative and quantitative similarities and/or differences observed in gut microbiota between fecal and cecal samples will be explored, aiming to draw conclusions regarding the potential utility of fecal samples in reflecting the presence and absence of the vast majority of members in the cecal community.**

1.2.1.2 A Dysbiotic Gut Microbiota in Obesity

Dysbiosis is characterized by changes in the microbial community, leading to reduced diversity and quantities of commensal bacteria [39]. Evidence indicates associations between gut

dysbiosis and various chronic health conditions, including inflammatory bowel disease, metabolic syndrome, cardiovascular disease and obesity [48].

While the cause of obesity is an imbalance between energy intake and expenditure, variations in gut microbial ecology among individuals may significantly contribute to energy homeostasis. It is hypothesized that the fecal microbiota of individuals living with obesity might have a higher ability to harvest energy from foods, particularly through the production of SCFAs [49]. However, human studies have shown mixed findings concerning the association between SCFAs and obesity [50]. While some human studies have indicated increased fecal SCFA concentrations in adults with obesity [51–53], others studies involving children living with obesity showed lower total fecal SCFAs [54,55], or reduced propionic and butyric acids compared to non-obese children [54,55]. On the other hand, obese mice exhibited increased SCFA levels in the cecum (acetate (100 μmol/g and butyrate (25 μmol/g)) compared to lean mice (acetate (80 μmol/g) and butyrate (12 μmol/g)). This increase in SCFAs suggests enhanced energy harvest, as evidenced by the lower energy content in the fecal matter of obese mice (~3.2 kcal/g) compared to their lean littermates (~3.45 kcal/g).[56]. Elevated fecal SCFAs have been suggested to serve as a potential indicator of increased microbial energy harvest, contributing to obesity development [57]. However, the precise contribution of SCFAs to excess energy harvesting remains a challenging issue and needs further investigation. In contrast, supplementing the diet with acetate, propionate, butyrate, or their combination has been demonstrated to markedly attenuate the body weight gain induced by HFD consumption in obese mice [58]. Similarly, acute colonic infusion of SCFAs, resulted in an increase in fasting fat oxidation and resting energy expenditure [59]. Additionally, other studies have highlighted the favorable health effects of supplementing with SCFAs, including improvements in insulin sensitivity [60,61] and the reduction of inflammation [62].

Furthermore, they may also increase energy expenditure and stimulate the production of anorexic hormones [57].

SCFAs have demonstrated a role in appetite regulation in human studies via increased secretion of gut hormones, namely peptide YY (PYY) and glucagon-like peptide–1 (GLP-1), accompanied by a significant reduction in adiposity and the prevention of weight gain [63]. Notably, the fecal excretion of SCFAs might not necessarily reflect SCFA levels in circulation, which could provide a more accurate representation of SCFA production and absorption [53], instead, they represent a net outcome derived from the balance between production and absorption [64]. A possible explanation for increased fecal SCFAs in obesity, could be that the GIT in individuals with obesity might contribute to reduced efficiency in the absorption of SCFAs, consequently resulting in elevated SCFA excretion [53]. Therefore, the conflicting evidence surrounding the role of SCFAs in obesity highlights the need for further investigation. Overall, these observations suggest a potential correlation between gut microbiota and obesity development through alterations in SCFA production and energy harvesting [56].

The initial evidence linking the gut microbiota to obesity emerged from studies involving germ-free mice [66]. Bäckhed and colleagues were the first who reported that conventionalization of germ-free mice with the gut microbiota derived from conventionally raised mice caused rapid weight gain and insulin resistance persisted despite a reduction in energy intake in recipient mice [67]. This demonstrated that gut microbes can contribute to the accumulation of adipose tissue in the host [68]. Additionally, transplanting the microbiota of twin pairs discordant for obesity into C57BL/6 germ-free mice increased body weight and fat mass in obese co-twin's microbiota recipients greater compared to the ones inoculated with lean microbiota [69]. These observations support the importance of alteration of microbiota diversity and composition as a contributing

factor in the pathogenesis of obesity and associated metabolic outcomes [70]. Additionally, 16S rRNA gene sequencing analysis of intestinal cecal bacteria revealed a potential association between obesity and two predominant bacterial phyla: Firmicutes and Bacteroidetes. In obese mice, the abundance of Bacteroidetes decreased by 50%, accompanied by a proportional increase in Firmicutes [65]. Further investigations confirmed a significant increase in the Firmicutes/Bacteroidetes ratio in obese mice [71]. Firmicutes were found to be more efficient in extracting energy from food compared to Bacteroidetes. This enhanced energy extraction promotes more efficient energy absorption, contributing to weight gain [72]. It is suggested that the over-representation of saccharolytic associated with gut dysbiosis contributes to enhanced food digestion, leading to increased energy harvest and fat deposition, ultimately contributing to obesity development [73]. Similarly, in a study on adult individuals, a positive correlation between the Firmicutes/Bacteroidetes ratio and increasing BMI was observed [74]. However, conflicting results have been reported in some studies. For instance, Zhang and colleagues [75] found no significant difference in the abundance of Bacteroidetes between individuals living with obesity and individuals with normal weight. These contradictory findings could be due to highly variable gut microbiota among individuals within the same population. This variability is likely influenced by numerous lifestyle-associated factors, including diet, physical activity, food additives and contaminants, antibiotic consumption, and other elements that impact the composition of the microbiota in GIT [40]. Consequently, more research is necessary to comprehensively understand the intricate relationship between the gut microbiota and obesity.

1.2.1.3 Altered Gut Microbiota During Weight Loss

Lifestyle modification serves as the primary strategy for both obesity treatment and effective weight management. While dietary modifications, including energy restriction, altered macronutrient composition, food choices, and dietary patterns, play a pivotal role in facilitating weight loss [76], it is important to recognize that their effectiveness may vary among individuals. Modifications in dietary patterns, especially those aimed at reducing energy intake, can result in weight loss and mitigate the risk of obesity-related complications [76,77], however, the contributing role of the gut microbiota in weight loss is not fully understood and may depend on an individual baseline microbiota [78]. In fact, studies have shown that the abundance of certain microbial members at baseline (prior to weight-loss interventions) can be predictors of subsequent weight-loss success, a finding which has initiated the notion that personalized therapies may require an initial assessment of the gut microbiota to optimize the achievement of the weight loss goals [78]. While weight reduction is suspected to influence gut microbiota composition irrespective of the cause of the weight loss, whether achieved through dietary modifications or bariatric surgery, an energy-restricted diet has been shown to reduce Firmicutes in individuals with obesity, both in the short-term (four weeks) and up to one year after adopting a low-energy diet [79]. Furthermore, alterations in diet composition rapidly impact gut microbiota composition [79,80]. Indeed, shifting from a high-fat, low-fiber diet to a low-fat, high-fiber diet has been demonstrated to induce acute changes in the gut microbiota composition within 24 hours of initiating controlled feeding [81].

A 2022 systematic review and meta-analysis [82], aiming to quantify the association between intentional weight loss and changes in the gut microbiota and intestinal permeability, reported a dose-response relationship. The study found that overall weight loss, achieved through lifestyle modifications, was associated with increases in gut microbiota α-diversity and reductions

in intestinal permeability in clinical studies. However, when specifically considering weight loss through diet intervention only, the evidence was inconsistent [82]. Notably, higher abundance of the fiber-fermenting SCFAs producing bacterial genera, such as *Prevotella*, have been identified as promising predictive biomarkers for the success of weight loss [78]. Similarly, other human studies underscored the significance of the baseline gut microbiota composition, with species like *Blautia wexlerae* and *Bacteroides dorei*, proved to be a strong predictive marker for weight loss trajectories [83]. On the other hand, in response to a calorie restriction program, a considerable inter-individual variation in the bacterial strain composition of the colonic microbiota was observed [84]. Despite all these findings, there is supporting evidence indicating a reduced Firmicutes/Bacteroidetes ratio and an increased abundance of *Akkermansia muciniphila* and *Faecalibacterium prausnitzii* after weight reduction [85]. However, some studies have reported reduced abundance of specific butyrate-producing bacteria within the Firmicutes phylum, like *Roseburia+Eubacterium* group known for their potential colonic health benefits, without an overall change in Firmicutes percentage [86]. Conversely, certain studies found limited or inconclusive changes in gut microbiome composition in overweight and adults living with obesity undergoing moderate weight loss through energy restriction, despite the presence of metabolic improvements [87]. Overall, the relationship between specific phyla/species or microbial-derived metabolites (such as SCFAs) and weight-loss requires further investigation [88]. **Therefore, an aim of this thesis was to investigate the impact of low-energy diet on gut- microbiota composition and SCFAs production and excretion in both the proximal (Chapter 3, Project 2) and distal (Chapter 2, Project 1) colon regions of the intestinal tract within the context of weight loss in obese mice.**

1.2.2 The Interplay Between Obesity, Gut Health and Inflammation

Obesity is linked to some degree of inflammation known as chronic low-grade systemic inflammation. Unlike typical inflammation, this form does not exhibit the usual visible signs (such as redness, heat, swelling, pain, loss of function, etc. [89]), but shares similarities in the disorders produced by typical inflammatory mediators and signaling pathways [90,91]. Adipose tissue serves not only as an energy storage site in the body but also plays a crucial role in regulating metabolic pathways, including immunity and inflammation [91]. The expansion of adipose tissue volume in individuals living with obesity is associated with elevated levels of cytokines including Tumor Necrosis Factor-Alpha (TNF-α), Interleukins (IL)-1, and IL-6, as well as acute-phase proteins like C-reactive protein (CRP) [92]. The adipose tissue also releases various pro-inflammatory and anti-inflammatory adipokines such as leptin, adiponectin, and resistin [91].

In obesity, adipose tissue experiences a substantial increase in macrophages, comprising about 50% of interstitial cells. These macrophages undergo a shift from an anti-inflammatory (M2) to a pro-inflammatory (M1) phenotype, releasing cytokines that promote tissue inflammation and various pathological effects [92,93]. Moreover, increased serum concentrations of microbiota-derived lipopolysaccharides (LPS) have been reported in patients with obesity [94]. LPS are produced by gram-negative bacteria as an essential component found in their outer membrane structure. LPS is highly immunogenic and can trigger robust pro-inflammatory responses in mammals, making it a potent stimulant for the immune system [95]. Consumption of a HFD may prolong the postprandial period, potentially intensifying the translocation of LPS into the bloodstream [92]. Additionally, HFDs have been shown to increase intestinal barrier permeability, facilitating the translocation of LPS into the systemic circulation [96].

Toll-Like Receptor 4 (TLR4) is expressed in immune cells, including macrophages and monocytes, and is activated by bacterial LPS [97]. TLR4 interacts with LPS with the assistance of LPS-binding protein (LBP), cluster of differentiation 14 (CD14) protein, and myeloid differentiation factor-2 (MD-2) protein [97]. LBP, a serum glycoprotein, is part of the lipid-binding protein family synthesized primarily by hepatocytes and intestinal epithelial cells [98]. Free LPS rapidly binds to LBP upon being released into the plasma [92]. LBP binds LPS micelles and forms complexes with cluster of differentiation 14 (CD14) protein [99]. The generation of CD14/LBP/LPS micelles, enhances the formation of complex with MD-2, a secreted glycoprotein containing an LPS-binding pocket. This protein plays a crucial role by firmly attaching to the extracellular fragment of the receptor, thereby facilitating the interaction between TLR4 and LPS [97,99]. The signalling complex (TLR4–MD-2–LPS), activates myeloid differentiation 88 (MyD88)-dependent pathway, leading to NF-κB activation and the release of inflammatory cytokines [92]. Macrophages have the capability to recognize LPS via TLR4, leading to a shift from an M2 to an M1 phenotype. This transition is associated with an augmented release of pro-inflammatory cytokines such as IL-1 and TNF-α [100].

Gut microbiota composition plays a role in gut-barrier integrity. For example, a decrease in Bifidobacterium is associated with reduced gene expression levels of tight junction proteins zona occludens 1 (ZO-1) and occludin, and increased gut permeability. Additionally, a deficiency in *Akkermansia muciniphila* abundance may be linked to a compromised gut mucosa, contributing to increased translocation of LPS to the circulation [92]. In contrast, SCFAs, mainly butyrate, have demonstrated the ability to alleviate the LPS-induced accumulation of macrophages, implying a potential anti-inflammatory effect in the context of obesity [100]. In this context, evidence similarly supports that the consumption of high fiber-containing foods, such as dietary pulses,

resistant starch, inulin, and oligofructose, results in the production of SCFAs and SCFA-producing bacteria in the gut, and therefore, hold promise for novel approaches to weight loss interventions and mitigating inflammatory state [57,101–103]. Calorie restriction induces a shift in gut microbiota composition, favoring the growth of beneficial bacteria that produce anti-inflammatory SCFAs. This promotes enhanced intestinal integrity while restricting the translocation of bacterial toxins in to the bloodstream [104]. Long-term calorie restriction in humans (approximately 30% less energy) resulted in significant weight loss accompanied by reductions in CRP, TNF-α, and IL-6 [105]. Similarly, weight loss (at least a 5% body weight) through caloric restriction in individuals living with overweight/obesity with metabolic syndrome was associated with an improvement in peripheral pro-inflammatory mediators such as IL-6 and TNF-α, IL-8 and macrophage inflammatory proteins- (MIP)-1β, resulting in an overall decrease in inflammatory score [106]. Additionally, transitioning from a HFD to a purified low-fat diet (LFD) in DIO animal models not only led to reductions in peripheral inflammatory cytokines like IL-6 and TNF-α, but also resulted in diminished macrophage infiltration in epididymal white adipose tissue (EAT), indicative of reduced inflammation. This was accompanied by a reduction in adipocyte size, similar to that observed in the obese control group [107]. Similarly, transitioning to a LFD in DIO mice resulted in higher adiponectin and lower leptin concentrations as well as reduced levels of chemokines (a subset of cytokines specifically involved in regulating the migration and activation of immune cells [108]) including monocyte chemoattractant protein (MCP)-1 in adipose tissue [109]. Overall, findings suggest that calorie restriction and dietary interventions, such as transitioning from a HFD to a LFD, exert beneficial effects on systemic and adipose tissue inflammation. **However, a comprehensive exploration of the alterations in gut microbiota and**

inflammation status resulting from dietary weight-loss interventions is warranted to enhance our understanding of these complex interactions.

1.2.3 The Interplay Between Obesity, Gut Health, and Mental Well-being

Recent research has emphasized the pivotal role of an imbalance in microbial homeostasis, referred to as dysbiosis, in the development and progression of obesity and associated metabolic disorders [66,110]. Moreover, individuals living with obesity are more likely to experience elevated levels of anxiety and depression [111–113]. A bidirectional relationship between depression and obesity has been reported, indicating that individuals with obesity have a 55% increased risk of developing depression over time, and individuals with depression have a 58% increased risk of obesity [112]. Furthermore, evidence has found higher odds of anxiety disorders in individuals with obesity compared to those with normal weight [114]. Additionally, in the past decade, evidence has also shown strong associations between microbial dysbiosis and other host diseases, affecting organs even at a considerable distance from the gut, including CNS [115]. The significant contribution of gut microbiota extends from its association with neuroinflammatory and psychiatric disorders to encompass a role in brain development [115]. The communication between the CNS, the intestine, and the microbiota occurs through the so-called gut-brain axis (GBA) [115]. GBA, is a bidirectional communication network linking the enteric and central nervous systems [116] **(Figure 1-3)**. This network involves not only anatomical connections but also extends to include endocrine, humoral, metabolic, and immune pathways of communications [116]. This axis is connected through the mutual activities of the CNS, the autonomic nervous system (ANS), enteric nervous system, the endocrine system, the hypothalamic-pituitary-adrenal axis (HPA), the immune system, and the gut microbiota and its metabolites [115,117].

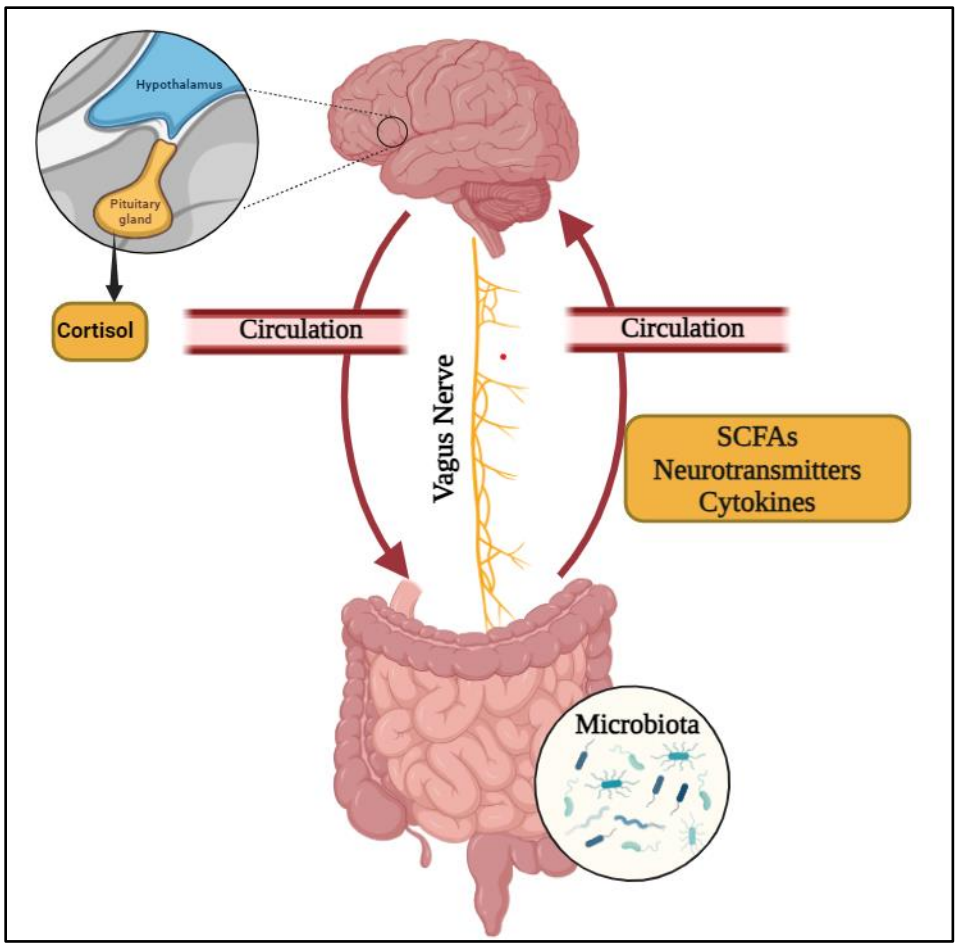

Figure 1-3. Gut-Brain-Axis. The gut microbiota and brain communicate bidirectionally through various pathways known as the gut microbiota-brain axis (GBA). These pathways include the neuroanatomical connections such as the vagus nerve, the neuroendocrine system, such as the hypothalamic-pituitary-adrenal axis, and both direct and indirect chemical pathways possibly involving microbial metabolites like short-chain fatty acids (SCFA) and specific neurotransmitters. Additionally, increased circulating cytokines subsequent to bacterial translocation contribute to this communication (Figure inspired by Han and Colleagues **[118]** and created with Biorender.com).

The CNS exerts influence over gut functions through the ANS. The ANS, comprised of sympathetic and parasympathetic branches, regulates various aspects of gut activity including motility, secretion of acids and mucus, and immune responses [119]. Changes in gastrointestinal transit, under ANS regulation, impact nutrient delivery to gut microbiota and alter the luminal environment. Additionally, ANS-mediated effects impact the size and quality of the intestinal mucus layer, affecting the habitat of gut microbiota. Furthermore, the CNS can modify immune activation in the gut, influencing how immune cells respond to luminal bacteria and affecting gut

permeability [119]. Environmental stressors or peripheral responses to intestinal inflammation are processed within the CNS, which in turn activates the HPA. This activation leads to the systemic release of glucocorticoids, like cortisol, which subsequently alter intestinal function, including gut transit time and nutrient availability [120]. Persistent high cortisol levels have been also linked to changes in gut microbiota composition and increased gut permeability, potentially fostering inflammation and playing a role in blood-brain-barrier (BBB) dysfunction and neuroinflammation, potentially leading to various CNS disorders **as observed in rodent and human studies** [121–123].

Conversely, the intestinal microbiota can release metabolites, cytokines, and other signaling mediators to the CNS through neuro-immune pathways, impacting the physiological function of the brain [117]. Several bacterial metabolites, such as essential vitamins, secondary bile acids, amino acids, and SCFAs, modulate numerous immune system pathways. These pathways, in turn, influence behavior, memory, learning, locomotion, and neurodegenerative disorders [115]. Neurotransmitters, including acetylcholine, gamma-aminobutyric acid, and serotonin, are produced by bacteria from Lactobacillus, Bifidobacteria, Enterococcus, and Streptococcus species [115]. These neurotransmitters can regulate brain functions. Remarkably, 90% of serotonin, crucial for regulating mood, behavior, sleep, and various functions in both the CNS and GIT, is synthesized in the gut [115]. Microbial dysbiosis can lead to increased gut permeability, causing the release of endotoxins like LPS into the bloodstream and triggering a neural immune response. The gut communicates its dysbiotic state with the brain via the vagus nerve, triggering heightened activity of HPA axis, and subsequent release of cortisol and proinflammatory cytokines [124,125]. The vagus nerve is a key part of the parasympathetic nervous system, consists mainly of afferent

fibers (80%) and efferent fibers (20%). It has the ability to sense microbiota metabolites through its afferent fibers and transfer this information from the gut to the CNS [126].

Individuals or mice with anxiety exhibit a notable reduction in microbial richness and diversity [127,128]. Anxiety is often associated with a lower abundance of Firmicutes but higher levels of Bacteroidetes and Fusobacteria at the phylum level [129]. At the genus (g) level, there are positive correlations between several gut microbiota genera (e.g., *Lactobacillales, Sellimonas, Streptococcus*, and *Enterococcus*) and anxiety, while some genera (e.g., *Lachnospira*, and *Butyricicoccus*) show an inverse relationship with anxiety [129]. Similarly, in individuals or animals with depression, a notable difference in the composition and abundance of gut microbiota compared to healthy controls have been observed [129]. At the family taxonomy level, certain gut microbiota exhibits a positive correlation with depression, including *Paraprevotella*, while others, like *Streptococcaceae* and *Gemella*, are negatively associated [130]. Furthermore, several gut microbiota genera, such as *Prevotella*, *Klebsiella*, and *Clostridium*, demonstrate a positive relationship with depression [131]. This evidence underscores the importance of targeting gut microbiota as an integral component of strategies used for preventing or treatment of mental disorders.

The CNS is traditionally considered immune-privileged, meaning it is protected from immune responses by the BBB, which tightly regulates exchanges with the periphery. [115,132]. However, this concept has been re-evaluated, as emerging evidence suggests that functional immune cells are capable of crossing the BBB and accessing the CNS [115]. Chronic low-grade systemic inflammation associated with obesity may disrupt the BBB [133,134]. This disruption has the potential to alter CNS homeostasis by challenging the BBB to modify its permeability and uptake capabilities, as well as by secreting mediators into the CNS [115,132]. This process can

result in the generation of neuroinflammation, increased oxidative stress, and potential behavioral and cognitive alterations [132,133]. The systemic inflammation facilitates the entry of pro-inflammatory molecules into the brain parenchyma, resulting in increased activation and proliferation of microglia and astrocytes in animal models and individuals living with obesity [133]. These cellular changes in the brain manifest as specific clinical symptoms, including impaired locomotor function, muscle weakness, paralysis, learning deficits, and dementia [125].

In obesity, the levels of various mediators, including not only gut derived LPS and fatty acids (FAs) but also adiponectin, leptin, and resistin, are chronically altered [132]. These changes also result in neuroinflammatory responses in numerous structures within the CNS [132]. HFD-fed obese C57BL/6 mice exhibited depressive and anxiety-like behaviors accompanied by the activation of microglia and astrocytes and increased neuroinflammation [135]. However, the impacts of dietary weight loss on mental well-being and behavior in animal models is unknown. While a potential link between obesity, dysbiosis, and mood and behavioral defects has been suggested, dietary modifications may also positively improve gut microbiota as a potential mediator for prevention and treatment of mental disorders [129,136].

1.2.3.1 Weight Loss and Mental Health Outcomes

Despite the potential metabolic benefits of weight loss induced by caloric restriction in humans, as discussed in previous sections, the impact of weight loss on psychological well-being within the context of obesity remains uncertain. Some evidence from studies involving individuals with normal to overweight state have demonstrated that weight loss induced by calorie restriction can improve quality of life [137], and overall mood [138]. In a 6-month weight loss intervention (−30% energy) in subjects with metabolic syndrome, significant reductions in body weight and

anxiety symptoms were observed [139]. Similarly, a very low-calorie ketogenic diet (600–800 kcal/day, low in carbohydrates for 4 months) resulted in substantial weight loss and enhanced psychological well-being parameters (as tested by assessment of food cravings, quality of life (QoL), daytime sleepiness and sleep quality, sexual functioning) [140]. On the contrary, in a recently published study involving adults with obesity, dietary weight loss (25% energy restriction daily for 12 months) was found to be associated with neither improvement in mood nor quality of life [141]. A comprehensive systematic review and meta-analysis on the impact of adult behavioural weight management interventions on mental health revealed significantly greater improvements across various mental health outcomes including depression and mental health-related quality of life in individuals with overweight or obesity. However, there was insufficient evidence available to comprehensively assess the impact of weight loss on anxiety [142]. These conflicting outcomes suggest that the effect of weight loss on mental well-being may significantly differ depending on the type of dietary interventions, potentially affecting gut microbiota in distinct ways. Furthermore, the simultaneous impacts of low-calorie diets on the intestinal microenvironment and mental well-being within the context of obesity remains unclear. **Therefore, an aim of this thesis (Chapter 3, Project 2) was to comprehensively investigate how targeting gut microbiota through low-calorie diets would impact anxiety-like behaviors and well-being, serving as indicators of mental health in DIO mice models.**

1.1 Dietary Pulses

Given that the gut microbiota has been suggested to play a role in the pathophysiology of obesity, it has been increasingly recognized as a promising target for therapeutic dietary interventions aimed at preventing and managing obesity and associated chronic diseases [143]. Recently, there has been a growing interest in the consumption of functional foods, like dietary

pulses [144]. Pulses have been demonstrated to improve intestinal health by closely interacting with the gut microbiota, promoting weight management, enhancing cognitive function, and contributing significantly to overall health [129,145–151]. Dietary pulses are ecologically sustainable protein food sources with a unique nutrient-dense profile [144]. The latest version of Canada's Food Guide [152] as well as the Dietary Guidelines for Americans [153] also emphasize the benefits of consuming plant-based foods, particularly dietary pulses.

Dietary pulses are defined as edible non-oilseed legumes in the Leguminosae family [154]. While a wide array of pulse varieties is available globally, the Food and Agriculture Organization (FAO) identifies 11 main types, including beans, broad beans, Bambara beans, chickpeas, lentils, cowpeas, peas, pigeon peas, vetches, lupins, and other 'minor' pulses [154]. Notably, lentils (*Lens culinaris L.*), beans (*Phaseolus vulgaris L.*), chickpeas (*Cicer arietinum L.*), and peas (*Pisum sativum L.*) stand out as the most commonly consumed pulses worldwide [155].

1.3.1 Nutritional Composition of Dietary Pulses: Focus on Common Beans

Pulses and in particular common beans are nutritious foods with protein content ranging from 21% to 25% by weight (wt), carbohydrates ranging from 55 to 65% wt, and high content of soluble and insoluble dietary fiber [144] (up to 30 g of fiber per 100 g dry weight [beans: 23–32 g; chickpeas: 18–22 g; lentils: 18–20 g; peas: 14–26 g] [156]). Dietary fibers are categorized into soluble and insoluble types [46,157] . Insoluble fibers, such as cellulose, certain hemicellulose, and lignin, are poorly fermented by gut microbes [46]. Instead, they tend to enhance gut transit rate, reducing the time available for bacterial fermentation of undigested food in the colon [46]. On the other hand, soluble fibers, including wheat dextrin, pectin, gums, β-glucan, psyllium, and fructans, are more accessible to bacterial fermentation, resulting in the production of SCFAs [46].

Dietary pulses also contain diverse bioactive compounds like polysaccharides, oligosaccharides, polyphenols/phytochemicals, and a spectrum of essential vitamins and minerals. Notably, the carbohydrate profile in pulses is dominated by starch, featuring a substantial amount of resistant starch (RS), accounting for 30 to 40% amylose content (wt) and displaying resistance to digestion [158]. The RS and other NDCs including galacto-oligosaccharides (such as raffinose, stachyose, and verbascose, making up between 3.5 and 6.9% (wt) of the cooked pulses [159–161]) undergo microbial fermentation producing SCFAs [162]. The dietary fiber content in beans and pulses is impressively high, with slight variations among types. For instance, a ½ cup of cooked kidney beans contains approximately 5.7 g of dietary fiber, while pinto beans contain 7.7 g, and navy beans contain 9.5 g [144]. Dietary fiber recommendations outlined by the Dietary Guidelines for Americans advocate for 14 g per 1000 kcal intake or 28 g for a 2000-calorie diet [153]. Despite these standards, an estimated 95% of American adults and children fail to meet the recommended amounts of fiber [163]. Similarly, Canadian guidelines suggest that women should consume 25 grams of fiber per day, while men need 38 grams. However, most Canadians are only getting about half of the recommended amount [164]. Given the exceptional fiber concentration in common beans, even a modest increase in bean consumption could lead to a significant enhancement in both fiber and RS profiles.

The dry bean is also a rich source of polyphenols (approximately 145 mg/g, constituting about 11% of the total seed). Among the phenolic compounds present in the seed coats are flavones, monomers, and oligomers of flavanols, flavanones, iso-flavonoids, anthocyanins, chalcones, and dihydrochalcones [165]. However, phenolic acids and non-flavonoid phenolic compounds, such as hydroxybenzoic and hydroxycinnamic acid, are primarily found in the cotyledons (seed leaf within the embryo of a seed) of the bean [165]. The presence and quantity of

these phenolic compounds vary based on factors such as the seed coat color pattern and the bean cultivar type. The color of the seed coat is influenced by polyphenols like anthocyanins, flavanols glucosides, and condensed tannins, with dark-colored beans typically having the highest anthocyanin content [165]. Red, black, and pink-colored varieties contribute color to the bean seed coat due to their anthocyanin content, while light yellow or pink spots on the seed coat are generally associated with the presence of condensed tannins [165].

There is a bidirectional relationship between gut microbiota and polyphenols, as the gut microbiota bio-transform polyphenols into simpler metabolites such as phenolic acids, modulating their absorption and biological activity [166]. In turn, polyphenols modulate gut dysbiosis by possessing prebiotic properties and enhancing the abundance of beneficial bacteria [167]. Evidence has shown that polyphenols enhance the growth of gut bacteria known as prebiotic targets, such as *Lactobacillus*, *Bifidobacterium*, *Akkermansia*, *Roseburia*, and *Faecalibacterium spp* [168]. More than 90% of polyphenols absorption occurs in the colon and their biotransformation is greatly dependant on gut microbiota composition and polyphenols structure [167]. Polyphenols have been shown to stimulate beneficial bacteria to produce a diverse array of metabolites, including SCFAs [169]. Dietary polyphenols, particularly catechins, anthocyanins, and proanthocyanidins, demonstrate a significant prebiotic effect, as supported by significant evidence from preclinical studies [168]. Furthermore, polyphenols have been reported to enhance the secretion of hormones and neurotransmitters such as serotonin and gamma-aminobutyric acid. These compounds play crucial roles in modulating the GBA, thereby may have potential to contribute to the prevention and treatment of neurodegenerative diseases [169].

1.3.2 Dietary Pulses and Obesity Management

Evidence suggests that promoting higher public consumption of pulses could serve as a practical and cost-effective strategy to address the ongoing obesity epidemic and mitigate the risk of various prevalent chronic diseases [148]. Pulses are suggested to play a pivotal role in impacting BMI through various factors such as the management of healthy body weight, satiety, and regulation of food intake [144,146,148]. Observational studies have shown an inverse relationship between pulse consumption and body weight [170,171]. Evidence from animal and human studies have shown beneficial effects of dietary pulses consumption on different metabolic outcomes including body weight [172–174]. Introducing raw kidney beans (Phaseolus vulgaris) at the dose of 260g/kg to low-fat or moderate-fat diets over 10 days resulted in significant weight reduction in obese Zucker rats (≈ -9.5 % and -2.7 %, respectively) and their lean littermates (≈ -8.1 % and -3.17 %, respectively) compared to controls [175]. Similarly, *ad libitum* consumption of either cooked whole bean, as well as a commercially prepared cooked bean powders, resulted in less weight gain and reduced storage of lipid in visceral fat depots in dietary induced obesity sensitive rats [172]. In randomized control trials on the impact of 8 weeks pulse consumption (4 days/week) with a hypocaloric diet in individuals living with obesity, higher weight loss in pulses consumers compared to the control group were found [176–178]. In a meta-analysis of 21 trials involving 940 participants with overweight or obesity, the overall pooled analysis showed that dietary pulse consumption was associated with a modest but significant weight reduction of -0.34 kg (1.74 kg in 4 trials and 0.29 kg in 17 trials with and without energy restriction, respectively) over a median duration of 6 weeks, with a median intake of 132 g/d (or approximately 1 serving/d). Overall, this study highlighted the potential versatility of dietary pulses as a weight management strategy irrespective of the implementation of energy restriction [149]. This study proposed the satiating

properties of dietary pulses as one of the mechanisms that could explain the observed weight loss. In another meta-analysis encompassing nine feeding trials with 126 participants, the impact of pulses on satiety and subsequent food intake was assessed. The findings indicated that while pulses led to a 31% increased acute satiety, which was determined to be clinically meaningful, they did not significantly affect intake during a subsequent meal [179]. However, the authors reported the limitations of their analysis, including small sample sizes and notable heterogeneity among the trials, a common challenge in studies examining the effects of pulses [179].

1.3.3 Exploring the Gut Health Benefits of Pulse Consumption in Obesity: Insights from Human Studies and Animal Models

Limited research has explored the impact of pulse consumption on the gut microbiota in individuals with obesity, particularly studies utilizing common beans as a dietary intervention [180]. A 2022 review paper highlighted that the inclusion of dietary pulses and their RS in the diet promotes the proliferation of beneficial gut bacteria and substantially increases SCFA production in the colon in clinical trials [101]. These studies involved the consumption of common pulses, ranging from 35 to 200g per day for 3 weeks to 4 months, and targeted various participant groups, including healthy individuals, those with pre-metabolic syndrome, and colorectal cancer survivors living with overweight or obesity [101,181–183]. However, there is a knowledge gap regarding the impact of pulse consumption in targeting gut microbiota composition during a low-calorie diet within the context of obesity. There was only one study conducted in individuals living with metabolic syndrome and obesity (BMI>30 kg/m2). The consumption of 1/2 cup (130 g) of cooked pinto bean per day for 12 weeks under energy maintenance conditions had limited effects on gut microbiota alterations, inducing an increase in *Peptostreptococcus* productus and a 50% reduction

in *Eubacterium limosum* compared to the control group [182]. However, this study selectively measured only six carbohydrate-fermenting bacterial populations. In another study in colorectal cancer survivors with participants BMI ranging from 18 to 46.4 kg/m^2, cooked navy bean powder led to an increase in *Clostridium*, *Lachnospira,* and *Coprococcus* along with a decrease in *Bacteroides fragilis* and *Anaerostipe* species, and a boost in microbial richness, although it had no impact on diversity [183]. Despite existing limited research specifically focusing on the impact of dietary pulses in obesity, there are other studies providing insights into the distinct effects of different dietary pulses on gut microbiota composition in healthy individuals [181]. Cooked chickpeas demonstrated a notable increase in the Bacteroidetes, *Megasphaera* (g), and *Faecalibacterium prausnitzii* species (sp), along with a decrease in various *Clostridium* clusters and *Subdoligranulum* (g) [181]. Overall, the limited number of human studies and the diversity in methodologies and outcomes used, create challenges in drawing definitive conclusions. **Therefore, there exists a significant knowledge gap that underscores the need for further extensive human research to establish the combined effects of different pulse types and low-calorie diets on the gut microenvironment and their subsequent health implications in individuals with obesity.**

With respect to animal studies, pulse consumption (ranging from 15.7% navy bean [184], 20% black Turtle bean [185], 30% whole mung bean flour [186], 40% white kidney bean flour [187], 40 % cooked whole pulses [145] or 17.5% to 70 % white kidney beans [188]) in HFD-fed C57BL/6 mice resulted in an elevation of the Bacteroidetes phylum [145,184,185,187,188] and a simultaneous reduction in Firmicutes [145,184,187,188] compared to purified HFD control diets within the duration of 6 to 17 weeks. The introduction of common beans to the HFD diet consistently demonstrated a decrease in the Firmicutes/Bacteroidetes (F/B) ratio, as indicated in

various studies [184,185,187,188]. However, navy bean supplementation for 8 weeks did not show a statistically significant alteration in this ratio [189]. Additional changes at the phylum level included an increased abundance of Cyanobacteria [190] (induced by the consumption of a diet supplemented with 78% dry-cooked black bean for two months), along with a reduced abundance of Actinobacteria reported in some studies [191] (induced by diets comprising 17.5% to 70% of the protein derived from white kidney bean for 12–14 weeks), while others showed no significant change [188]. Moreover, there were varied findings regarding the abundance of Proteobacteria, with some studies indicating an increase [190], while others reported a decrease [188]. Further, the abundance of bacterial genera like *Akkermansia,* [145,184,186–188]; recognized for its beneficial effects in alleviating obesity [192–194], Bacteroides, Bifidobacterium [186], *Allobaculum, Sutterella (II)* [188,189,191], *rc4-4* (of *Peptococcaceae*), *RF32* (of *Alphaproteobacteria*) and *Prevotella* and *S24-7* [184,189], have increased in response to pulse consumption. Conversely, the abundance of *Oscillospira, Dorea, Lactococcus, Streptococcus* [188], *Ruminiclostridium, Mucispirillum, Ruminiclostridium, Oscillibacter* [186] reduced following pulses consumption. Notably, the microbiota exhibited distinct responses to dietary pulses, showing unique effects influenced by variations in pulse types (i.e., lentil- and bean-fed mice saw increases in *Akkermansia. muciniphila* cecal abundance by 25-fold and 49-fold increase, respectively, relative to the control diet, but chickpea- and dry pea-fed mice did not [145]), dosage (17% to 70%) [191]. Notably, a dose-responsive shift in microbial composition was observed with increasing bean doses, leading to enhanced levels of health-associated genera such as *Rikenellaceae, Bacteroides*, and *RF39*. Conversely, there was a suppression observed in genera linked to chronic disease risk, including *Allobaculum, Oscillospira, Dorea*, and *Ruminococcus* [191]. On the other hand, certain bacterial genera, such as rc4-4, demonstrated an increase in

cecum samples in one study [188], whereas they exhibited a decrease in feces samples in other reports [184,189] following pulse consumption. This may underscore the unique composition of the microbiota across different gut regions. These microbiota modifications within the gut were associated with inconsistent alterations in alpha-diversity, while beta-diversity showed significantly separate clustering in pulses supplemented groups from the control group [145,185,186,188,189,189–191]. The observed inconsistencies between studies could be attributed to the variations in fat type and percentage in the diet, duration of HFD consumption and dysbiosis state prior to introducing dietary pulses to the diet, pulse type, duration of supplementation, sex, and location of the gastrointestinal tract from which samples are taken.

The modulation of the colonic microenvironment resulted from pulse consumption has demonstrated significant improvements in various aspects of gut health. These improvements included enhanced colon histology score (crypt length, epithelial cell proliferation, goblet cell number, increased crypt mucus content), as well as increased mucin mRNA expression, and the expression of epithelial tight junction proteins [101,189,195–197]. However, none of those studies were conducted within the context of obesity and calorie restriction. Additionally, the high dosage of pulses (up to 70% of cooked bean powder) that were utilized in established obese mice models [191], may not be feasible or translatable to human studies due to practical limitations. For instance, based on average calorie intake conversions in mice and humans, 70% w/w of cooked pulses in mice diets is approximately equivalent to 4 ½ cups of cooked pulses in adult diets, which exceeds typical daily intake recommendations for pulses in human diets in most populations [154]. **As can be seen from the above literature review, there is a significant knowledge gap in literature concerning the impact of dietary pulses, notably common beans, on gut health during the transition from a dysbiotic state induced by a HFD to a reduced calorie diet. This**

understanding is crucial for better weight loss strategies in individuals living with obesity with potential pre-existing gut microbiota dysbiosis.

1.3.4 Exploring the Benefits of Pulse consumption on Systemic Inflammation and Metabolic Health in Obesity

In this section, the impacts of dietary pulses on inflammation status during obesity development or established obesity animal models, as well as their effects on individuals living with overweight or obesity are discussed.

White adipose tissue plays a central role as the primary fat-storing depot and functions as the largest endocrine organ, releasing adipokines and cytokines into the systemic circulation [198]. Despite the significant interest in evaluating inflammatory changes in adipose tissue of individuals living with obesity to facilitate early detection and disease prevention, there is currently a lack of reliable non-invasive diagnostic methods [199]. As a result, there has been a predominant shift towards investigating adipose tissue in animal studies, with human studies placing a greater emphasis on inflammation markers in the bloodstream.

Feeding rats for two months with 78% dry cooked black beans in a diet referred to as HFD (24 % fat) resulted in reduced NF-κB protein abundance in the colon, with a negative association between fecal butyrate along with significant reduced fat mass, lower serum leptin and insulin concentrations and enhanced glucose tolerance compared to the control group [190]. Introducing black turtle bean to a HFD during obesity development led to decreased plasma levels of GIP, GLP-1, glucagon, leptin, IL-4, IL-5, IL-10, IL-12, TNF-α, and IFN-γ, while final body weight as well as insulin and resistin levels did not differ between the been-fed and control groups [185]. Similarly, cooked navy bean powder supplementation into a purified HFD [189] resulted in

reduced mRNA expression levels of inflammatory markers, including MCP-1, IL-6, and TNF-α, and suppressed the activation of inflammatory transcription factors like NF-κB p65 and STAT3 in EAT of obesity development mouse models. Adiponectin levels increased in both serum and EAT. However, leptin: adiponectin ratio decreased only in serum, with EAT leptin remaining unchanged in beans supplemented group compared to the control group. Despite no difference was observed in body weight between bean-fed and control groups, beans consumption was accompanied by a decrease in insulin resistance and a reduction in the formation of crown-like structures in EAT, along with a decrease in adipocyte size in the group supplemented with beans. These findings suggest that beans play a role in mitigating the severity of the obese phenotype during obesity development [189].

Other studies have investigated the potential of common beans to alleviate the inflammatory profile in mouse models following the establishment of obesity, providing insights that may be more translatable to humans and reflective of the inflammatory phenotype observed in human obesity. Similar to the previous study [189], feeding established obese mouse models with a HFD supplemented with Navy beans, despite no significant change in body weight, led to reduced EAT protein expressions of IL-6, MCP-1, MIP-1α, and TNF-α as well as activated NF-κB p65, STAT3, with no significant effect on serum levels of leptin, PAI-1, and resistin compared to the control group [184].

Human studies have investigated the impact of dietary pulses on inflammation and metabolic health under both calorie-restriction for weight loss and weight maintenance conditions in individuals living with overweight and obesity. The consumption of mixed pulses (896 g per week), comprising yellow split peas, chickpeas, navy beans, and lentils, or counselling to reduce energy intake (−500 kcal) by men and women with metabolic syndrome and a BMI of 27–39·9

kg/m^2 for eight weeks did not reveal differences in adiponectin and CRP between the diet groups, however, fasting plasma leptin increased. Additionally, both interventions led to reduced energy intake and improvements in blood glucose control and insulin sensitivity [200]. Overall, the findings of this study suggest that incorporating pulses into the diet may offer comparable or superior benefits to dietary energy reduction in managing metabolic syndrome risk factors [200]. In another 8-week randomized controlled trial, participants with an average BMI of 32.5 ± 4.5 kg/m^2 followed an energy-restricted diet (−30% total energy expenditure) supplemented with 240-360 g of pulses per week, including lentils, chickpeas, peas, and beans, the pulse diet resulted in decreased plasma levels of complement C3 (synthesize by activated macrophages and adipocytes), high-sensitivity TNF-α, and CRP, while IL-6 levels remained relatively unchanged when compared to the calorie-restricted legume-free diet [178]. In contrast, in a similar design study but of shorter duration (6 weeks), an energy-restricted diet (−500 kcal) supplemented with one cup of mixed pulses, the plasma concentrations of high-sensitivity CRP (hs-CRP) remained unchanged [201]. Additionally, under weight-stable conditions, a 4-week randomized crossover feeding trial involving participants with average BMI of 28.7 ± 3.5 kg/m2, followed either a low-glycemic index diet supplemented with 250 g of beans per day (including navy, pinto, kidney, and black beans) or a healthy American control diet, both diets exhibited favorable effects on inflammatory markers, leading to reduced serum CRP and TNF-α receptors, possibly attributed to their overall healthier nutrient profiles, including higher vitamin C and lower cholesterol, compared to the participants pre-trial diets. However, 2h-postprandial insulin levels increased less by the legume diet [202]. In a 6-week randomized controlled trial involving individuals with a family history of diabetes and an average BMI of 28.92 ± 0.85 kg/m^2, the addition of 250 g of pulses per week, specifically pinto beans, and brown lentils, to their habitual diet led to decreased levels of hs-CRP,

while there were no significant differences in IL-6, TNF-α, and adiponectin between groups [203]. In an 8-week randomized controlled trial with an average BMI of 27.5 ± 4.5 kg/m2, participants following either their habitual diet or pulse-based foods supplemented with 150 g of pulses per day, comprising green and red split lentils, chickpeas, yellow split peas, and various beans, demonstrated improved serum cholesterol concentrations. However, no significant differences were observed in CRP, glucose, and insulin levels between the two dietary groups [204].

Based on the above literature review, despite some conflicting evidence, that could be a result of various dosage and duration of dietary pulses supplementation, the overall inclusion of pulses in the diet can be considered to have favorable effects on inflammatory markers and metabolic health. Furthermore, as previously mentioned, certain cultivars of beans, including red, black, and blue-violet-colored beans, are enriched in a significant concentration of phenolic compounds [205]. These compounds may contribute to the additional health benefits observed in limited research conducted on beans with dark-colored seed coats compared to their light-colored counterparts, particularly in terms of intestinal health, as indicated by greater impacts of dark beans on increased proximal colon goblet cell number, crypt length and mucus content, and epithelial cell proliferation in healthy mice [196]. In contrast, in another study involving colitis mouse models, despite observing differential effects of diets supplemented with white and dark beans in reducing the mRNA expression of inflammatory markers in the colon [195,206], dark beans did not strongly influence the colitis phenotype [195]. **However, to the best of my knowledge, no study has comprehensively explored the effects of distinct bean varieties within the same genetic background on intestinal inflammation and metabolic health within the context of obesity, leaving this area to be further investigated. Therefore, this thesis also aimed to**

determine if the beneficial effects of the consumed kidney beans can be depending on the variety (dark or white) and phenolic compound contents of the beans.

1.3.5 Mechanisms Underlying the Beneficial Impact of Dietary Pulses on Obesity Management, Gut Health and Systemic Inflammation

Dietary pulses may contribute to weight loss through two primary mechanisms. Firstly, their high fiber and protein content, combined with a low glycemic index, promote feelings of fullness and delay hunger by slowing digestion and nutrient absorption [149,174]. High-fiber foods like dietary pulses enhance the feeling of fullness by increasing chewing time, reducing food intake, and triggering early satiety signals [149]. Additionally, the soluble fibers in dietary pulses, forming viscous gels, may delay gastric emptying and nutrient absorption, slowing their passage through the digestive system [149]. The high protein content in dietary pulses stimulates the secretion of gastric hormones, such as cholecystokinin and GLP-1, inducing a sensation of fullness. Lastly, low-glycemic index diets help regulate blood glucose concentrations and insulin release, potentially preventing overeating and promoting weight control [149]. Additionally, pulses contain various compounds, including intact cell walls, resistant starch, and fiber, as well as protease and amylase inhibitors, and phenolic compounds. These components may reduce the absorption of calories from pulses. As a result, traditional methods of estimating calorie intake may be challenged. This reduced bioavailability of calories from pulses could potentially lead to lower energy intake and aid in weight loss efforts [174].

Further, dietary fibers are involved in shaping the gut microbiota composition and its fermentative metabolism [207]. For example, it is proposed that the abundance of mucus-degrading bacteria rises in the absence of dietary fiber polysaccharides, given that they constitute

the primary energy source for the gut microbiota [208]. Among all macronutrients, dietary fibers (including NDCs) stand out for their crucial role in fostering a robust and healthy gut microbiota, contributing to overall health and well-being [207]. Microbial fermentation of NDCs promote the production of SCFAs [162]. Various gut bacteria produce distinct types of SCFAs [46]. Key fermentation byproducts, namely acetate, propionate, and butyrate, play pivotal roles in maintaining gut health [39]. They provide energy for epithelial cells, enhance the development of intestinal mucosa and bolster epithelial barrier integrity, and protect the host against enteric pathogens [38,39]. These SCFAs can also lower the colonic pH, thereby promoting the growth of beneficial bacteria such as *Lactobacillus* and *Bifidobacterium* [209]. SCFAs also play regulatory roles in lipids, cholesterol, and glucose metabolism, as well as contribute to anti-inflammatory responses [63]. SCFAs serve as signaling molecules for gut cells and other tissues by interacting with G-protein coupled receptors (GPR) including GPR41 and GPR43 (also known as free-fatty acid receptor 3 (FFA3) and 2 (FFA2), respectively), and GPR109a [63]. Butyrate is served as the major energy source for colonocytes [210]. Additionally, butyrate has been noted for its ability to upregulate the mucin 2 (MUC2) expression, the predominant mucin on the intestinal mucosal surface, promoting heightened mucus production and secretion, and providing enhanced protection against luminal pathogens [210]. The consumption of a western-style diet (characterized by high fat, high sucrose and low fiber content) is associated with altered gut microbiota composition and reduced SCFA production, resulting in a compromised colonic inner mucus layer, reduced mucus layer thickness and increased mucus penetrability [208]. SCFAs enhance intracellular gut permeability by altering tight junction proteins expression or distribution, including ZO-1, which are collectively considered as contributors to the maintenance of the intestinal barrier [46]. As mentioned earlier, a significant outcome of an intestinal barrier disruption is the increased

translocation of bacterial endotoxin LPS into the systemic circulation and initiation of downstream systemic inflammation pathways [92]. Therefore, enhanced intestinal barrier integrity could be a mechanism involved in enhanced systemic inflammation induced by foods containing fiber, like dietary pulses. In addition, SCFAs, particularly butyrate, contribute to anti-inflammatory effects by inhibiting NF-κB activation (a transcription factor regulating genes in inflammation and immunity), suppressing IFN-γ signaling, and upregulating PPAR-γ (a nuclear hormone receptor highly expressed in colonic epithelial cells involved in reducing inflammation and promoting epithelial barrier function) [210]. SCFAs can modulate inflammation by regulating immune cell cytokine production. Butyrate and propionate, for instance, reduce LPS-induced TNF-α and nitric oxide synthase expression in monocytes. These effects are mediated through the activation of FFA2 and FFA3 receptors, GPR109A, or inhibition of Histone deacetylases (HDACs) [211]. Moreover, butyrate and propionate play a crucial role in inhibiting HDAC activation, involved in the regulation of inflammatory and immune pathways [63]. SCFAs represent only a fraction of the diverse metabolites generated by gut bacteria but having profound effects on the host metabolism and homeostasis. It is evident that both the function and composition of the gut microbiota are closely linked to diet, with dietary fibers increasing SCFA production. However, the precise mechanism through which the composition of the gut microbiota influences this dynamic relationship is unclear [102].

As mentioned earlier, dietary pulses are enriched in polyphenolic compounds with numerous health promoting properties [158,165]. Research indicates that polyphenols exert their anti-inflammatory effects by interacting with proteins engaged in gene expression and cell signaling, thereby inhibiting pro-inflammatory transcription factors. This interaction contributes to protective effects against various chronic diseases mediated by inflammation [212].

Furthermore, dietary polyphenols and their metabolites contribute to gut health by exhibiting prebiotic-like effects [213]. These polyphenols are primarily located in the seed coat of beans, and their content varies among different pulse types and varieties based on the color of the seed coat [165]. Dietary polyphenols play a dual role in modulating the gut microbiota composition and improving polyphenol bioavailability through microbial conversion [214]. In this context, colonic gut bacteria play a role in metabolizing polyphenols, transforming them into metabolites such as phenolic acids with potentially greater bioavailability than their original structures. Polyphenols contribute to the growth of beneficial probiotics like *Lactobacillus* and *Bifidobacterium* while inhibiting pathogenic bacteria such as *Clostridium histolyticum* and *Clostridium perfringens*, known for causing inflammatory bowel disease. Polyphenols also regulate the Firmicutes to Bacteroides ratio [214]. Polyphenols contribute to the preservation of the mucus barrier, crucial for preventing colonic inflammation [213]. Evidence indicates that polyphenol-rich diets, can enhance the population of SCFAs producing bacteria, notably *Akkermansia* [214], known for stimulating mucin production. Promoting SCFA production, leading to anti-inflammatory effects and improved colon barrier integrity [214]. They promote mucus secretion by stimulating interleukins (like IL-4 and IL-13), goblet cell proliferation, and MUC2 production. On the contrary, polyphenols inhibit the overgrowth of mucus-eroding bacteria, such as *Citrobacter rodentium*, preventing colonic damage [213].

In conclusion, the intricate mechanisms through which dietary pulses positively impact gut health and systemic inflammation are multifaceted. The synergistic effects of NDCs and polyphenols in pulses have the potential to play pivotal roles in shaping the gut microbiota, promoting the production of SCFAs, enhancing intestinal barrier integrity, and exerting anti-inflammatory effects. **These findings underscore the intricate interplay between diet, gut**

microbiota, and systemic health, highlighting the potential of dietary pulses as valuable contributors to overall well-being through impacting gut-brain-axis.

1.3.6 Exploring the Impact of Pulse Consumption and Key Components on Mental Health

Observational evidence indicates that maintaining a healthy diet, particularly the traditional Mediterranean diet, and avoiding from pro-inflammatory food (such as processed meats and trans fats) are linked to a lower risk of experiencing depressive symptoms or clinical depression [215]. The evidence regarding the role of pulses in enhancing mental health is very limited. In a longitudinal study in humans [216], a moderate intake of legumes was associated with a reduced risk of depression among women undergoing menopausal transition. However, no significant association was found between legume consumption and depressive risk among men, premenopausal women, or postmenopausal women. Since the evidence regarding the effects of pulse consumption on mental health remains limited, the following paragraphs discuss the findings of studies focusing on key components of pulses, such as dietary fiber and polyphenols, with the potential in altering gut microbiota composition, which in turn could have implications for mental well-being.

In a pre-clinical study on obese C57BL/6 mice, supplementation of the diet with NDCs at a concentration of 10 g per 100 g, alongside improving gut microbiota composition (such as increased relative abundance of Bacteroidetes phylum and genera including *Faecalibacterium*, *Prevotella*, and *Bifidobacterium*), prevented cognitive impairment induced by a HFD observed through improvements in nest building behavior and temporal order memory tests [35]. According to a recently published systematic review and meta-analysis, human studies focusing on the

relationship between dietary fiber intake and mental disorders primarily examine depressive symptoms, with a lack of data regarding the association between dietary fiber and anxiety [217]. Overall, the findings of observational studies included in this systematic review suggest that a higher intake of dietary fiber is associated with a reduced likelihood of depression in both adolescents and adults. Specifically, for every 5-g/day increase in total dietary fiber intake, there was a corresponding 5% reduction in the odds of experiencing depression. Furthermore, consuming higher amounts of dietary fiber from vegetables and soluble sources has shown to have a protective association with depression, while intake of dietary fiber from cereals, fruits, and insoluble sources was only marginally connected [217]. In contrast, findings from the randomised clinical trials did not find significant differences between fiber supplementation and placebo for depressive or anxiety outcomes. It is important to note that the selection criteria for these studies were not exclusively based on individuals with obesity. In a cross-sectional study, higher consumption of dietary fiber by adults with overweight and obesity was associated with a reduced likelihood of psychological distress while no significant association was found between higher intake of dietary fiber and depression or anxiety [218]. Additionally, prebiotic supplementation (16 g/d for 3 months) improved mood in individuals with obesity, particularly those with specific gut microbiota profiles (higher baseline *Coprococcus* and increased *Bifidobacterium* and *Haemophilus* levels at the of the intervention) [219]. However, further research is warranted to explore the effects of dietary interventions, including pulse consumption, on simultaneous modulation of gut microbiota and mental well-being, particularly in populations living with obesity.

Similarly, literature suggests varying effects of polyphenol compounds and polyphenol-rich foods on mental health outcomes including depression. While some, like naringenin and quercetin

found in certain foods, appear to be protective against depression, others, including icariin (a type of flavonoid) and soy, may increase depressive symptoms and risks. Certain dietary patterns rich in polyphenol compounds like curcumin and resveratrol, as well as polyphenol-rich foods such as cocoa, blueberries, tea, red clover, and oranges, could serve as potential adjunctive treatments for depression. However, the inconsistent findings emphasize the need for further research to better understand the complex relationship between polyphenols and depression [220]. Cocoa extract supplementation (providing 645 mg total polyphenols/d for 4 weeks) in combination with a moderate energy restriction (15% energy deficit) in individuals with obesity, did not significantly change anxiety and depression scores compared to the control group [221]. On the other hand, supplementation with polyphenol curcumin (1 g/day for 30 days) significantly reduced symptoms of anxiety in individuals with obesity, while did not exert a significant effect on symptoms of depression [222]. This suggests that curcumin may hold promise as a natural intervention for managing anxiety in individuals living with obesity. Overall, while numerous other animal and human studies have explored the correlation between dietary compounds, including fiber and polyphenols, and mental disorders [215,220,223], there is a notable gap in research comprehensively investigating the effects of metabolites produced by the gut microbiota from these dietary compounds (such as SCFAs) available in dietary pulses on mental health outcomes within the context of obesity. **Therefore, another aim of this thesis was to investigate how targeting gut microbiota through low-calorie diets supplemented with dietary pulses would impact anxiety-like behaviors and well-being, in DIO mice models (Chapter 3, Project 2).**

1.4 Thesis Specific Objectives and Hypotheses

The following outlines the specific objectives and hypotheses of each project, offering a comprehensive overview of the investigations undertaken for the purpose of this thesis **(Figure 1-4).**

1. **Project 1 (Chapter 2)**
    - **Objective:** Investigate the effects of incorporating white and dark red kidney beans into a low-fat-diet in C57BL/6 mice with HFD-induced obesity on fecal gut microbiota composition and function, and inflammatory and metabolic outcomes, including body weight, body composition, adipose tissue cytokines, and circulating biomarkers of adipose tissue function and glucose homeostasis.
    - **Hypothesis:** It was hypothesized that transitioning from a high-fat to a low-fat would alleviate obesity-associated gut dysbiosis, inflammatory and metabolic dysfunctions. Furthermore, the introduction of beans was expected to beneficially impact gut microbiota composition and function, resulting in a reduction in inflammation and an enhancement of metabolic outcomes. Additionally, dark-red kidney beans were anticipated to exhibit further benefits due to enriched amounts of phenolic compounds, including increased flavonoids and anthocyanins, present in the dark-colored seed coats, when compared to the white-red kidney beans.

2. **Project 2 (Chapter 3)**
    - **Objective:** Investigate the effects of incorporating white and dark red kidney beans into a low-fat diet in C57BL/6 mice with obesity induced by a high-fat diet, on cecal

gut microbiota composition and function, proximal colon histomorphology, and behavioral outcomes.

- **Hypothesis:** It was hypothesized that incorporating white and dark red kidney beans into a low-fat diet in C57BL/6 mice exposed to a high-fat diet resulted in significant improvements in intestinal and mental health. Specifically, the intervention was expected to lead to favorable alterations in cecal gut microbiota composition and function. Additionally, positive changes in proximal colon histomorphology were anticipated, indicative of improved intestinal health. These physiological improvements were further anticipated to appear in behavioral outcomes, reflecting a positive impact on mental health. Notably, dark-red kidney beans were speculated to provide additional benefits when compared to the white-red kidney beans.

3. **Project 3**

- **Objective:** Investigate the gut microbiota composition, and inflammatory and metabolic factors potentially contributing to obesity resistance in C57BL/6 mice exposed to a HFD.
- **Hypothesis:** It was hypothesized that the gut microbial community of C57BL/6 mice resistant to HFD-induced obesity would differ from that of mice prone to HFD-induced obesity, with distinct variations in inflammatory and metabolic profiles.

Thesis Projects Study Design

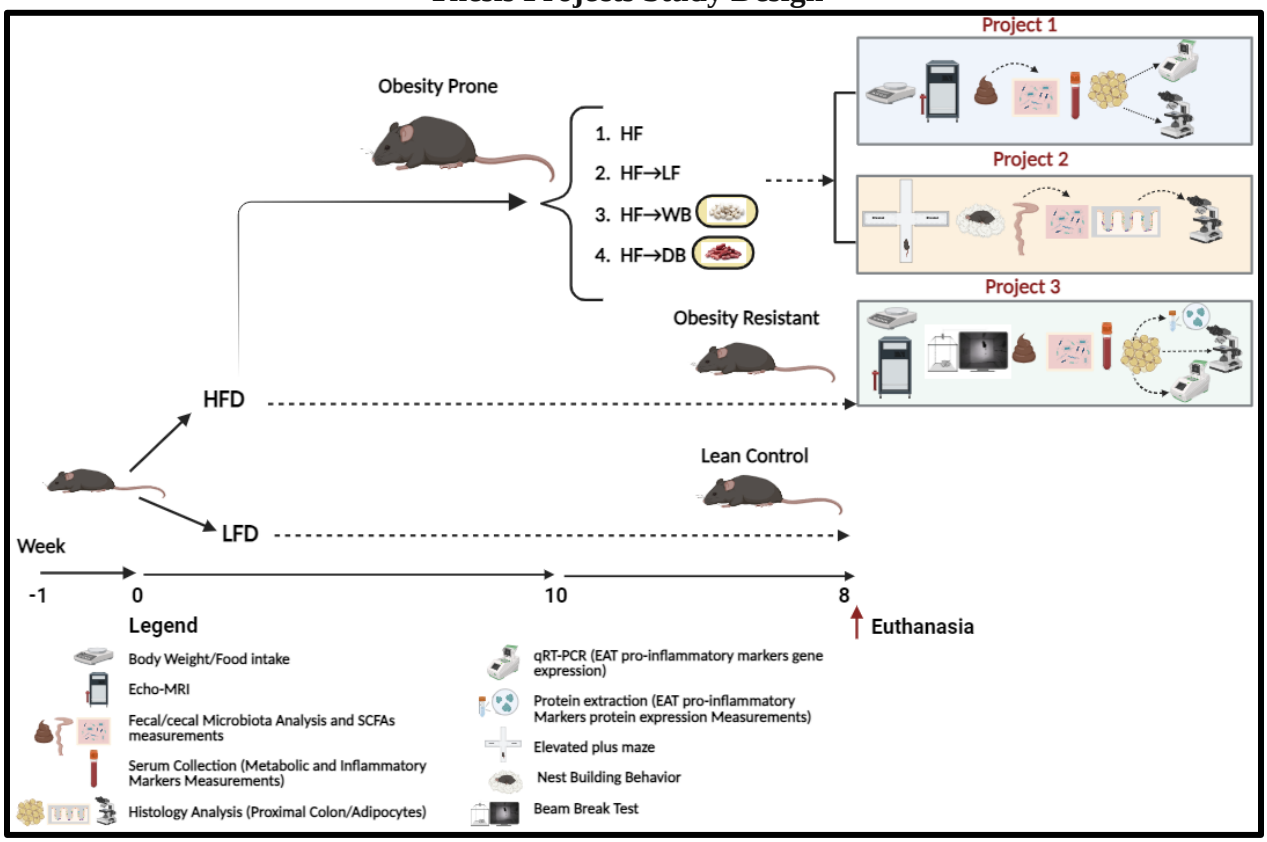

Figure 1-4. Schematic Overview of Three Research Projects. A visual representation of the study design and outcomes measured in each of the three research projects conducted in this thesis. HFD: High-fat diet, LFD: Low-fat diet, HF: High-fat diet fed group, HF→LF: High-fat to low-fat diet transition group, HF→WB: High-Fat to low fat + white kidney beans diet transition group, HF→DB: High-fat to low-fat + dark-red kidney beans diet transition group. EAT: Epididymal adipose tissue.

2 CHAPTER 2 - Project 1 Manuscript

Targeting the Gut Microbiota with White and Dark-Red Kidney Beans as an Approach to Improve Obesity-Associated Metabolic and Inflammatory Outcomes in Male C57Bl/6 Mice

Salma Mahmoodianfard[1], Lalit Kishore[2], Alexane Rodrigue[3], Giorgio Freije[3], Valérie Roumelis[4], Laili Mahmoudian[2], Dawson B.H. Livingston[3], K. Peter Pauls[5], Éric Doucet[1], Krista A. Power[2,3*]

Affiliations:

1. School of Human Kinetics, Faculty of Health Science, University of Ottawa, Ottawa K1N 6N5, Canada
2. School of Nutrition Sciences, Faculty of Health Science, University of Ottawa, Ottawa, Canada, K1N 6N5
3. Department of Biochemistry, Microbiology and Immunology, Faculty of Medicine, University of Ottawa, Ottawa, Canada, K1H 8L1
4. Department of Biology, Faculty of Science, University of Ottawa
5. Department of Plant Agriculture, University of Guelph

***Corresponding Author:**
Krista A. Power
School of Nutrition Sciences
University of Ottawa
Roger Guindon Hall; Room 3260
Phone: 613-562-5800 ext. 2200
Krista.Power@uottawa.ca

Abstract

Gut microbiota dysbiosis has been linked to the development of obesity and contributing to metabolic disturbances. Calorie-restricted low-fat diets are known as effective strategies in mitigating obesity and associated metabolic dysfunctions. Weight loss strategies that target the microbiota such as prebiotic supplements, have demonstrated superior health outcomes when compared to interventions solely focused on calorie restriction. Consumption of dietary pulses can modulate gut microbiota composition and function and thus may offer a promising approach for mitigating obesity-related complications. This study investigated the potential for white (WB) and dark red (DB) kidney bean supplemented diet to beneficially modulate the gut microbiota and metabolic status in obese mice undergoing a weight loss intervention. High-fat diet (HFD)-induced obese C57BL/6 male mice were randomized into four groups: HF-control; HF→LF (transition to a low-fat diet, LFD); HF→WB (LFD+15% WB [wt/wt]); and HF→DB (LFD+15% DB [wt/wt]) for 8 weeks. Transitioning to LFD, led to reduced homeostasis model assessment of insulin resistance (HOMA-IR) and inflammatory-associated markers including serum leptin and adipose tissue monocyte chemoattractant protein-1 (MCP-1) expression compared to the HF-controls. DB provided extra benefits by lowering Resistin levels. Beans led to distinct fecal microbiota β-diversity, elevated short-chain fatty acids (SCFAs), and significant shifts in relative abundance of fecal bacterial genera including reduced *Parabacteroides* and *Dorea* along with an increased ***Prevotella*** **and** ***Rikenellaceae,*** *Clostridium* (methylpentosum sp.) and *Lactobacillus* compared to the HF→LF and HF controls. Additionally, bean-fed mice showed greater lean mass when compared to other groups. Overall, transitioning from HFD to LFD had the greatest impact on enhancing obesity-associated inflammatory and metabolic outcomes in diet-induced obese male mice, while consumption of beans resulted in distinct changes in gut microbiota composition and function and enhanced body composition

Keywords: Obesity; gut microbiota; common beans; adipose tissue dysfunction, inflammation, weight-loss

1. Introduction

Obesity is an alarming public health concern worldwide and a predictor of early death, as it is associated with a higher prevalence of chronic diseases such as diabetes, cardiovascular disease, stroke, hypertension, and cancer [1]. Intestinal microbial dysbiosis (i.e., reduced phylogenetic diversity, increased abundance of pathobionts), is typically observed in individuals living with obesity, as well as in rodent models of obesity, and is associated with metabolic dysfunctions, including insulin resistance, low-grade systemic inflammation insulin resistance, and appetite dysregulation [2–4].

Interventions to treat obesity often include diet modifications (e.g., calorie-restriction, low-carbohydrate, low-fat diets), which have been shown to stimulate weight loss and metabolic homeostasis [5–7], reduce inflammation [6,8], improve intestinal barrier function [6,9], alter the composition and function of the intestinal microbiome [10–12]. Importantly, studies in which weight-loss strategies are concurrent with adjuvant therapies designed to target the gut microbiome (e.g., prebiotics (inulin, oligosaccharides, polyphenols), probiotics, synbiotics), often result in better health outcomes compared to calorie-restriction alone [13–15]. Mechanistically, these treatments can enhance microbial diversity and function leading to the production of microbial metabolites (i.e., short chain fatty acids (SCFAs)), that can directly or indirectly improve intestinal function, promote energy homeostasis, reduce inflammation, and supress appetite [16–22].

Given the growing interest in exploring dietary alternatives for achieving weight loss, targeting the gut microbiota through the consumption of functional foods could offer a promising and affordable approach to mitigate obesity-associated complications. Dietary pulses, including common beans, chickpeas, and lentils, are an inexpensive and highly accessible source of plant-based proteins [23], that are also enriched in microbial-accessible non-digestible carbohydrates

(NDCs; fibers) and polyphenols [24–28]. Our group and others have continuously shown in rodent models of obesity, that supplementation of obesogenic diets (e.g., high-fat diets), can beneficially alter the gut microbiome and attenuate obesity-associated metabolic impairments and systemic and adipose tissue inflammation when consumed i) during obesity, and ii) once obesity has been established [23,29–36]. Furthermore, weight-loss intervention trials with individuals living with obesity have shown that incorporating dietary pulses into hypocaloric diet regimens results in greater body weight reduction, improvements in blood lipid profiles, and reductions in pro-inflammatory mediators, compared to calorie-restrictive diet alone [37–41]. However, no studies have investigated the impact of pulse consumption on the gut microbiota during weight-loss interventions, and its association with improvements in metabolic health and inflammation-associated outcomes.

Therefore, the objective of this study was to determine if incorporating pulses, specifically different varieties of kidney beans, into a weight-loss intervention diet in obese mice, would beneficially modulate the gut microbiota composition and function, and improve metabolic homeostasis and inflammation. Importantly, common beans have a distinct profile of polyphenolic compounds, including phenolic acids, flavonoids, proanthocyanidins, and anthocyanins, which collectively contribute to their diverse seed coat color [42]. Anthocyanins are a type of flavonoid that can create red, blue, or purple pigmentation in bean seed coats with black coat beans having the highest concentrations [43]. Therefore, due to the different profile of white and dark red kidney beans in terms of antioxidant capacities, as well as anthocyanin, flavonoids, and overall polyphenol content [44], we also investigated if beans with darker seed coats would have additional benefits on the aforementioned outcomes.

2. Materials and Methods

2.1 Preparation of cooked bean powders and experimental diet formulation

White and dark-red kidney beans (Yeti and Dynasty cultivars) were generously provided by the University of Guelph Bean Breeding Program. Two hundred grams of dry beans were soaked in 700 mL of tap water overnight and then boiled in 1250 mL of fresh tap water for 10 minutes at the heat setting 7 on an induction ceramic cooktop (Bertazonni, Model # PRO304INSX). Subsequently, they were simmered over the heat setting 4 until fully cooked and reached the desired uniform tenderness. The cooked beans were blended using a Ninja blender (Model # 900W) for a duration of 30-60 seconds. The resulting bean purees were spread out in a thin layer on a parchment paper, placed on a metal tray, and dried using a Turbofan® convection oven (Moffat Ltd., Model # E32D5) set at 221°F for 90-120 minutes. The dried bean purees were then processed into a powder using the KitchenAid KGM Grain Mill Attachment, mounted on a KitchenAid® stand mixer (Model # Pro 600™). The resulting bean powders was then sifted through an 850 μm mesh sieve (VWR, Cat. #57334-562) to ensure uniform particle size and subsequently packaged and stored in a -20°C freezer until ready for use. Proximate analysis and total and insoluble fibre content of the bean powders was analyzed by Maxxam Analytics (Mississauga, Ontario, Canada) **(See Table 2-4 (S1) for detailed methods and results)**.

Four experimental diets were prepared by Envigo/Teklad USA **(Table 2-1)**: low fat diet (AIN-93G; LFD; 13% kcal from fat), high fat diet (HFD; 60% kcal from fat), LFD supplemented with 15% white kidney bean powder (WB), and LFD supplemented with 15% dark kidney bean powder (DB). The bean powder was incorporated into the low-fat diet at a ratio of 15% (w/w) which is equal to 1 cup of pulses for adults; representing a realistic and achievable daily intake of

pulses in humans [45]. Diets were stored at 4°C (LFD, WB, DB) or -20°C (HFD) for the duration of the study.

Table 2-1. Experimental Diet Composition

Nutrients g/Kg	TD.190833 Low Fat Diet (LFD)	TD.190378 High Fat Diet (HFD)	TD.190834 - LFD + 15% White Kidney Bean Flour (WB)	TD.190835 LFD + 15% Dark red Kidney Bean Flour (DB)
Casein	200	265	160	161.22
L-Cystine	3	4	3	3
Corn Starch	414.49	0	349.21	345.8
Maltodextrin	132	160	132	132
Sucrose	100	92.59	100	100
Soybean Oil	34	30	32.33	32.27
Lard	19	310	19	19
Cellulose	50	70	6.95	9.2
Mineral Mix, AIN-93G-MX (94046)	35	48	35	35
Calcium Phosphate, dibasic	0	3.4	0	0
Vitamin Mix, AIN-93-VX (94047)	10	14	10	10
Choline Bitartrate	2.5	3	2.5	2.5
TBHQ, antioxidant	0.01	0.01	0.01	0.01
Bean flour			150	150
Sum	1000	1000	1000	1000
Macronutrient Contribution of Diets g/kg				
Protein, g/kg	177	235	177	177
Carbohydrate, g/kg	616	269	613	615
Fat, g/kg	55	343	55	55
Fiber, g/kg	50	70	50	50
Macronutrient Contribution of total Kcal %				
Protein, % kcal	19.3	18.4	19.4	19.3
Carbohydrate, % kcal	67.2	21.1	67.1	67.2
Fat, % kcal	13.5	60.5	13.5	13.5
Expected Daily Total Food Intake, g	3	2	3	3
Expected Daily Fiber intake, g	0.15	0.14	0.15	0.15
kcal/g	**3.7**	**5.1**	**3.7**	**3.7**

2.2 Experimental Design

The experimental protocol was approved by the University of Ottawa Animal Care Committee (ACC, Protocol number HSe-2857-R3). Five-week-old wild-type C57BL/6 male mice

(n=56) were purchased from Charles River (Kingston, NY, USA). The mice were individually housed in polycarbonate rodent cages containing corncob bedding and cotton nesting material, under a 12-hour light/dark cycle at a temperature range of 22-26 °C with 40% relative humidity. They were acclimatized to the controlled environment with *ad libitum* access to food (LFD) and water for a period of one week. A subset of mice (n=8), referred to as the lean (LF) group, were maintained on the LFD throughout the study, while the remaining mice (n=48) were switched to HFD for 10 weeks to establish obesity. The obese mice were then randomly assigned into four dietary groups for the interventional phase of the study: (1) HF control (maintained on HFD), (2) HF→LF; switched from HFD to LFD, (3) HF→WB; switched from HFD to WB, and (4) HF→DB; switched from HFD to DB. The mice were given *ad libitum* access to their respective diets for an additional 8 weeks (n=12 mice/dietary group) with fresh food provided 3 times/week. At the end of the study, the mice were euthanized by decapitation, trunk blood was collected, and tissues including epididymal adipose tissue (EAT) were excised, weighed, and processed for further analyses as described below.

2.3 Assessment of Body Weight, Diet Intake, and Body Composition

Body weight (BW) and food intake were measured 2-3 times per week throughout the study using a digital scale. Body composition, including lean and fat mass, was quantified using the Echo-MRI™-700 body composition analyzer at week 10 and at the end of week 18.

2.4 Assessment of Fecal Microbial Community Structure and Function

2.4.1 Microbiota DNA Sequencing and Diversity Analysis

Fresh fecal pellets were collected at week 18 from each mouse and stored in cryogenic storage vials at -80°C until analysis. Genomic DNA was extracted using the QIAamp Fast DNA

Stool Mini Kit (Qiagen, Cat. #51604, Germany) following the manufacturer's instructions. The V3-V4 regions of the 16S rRNA gene were amplified, and the libraries were quantified, normalized, and pooled according to the Illumina 16S Metagenomic Sequencing Library Preparation Guide [46]. Sequencing of the libraries was performed on the Illumina MiSeq platform (Illumina®, Miseq). Microbial diversity and community structure were analyzed using the QIIME2 bioinformatics pipeline (version 2022.2) [47]. The 300 bp Casava 1.8 paired-end demultiplexed files were imported and subjected to quality filtering using DADA2 [48]. This process involved denoising, removal of chimeric sequences, correction of Illumina-sequenced amplicon errors, and generation of amplicon sequence variants (ASVs). A phylogenetic tree was constructed using the Greengenes 13_8 99% identity reference tree [49]. Core diversity analysis was conducted using the QIIME2 core-metric method at a sampling depth of 15,000. Alpha (α)-diversity metrics, including Shannon, observed features, Pielou's evenness, and Faith's phylogenetic diversity (PD), were calculated. Microbiota beta (β)-diversity dissimilarity was measured using the Bray-Curtis metric [50], and then visualized using Principal Coordinate Analysis (PCoA). Statistical significance of differences in α-diversity between groups was assessed by Kruskal-Wallis test with Benajmini–Hochberg corrections in Qiime2. PERMANOVA analysis was employed to identify differences in β-diversity between dietary groups in Qiime2, and p-values were adjusted using the Benjamini-Hochberg FDR correction. Taxa relative abundance comparison between groups was performed using the Mann-Whitney U test followed by the two-stage linear step-up method of Benjamini, Kreiger, and Yekutieli ($p<0.05$; FDR<5%).

2.4.2 Predicted Functions of the Metagenome

The microbial community predictive functional profiling was analyzed using the Phylogenetic Investigation of Communities by Reconstruction of Unobserved States 2 (PICRUSt2) [51,52], version 2.51. Initially, the fragment insertion Qiime2 plugin [53] was run for aligning ASVs to the HMMER sequence databases (www.hmmer.org), placing them into the optimal position onto the reference phylogeny using the SATé-Enabled Phylogenetic Placement (SEPP) tool [54] and constructing a new phylogenetic tree using the genesis applications for phylogenetic placement analysis (GAPPA) [55]. Next, core hidden state prediction functions (hsp.py) were performed using the castor R-package [56] to predict gene family abundances for each ASV and Kyoto Encyclopedia of Genes and Genomes (KEGG) orthologs [57] (KO). Subsequently, the metagenome_pipeline.py command was employed to normalize the KO abundances based on 16S abundance. The resulting file (pred_metagenome_unstrat.tsv), containing mouse-specific KO abundances, was processed in RStudio (R =V4.2.2, R Studio: V2022.12.0+353) to determine the inferred function of the microbiota. Employing a custom R code analogous to the categorize_by_function.py used in PICRUST1 [58], the KOs were aligned with a manually curated mapping file sourced from https://www.genome.jp/kegg-bin/get_htext?ko00001.keg (accessed on 17 June 2023) [57]. Finally, STAMP (Statistical Analysis of Taxonomic and Functional Profiles), version 2.1.3 [59], was applied for the outcomes representing the inferred functional aspects and two groups comparisons using Welch's two-sided t-test with Benjamini-Hochberg multiple test correction ($q<0.05$).

2.5 Quantification of Fecal Short Chain Fatty Acids

Gut microbiota function was evaluated by quantifying the levels of SCFAs, including acetic acid, butyric acid, propionic acid, and valeric acid, as well as branched-chain fatty acids (BCFAs), iso-butyric and iso-valeric acids, as previously described [60]. In summary, the methodology included freeze-drying fecal samples, recording dry weight, dilution in MilliQ water to attain a 10% homogeneous fecal solution, centrifugation, pH measurement, acidification, filtration, and utilizing gas chromatography analysis with a standard curve for calibration. This process identified various SCFAs based on retention times and determined their concentrations using analytical standards.

2.6 Serum Metabolic, Inflammatory Biomarkers and Endotoxemia Analysis

Biomarkers of metabolic health were measured from mouse serum collected during week 17 of the study, after an 8 hour overnight fast. Fasting blood samples were collected between 7:00 to 9:00 AM by snipping the tip of the tail using Microvette® CB 300 K2 EDTA capillary blood collection tube (Sarstedt, Cat #16.444.100). Fasting blood glucose levels were measured using a glucometer (Contour®Next blood glucose monitoring system, Bayer, model 7268). Fasting serum was obtained from clotted blood after 30 min incubation at room temperature followed by 15 min on ice and then centrifugation at 10,000 g, 4°C for 30 minutes. The resulting supernatant was separated, and aliquots were stored at -20°C for 48 hours, and then transferred to -80°C until analysis.

Concentrations of Ghrelin, glucose-dependent insulinotropic polypeptide (GIP), glucagon-like peptide-1 (GLP-1), glucagon, insulin, leptin, plasminogen activator inhibitor-1 (PAI-1), and resistin were measured using a multiplex magnetic bead-based fluorescence sandwich

immunoassay kit (Bio-Plex Pro Mouse Diabetes 8-Plex Immunoassay, Bio-Rad, Cat. #171F7001M), and adiponectin concentrations were measured using a single-plex assay (Bio-Plex Pro Mouse Diabetes Adiponectin Assay, Cat. #171F7002M), following the manufacturer's provided instruction manual. Once the samples were prepared and loaded onto the plate, the plate was read on a Luminex® analyzer (MAGPIX®) equipped with Milliplex Analyst software, version 5.1.0.0., developed by VigeneTech Inc. The standards were measured in duplicates to ensure accuracy and reliability, while each sample was read as a single measurement. Therefore, the coefficient of variation (CV%) for the parameters measured was not applicable.

The homeostatic model assessment of insulin resistance (HOMA-IR) index was calculated using the fasting glucose and insulin levels using the following formula: [fasting serum insulin (μIU/L) × fasting serum glucose (mM)] / 22.5. Insulin concentrations were converted from pg/mL to μIU/L using a molar mass of 5808 Da and a conversion factor of 1 μIU/L = 6.00 pmol/L [61].

Mouse LBP enzyme- linked immunosorbent assay (ELISA) kits (HyCultBiotech, Cat# HK205-01) were used to measure lipopolysaccharide binding protein (LBP) levels in duplicates in mice serum as a biomarker of systemic lipopolysaccharide (LPS) exposure [62]. The assay was performed based on the sandwich principle using the manufactures instruction.

2.7 Adipose tissue mRNA Expression

At euthanasia, approximately 500 mg of excised EAT were snap frozen in liquid nitrogen and stored at –80°C for later RNA extraction. RNA was extracted and purified using the Total RNA Purification Plus Kit (Norgen Biotek, #48400). The Purified RNA was normalized to a concentration of 1μg RNA/10μL using the UltraPure™ DNase/RNase-Free Distilled Water (Invitrogen, Cat. #10977015). The normalized RNA was reverse transcribed to complementary

DNA (cDNA) using High-Capacity cDNA Reverse Transcription Kit (Applied Biosystems, Cat. #4368814) in a thermal cycler (Bio-rad, Cat. #1861096. Quantitative real-time PCR (qRT-PCR) analyses were performed using a SYBR Green (Applied Biosystems™, Cat. #A25742) master mix in a CFX96 real-time PCR detection system (Bio-rad, model C1000 Touch™). The Cq values for each of the samples were obtained from CFX Maestro Software. To compare relative expression of the target genes between samples, ΔΔCq method was applied while the gene expression levels were normalized to the expression levels of RPLP0 housekeeping reference gene. Primer sequences are displayed in Supplemental **Table 2-5(S2)**.

2.8 *Histology and Adipocyte Size Measurements*

EAT was fixed in 10% formalin for 48 hours and then in 70% ethanol until processing. EAT were paraffin-embedded, cut at 4 μm thickness, and stained using Hematoxylin and eosin (H&E) at the University of Ottawa Histology Core Facility (Roger-Guidon Hall, Ottawa ON, Canada). Images were captured at 20x magnification using Zeiss, Axiocam 506 microscope camera and analyzed using the Fiji (Image J2) software (version:2.9.0/1.53t) with Adiposoft plugin. To measure the adipocyte size, an average of 25 adipocytes per mouse were analyzed, and their diameter and area were recorded.

2.9 *Statistical Analysis*

Statistical analyses were conducted using GraphPad Prism (Version 9.5.1) software. The ROUT method (q = 1%) was applied to identify the outliers. To assess the normality assumption, the D'Agostino-Pearson omnibus test (K2) was employed. Additionally, the homogeneity of variances for the parametric data was evaluated through the Brown-Forsythe and Bartlett's tests. To evaluate the impact of the intervention on parametric data among the different dietary groups,

a one-way analysis of variance (ANOVA) was performed. Post-hoc analyses, including the Student-Newman-Keuls (SNK) or Tukey's multiple comparison test, were conducted to examine specific pairwise differences between the dietary groups if the ANOVA results were statistically significant. For non-parametric data, two different approaches were used depending on the data distribution. If the non-parametric data could be log-transformed to achieve normality, a One-way ANOVA was performed after the data transformation. Alternatively, a Kruskal-Wallis test was conducted followed by Dunn's multiple comparisons test as a post-hoc analysis. Additionally, Spearman correlation analysis was employed to investigate associations between select variables. The significance level for all statistical tests was set at $p < 0.05$. The detailed statistical results from the ANOVA, Kruskal-Wallis, and other relevant analyses, are provided in Appendix 6-10 for further reference.

3. Results

3.1 Effects of diet on food and energy intake and body weight and composition

The weekly food intake (g) and cumulative energy intake (Kcal) during the intervention period (weeks 10-18) are shown in **Figure 2-1C** and **2-1D,** respectively. The cumulative energy intake was calculated by considering the different energy density of the intervention diets. The total cumulative energy intake was significantly higher in HF (890.3±11.55 kcal) compared with mice in LF (766.1 ±20.35 kcal), HF→LF (756.4±11.65 kcal), HF→WB (833.3±12.45 kcal) and HF→DB (829.9±11.35 kcal) groups. Energy intake was found to be significantly lower in HF→LF mice compared to the bean supplemented groups, while no significant difference was observed among bean groups.

The growth chart and final BW are shown in **Figure 2-1A** and **2-1B**, respectively. After 10 weeks, the BW of HFD-fed mice (n = 48) was significantly greater than their LFD-fed counterparts

(n=8) (40.98±0.67 vs 30.80±0.73g). The HFD-fed mice were then randomly assigned to four groups, such that BW was equivalent across groups, and either fed HFD, LFD (HF→LF), WB (HF→WB), or DB (HF→DB) diets for an additional 8 weeks. A two-way repeated measures ANOVA was performed for the main effects (group and time), which showed a significant difference between groups and over time, as well as a group-time interaction. Dunnett's multiple comparisons test showed that compared to the HF group, the BW of the HF→LF group started to reduce at week 12 and stayed lower until the end of the study. Similarly, at week 13, mice in the HF→WB and HF→DB groups had lower BW compared to HF mice, which continued until the end of the study. The lean control group remained significantly lower than those in the HF group throughout the 8-week intervention period **(Figure 2-1A)**. Final BW showed significant differences among the groups. Notably, BW in all mice consuming low fat-based diets (LF, HF→LF, HF→WB, HF→DB) were lower than HF mice, although amongst the intervention groups (HF→LF, HF→WB, HF→DB), the BW of the HF→LF group were significantly lower than bean-fed groups **(Figure 2-1B)**.

The cumulative energy intake agreed with the final BW, indicating a relationship between diet intake and BW gain.

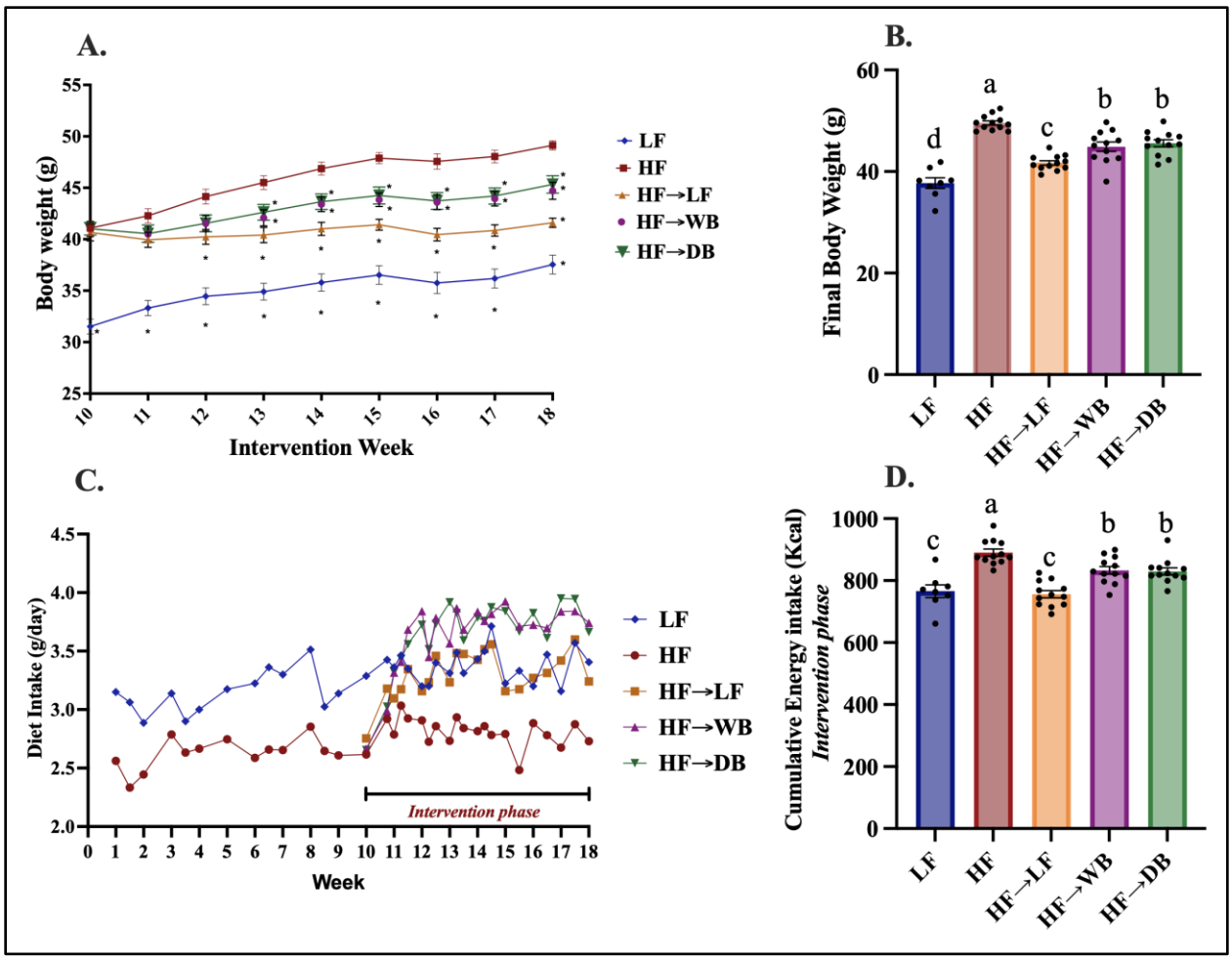

Figure 2-1. Body weight, Food consumption and Dietary Energy Intake. A. Body weight (g) throughout the intervention phase (Week 10-18); An asterisk (*) indicates a significant difference from the high-fat (HF) group, as determined by Kruskal-Wallis test with Dunnett's multiple comparisons test. ($P<0.05$), B. Final body weight (g) at week 18; bars with letters that are not shared differ significantly, as determined by One-way ANOVA followed by Tukey's multiple comparisons test ($P<0.05$), C. Weekly diet intake (g) throughout the study, D. Cumulative energy intake (kcal) during the intervention phase; bars with letters that are not shared are significantly different as indicated by One-way ANOVA followed by Tukey's multiple comparisons test ($P<0.05$). Values are shown as mean±SEM. (n=8 LF, n=12 mice in other groups). LF: Low-fat diet fed lean control group, HF: High-fat diet fed group, HF→LF: High-fat to low-fat diet transition group, HF→WB: High-Fat to low fat + white kidney beans diet transition group, HF→DB: High-fat to low-fat + dark-red kidney beans diet transition group.

Body fat and lean mass were analysed using Echo-MRI at weeks 10 and 18 (**Figure 2-2**). From the start of the intervention phase (End of week 10), fat mass increased over time in the HF group, compared to all other groups, indicating that in obese mice, transitioning from HFD to LFD, with/without bean supplementation, attenuates further gain in fat mass. Amongst the intervention

groups, there was no difference in % fat mass at the end of the intervention period. On the contrary, there was a significant greater lean mass in the groups that received bean diets compared to all other groups. The lean mass gain percentage, calculated as [(Δ lean mass (week 18 - week 10)) / lean mass (week 10)] * 100, showed an increase of 12.1% in both the HF→WB and HF→DB groups, compared to 6.9% and 5.8% in the HF and HF→LF groups, respectively. These results indicate that although the HF→WB and HF→DB groups had a higher final body weight compared to the HF→LF group (as shown in **Figure 2-1B**), this difference was primarily due to an increase in lean mass and not fat mass. Overall, these findings suggest an improvement in body composition in mice consuming bean-supplemented diet as a part of a weight-loss intervention.

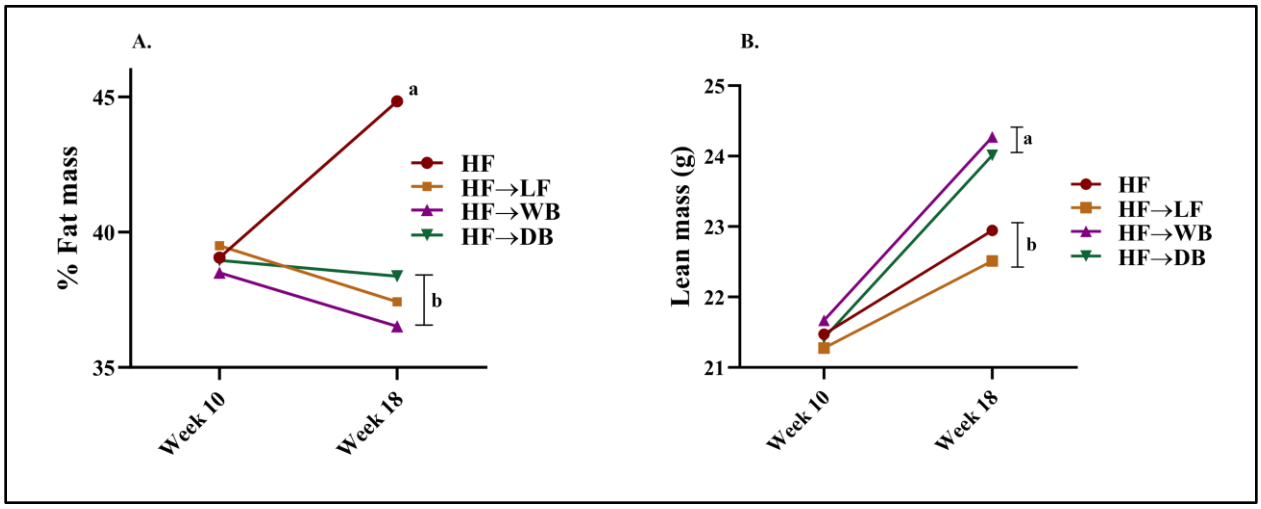

Figure 2-2. Body Composition at 10 and 18 Weeks. A. Fat mass as a percentage of body weight (% fat mass), B. Lean mass (g). Values were independently compared between groups before initiating the intervention at week 10 and after the study termination at week 18 using One-way ANOVA, followed by the Newman-Keuls multiple comparisons test. Values are displayed as mean±S.E.M. SEM (n=12/ dietary group). Body composition differences at the end of the week 18 are shown with a lower-case letter on the respective connecting lines, values not sharing a lowercase letter are considered significantly different ($p<0.05$). HF: High-fat diet fed group, HF→LF: High-fat to low-fat diet transition group, HF→WB: High-Fat to low fat + white kidney beans diet transition group, HF→DB: High-fat to low-fat + dark-red kidney beans diet transition group.

3.2 Fecal Microbial Community Structure

Stool samples have been extensively utilized in numerous human studies, making the analysis of mice fecal microbiota highly informative for potential translation to the human gut microbiome. This section presents a comprehensive examination of the gut microbial community structure in mice fecal samples.

3.2.1. High-fat Diet Induces fecal microbial Dysbiosis

To evaluate the impact of the LFD and HFD on the microbiota structure, microbial richness, evenness, and abundance, α-diversity was analyzed. Among the α-diversity indices examined, including Shannon diversity, observed species, and evenness, no significant differences were observed between the two groups (Data not shown). However, Faith's PD was significantly reduced in the HFD-fed obese mice compared to the LFD-fed lean group **(Figure 2-S1A)**. Analysis of β-diversity, conducted using PCoA based on Bray Curtis distance matrices, clearly demonstrated a distinct separation between the HF and LF groups **(Figure 2-S1B)**, indicating a significant influence of diet composition on gut microbiota dysbiosis. Furthermore, the analysis of feces microbiota composition revealed a total of eight phyla across LF and HF groups (**Figure 2-S1C**) with Firmicutes and Bacteroidetes as the dominant phylum. No significant difference was observed at the phylum level between LF and HF groups. However, at the genus (g) level (**Figure 2-S1D**), comparing the lean LF mice to obese HF mice, we observed significant differences in the relative abundance of certain bacterial members. Notably, the obese HF mice showed a lower relative abundance of *Papillibacter* (g) from the Firmicutes phylum, along with *Prevotella* (g) and *S24-7* (f), both belonging to the Bacteroidetes phylum, known as carbohydrate-fermenting bacteria [63,64]. Conversely, there was a significant increase in relative abundance of *Clostridium* (g) and

Clostridiales (o), both from the Firmicutes phylum in the HF group when compared to the lean mice **(Figure 2-S2)**.

3.2.2 Low fat and bean supplement Intervention Diets Improve the obese dysbiotic fecal microbial Composition and Function

3.2.2.1 Fecal Microbiota Diversity

As shown **Figure 2-3A-D**, Pielou's Evenness and Shannon diversity reduced in both bean-fed mice compared to the HF, and HF→LF groups. Conversely, no significant differences were found in Observed Features and Faith's PD among groups. Microbiota β-diversity visualization using PCoA of Bray-Curtis distance matrices indicated a very distinct microbiota profile of both the HF→WB and HF→DB groups in comparison to other dietary groups **(Figure 2-3E)**. PERMANOVA analysis of β-diversity distance matrices showed that both bean supplemented groups clustered together with no significant differences from each another, while β-diversity distance matrices differed between all other groups **(Figure 2-3F)**.

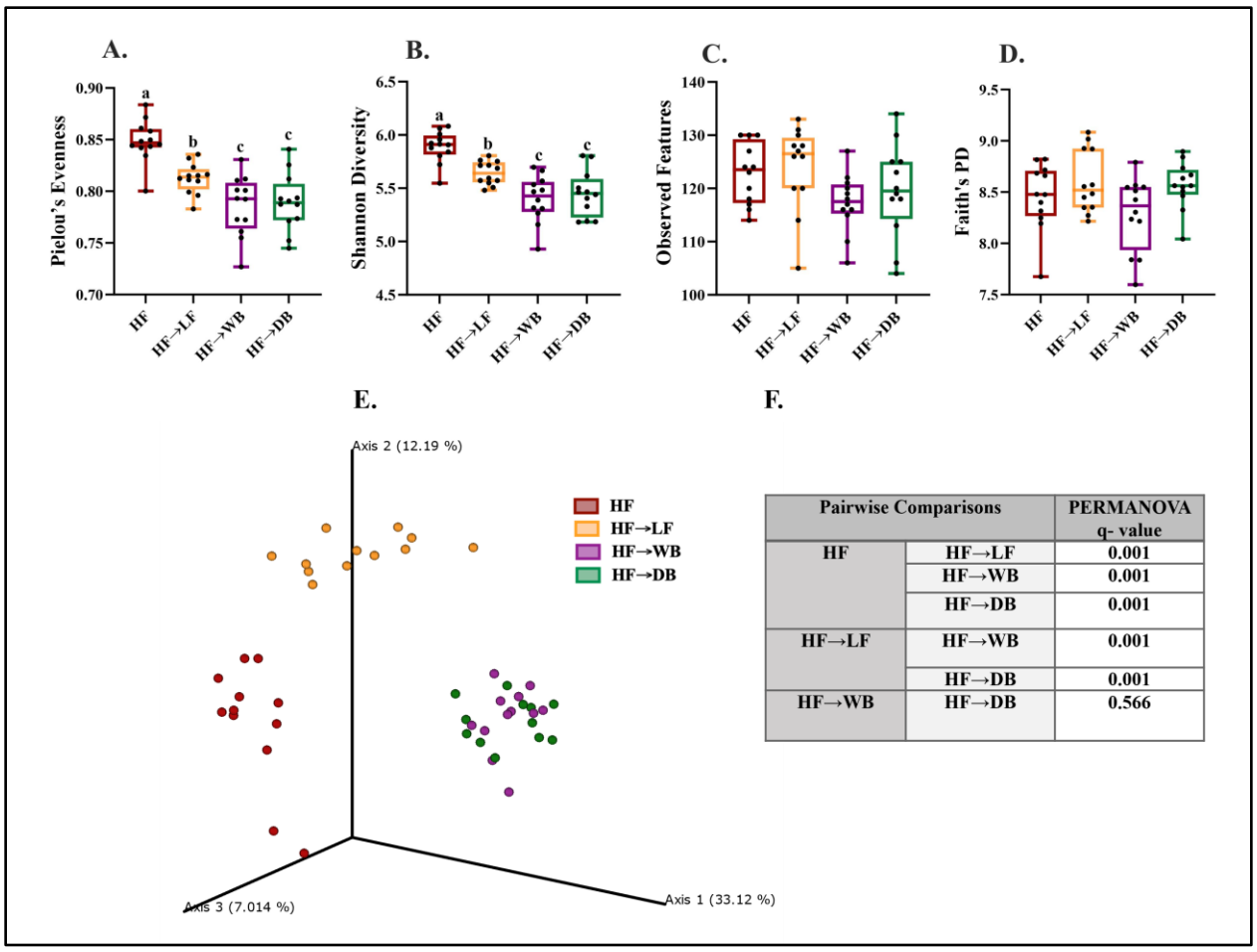

Pairwise Comparisons		PERMANOVA q- value
HF	HF→LF	0.001
	HF→WB	0.001
	HF→DB	0.001
HF→LF	HF→WB	0.001
	HF→DB	0.001
HF→WB	HF→DB	0.566

Figure 2-3. Microbiota α-diversity Metrics. A. Pielou's Evenness, B. Shannon diversity, C. Observed features, D. Faith's phylogenetic diversity (PD) E. Microbiota β-diversity across the diet groups at the ASVs level visualized by principal component analysis (PCoA) of Bray-Curtis distance matrices. The results are shown in a 3D plot, where the three axes, PC1, PC2, and PC3, indicate the distance between bacterial communities. The microbial communities of samples from each of the intervention groups, including HF, HF→LF, HF→WB, and HF→DB, were clustered together based on their respective diets. Each dot in the plot represented a mouse bacterial community, and each color represented a different dietary group. The percentage of variation in the data set explained by each principal coordinate was shown in brackets. F. Permutational Multivariate Analysis of Variance (PERMANOVA) pairwise comparisons q-values. Kruskal-Wallis test was used to analyze the α-diversity data. Adjusted P value (q-value<0.05) was computed following the Benjamini-Hochberg procedure. The plots that did not share a lowercase letter were significantly different. The differences in β-diversity data were analyzed by the permutational multivariate analysis of variance using distance matrices (PERMANOVA), p-value=0.001. (n=12/ groups). HF: High-fat diet fed group, HF→LF: High-fat to low-fat diet transition group, HF→WB: High-Fat to low fat + white kidney beans diet transition group, HF→DB: High-fat to low-fat + dark-red kidney beans diet transition group.

3.2.2.2 Fecal Microbiota Composition

The taxonomic composition of fecal microbiota from all the different dietary groups is shown in **Figure 2-4A-C** and **Table 2-2**. Similar to the observed differences in microbiota composition between LF and HF group **(Figure 2-10-(S1))**, transitioning mice to a LFD resulted in higher relative abundance of *Papillibacter* (g), *Prevotella* (g) and and *S24-7* (f), while the relative abundance of *Clostridium* (g) and *Clostridiales* (o) reduced when compared to the obese control group. Furthermore, some other additional alterations included a reduced presence of certain bacterial groups, such as Deferribacteres (*Mucispirillum* (g)) and Firmicutes mainly driven by a reduction in *Ruminococcaceae* (f), *Clostridiales* (another unassigned order), *Defluviitalea* (g), and *Sporobacter* (g). On the other hand, there was an increase in relative abundance of Bacteroidetes primarily driven by *Alistipes* (g) and *Bacteroidales* (o) and Proteobacteria (*Alphaproteobacteria* (c)) in HF→LF when compared to the HFD-fed obese controls (**Table 2-2**).

Furthermore, transitioning from HFD to LFD, resulted in significant reduction of Firmicutes/Bacteroidetes ratio across all DIO mice fed with LFD with/without beans supplementation when compared to the HF controls. Importantly, there were no additional alterations induced by diets incorporating beans in this ratio. However, as expected and consistent with the distinct differences observed in the microbiota β-diversity distances in bean-supplemented groups, both varieties of beans, exerted more profound changes in the fecal microbial structure compared to the HF mice. In addition to the above mentioned altered fecal bacterial composition induced by transitioning from HFD to LFD, both varieties of beans, regardless of seed coat color, reduced the abundance of TM7 (F16 (f)), *Parabacteroides* from Bacteroidetes, as well as *Ruminococcaceae* (f) and *Dorea*, both of which belonging to Firmicutes phylum, when compared to HF obese mice. Conversely, bean-incorporated diets resulted in an increase in relative

abundance of *Rikenellaceae* (f) from Bacteroidetes, *Clostridium* (g *(methylpentosum* species (s)), *Lactobacillus* (g) and *Lachnospiraceae* (f), all belonging to Firmicutes, in comparison to mice in HF group. Although similar alterations were observed on the fecal microbiota community structure by bean diets, few bacterial taxa changed differently compared to the HF group. In the HF→WB group, the relative abundance of bacterial genera *Parabacteroides* from Bacteroidetes and *rc4-4* from Firmicutes decreased, while there was a higher relative abundance of *Bacillaceae* (f), *Alphaproteobacteria* (c) and *Lactobacillales* (o) from Firmicutes compared to the HF mice. In comparison to HF controls, there was a reduction in relative abundance of Actinobacteria (*Paraeggerthella* (g)) and *Papillibacter* (g) in both HF→LF and HF→DB groups, but this reduction was not observed in HF→WB. In addition, there was an exclusive higher relative abundance of *Enterobacteriaceae* (f) from Proteobacteria in HF→DB compared to the HF mice (**Table 2-2)**.

Both bean diets increased the relative abundance of *Clostridium* (g (*Methylpentosum* (s)), *Prevotella* (g), and *Rikenellaceae* (f), while concurrently led to a decrease in the relative abundance of *Alistipes* (g), *Papillibacter* (g), *Dorea* (g), *Parabacteroides* (g), and *Ruminococcaceae* (f). Additionally, compared to HF→LF group, the relative abundance of rc4-4 and *Clostridium* (unassigned species) reduced by HF→WB and HF→DB, respectively **Table 2-2**.

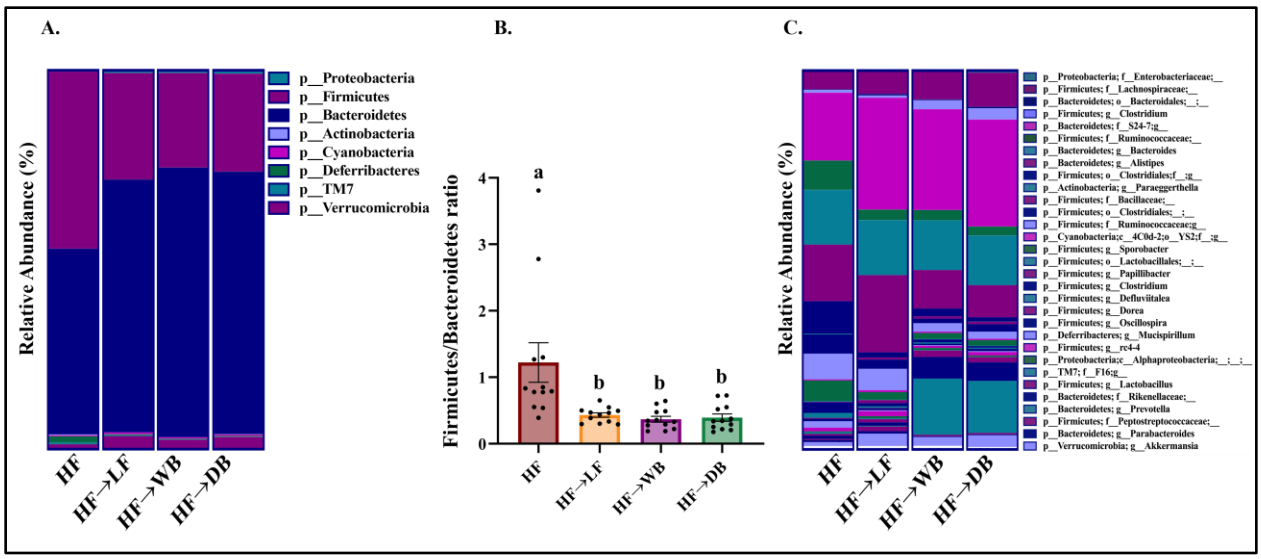

Figure 2-4. Taxonomic Structure of Fecal Microbiota. A. Taxonomic relative abundance of fecal microbiota at the phylum level (p), **B.** Firmicutes/Bacteroidetes ratio, Values are displayed as means±S.E.M. Data was analysed by Kruskal-Wallis test followed by Dunn's multiple comparisons test. **C.** Taxonomic relative abundance of fecal microbiota at the genus level (g) (labels show microbiota taxa composition according to the phyla and genus where applicable, or the family (f)/order (o) for the unclassified genera), (n=12/ groups). HF: High-fat diet fed group, HF→LF: High-fat to low-fat diet transition group, HF→WB: High-Fat to low fat + white kidney beans diet transition group, HF→DB: High-fat to low-fat + dark-red kidney beans diet transition group.

Table 2-2. Relative abundance of the fecal microbiota at the phyla and genus levels

Taxonomy	Relative abundance (%)			
	HF	**HF→LF**	**HF→WB**	**HF→DB**
p-Firmicutes	46.76±4.11	28.14±1.37[1]	24.98±2.15[1]	25.88±2.76[1]
f__Bacillaceae;__	0.00±0.00	0.57±0.27	0.61±0.29[1]	0.63±0.31
f__Lachnospiraceae;__	4.90±0.91	6.10±0.73	7.54±0.98[1]	9.05±1.54[1]
f__Peptostreptococcaceae;__	0.35±0.15	1.22±0.55	0.38±0.10	0.39±0.11
f__Ruminococcaceae;__	7.74±0.87	2.81±0.36[1]	2.73±0.46[1]	2.39±0.39[1]
f__Ruminococcaceae;g__	6.78±0.67	5.72±1.03	2.25±0.46[1, 2]	1.88±0.34[1, 2]
g__Clostridium (;s__methylpentosum)	0.77±0.17	0.65±0.19	2.41±0.45[1, 2]	2.97±0.59[1, 2]
g__Clostridium	2.89±0.16	0.87±0.11[1]	0.80±0.18[1]	0.44±0.10[1, 2]
g__Defluviitalea	1.31±0.25	0.40±0.05[1]	0.35±0.06[1]	0.33±0.08[1]
g__Dorea	0.27±0.08	0.14±0.04	0.01±0.01[1, 2]	0.01±0.01[1, 2]
g__Lactobacillus	0.49±0.13	0.87±0.28	1.75±0.0.43[1]	1.43±0.25[1]
g__Oscillospira	0.68±0.16	0.56±0.13	0.46±0.10	0.62±0.17
g__Papillibacter	0.14±0.05	0.82±0.23[1]	0.05±0.03 [2]	0.01±0.01[1, 2]
g__rc4-4	1.02±0.11	1.39±0.24	0.59±0.14[1, 2]	0.91±0.15
g__Sporobacter	5.47±0.94	2.02±0.37[1]	1.61±0.25[1]	1.48±0.23[1]
o__Clostridiales;__;__	5.12±0.74	2.42±0.59[1]	1.22±0.32[1]	2.00±0.38[1]
o__Clostridiales;f__;g__	8.60±1.71	1.44±0.41[1]	2.07±0.76[1]	1.19±0.20[1]
o__Lactobacillales;__;__	0.22±0.04	0.14±0.01	0.14±0.03[1]	0.15±0.3
p-Bacteroidetes	49.03±4.27	66.78±1.99[1]	71.17±2.46[1]	69.30±2.40[1]
f__Rikenellaceae;__	0.85±0.10	0.91±0.13	5.78±0.53[1, 2]	4.90±0.51[1, 2]
f__S24-7;g__	17.92±1.53	29.52±1.28[1]	26.64±1.29[1]	28.25±1.64[1]
g__Alistipes	15.00±1.70	20.42±1.50[1]	10.17±1.05[1, 2]	8.49±0.59[1, 2]
g__Bacteroides	14.46±1.40	14.54±1.17	13.17±1.26	13.17±0.93
g__Parabacteroides	0.60±0.10	0.72±0.15	0.25±0.05[1, 2]	0.24±0.04[1, 2]
g__Prevotella	0.02±0.01	0.21±0.03[1]	14.87±1.26[1, 2]	13.77±1.19[1, 2]
o__Bacteroidales;__;__	0.19±0.03	0.44±0.11[1]	0.28±0.02[1]	0.47±0.13[1]
p-Deferribacteres	1.73±0.59	0.25±0.07[1]	0.18±0.06[1]	0.226±0.07[1]
g__Mucispirillum	1.73±0.59	0.25±0.07[1]	0.18±0.06[1]	0.226±0.07[1]
p-Proteobacteria	0.36±0.10	0.74±0.12[1]	0.75±0.15[1]	0.93±0.22[1]
f__Enterobacteriaceae;__	0.08±0.02	0.16±0.05	0.18±0.09	0.55±0.24[1]
c__Alphaproteobacteria;__;__;	0.29±0.10	0.58±0.11[1]	0.57±0.13[1]	0.38±0.08
p-TM7	0.45±0.07	0.24±0.08	0.15±0.05[1]	0.09±0.02[1]
p__TM7; f__F16;g__	0.45±0.07	0.24±0.08	0.15±0.05[1]	0.09±0.02[1]
p-Verrucomicrobia	1.08±0.34	3.28±1.36	2.35±0.73	3.09±1.05
g__Akkermansia	1.08±0.34	3.28±1.36	2.35±0.73	3.09±1.05
p-Cyanobacteria	0.35±0.07	0.53±0.10	0.37±0.12	0.37±0.13
o__YS2;f__;g__	0.35±0.07	0.53±0.10	0.37±0.12	0.37±0.13
p__Actinobacteria	0.23±0.06	0.04±0.01[1]	0.04±0.02[1]	0.07±0.02[1]
g__Paraeggerthella	0.23±0.06	0.04±0.01[1]	0.04±0.02[1]	0.07±0.02[1]

Relative abundance (mean±S.E.M.) of cecal bacterial taxa at the phylum level (rows highlighted in grey), or the corresponding order (o), family (f), or genus level (g) (white rows). The data analysed by Mann-Whitney test followed by a two-stage linear step-up procedure of Benjamini, Kreiger and Yekutieli to correct for multiple comparisons (corrected p-value<0.05; FDR<5%) (n=12/groups) to compare HF vs HF→LF, HF→WB and HF→DB; HF→LF vs HF→WB and HF→WD; and HF→WB vs HF→DB. Significantly different values are indicated by [1, 2]superscripts. [1] Significantly different from the HF group; [2] Significantly different from HF→LF. HF: High-fat diet fed group, HF→LF: High-fat to low-fat diet transition group, HF→WB: High-Fat to low fat + white kidney beans diet transition group, HF→DB: High-fat to low-fat + dark-red kidney beans diet transition group.

3.3 Fecal Microbial Community Function

3.3.1 Fecal pH and Short-Chain Fatty Acids

Fecal pH showed a reduction in both bean supplemented groups compared to other groups with no difference from each other **(Figure 2-5B)**. In accordance with the fecal pH results, concentrations of individual SCFAs including acetic acid, propionic acid, butyric acid, as well as total SCFAs increased in beans fed mice compared to other groups **(Figure 2-5A)**. Despite a greater level of SCFAs in HF→WB, only butyric acid reached significant levels compared to that in HF→DB. Fecal valeric acid concentrations increased in HF→WB in relation to the both HF and HF→LF group, with no further difference compared to the HF→DB. Fecal concentrations of branched-chain fatty acids (BCFAs), including Iso-butyric acid, Iso-valeric acid, and total BCFAs did not reveal any difference between groups **(Figure 2-5A)**. Notably, as shown in **Figure 2-5C**, a significant positive correlation was found between Total SCFAs and lean mass ($r=0.48$, $p=0.007$).

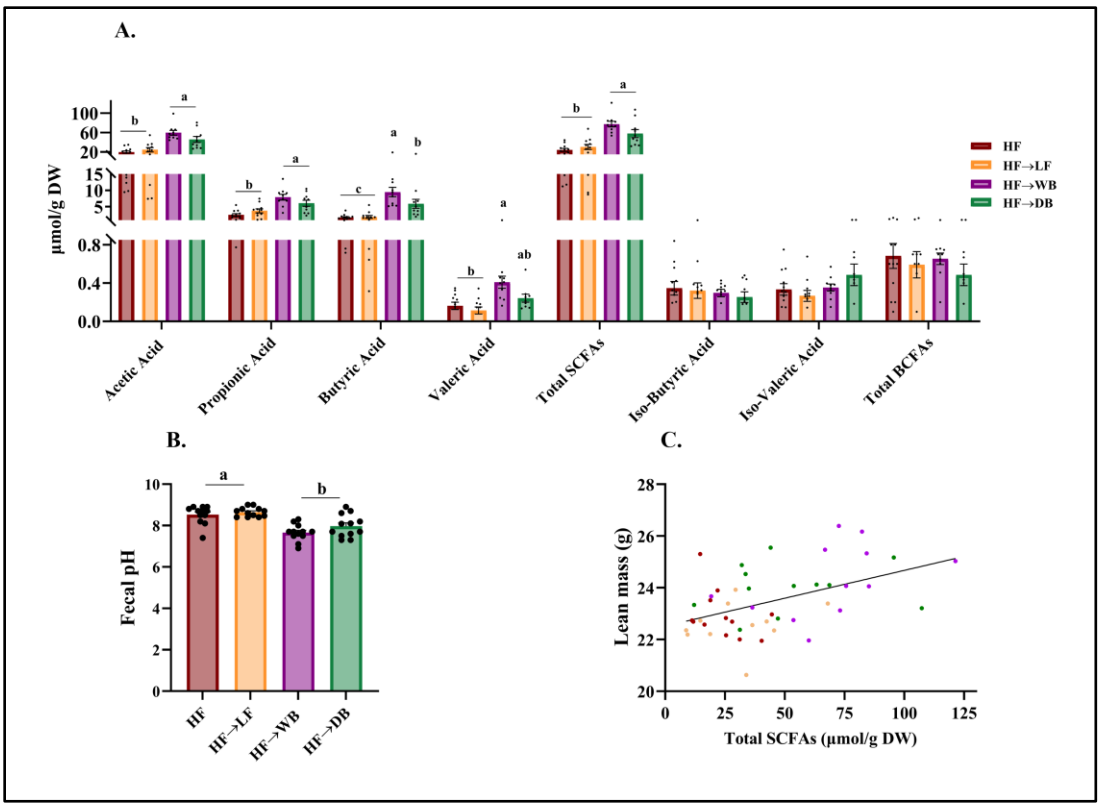

Figure 2-5. Analysis of Fecal Short-chain Fatty Acids (SCFAs). A. Short-chain fatty acid (SCFAs) and Branched-chain fatty acid BCFAs, µmol/g DW, **B.** Fecal pH**, C.** Linear regression and Pearson's correlation coefficient relationship between Total SCFAs (µmol/g DW) and Lean mass (g). Values are displayed as means±S.E.M. (n=12/groups). Parametric data (including fecal pH, Iso-Butyric Acid, Total BCSFAs) was analysed by One-way ANOVA followed by Newman-Keuls multiple comparisons test and non-parametric data was either log-transformed to normalize, followed by performing the ANOVA (including Acetic Acid, Propionic Acid, Butyric Acid and Total SCFAs), or analysed by Kruskal-Wallis test (Valeric and Iso-Valeric Acids) followed by Dunn's multiple comparisons test. Bars not sharing a lower-case letter are significantly different ($p<0.05$). HF: High-fat diet fed group, HF→LF: High-fat to low-fat diet transition group, HF→WB: High-Fat to low fat + white kidney beans diet transition group, HF→DB: High-fat to low-fat + dark-red kidney beans diet transition group.

3.3.2 Functional Metagenome Prediction Analysis

PICRUSt2 results, visualized by STAMP, revealed differential predicted metagenomic functional pathways in microbial populations among the dietary groups. Overall, HF→LF resulted in 193 significantly different pathways when compared to the HF control. Introducing beans increased the number of differences in the inferred bacterial metagenomic pathways compared to the HF control. While no significant differences were found in the bacterial predicted metagenomic functional pathways between the beans supplemented groups, HF→DB derived greater impacts

on the functionality of the microbiota by inducing 204 significantly different functional pathways, compared to 195 pathways in HF→WB when compared to the HF group **(Figure 2-6A-C)**.

Venn diagram analysis revealed a total of 63 shared pathways were overrepresented in HF→LF, HF→WB and HF→DB groups, compared to the HF group **(Figure 2-6D)**. Most notably this included PPAR signalling, adipocytokine signalling, thermogenesis, apoptosis, lysosome, protein digestion and absorption, and LPS biosynthesis pathways. Conversely, a total of 51 pathways were underrepresented in the HF→LF, HF→WB and HF→DB groups, compared to the HF group, **(Figure 2-6E)**, including Flagellar assembly, bacterial chemotaxis, bacterial motility proteins, NOD-like receptor signalling, glucagon and insulin signalling pathways, transcription factors, two-component system, and fat digestion and absorption.

Additionally, 36 pathways were overexpressed, unique to the bean groups. Notably, there were 6 pathways up-regulated exclusively within the HF→WB group, while an additional 9 pathways demonstrated unique elevation in the HF→DB group, both as relative to the HF control group. In contrast, 25 pathways exhibited reduced representation across the beans supplemented groups. Additionally, in the two-by-two comparison with the HF control, distinct patterns emerged, identifying 7 and 9 unique pathways that were suppressed in the HF→WB, and HF→DB groups, respectively. To provide specific examples, the following pathways were enriched in the HF control group when compared to the bean groups: Fat digestion and absorption, fatty acid biosynthesis pathway, NOD-like receptor signaling pathway, and insulin signaling pathway, while some pathways, such as lipopolysaccharide biosynthesis and a pathway related to protein digestion and absorption were suppressed. Conversely, both bean-supplemented groups demonstrated an enhancement in pathways related to carbohydrate digestion and absorption in comparison to the HF group. Simultaneously, they showed suppressed pathways associated with the metabolism of

predominant essential amino acids found in common beans, such as lysine degradation and valine, leucine and isoleucine biosynthesis. This suppression might be attributed to the high content of these essential amino acids in the beans [65].

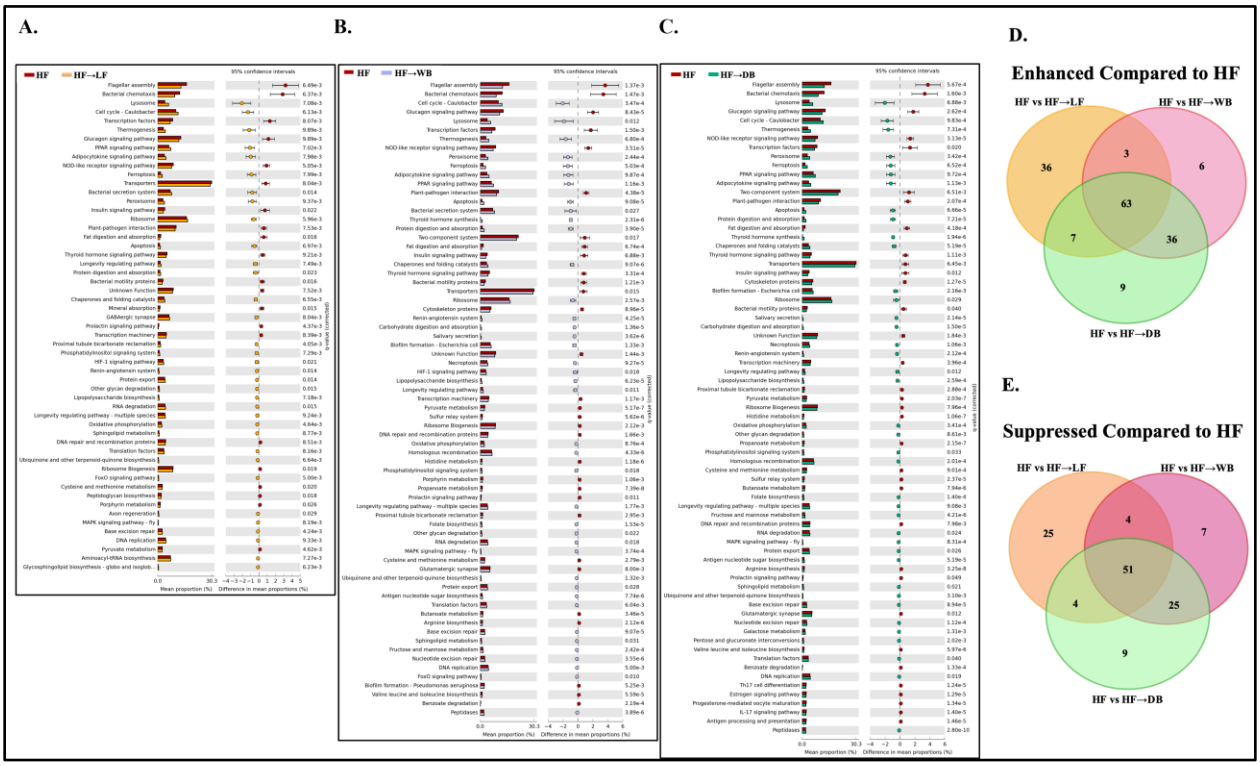

Figure 2-6. Predicted Functional Differences of the Microbial Communities. PICRUSt2 results indicating significantly altered bacterial Kyoto Encyclopedia of Genes and Genomes (KEGG) pathways at level 3 for the following comparisons: **A.** HF vs HF→LF, **B.** HF vs HF→WB, **C.** HF vs HF→DB. To refine the number of active features in the extended error bars, the pathways associated with "Human Diseases" category were excluded. Among the retained pathways, only those with an effect size difference greater than 0.1 are displayed, **D**. and **E.** Venn diagrams displaying the total number of unique and common bacterial functional pathways that were up-regulated and down-regulated in HF →LF, HF →WB, and HF →DB compared to the HF control group, respectively. The PICRUSt2 data was analyzed in STAMP using Welch's two-sided t-test with Benjamini-Hochberg multiple test correction ($q<0.05$), Difference between proportions and ratio of proportion effect size, (n=12/ groups). HF: High-fat diet fed group, HF→LF: High-fat to low-fat diet transition group, HF→WB: High-Fat to low fat + white kidney beans diet transition group, HF→DB: High-fat to low-fat + dark-red kidney beans diet transition group.

3.4 Systemic Endotoxemia, LPS Biosynthesis and Gut Microbiota

Following to the observed up-regulation in the predicted functional pathways associated to LPS biosynthesis in groups transitioning from HFD to LFD in comparison to the HF controls **(Figure 2-6A-C)**, the regression analysis also revealed notable positive correlations between the relative frequency of LPS biosynthesis pathways and the Bacteroidetes and Proteobacteria phyla ($r=0.9$ and $r=0.6$, respectively, $p<0.001$ for both) **(Figure 2-7A-B)**. LBP concentrations did not differ significantly among the dietary groups **(Figure 2-7C)**. Since LPS is mainly known to be associated with gram negative species from Proteobacteria and Bacteroidetes phyla [66], serum LBP levels were then adjusted in relation to the relative abundance of these two phyla. The findings showed a significant reduction in the ratio of LBP in relation to the relative abundance of Bacteroidetes (LBP/ Bacteroidetes RA) by both bean diets when compared to HF, while LBP ratio in relation to the relative abundance of Proteobacteria (LBP/ Proteobacteria RA) reduced only in HF→DB compared with HF **(Figure 2-7D)**.

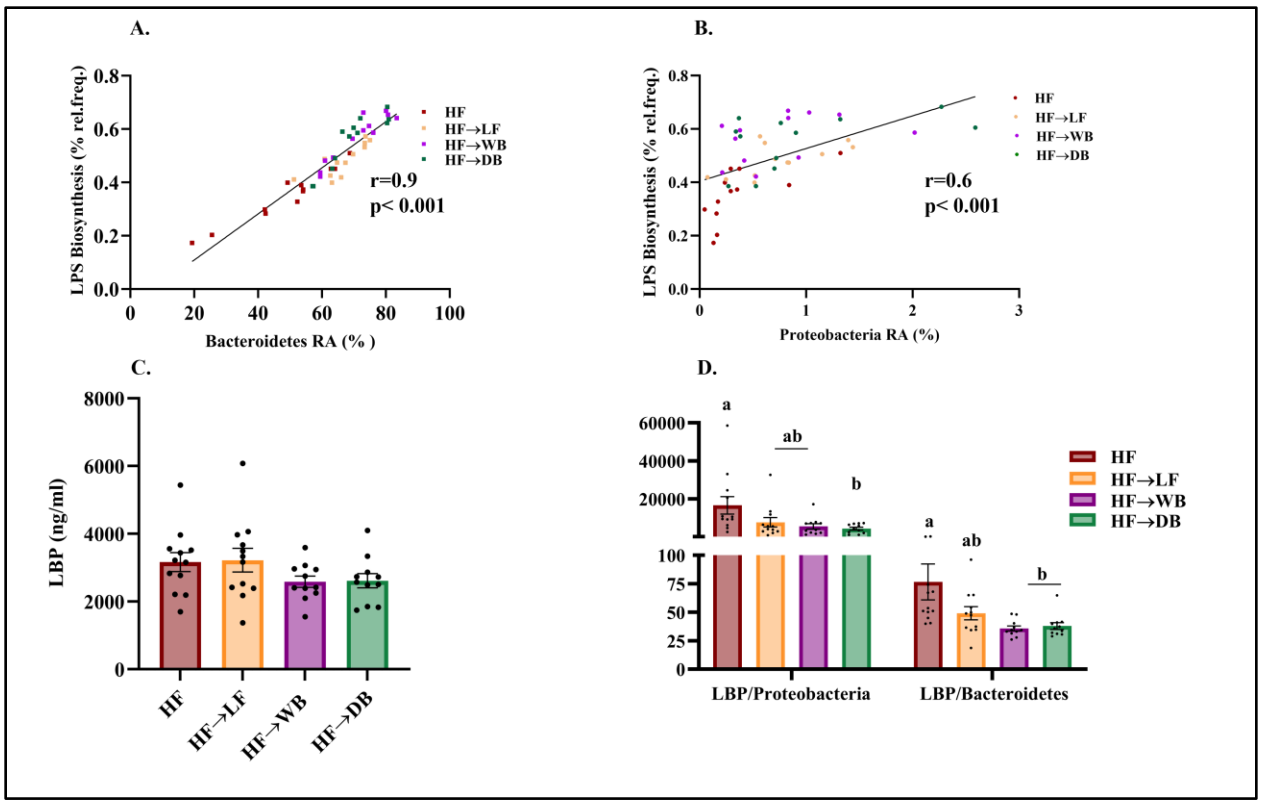

Figure 2-7. Endotoxemia, LPS Biosynthesis and Gut Microbiota. A) Linear regression and Spearman 's correlation coefficient relationship between the relative abundance of Bacteroidetes and lipopolysaccharide biosynthesis pathway. **B.** Linear regression between Proteobacteria and lipopolysaccharide biosynthesis pathway. **C.** Serum LBP levels (ng/ml), **D.** Ratio of LBP levels to the relative abundance of Proteobacteria and Bacteroidetes. In bar graphs, Values are displayed as means±S.E.M. (n=11-12/groups). LBP data was log-transformed to normalize then analysed by One-way ANOVA followed by Newman-Keuls multiple comparisons test. LBP/Bacteroidetes and LBP/Proteobacteria ratios were analysed by Kruskal-Wallis test followed by Dunn's multiple comparisons test. LBP: Lipopolysaccharide binding protein. Bars not sharing a lower-case letter are significantly different ($p<0.05$). HF: High-fat diet fed group, HF→LF: High-fat to low-fat diet transition group, HF→WB: High-Fat to low fat + white kidney beans diet transition group, HF→DB: High-fat to low-fat + dark-red kidney beans diet transition group. LPS: Lipopolysaccharide from the outer membrane of Gram-negative bacteria, LBP: LPS binding protein.

3.5 Dysfunctional adipose tissue markers

3.5.1 Histology

Total EAT weight, as well as the diameter and area of adipocytes in EAT histological sections, were measured as markers of adipose tissue dysfunction. As anticipated, analysis of H&E stained adipocyte images **(Figure 2-8D)** revealed that HFD induced an increase in adipocyte hypertrophy

and the average adipocyte size, quantified by adipocyte diameter and area, compared to HF→LF, HF→WB and HF→DB groups, with no further difference between groups **(Figure 2-8A-C).**

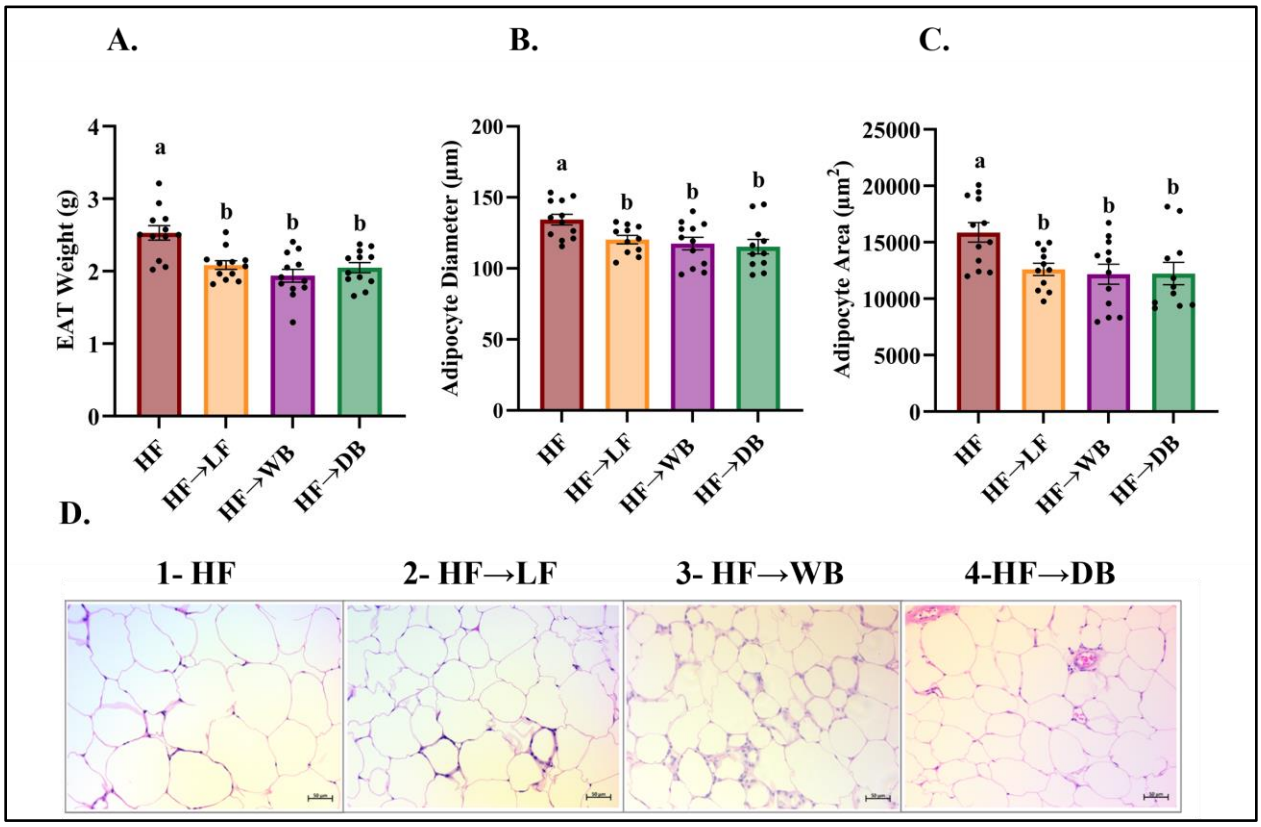

Figure 2-8. Effects of the Dietary Intervention on Fat-pad Weight and Adipocyte Size. A. EAT weight (g), **B.** Adipocyte diameter, **C.** Adipocyte area, **D.** Representative H&E staining of EAT obtained from mice in: 1- HF, 2- HF→LF, 3- HF→WB, 4- HF→DB groups. Bars not sharing a lower-case letter are significantly different**.** Values are presented as means ± S.E.M (n = 11-12/ group). Data was analyzed using One-way ANOVA followed by the Newman-Keuls multiple comparisons test. Statistical significance was set at $p < 0.05$. HF: High-fat diet fed group, HF→LF: High-fat to low-fat diet transition group, HF→WB: High-Fat to low fat + white kidney beans diet transition group, HF→DB: High-fat to low-fat + dark-red kidney beans diet transition group. EAT: epididymal adipose tissue.

3.5.2 Gene Expression of Inflammatory Mediators and SCFA Receptors in Adipose tissue

Dietary intervention did not reveal significant differences in the mRNA expression levels of pro-inflammatory markers TNF-α, IL-6, TLR-4, as well as SCFAs receptors GPR41 and GPR43 in EAT across the studied groups, as depicted in **Figure 2-9.** Conversely, MCP-1 demonstrated the highest expression in HF obese controls, with a significant reduction observed upon transitioning to LFD in other groups.

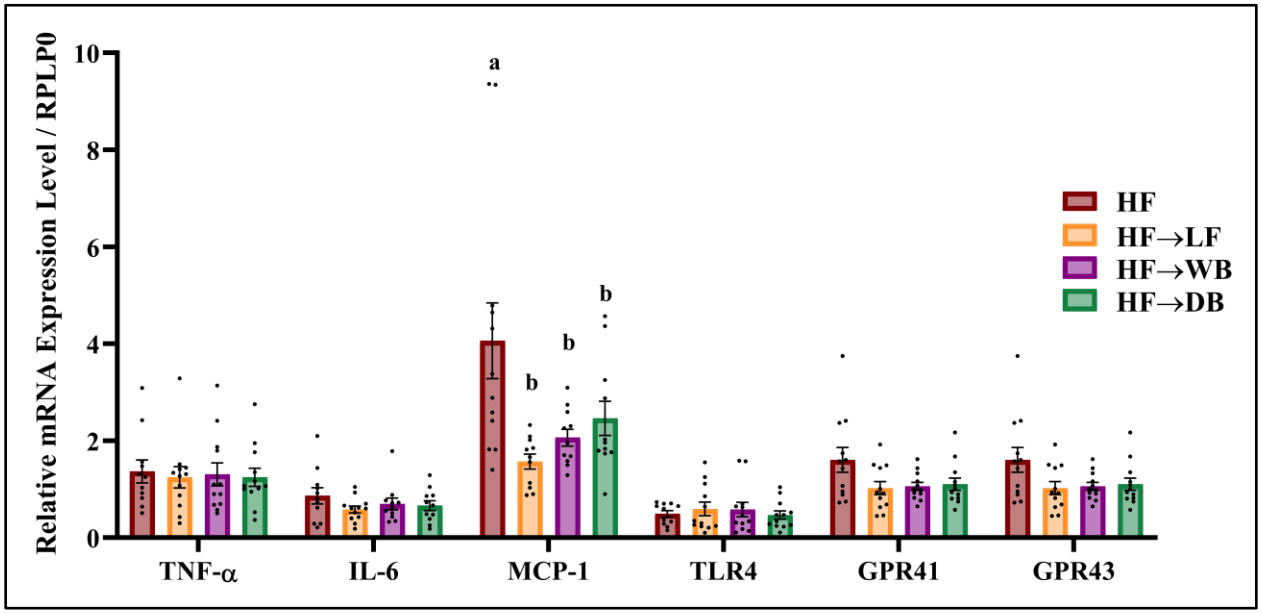

Figure 2-9. Effects of the Dietary Intervention on EAT mRNA Expression of Pro-inflammatory markers and SCFAs receptors. Values are displayed as means±S.E.M. (n=10-12/ groups). Data was log-transformed to normalize then analysed by One-way ANOVA followed by Newman-Keuls multiple comparisons test. Bars not sharing a lower-case letter are significantly different ($p<0.05$). Data related to gene expression of each target gene was normalized to the expression levels of ribosomal protein lateral stalk subunit P0 (RPLP0) as the housekeeping gene. HF: High-fat diet fed group, HF→LF: High-fat to low-fat diet transition group, HF→WB: High-Fat to low fat + white kidney beans diet transition group, HF→DB: High-fat to low-fat + dark-red kidney beans diet transition group. EAT: Epididymal adipose tissue. TNF-α: Tumor Necrosis Factor-alpha, TLR-4: Toll-like receptor 4, IL-6: Interleukin-6, MCP-1: Monocyte Chemoattractant Protein-1, GPR-41: G-protein coupled receptor 41, GPR-43: G-protein coupled receptor 43.

3.6 Serum Metabolic Profile

The effects of our dietary intervention on fasting serum adipokines and biomarkers associated with glucose and insulin homeostasis are presented in **Table 2-3.** There were no

significant differences observed in concentrations of anti-inflammatory adiponectin and pro-inflammatory PAI-I adipokines. However, serum concentrations of other pro-inflammatory adipokines, including Resistin, exhibited a reduction in the HF→DB in contrast to the HF group. Furthermore, leptin levels decreased in HF→LF, HF→WB, and HF→DB groups, when compared to the HF control group. Meanwhile, the adiponectin-to-leptin (Adpn/Lep) ratio, (a recognized functional biomarker of adipose tissue dysfunction that inversely correlates with inflammation [67]), showed a significant reduction in HF compared to other groups. There was no difference in serum concentrations of ghrelin, glucagon, GLP-1, GIP and FBG between dietary groups. Insulin levels reduced significantly in HF→LF and HF→WB when compared to the HF controls, with no significant difference from the HF→DB group. However, there was a significant reduction in HOMA-IR in all mice from the HF→LF, HF→WB, and HF→DB groups in comparison to the HF mice.

Table 2-3. Effects of Dietary Intervention on Serum Adipokines, Glucose and Insulin Homeostasis and Gut Peptides.

Fasting Serum Biomarkers	HF	HF→LF	HF→WB	HF→DB
Adipokine Hormones				
Resistin (pg/mL)	123714± 8795 [a]	97173± 9369 [a]	99836± 8480 [a]	90545± 5988[b]
PAI-I (pg/mL)	2133±170.3	1761±144.8	2389±154.8	2162±152.9
Adiponectin (mg/mL)	42.23±4.12	41.86±4.05	39.96±3.70	37.78±2.62
Leptin (mg/mL)	0.11±0.01[a]	0.03±0.00[b]	0.04±0.01[b]	0.04±0.01[b]
Adpn/Lep	389.9±38.85 [b]	1725±199.1 [a]	1315±285.0 [a]	1207±272.9 [a]
Glucose and Insulin Homeostasis				
Glucagon (pg/mL)	728.26±89.69	615.45±58.62	526.78±52.59	630.59±64.20
GIP (pg/mL)	379.26±89.69	302.56±58.62	374.44±52.59	316.70±64.20
Insulin(pg/mL)	8496.82±724.41 [a]	6388.17±948.86 [b]	5932.40±351.95[b]	6942.09±563.16 [ab]
FBG (mmol/L)	9.17±0.35	8.30±0.24	8.34±0.65	8.84±0.36
HOMA-IR	106.8±10.62 [a]	66.02±8.23 [b]	59.41±5.69[b]	78.26±8.32[b]

Gut Peptides				
Ghrelin (pg/mL)	6819.75±717.82	7455.92±962.25	6563.33±531.23	5940.08±308.63
GLP-1 (pg/mL)	129.41±29.40	95.19±24.26	90.20±30.19	95.61±29.70

Values are displayed as mean±S.E.M. (n=10-12/group). Parametric data (including Resistin, PAI-I, Adiponectin, GIP and Glucagon) were analysed by One-way ANOVA followed by Newman-Keuls multiple comparisons test and non-parametric data either was either log-transformed to normalize (including Ghrelin, GLP-1, Leptin, Adpn/Lep and HOMA-IR) followed by performing the ANOVA or analysed by Kruskal-Wallis test (Insulin andFBG) followed by Dunn's multiple comparisons test. Values that do not share a lowercase letter are significantly different ($p<0.05$). HF: High-fat diet fed group, HF→LF: High-fat to low-fat diet transition group, HF→WB: High-Fat to low fat + white kidney beans diet transition group, HF→DB: High-fat to low-fat + dark-red kidney beans diet transition group. PAI-Plasminogen Activator Inhibitor-1, Adpn/Lep=Adiponectin-to-Leptin ratio, FBG=Fasted-blood glucose, GIP=Glucose-dependent insulinotropic polypeptide HOMA-IR=Homeostatic Model Assessment of Insulin Resistance. GLP-1: Glucagon-like Peptide-1.

4. Discussion

Interventions to treat obesity often include diet modifications (e.g., calorie-restriction, low-fat diets), which have been shown to stimulate weight loss and metabolic homeostasis [5,6], reduce inflammation [6,8], improve intestinal barrier function [6,9], and alter the composition and function of the intestinal microbiome [10–12]. Importantly, studies in which weight-loss strategies are concurrent with adjuvant therapies designed to target the gut microbiome (e.g., prebiotics (inulin, oligosaccharides, polyphenols), probiotics, synbiotics), often result in better health outcomes compared to calorie-restriction alone [13–15,68]. Previously, we and others have demonstrated in rodent models, that consumption of HFD supplemented with dietary pulses, in particular common beans, beneficially impact the intestinal microbiome during the development of HFD-induced obesity [32], as well as in mice with established obesity [69]. On the other hand, the impact of bean consumption concurrent with weight-loss interventions (e.g. reduced calorie diet) on the microbiome and obesity-associated metabolic dysfunctions has not been investigated. In the study reported herein, we aimed to determine in mice with established HFD-induced obesity, if switching to a low-fat diet supplemented with cooked common beans would result in beneficial changes to the fecal microbiome and metabolic health, more so than low-fat diet alone. We further aimed to investigate whether consumption of dark red kidney beans, which is considered a

polyphenol-rich variety of common beans [44], could have additional positive impacts compared to white kidney beans.

Overall, our findings show that in obese mice, switching the mice to a low-fat kidney bean supplemented diet induced 1) alterations to the fecal microbial community structure and function, 2) improvements in body composition (enhanced lean mass), and 3) dark red kidney bean induced improvement in serum resistin concentrations.

Pre-clinical rodent models of obesity mimic aspects of obesity development in humans, enabling a comprehensive exploration of obesity-linked pathways [35,70] and novel therapeutic dietary approaches with translational implications to humans [71]. Excessive dietary fat intake is linked to obesity exacerbation and the development of obesity-associated metabolic dysfunction [72]. Our findings indicated that transitioning from a HFD to a LFD diet limited weight gain in HF→LF mice, whereas bean-supplemented diets only mitigated weight gain compared to the HF controls **(Figure 2-1A-B).** These findings contrast with existing literature where DIO mice exhibited weight loss when shifting from high-fat to low-fat diets [73–75]. It is important to note that even the age-matched lean mice, without prior DIO exposure, gained weight during the study, preventing speculation about weight loss in HF→LF, HF→WB, or HF→DB mice with established obesity phenotype. On the other hand, although it is controversial, systematic reviews reported greater weight loss with dietary pulse interventions, especially when combined with energy-restricted diets [76,77]. In our study, mice were not subjected to an intentional energy restriction, as they had *ad libitum* access to food. However, the cumulative calorie intake varied significantly among groups during the intervention (**Figure 2-1D)**, explaining differences in body weights among the dietary groups.

Concurrently, consumption of bean-enriched diets led to increased microbial fermentation activity as indicated by elevated fecal SCFAs. These SCFAs could potentially provide an additional source of energy and result in subsequent weight gain [78,79]. Additionally, the increased body weight by beans supplemented diets could be partially explained by increased lean mass in the respective groups. These results are aligned with prior research that reported increased muscle mass by HFD supplemented with SCFAs [80,81] or prebiotics in obese mice [82]. Similarly, the findings of a cross-sectional study confirmed the presence of a significant positive association between fiber intake with increased body lean mass [83]. SCFAs are assumed to be as mediating factors that have the potential to establish a link between gut microbiota and skeletal muscle [84] evidenced by studies in which diet-incorporated butyrate preserved the muscle mass in HF-fed DIO mice [80,81] or prevented muscle atrophy in aged mice under an LFD [85]. Our findings also showed a slightly greater lean mass in HF →WB **(Figure 2-2B),** which aligns with higher concentrations of fecal butyric acid compared to that in HF →DB **(Figure 2-5B)**.

Consumption of beans incorporated diets regardless of the bean variety, enhanced growth of specific bacterial taxa likely responsible for breakdown and fermenting of NDCs including *Lachnospiraceae* (f), *Prevotella* (g), *Lactobacillus (g)*, and *Rikenellaceae* (g) **(Table 2-2)**. Increased *Rikenellaceae* abundance correlated with enhanced visceral adipose tissue, improved metabolic profile, reduced oxidative stress [86], and alleviated inflammatory bowel disease symptoms [87]. Conversely, bean diets suppressed *Alistipes*, *Dorea*, *Papillibacter, and Parabacteroides genera* **(Table 2-2)**, which among them some are linked to obesity, inflammation and chronic diseases [88–95]. Given that each genus could consist of various species with different metabolic functions, understanding the relationship between the gut microbial genera and human health and diseases might be complicated and need further investigation.

Gut microbiota changes induced by WB and DB align with previous studies, where alterations in gut microbiota were induced by navy bean supplementation during both obesity development [32] and established obesity [69], or by increasing doses of WB in male and female mice with an obese phenotype [88]. Our findings in particular are consistent with the gut microbiota changes in the latter study with male mice fed a diet enriched in 17.5 % of WB, which was closest to the dosage consumed in our study, implying dose and sex differences in responses [88]. Concomitants to improved intestinal microbiota composition induced by beans, metagenomic functions of microbiota were also differently changed by both bean types as compared to the obese control groups **(Figure 2-6)**. It is noteworthy that the HF group exhibited enhanced fat digestion and absorption pathway compared to other groups, which is in-line with their high-fat diet content, while carbohydrate digestion and absorption pathway enhanced by bean-supplemented groups compared to HF group, which is in-line with higher dietary carbohydrate content and increased NDCs fermentation. These findings emphasize the dietary influence on metabolic pathways and underscore distinct responses to macronutrient composition.

Obesity triggers the recruitment of immune cells, particularly monocyte-derived macrophages, into the various tissues, with adipose tissue being as a major source of inflammatory mediators [96]. Our findings revealed that adipose tissue mRNA expression of pro-inflammatory cytokines like MCP-1, was suppressed in all DIO mice transitioned to be fed by LFD, when compared to the HF obese controls with no additional effects of beans **(Figure 2-9)**. This aligns with the results of some other experimental studies demonstrating reduced pro-inflammatory cytokine expressions in adipose tissue after calorie restriction [97,98] or low-fat diets [99], indicating amelioration of macrophage infiltration in adipose tissue [75,100]. Further, the observed suppression of adipocyte hypertrophy compared to the obese controls **(Figure 2-8)** implies an

alleviation of obesity-associated dysfunction in adipose tissue for all groups transitioned from HFD to LFD. . This suggests that gene expression of inflammatory markers is influenced by the levels of fat accumulation in adipose tissue, as the EAT weight was significantly greater in obese control mice but did not differ among any of the HF→LF, HF→WB, and HF→DB groups with comparable amounts of the associated fat pad weight. Overall, beans did not have a pronounced effect on adipocyte hypertrophy, which contrasts with findings from a study where 5% cooked adzuki bean (red beans rich in polyphenols) supplementation effectively inhibited the increase of adipocyte size during obesity development [101], and a parallel effect was observed in mice fed WB but at a higher dose of 40% [102].

Beyond the alterations that occurred in the intestinal microenvironment and adipose tissue, transitioning obese mice to consume LFD induced changes in systemic metabolic and inflammation-associated hormones, which is similar to previous reports [73,75,97,100,103,104]. These changes were characterised by lower levels of leptin, insulin resistance and higher Adpn/Lep when compared to the HF control mice. Notably, the consumption of beans had no additional impact, except for the reduction in Resistin induced by DB **(Table 2-3)**. Moreover, DB despite having a higher phenolic profile, did not induce a pronounced difference with respect to other systemic and metabolic obesity-associated outcomes when compared to WB. This might be due to the impacts of thermal processing methods (cooking or steaming) on reducing the bioavailability of total polyphenols, especially flavonoids and isoflavones, contents of dark beans and decreasing their antioxidant activity [101,105]. This is in contrasts with the lower GIP, leptin, glucagon and index of insulin resistance in high-fat black bean fed mice, as reported elsewhere [29]. The discrepancy observed in the research findings could be attributed to multiple factors, including differences in diet composition and supplementation level, obesity status prior to the intervention

commencement and the specific disease models utilized. A systematic review of randomized controlled trials focusing on pulses intake and potential health benefits, reported improved insulin resistance and inflammation biomarkers when coupled with the moderate calorie-restricted diets resulting in weight-loss [106]. But, as mentioned earlier, all groups of mice in the current study had unrestricted access to their respective diets. This resulted in higher food intake in the bean-supplemented groups, possibly due to the increased palatability of diets containing beans, which could have influenced the metabolic responses. Therefore, a notable limitation of this study is the absence of pair-feeding food access after transitioning from HFD to LFD, potentially impacting weight alterations and other outcomes. Additionally, in this study only male mice were included, therefore, use of females in designing future studies are recommended.

In summary, this study showed that common beans, regardless of the bean variety, effectively modulated gut microbiota community and reversed the dysbiosis in established obese mice. While transitioning to a low-fat diet had the greatest impact on recovering adipose tissue inflammation and insulin resistance, it is worth noting that incorporating beans into the diet also led to significant increases in lean mass and fecal SCFAs concentrations.

Supplementary Materials

Table 2-4 (S1). Cooked white and dark red kidney bean powder macronutrient composition.

	WK powder (g/100g DW)	DK powder (g/100g DW)	Method
Protein	23.22	22.49	AOAC 992.15
Fat	1.38	1.41	AOAC 922.06, 933.05
Carbohydrate	67.8	66.0	Calculated by difference
Available Carbohydrate	39.1	38.8	Calculated by difference: carbohydrate -total fibre
Total Fiber	28.7	27.2	AOAC 991.43, 985.29
Soluble Fiber	7.2	6.2	AOAC 991.43(mod)
Insoluble Fiber	21.5	21	Calculated by difference: total fiber-soluble fiber
Ash	4.2	4.3	AOAC 923.03
Moisture	5.2	4.0	AOAC methodology
Energy (kcal)	311.9	319.6	Calculated

WK: White kidney beans, DK: Dark-red kidney beans

Table 2-5(S2). Forward and reverse primer sequences utilized for Real-Time Quantitative Reverse Transcription PCR (qRT-PCR).

Target gene	Forward Primer (5'-3')	Reverse Primer (5'-3')
RPLP0	ACTGGTCTAGGACCCGAGAAG	TCCCACCTTGTCTCCAGTCT
TNF-α	CATCTTCTCAAAATTCGAGTGACAA	TGGGAGTAGACAAGGTACAACCC
IL-6	AACGATGATGCACTTGCAGA	GAGCATTGGAAATTGGGGTA
MCP-1	GCCTGCTGTTCACACAGTTGC	CAGGTGAGTGGGGCGTTA
TLR-4	AGAAAATGCCAGGATGATGC	CTGATCCATGCATTGGTAGGT
GPR-41	GTGACCATGGGGACAAGCTTC	CCCTGGCTGTAGGTTGCATT
GPR-43	GGCTTCTACAGCAGCATCTA	AAGCACACCAGGAAATTAAG

LF: Low-fat diet fed lean control group, HF: High-fat diet fed group, RPLP0-TNF-α: Tumor Necrosis Factor-alpha, IL-6: Interleukin-6, MCP-1: Monocyte Chemoattractant Protein-1, TLR-4: Toll-like Receptor-4, GPR-41: G-Protein Coupled Receptor-41, GPR-43: G-Protein Coupled Receptor-43

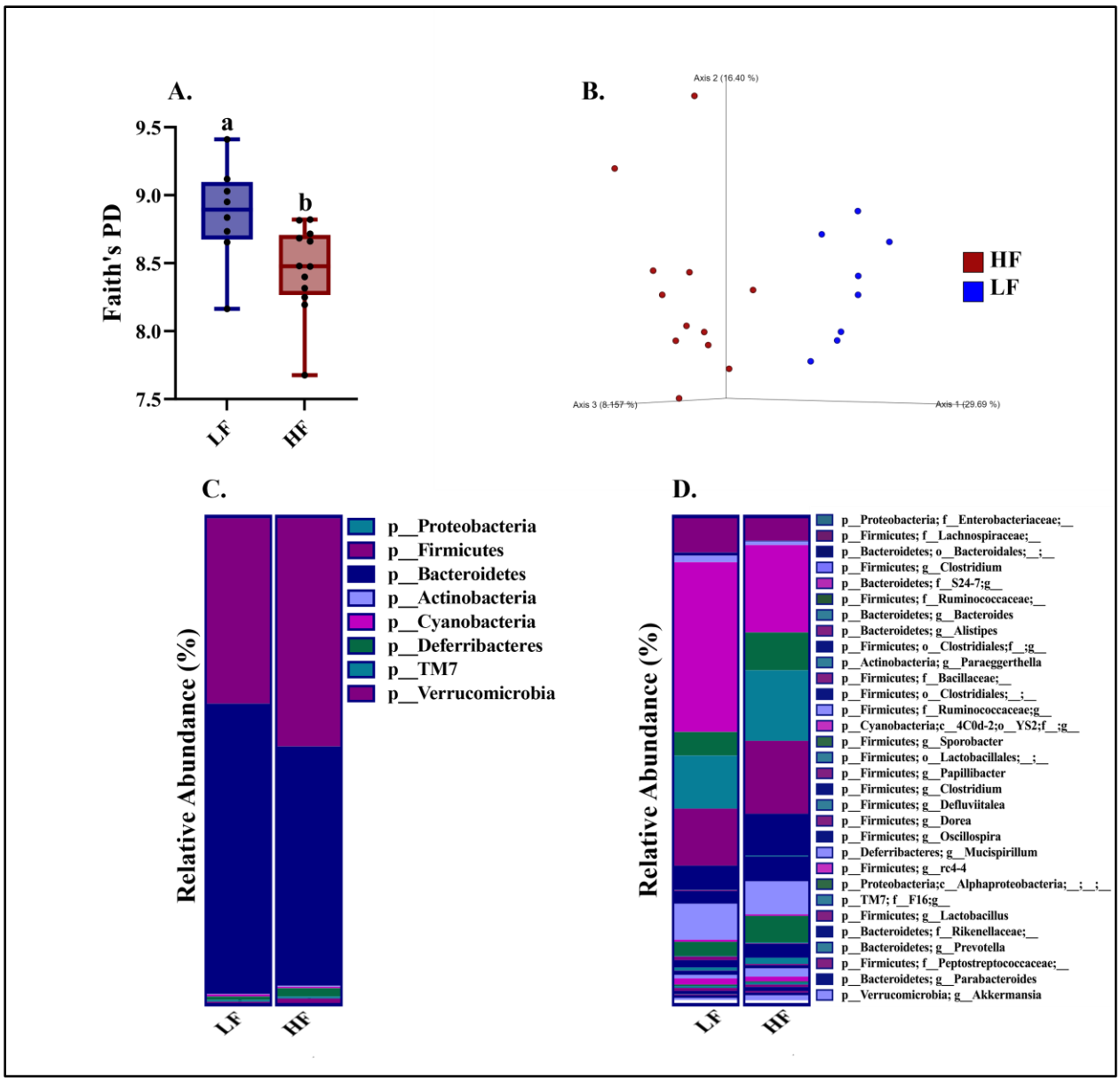

Figure 2-10 (S1). Fecal Microbiota Diversity and Taxonomic Structure A. Microbiota α-diversity visualized by Faith's phylogenetic diversity (PD); Box plots not sharing a lower-case letter are significantly different ($p<0.05$) **B.** Microbiota β-diversity visualized by Bray-Curtis distance matrices, analyzed by PERMANOVA, **C.** Relative abundance of fecal microbiota at the phylum level (p), **D.** Taxonomic relative abundance of fecal microbiota at the genus level (g) (labels show microbiota taxa composition according to the phyla and genus where applicable, or the family(f)/order (o) for the unclassified genera). (n=8 in LF and n=12 in HF group). LF: Low-fat diet fed lean control group, HF: High-fat diet fed group,

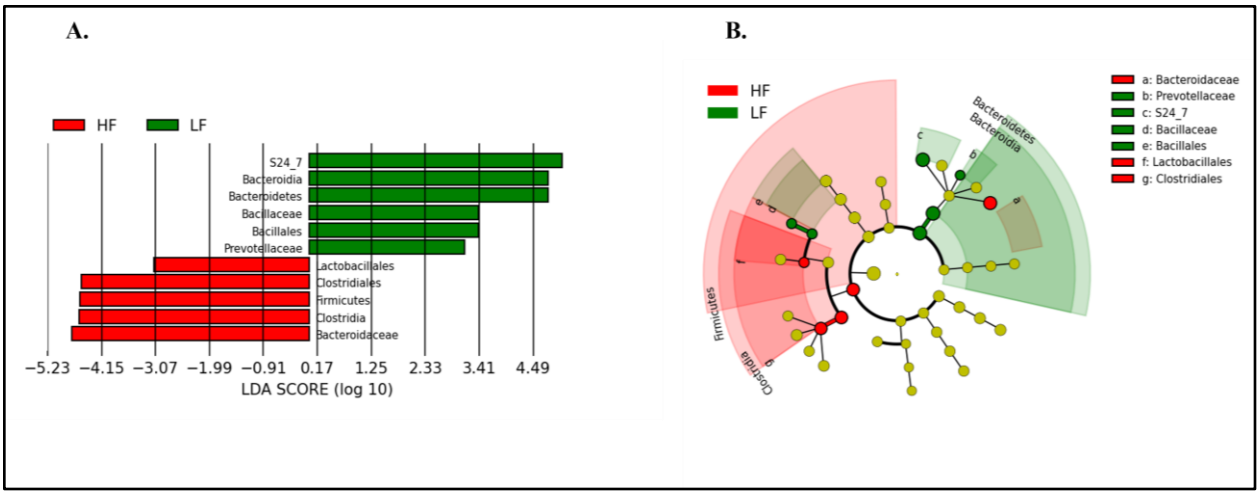

Figure 2-11 (S2). The Linear Discriminant Analysis (LDA) Effect Size (LEfSe) analysis of gut microbiota composition. A. LEfSE bar plot denoting LDA scores of taxa between the LF and HF groups. **B.** Taxonomic Cladogram (phylum to genus) from LEfSe, depicting taxonomic association between microbiome communities from LF and HF groups. Each node represents a specific taxonomic type. Red nodes denote the taxonomic types with more abundance in HF than in LF, while the green nodes represent the taxonomic types more abundant LF group. (LDA > 2, $p < 0.05$). LF: Low-fat diet fed lean control group, HF: High-fat diet fed group,

Author Contributions:

Conceptualization, S.M., É. D., and K.A.P.; Methodology, S.M., and L.K.; Investigation, S.M., L.K., G.F., V.R., D.B.H.L., L.M.; Formal analysis, S.M., and K.A.P.; Resources/Equipment, K.A.P.; Writing– Original Draft Preparation, S.M.; Writing – Review & Editing, S.M., and K.A.P.; Supervision, É. D., and K.A.P.; Project Administration, S.M.; Funding Acquisition, K.A.P.

Funding:
This research was supported by the following funding sources: NSERC Discovery, Ontario Research Fund, and the Nutrition and Mental Health Doctoral Scholarship from the School of Nutrition at the University of Ottawa.

Institutional Review Board Statement:
This study was conducted according to the National Institute of Health Guide for the Care and Use of Laboratory Animals and received approval from the Institutional Review Board at the University of Ottawa (Animal Care Committee, Protocol#HS-2857).

Data Availability Statement:
The data presented in this study are available on request from the corresponding author.

Acknowledgments:
The authors would like to express their gratitude to the department of Plant Agriculture, University of Guelph, Guelph, ON, for generously supplying the donation of kidney beans. Additionally, we would like to acknowledge the valuable assistance provided by the University of Ottawa, animal care and veterinary services (ACVS) team in animal care aspect of this research, and the Animal Behaviour and Physiology Core Facility team for supporting the behavior tests training and provision of essential equipment. We gratefully acknowledge Histology/ Staining services provided by the Louise Pelletier Histology Core RRID: SCR_021737.

Conflicts of Interest:
The authors declare no conflicts of interest.

5. **References**

1. Tiwari, A.; Balasundaram, P. Public Health Considerations Regarding Obesity. [Updated 2022 Sep 3]. In *StatPearls*; StatPearls Publishing: Treasure Island (FL), 2022.
2. Soto, M.; Herzog, C.; Pacheco, J.A.; Fujisaka, S.; Bullock, K.; Clish, C.B.; Kahn, C.R. Gut Microbiota Modulate Neurobehavior through Changes in Brain Insulin Sensitivity and Metabolism. *Mol. Psychiatry* **2018**, *23*, 2287–2301, doi:10.1038/s41380-018-0086-5.
3. Liu, B.-N.; Liu, X.-T.; Liang, Z.-H.; Wang, J.-H. Gut Microbiota in Obesity. *World J. Gastroenterol.* **2021**, *27*, 3837–3850, doi:10.3748/wjg.v27.i25.3837.
4. Scheithauer, T.P.M.; Rampanelli, E.; Nieuwdorp, M.; Vallance, B.A.; Verchere, C.B.; van Raalte, D.H.; Herrema, H. Gut Microbiota as a Trigger for Metabolic Inflammation in Obesity and Type 2 Diabetes. *Front. Immunol.* **2020**, *11*, 571731, doi:10.3389/fimmu.2020.571731.
5. Sun, J.; Ruan, Y.; Xu, N.; Wu, P.; Lin, N.; Yuan, K.; An, S.; Kang, P.; Li, S.; Huang, Q.; et al. The Effect of Dietary Carbohydrate and Calorie Restriction on Weight and Metabolic Health in Overweight/Obese Individuals: A Multi-Center Randomized Controlled Trial. *BMC Med.* **2023**, *21*, 192, doi:10.1186/s12916-023-02869-9.
6. Ott, B.; Skurk, T.; Hastreiter, L.; Lagkouvardos, I.; Fischer, S.; Büttner, J.; Kellerer, T.; Clavel, T.; Rychlik, M.; Haller, D.; et al. Effect of Caloric Restriction on Gut Permeability, Inflammation Markers, and Fecal Microbiota in Obese Women. *Sci. Rep.* **2017**, *7*, 11955, doi:10.1038/s41598-017-12109-9.
7. Lei, L.; Huang, J.; Zhang, L.; Hong, Y.; Hui, S.; Yang, J. Effects of Low-Carbohydrate Diets versus Low-Fat Diets on Metabolic Risk Factors in Overweight and Obese Adults: A Meta-Analysis of Randomized Controlled Trials. *Front. Nutr.* **2022**, *9*, 935234, doi:10.3389/fnut.2022.935234.
8. Alemán, J.O.; Iyengar, N.M.; Walker, J.M.; Milne, G.L.; Da Rosa, J.C.; Liang, Y.; Giri, D.D.; Zhou, X.K.; Pollak, M.N.; Hudis, C.A.; et al. Effects of Rapid Weight Loss on Systemic and Adipose Tissue Inflammation and Metabolism in Obese Postmenopausal Women. *J. Endocr. Soc.* **2017**, *1*, 625–637, doi:10.1210/js.2017-00020.
9. Rosendo-Silva, D.; Viana, S.; Carvalho, E.; Reis, F.; Matafome, P. Are Gut Dysbiosis, Barrier Disruption, and Endotoxemia Related to Adipose Tissue Dysfunction in Metabolic Disorders? Overview of the Mechanisms Involved. *Intern. Emerg. Med.* **2023**, *18*, 1287–1302, doi:10.1007/s11739-023-03262-3.
10. Rondanelli, M.; Gasparri, C.; Peroni, G.; Faliva, M.A.; Naso, M.; Perna, S.; Bazire, P.; Sajuox, I.; Maugeri, R.; Rigon, C. The Potential Roles of Very Low Calorie, Very Low Calorie Ketogenic Diets and Very Low Carbohydrate Diets on the Gut Microbiota Composition. *Front. Endocrinol.* **2021**, *12*, 662591, doi:10.3389/fendo.2021.662591.
11. Alemán, J.O.; Bokulich, N.A.; Swann, J.R.; Walker, J.M.; De Rosa, J.C.; Battaglia, T.; Costabile, A.; Pechlivanis, A.; Liang, Y.; Breslow, J.L.; et al. Fecal Microbiota and Bile Acid Interactions with Systemic and Adipose Tissue Metabolism in Diet-Induced Weight Loss of Obese Postmenopausal Women. *J. Transl. Med.* **2018**, *16*, 244, doi:10.1186/s12967-018-1619-z.
12. Wang, H.; Song, W.; Yuan, W.; Zhou, Q.; Sadiq, F.A.; Zhao, J.; Wu, W.; Lu, W. Modulating the Human Gut Microbiota through Hypocaloric Balanced Diets: An Effective Approach for Managing Obesity. *Nutrients* **2023**, *15*, 3101, doi:10.3390/nu15143101.

13. Vaghef-Mehrabany, E.; Ranjbar, F.; Asghari-Jafarabadi, M.; Hosseinpour-Arjmand, S.; Ebrahimi-Mameghani, M. Calorie Restriction in Combination with Prebiotic Supplementation in Obese Women with Depression: Effects on Metabolic and Clinical Response. *Nutr. Neurosci.* **2021**, *24*, 339–353, doi:10.1080/1028415X.2019.1630985.
14. Peckmezian, T.; Garcia-Larsen, V.; Wilkins, K.; Mosli, R.H.; BinDhim, N.F.; John, G.K.; Yasir, M.; Azhar, E.I.; Mullin, G.E.; Alqahtani, S.A. Microbiome-Targeted Therapies as an Adjunct to Traditional Weight Loss Interventions: A Systematic Review and Meta-Analysis. *Diabetes Metab. Syndr. Obes. Targets Ther.* **2022**, *15*, 3777–3798, doi:10.2147/DMSO.S378396.
15. Aoun, A.; Darwish, F.; Hamod, N. The Influence of the Gut Microbiome on Obesity in Adults and the Role of Probiotics, Prebiotics, and Synbiotics for Weight Loss. *Prev. Nutr. Food Sci.* **2020**, *25*, 113–123, doi:10.3746/pnf.2020.25.2.113.
16. Tandon, D.; Haque, M.M.; Gote, M.; Jain, M.; Bhaduri, A.; Dubey, A.K.; Mande, S.S. A Prospective Randomized, Double-Blind, Placebo-Controlled, Dose-Response Relationship Study to Investigate Efficacy of Fructo-Oligosaccharides (FOS) on Human Gut Microflora. *Sci. Rep.* **2019**, *9*, 5473, doi:10.1038/s41598-019-41837-3.
17. Krumbeck, J.A.; Rasmussen, H.E.; Hutkins, R.W.; Clarke, J.; Shawron, K.; Keshavarzian, A.; Walter, J. Probiotic Bifidobacterium Strains and Galactooligosaccharides Improve Intestinal Barrier Function in Obese Adults but Show No Synergism When Used Together as Synbiotics. *Microbiome* **2018**, *6*, 121, doi:10.1186/s40168-018-0494-4.
18. Hald, S.; Schioldan, A.G.; Moore, M.E.; Dige, A.; Lærke, H.N.; Agnholt, J.; Bach Knudsen, K.E.; Hermansen, K.; Marco, M.L.; Gregersen, S.; et al. Effects of Arabinoxylan and Resistant Starch on Intestinal Microbiota and Short-Chain Fatty Acids in Subjects with Metabolic Syndrome: A Randomised Crossover Study. *PloS One* **2016**, *11*, e0159223, doi:10.1371/journal.pone.0159223.
19. You, H.; Tan, Y.; Yu, D.; Qiu, S.; Bai, Y.; He, J.; Cao, H.; Che, Q.; Guo, J.; Su, Z. The Therapeutic Effect of SCFA-Mediated Regulation of the Intestinal Environment on Obesity. *Front. Nutr.* **2022**, *9*, 886902, doi:10.3389/fnut.2022.886902.
20. Brooks, L.; Viardot, A.; Tsakmaki, A.; Stolarczyk, E.; Howard, J.K.; Cani, P.D.; Everard, A.; Sleeth, M.L.; Psichas, A.; Anastasovskaj, J.; et al. Fermentable Carbohydrate Stimulates FFAR2-Dependent Colonic PYY Cell Expansion to Increase Satiety. *Mol. Metab.* **2017**, *6*, 48–60, doi:10.1016/j.molmet.2016.10.011.
21. Lecerf, J.-M.; Dépeint, F.; Clerc, E.; Dugenet, Y.; Niamba, C.N.; Rhazi, L.; Cayzeele, A.; Abdelnour, G.; Jaruga, A.; Younes, H.; et al. Xylo-Oligosaccharide (XOS) in Combination with Inulin Modulates Both the Intestinal Environment and Immune Status in Healthy Subjects, While XOS Alone Only Shows Prebiotic Properties. *Br. J. Nutr.* **2012**, *108*, 1847–1858, doi:10.1017/S0007114511007252.
22. Gill, P.A.; Zelm, M.C.; Muir, J.G.; Gibson, P.R. Review Article: Short Chain Fatty Acids as Potential Therapeutic Agents in Human Gastrointestinal and Inflammatory Disorders. *Aliment. Pharmacol. Ther.* **2018**, *48*, 15–34, doi:10.1111/apt.14689.
23. Kadyan, S.; Sharma, A.; Arjmandi, B.H.; Singh, P.; Nagpal, R. Prebiotic Potential of Dietary Beans and Pulses and Their Resistant Starch for Aging-Associated Gut and Metabolic Health. *Nutrients* **2022**, *14*, doi:10.3390/nu14091726.
24. Cruz-Bravo, R.K.; Guevara-Gonzalez, R.; Ramos-Gomez, M.; Garcia-Gasca, T.; Campos-Vega, R.; Oomah, B.D.; Loarca-Piña, G. Fermented Nondigestible Fraction from Common

Bean (Phaseolus Vulgaris L.) Cultivar Negro 8025 Modulates HT-29 Cell Behavior. *J. Food Sci.* **2011**, *76*, T41-47, doi:10.1111/j.1750-3841.2010.02025.x.

25. Aquino-Bolaños, E.N.; García-Díaz, Y.D.; Chavez-Servia, J.L.; Carrillo-Rodríguez, J.C.; Vera-Guzmán, A.M.; Heredia-García, E. Anthocyanin, Polyphenol, and Flavonoid Contents and Antioxidant Activity in Mexican Common Bean (Phaseolus Vulgaris L.) Landraces. *Emir. J. Food Agric.* **2016**, *28*, 581–588, doi:10.9755/ejfa.2016-02-147.
26. Campos-Vega, R.; Reynoso-Camacho, R.; Pedraza-Aboytes, G.; Acosta-Gallegos, J.A.; Guzman-Maldonado, S.H.; Paredes-Lopez, O.; Oomah, B.D.; Loarca-Piña, G. Chemical Composition and *In Vitro* Polysaccharide Fermentation of Different Beans (*Phaseolus Vulgaris* L.). *J. Food Sci.* **2009**, *74*, T59–T65, doi:10.1111/j.1750-3841.2009.01292.x.
27. shuncheng, R.; Ze-long, L.; Peng, W.F. Proximate Composition and Flavonoids Content and in Vitro Antioxidant Activity of 10 Varieties of Legume Seeds Grown in China. *J. Med. Plants Res.* **2012**, *6*, 301–308.
28. Hernández-Salazar, M.; Osorio-Diaz, P.; Loarca-Piña, G.; Reynoso-Camacho, R.; Tovar, J.; Bello-Pérez, L.A. In Vitro Fermentability and Antioxidant Capacity of the Indigestible Fraction of Cooked Black Beans (Phaseolus Vulgaris L.), Lentils (Lens Culinaris L.) and Chickpeas (Cicer Arietinum L.). *J. Sci. Food Agric.* **2010**, *90*, 1417–1422, doi:10.1002/jsfa.3954.
29. Tan, Y.; Tam, C.C.; Meng, S.; Zhang, Y.; Alves, P.; Yokoyama, W. Cooked Black Turtle Beans Ameliorate Insulin Resistance and Restore Gut Microbiota in C57BL/6J Mice on High-Fat Diets. *Foods Basel Switz.* **2021**, *10*, 1691, doi:10.3390/foods10081691.
30. Feng, Q.; Niu, Z.; Zhang, S.; Wang, L.; Dong, L.; Hou, D.; Zhou, S. Protective Effects of White Kidney Bean (Phaseolus Vulgaris L.) against Diet-Induced Hepatic Steatosis in Mice Are Linked to Modification of Gut Microbiota and Its Metabolites. *Nutrients* **2023**, *15*, 3033, doi:10.3390/nu15133033.
31. Lutsiv, T.; McGinley, J.N.; Neil-McDonald, E.S.; Weir, T.L.; Foster, M.T.; Thompson, H.J. Relandscaping the Gut Microbiota with a Whole Food: Dose-Response Effects to Common Bean. *Foods Basel Switz.* **2022**, *11*, doi:10.3390/foods11081153.
32. Monk, J.M.; Wu, W.; Lepp, D.; Wellings, H.R.; Hutchinson, A.L.; Liddle, D.M.; Graf, D.; Pauls, K.P.; Robinson, L.E.; Power, K.A. Navy Bean Supplemented High-Fat Diet Improves Intestinal Health, Epithelial Barrier Integrity and Critical Aspects of the Obese Inflammatory Phenotype. *J Nutr Biochem* **2019**, *70*, 91–104, doi:10.1016/j.jnutbio.2019.04.009.
33. Zhu, Z.; Jiang, W.; Thompson, H.J. Edible Dry Bean Consumption (Phaseolus Vulgaris L.) Modulates Cardiovascular Risk Factors and Diet-Induced Obesity in Rats and Mice. *Br. J. Nutr.* **2012**, *108 Suppl 1*, S66-73, doi:10.1017/S0007114512000839.
34. Zhu, Z.; Jiang, W.; Thompson, H.J. Edible Dry Bean Consumption (Phaseolus Vulgaris L.) Modulates Cardiovascular Risk Factors and Diet-Induced Obesity in Rats and Mice. *Br. J. Nutr.* **2012**, *108*, S66–S73, doi:DOI: 10.1017/S0007114512000839.
35. Neil, E.S.; McGinley, J.N.; Fitzgerald, V.K.; Lauck, C.A.; Tabke, J.A.; Streeter-McDonald, M.R.; Yao, L.; Broeckling, C.D.; Weir, T.L.; Foster, M.T.; et al. White Kidney Bean (Phaseolus Vulgaris L.) Consumption Reduces Fat Accumulation in a Polygenic Mouse Model of Obesity. *Nutrients* **2019**, *11*, doi:10.3390/nu11112780.
36. Sánchez-Tapia, M.; Hernández-Velázquez, I.; Pichardo-Ontiveros, E.; Granados-Portillo, O.; Gálvez, A.; R Tovar, A.; Torres, N. Consumption of Cooked Black Beans Stimulates a

Cluster of Some Clostridia Class Bacteria Decreasing Inflammatory Response and Improving Insulin Sensitivity. *Nutrients* **2020**, *12*, doi:10.3390/nu12041182.
37. Crujeiras, A.B.; Parra, D.; Abete, I.; Martínez, J.A. A Hypocaloric Diet Enriched in Legumes Specifically Mitigates Lipid Peroxidation in Obese Subjects. *Free Radic. Res.* **2007**, *41*, 498–506, doi:10.1080/10715760601131935.
38. Abete, I.; Parra, D.; Martinez, J.A. Legume-, Fish-, or High-Protein-Based Hypocaloric Diets: Effects on Weight Loss and Mitochondrial Oxidation in Obese Men. *J. Med. Food* **2009**, *12*, 100+.
39. Hermsdorff, H.H.M.; Zulet, M.Á.; Abete, I.; Martínez, J.A. A Legume-Based Hypocaloric Diet Reduces Proinflammatory Status and Improves Metabolic Features in Overweight/Obese Subjects. *Eur. J. Nutr.* **2011**, *50*, 61–69, doi:10.1007/s00394-010-0115-x.
40. Kim, S.J.; de Souza, R.J.; Choo, V.L.; Ha, V.; Cozma, A.I.; Chiavaroli, L.; Mirrahimi, A.; Blanco Mejia, S.; Di Buono, M.; Bernstein, A.M.; et al. Effects of Dietary Pulse Consumption on Body Weight: A Systematic Review and Meta-Analysis of Randomized Controlled Trials. *Am. J. Clin. Nutr.* **2016**, *103*, 1213–1223, doi:10.3945/ajcn.115.124677.
41. McCrory, M.A.; Lovejoy, J.C.; Palmer, P.A.; Eichelsdoerfer, P.E.; Gehrke, M.M.; Kavanaugh, I.T.; Buesing, S.A.; Rose, T.L. Effectiveness of Legume Consumption for Facilitating Weight Loss: A Randomized Trial. *FASEB J.* **2008**, *22*, 1084.8-1084.8, doi:10.1096/fasebj.22.1_supplement.1084.8.
42. Yang, Q.-Q.; Gan, R.-Y.; Ge, Y.-Y.; Zhang, D.; Corke, H. Polyphenols in Common Beans (Phaseolus Vulgaris L.): Chemistry, Analysis, and Factors Affecting Composition. *Compr. Rev. Food Sci. Food Saf.* **2018**, *17*, 1518–1539, doi:10.1111/1541-4337.12391.
43. Rodríguez Madrera, R.; Campa Negrillo, A.; Suárez Valles, B.; Ferreira Fernández, J.J. Phenolic Content and Antioxidant Activity in Seeds of Common Bean (Phaseolus Vulgaris L.). *Foods Basel Switz.* **2021**, *10*, doi:10.3390/foods10040864.
44. Ombra, M.N.; d'Acierno, A.; Nazzaro, F.; Riccardi, R.; Spigno, P.; Zaccardelli, M.; Pane, C.; Maione, M.; Fratianni, F. Phenolic Composition and Antioxidant and Antiproliferative Activities of the Extracts of Twelve Common Bean (*Phaseolus Vulgaris* L.) Endemic Ecotypes of Southern Italy before and after Cooking. *Oxid. Med. Cell. Longev.* **2016**, *2016*, 1398298, doi:10.1155/2016/1398298.
45. John, H.S.; Doucet, É.; Power, K.A. Dietary Pulses as a Means to Improve the Gut Microbiome, Inflammation, and Appetite Control in Obesity. *Obes. Rev. Off. J. Int. Assoc. Study Obes.* **2023**, *24*, e13598, doi:10.1111/obr.13598.
46. Illumina 16S Metagenomic Sequencing Library. *Illumina.com* **2013**, 1–28.
47. Bolyen, E.; Rideout, J.R.; Dillon, M.R.; Bokulich, N.A.; Abnet, C.C.; Al-Ghalith, G.A.; Alexander, H.; Alm, E.J.; Arumugam, M.; Asnicar, F.; et al. Reproducible, Interactive, Scalable and Extensible Microbiome Data Science Using QIIME 2. Nat. Biotechnol. 2019, 37, 852–857, doi:10.1038/s41587-019-0209-9.
48. Callahan, B.J.; McMurdie, P.J.; Rosen, M.J.; Han, A.W.; Johnson, A.J.A.; Holmes, S.P. DADA2: High-Resolution Sample Inference from Illumina Amplicon Data. Nat. Methods 2016, 13, 581–583, doi:10.1038/nmeth.3869.
49. McDonald, D.; Price, M.N.; Goodrich, J.; Nawrocki, E.P.; DeSantis, T.Z.; Probst, A.; Andersen, G.L.; Knight, R.; Hugenholtz, P. An Improved Greengenes Taxonomy with Explicit Ranks for Ecological and Evolutionary Analyses of Bacteria and Archaea. ISME J. 2012, 6, 610–618, doi:10.1038/ismej.2011.139.

50. Bray, J.R.; Curtis, J.T. An Ordination of the Upland Forest Communities of Southern Wisconsin. Ecol. Monogr. 1957, 27, 326–349, doi:10.2307/1942268.
51. Douglas, G.M.; Maffei, V.J.; Zaneveld, J.R.; Yurgel, S.N.; Brown, J.R.; Taylor, C.M.; Huttenhower, C.; Langille, M.G.I. PICRUSt2 for Prediction of Metagenome Functions. *Nat. Biotechnol.* **2020**, *38*, 685–688, doi:10.1038/s41587-020-0548-6.
52. Langille, M.G.I.; Zaneveld, J.; Caporaso, J.G.; McDonald, D.; Knights, D.; Reyes, J.A.; Clemente, J.C.; Burkepile, D.E.; Vega Thurber, R.L.; Knight, R.; et al. Predictive Functional Profiling of Microbial Communities Using 16S rRNA Marker Gene Sequences. *Nat. Biotechnol.* **2013**, *31*, 814–821, doi:10.1038/nbt.2676.
53. Janssen, S.; McDonald, D.; Gonzalez, A.; Navas-Molina, J.A.; Jiang, L.; Xu, Z.Z.; Winker, K.; Kado, D.M.; Orwoll, E.; Manary, M.; et al. Phylogenetic Placement of Exact Amplicon Sequences Improves Associations with Clinical Information. *mSystems* **2018**, *3*, e00021-18, doi:10.1128/mSystems.00021-18.
54. MIRARAB, S.; NGUYEN, N.; WARNOW, T. SEPP: SATé-Enabled Phylogenetic Placement. In *Biocomputing 2012*; WORLD SCIENTIFIC, 2011; pp. 247–258 ISBN 978-981-4596-37-4.
55. Czech, L.; Stamatakis, A. Scalable Methods for Analyzing and Visualizing Phylogenetic Placement of Metagenomic Samples. *PloS One* **2019**, *14*, e0217050, doi:10.1371/journal.pone.0217050.
56. Louca, S.; Doebeli, M. Efficient Comparative Phylogenetics on Large Trees. *Bioinformatics* **2018**, *34*, 1053–1055, doi:10.1093/bioinformatics/btx701.
57. Kanehisa, M.; Goto, S. KEGG: Kyoto Encyclopedia of Genes and Genomes. *Nucleic Acids Res.* **2000**, *28*, 27–30, doi:10.1093/nar/28.1.27.
58. Douglas, G. PiCrust2 Categorize_by_function.Py · Issue #1 · Gavinmdouglas/Picrust2_manuscript Available online: https://github.com/gavinmdouglas/picrust2_manuscript/issues/1 (accessed on 17 June 2022).
59. Parks, D.H.; Tyson, G.W.; Hugenholtz, P.; Beiko, R.G. STAMP: Statistical Analysis of Taxonomic and Functional Profiles. *Bioinforma. Oxf. Engl.* **2014**, *30*, 3123–3124, doi:10.1093/bioinformatics/btu494.
60. Livingston, D.B.H.; Sweet, A.; Rodrigue, A.; Kishore, L.; Loftus, J.; Ghali, F.; Mahmoodianfard, S.; Celton, C.; Hosseinian, F.; Power, K.A. Dietary Flaxseed and Flaxseed Oil Differentially Modulate Aspects of the Microbiota Gut–Brain Axis Following an Acute Lipopolysaccharide Challenge in Male C57Bl/6 Mice. *Nutrients* **2023**, *15*, 3542, doi:10.3390/nu15163542.
61. Chen, S.-Y.; Beretta, M.; Olzomer, E.M.; Shah, D.P.; Wong, D.Y.H.; Alexopoulos, S.J.; Aleksovska, I.; Salamoun, J.M.; Garcia, C.J.; Cochran, B.J.; et al. Targeting Negative Energy Balance with Calorie Restriction and Mitochondrial Uncoupling in Db/Db Mice. *Mol. Metab.* **2023**, *69*, 101684, doi:https://doi.org/10.1016/j.molmet.2023.101684.
62. Dalby, M.J.; Aviello, G.; Ross, A.W.; Walker, A.W.; Barrett, P.; Morgan, P.J. Diet Induced Obesity Is Independent of Metabolic Endotoxemia and TLR4 Signalling, but Markedly Increases Hypothalamic Expression of the Acute Phase Protein, SerpinA3N. *Sci. Rep.* **2018**, *8*, 15648, doi:10.1038/s41598-018-33928-4.
63. Sawicka-Śmiarowska, E.; Moniuszko-Malinowska, A.; Kamiński, K.A. Which Microbes Like My Diet and What Does It Mean for My Heart? *Nutrients* **2021**, *13*, doi:10.3390/nu13114146.

64. Chen, T.; Long, W.; Zhang, C.; Liu, S.; Zhao, L.; Hamaker, B.R. Fiber-Utilizing Capacity Varies in Prevotella- versus Bacteroides-Dominated Gut Microbiota. *Sci. Rep.* **2017**, *7*, 2594, doi:10.1038/s41598-017-02995-4.
65. Margier, M.; Georgé, S.; Hafnaoui, N.; Remond, D.; Nowicki, M.; Du Chaffaut, L.; Amiot, M.-J.; Reboul, E. Nutritional Composition and Bioactive Content of Legumes: Characterization of Pulses Frequently Consumed in France and Effect of the Cooking Method. *Nutrients* **2018**, *10*, 1668, doi:10.3390/nu10111668.
66. Lin, T.-L.; Shu, C.-C.; Chen, Y.-M.; Lu, J.-J.; Wu, T.-S.; Lai, W.-F.; Tzeng, C.-M.; Lai, H.-C.; Lu, C.-C. Like Cures Like: Pharmacological Activity of Anti-Inflammatory Lipopolysaccharides From Gut Microbiome. *Front. Pharmacol.* **2020**, *11*, 554, doi:10.3389/fphar.2020.00554.
67. Frühbeck, G.; Catalán, V.; Rodríguez, A.; Ramírez, B.; Becerril, S.; Salvador, J.; Colina, I.; Gómez-Ambrosi, J. Adiponectin-Leptin Ratio Is a Functional Biomarker of Adipose Tissue Inflammation. *Nutrients* **2019**, *11*, doi:10.3390/nu11020454.
68. Wu, Z.; Du, Z.; Tian, Y.; Liu, M.; Zhu, K.; Zhao, Y.; Wang, H. Inulin Accelerates Weight Loss in Obese Mice by Regulating Gut Microbiota and Serum Metabolites. *Front. Nutr.* **2022**, *9*, 980382, doi:10.3389/fnut.2022.980382.
69. Monk, J.M.; Wu, W.; Lepp, D.; Pauls, K.P.; Robinson, L.E.; Power, K.A. Navy Bean Supplementation in Established High-Fat Diet-Induced Obesity Attenuates the Severity of the Obese Inflammatory Phenotype. *Nutrients* **2021**, *13*, doi:10.3390/nu13030757.
70. Guillemot-Legris, O.; Muccioli, G.G. Obesity-Induced Neuroinflammation: Beyond the Hypothalamus. *Trends Neurosci.* **2017**, *40*, 237–253, doi:10.1016/j.tins.2017.02.005.
71. Della Vedova, M.C.; Muñoz, M.D.; Santillan, L.D.; Plateo-Pignatari, M.G.; Germanó, M.J.; Tosi, M.E.R.; Garcia, S.; Gomez, N.N.; Fornes, M.W.; Mejiba, S.E.G.; et al. A Mouse Model of Diet-Induced Obesity Resembling Most Features of Human Metabolic Syndrome. *Nutr. Metab. Insights* **2016**, *9*, NMI.S32907, doi:10.4137/NMI.S32907.
72. Duan, Y.; Zeng, L.; Zheng, C.; Song, B.; Li, F.; Kong, X.; Xu, K. *Inflammatory Links Between High Fat Diets and Diseases*; 2018; Vol. 9; ISBN 1664-3224.
73. Wu, S.-C.; Rau, C.-S.; Lu, T.-H.; Tzeng, S.-L.; Wu, Y.-C.; Wu, C.-J.; Lin, C.-W.; Hsieh, C.-H. Effect of Weight-Reduction in Obese Mice Lacking Toll-Like Receptor 5 and C57BL/6 Mice Fed a Low-Fat Diet. *Mediators Inflamm.* **2015**, *2015*, 852126, doi:10.1155/2015/852126.
74. Hoevenaars, F.P.M.; Keijer, J.; Swarts, H.J.; Snaas-Alders, S.; Bekkenkamp-Grovenstein, M.; van Schothorst, E.M. Effects of Dietary History on Energy Metabolism and Physiological Parameters in C57BL/6J Mice. *Exp. Physiol.* **2013**, *98*, 1053–1062, doi:10.1113/expphysiol.2012.069518.
75. Shi, H.; Akunuru, S.; Bierman, J.C.; Hodge, K.M.; Mitchell, M.C.; Foster, M.T.; Seeley, R.J.; Reizes, O. Diet-Induced Obese Mice Are Leptin Insufficient after Weight Reduction. *Obes. Silver Spring Md* **2009**, *17*, 1702–1709, doi:10.1038/oby.2009.106.
76. Li, S.S.; Kendall, C.W.C.; De Souza, R.J.; Jayalath, V.H.; Cozma, A.I.; Ha, V.; Mirrahimi, A.; Chiavaroli, L.; Augustin, L.S.A.; Blanco Mejia, S.; et al. Dietary Pulses, Satiety and Food Intake: A Systematic Review and Meta-Analysis of Acute Feeding Trials. *Obesity* **2014**, *22*, 1773–1780, doi:10.1002/oby.20782.
77. McCrory, M.A.; Hamaker, B.R.; Lovejoy, J.C.; Eichelsdoerfer, P.E. Pulse Consumption, Satiety, and Weight Management. *Adv. Nutr. Bethesda Md* **2010**, *1*, 17–30, doi:10.3945/an.110.1006.

78. Turnbaugh, P.J.; Ley, R.E.; Mahowald, M. a; Magrini, V.; Mardis, E.R.; Gordon, J.I. An Obesity-Associated Gut Microbiome with Increased Capacity for Energy Harvest. *Nature* **2006**, *444*, 1027–1031, doi:10.1038/nature05414.
79. McNeil, N.I. The Contribution of the Large Intestine to Energy Supplies in Man. *Am. J. Clin. Nutr.* **1984**, *39*, 338–342.
80. Gao, Z.; Yin, J.; Zhang, J.; Ward, R.E.; Martin, R.J.; Lefevre, M.; Cefalu, W.T.; Ye, J. Butyrate Improves Insulin Sensitivity and Increases Energy Expenditure in Mice. *Diabetes* **2009**, *58*, 1509–1517, doi:10.2337/db08-1637.
81. Henagan, T.M.; Stefanska, B.; Fang, Z.; Navard, A.M.; Ye, J.; Lenard, N.R.; Devarshi, P.P. Sodium Butyrate Epigenetically Modulates High-fat Diet-induced Skeletal Muscle Mitochondrial Adaptation, Obesity and Insulin Resistance through Nucleosome Positioning. *Br. J. Pharmacol.* **2015**, *172*, 2782–2798, doi:10.1111/bph.13058.
82. Everard, A.; Lazarevic, V.; Derrien, M.; Girard, M.; Muccioli, G.G.; Neyrinck, A.M.; Possemiers, S.; Van Holle, A.; François, P.; de Vos, W.M.; et al. Responses of Gut Microbiota and Glucose and Lipid Metabolism to Prebiotics in Genetic Obese and Diet-Induced Leptin-Resistant Mice. *Diabetes* **2011**, *60*, 2775–2786, doi:10.2337/db11-0227.
83. Frampton, J.; Murphy, K.G.; Frost, G.; Chambers, E.S. Higher Dietary Fibre Intake Is Associated with Increased Skeletal Muscle Mass and Strength in Adults Aged 40 Years and Older. *J. Cachexia Sarcopenia Muscle* **2021**, *12*, 2134–2144, doi:10.1002/jcsm.12820.
84. Frampton, J.; Murphy, K.G.; Frost, G.; Chambers, E.S. Short-Chain Fatty Acids as Potential Regulators of Skeletal Muscle Metabolism and Function. *Nat. Metab.* **2020**, *2*, 840–848, doi:10.1038/s42255-020-0188-7.
85. Walsh, M.E.; Bhattacharya, A.; Sataranatarajan, K.; Qaisar, R.; Sloane, L.; Rahman, M.M.; Kinter, M.; Van Remmen, H. The Histone Deacetylase Inhibitor Butyrate Improves Metabolism and Reduces Muscle Atrophy during Aging. *Aging Cell* **2015**, *14*, 957–970, doi:10.1111/acel.12387.
86. Tavella, T.; Rampelli, S.; Guidarelli, G.; Bazzocchi, A.; Gasperini, C.; Pujos-Guillot, E.; Comte, B.; Barone, M.; Biagi, E.; Candela, M.; et al. Elevated Gut Microbiome Abundance of Christensenellaceae, Porphyromonadaceae and Rikenellaceae Is Associated with Reduced Visceral Adipose Tissue and Healthier Metabolic Profile in Italian Elderly. *Gut Microbes* **2021**, *13*, 1–19, doi:10.1080/19490976.2021.1880221.
87. Xie, Y.; Li, W.; Zhu, L.; Zhai, S.; Qin, S.; Du, Z. Effects of Phycocyanin in Modulating the Intestinal Microbiota of Mice. *MicrobiologyOpen* **2019**, *8*, e00825, doi:10.1002/mbo3.825.
88. Lutsiv, T.; McGinley, J.N.; Neil-McDonald, E.S.; Weir, T.L.; Foster, M.T.; Thompson, H.J. Relandscaping the Gut Microbiota with a Whole Food: Dose-Response Effects to Common Bean. *Foods Basel Switz.* **2022**, *11*, doi:10.3390/foods11081153.
89. Parker, B.J.; Wearsch, P.A.; Veloo, A.C.M.; Rodriguez-Palacios, A. The Genus Alistipes: Gut Bacteria With Emerging Implications to Inflammation, Cancer, and Mental Health. *Front. Immunol.* **2020**, *11*, 906, doi:10.3389/fimmu.2020.00906.
90. Guo, S.; Zhao, H.; Ma, Z.; Zhang, S.; Li, M.; Zheng, Z.; Ren, X.; Ho, C.-T.; Bai, N. Anti-Obesity and Gut Microbiota Modulation Effect of Secoiridoid-Enriched Extract from Fraxinus Mandshurica Seeds on High-Fat Diet-Fed Mice. *Molecules* **2020**, *25*, doi:10.3390/molecules25174001.
91. Zeng, Q.; Li, D.; He, Y.; Li, Y.; Yang, Z.; Zhao, X.; Liu, Y.; Wang, Y.; Sun, J.; Feng, X.; et al. Discrepant Gut Microbiota Markers for the Classification of Obesity-Related Metabolic Abnormalities. *Sci. Rep.* **2019**, *9*, 13424, doi:10.1038/s41598-019-49462-w.

92. Verdam, F.J.; Fuentes, S.; De Jonge, C.; Zoetendal, E.G.; Erbil, R.; Greve, J.W.; Buurman, W.A.; De Vos, W.M.; Rensen, S.S. Human Intestinal Microbiota Composition Is Associated with Local and Systemic Inflammation in Obesity. *Obesity* **2013**, *21*, doi:10.1002/oby.20466.
93. Dan, X.; Mushi, Z.; Baili, W.; Han, L.; Enqi, W.; Huanhu, Z.; Shuchun, L. Differential Analysis of Hypertension-Associated Intestinal Microbiota. *Int. J. Med. Sci.* **2019**, *16*, 872–881, doi:10.7150/ijms.29322.
94. Jennings, A.; Koch, M.; Bang, C.; Franke, A.; Lieb, W.; Cassidy, A. Microbial Diversity and Abundance of Parabacteroides Mediate the Associations Between Higher Intake of Flavonoid-Rich Foods and Lower Blood Pressure. *Hypertens. Dallas Tex 1979* **2021**, *78*, 1016–1026, doi:10.1161/HYPERTENSIONAHA.121.17441.
95. Ishioka, M.; Miura, K.; Minami, S.; Shimura, Y.; Ohnishi, H. Altered Gut Microbiota Composition and Immune Response in Experimental Steatohepatitis Mouse Models. *Dig. Dis. Sci.* **2017**, *62*, 396+.
96. Monk, J.M.; Wu, W.; Hutchinson, A.L.; Pauls, P.; Robinson, L.E.; Power, K.A. Navy and Black Bean Supplementation Attenuates Colitis-Associated Inflammation and Colonic Epithelial Damage. *J. Nutr. Biochem.* **2018**, *56*, 215–223, doi:10.1016/j.jnutbio.2018.02.013.
97. Vangoitsenhoven, R.; van der Ende, M.; Corbeels, K.; Monteiro Carvalho Mori Cunha, J.P.; Lannoo, M.; Bedossa, P.; van der Merwe, S.; Mertens, A.; Gesquiere, I.; Meulemans, A.; et al. At Similar Weight Loss, Dietary Composition Determines the Degree of Glycemic Improvement in Diet-Induced Obese C57BL/6 Mice. *PLOS ONE* **2018**, *13*, e0200779.
98. Kurki, E.; Shi, J.; Martonen, E.; Finckenberg, P.; Mervaala, E. Distinct Effects of Calorie Restriction on Adipose Tissue Cytokine and Angiogenesis Profiles in Obese and Lean Mice. *Nutr. Metab.* **2012**, *9*, 64, doi:10.1186/1743-7075-9-64.
99. Rodrigues, M.O.M.; Evangelista-Silva, P.H.; Neves, N.N.; Moreno, L.G.; Santos, C.S.; Rocha, K.L.S.; Ottone, V.O.; Batista-da-Silva, B.; Dias-Peixoto, M.F.; Magalhães, F.C.; et al. Caloric Restriction-Induced Weight Loss with a High-Fat Diet Does Not Fully Recover Visceral Adipose Tissue Inflammation in Previously Obese C57BL/6 Mice. *Appl. Physiol. Nutr. Metab. Physiol. Appl. Nutr. Metab.* **2020**, *45*, 1353–1359, doi:10.1139/apnm-2020-0220.
100. Hoevenaars, F.P.M.; Keijer, J.; Herreman, L.; Palm, I.; Hegeman, M.A.; Swarts, H.J.M.; van Schothorst, E.M. Adipose Tissue Metabolism and Inflammation Are Differently Affected by Weight Loss in Obese Mice Due to Either a High-Fat Diet Restriction or Change to a Low-Fat Diet. *Genes Nutr.* **2014**, *9*, 391, doi:10.1007/s12263-014-0391-9.
101. Zhao, Q.; Liu, Z.; Zhu, Y.; Wang, H.; Dai, Z.; Yang, X.; Ren, X.; Xue, Y.; Shen, Q. Cooked Adzuki Bean Reduces High-Fat Diet-Induced Body Weight Gain, Ameliorates Inflammation, and Modulates Intestinal Homeostasis in Mice. *Front. Nutr.* **2022**, *9*, 918696, doi:10.3389/fnut.2022.918696.
102. Lutsiv, T.; Weir, T.L.; McGinley, J.N.; Neil, E.S.; Wei, Y.; Thompson, H.J. Compositional Changes of the High-Fat Diet-Induced Gut Microbiota upon Consumption of Common Pulses. *Nutrients* **2021**, *13*, doi:10.3390/nu13113992.
103. Rodriguez-Echevarria, R.; Macias-Barragan, J.; Parra-Vargas, M.; Davila-Rodriguez, J.R.; Amezcua-Galvez, E.; Armendariz-Borunda, J. Diet Switch and Omega-3 Hydroxy-Fatty Acids Display Differential Hepatoprotective Effects in an Obesity/Nonalcoholic Fatty

Liver Disease Model in Mice. *World J. Gastroenterol.* **2018**, *24*, 461–474, doi:10.3748/wjg.v24.i4.461.
104. Wheatley, K.E.; Nogueira, L.M.; Perkins, S.N.; Hursting, S.D. Differential Effects of Calorie Restriction and Exercise on the Adipose Transcriptome in Diet-Induced Obese Mice. *J. Obes.* **2011**, *2011*, 265417, doi:10.1155/2011/265417.
105. Feng, Y.; Fan, X.; Zhang, S.; Yu, M.; Wu, T.; Liang, Y.; Wang, C.; Yang, H. Effect of Thermal Processing on the Metabolic Components of Black Beans on Ultra-High-Performance Liquid Chromatography Coupled with High-Field Quadrupole-Orbitrap High-Resolution Mass Spectrometry. *Molecules* **2022**, *27*, doi:10.3390/molecules27123919.
106. Ferreira, H.; Vasconcelos, M.; Gil, A.M.; Pinto, E. Benefits of Pulse Consumption on Metabolism and Health: A Systematic Review of Randomized Controlled Trials. *Crit. Rev. Food Sci. Nutr.* **2021**, *61*, 85–96, doi:10.1080/10408398.2020.1716680.

3 CHAPTER 3 - Project 2 Manuscript

Assessing the Impact of Introducing White and Dark-Red Kidney Beans into a Low-Fat Diet on Intestinal and Mental Health in Diet-Induced Obese Mice

Authors

Salma Mahmoodianfard[1], Lalit Kishore[2], Alexane Rodrigue[3], Giorgio Freije[4], Valérie Roumelis[4], Éric Doucet[1], Krista A. Power[2,5]

Affiliations:

1. School of Human Kinetics, University of Ottawa, Ottawa K1N 6N5, Canada
2. School of Nutrition Sciences, Faculty of Health Science, University of Ottawa, Ottawa, Canada, K1N 6N5
3. Department of Biochemistry, Microbiology and Immunology, Faculty of Medicine, University of Ottawa, Ottawa, Canada, K1H 8L1
4. Department of Biology, Faculty of Science, University of Ottawa
5. Department of Plant Agriculture, University of Guelph

Corresponding Author Contact:
Krista A. Power, Krista.Power@uottawa.ca

Abstract

Dietary pulses, like common beans, rich in non-digestible carbohydrates (NDCs) and polyphenols, may impact gut microbiome-metabolome interactions during weight loss. This study investigated the impact of white (WB) and dark red kidney beans (DB) in a low-fat diet (LFD) on intestinal health and behavior well-being in obesity mouse models. Obesity was established in C57BL/6 male mice through a high-fat diet (HFD) for 10 weeks, followed by division into four groups: 1. HF control (remaining on HFD); 2. HF→LF (transitioning to LFD); 3. HF→WB (LFD with 15% white kidney beans powder [wt/wt]); and 4. HF→DB (LFD with 15% dark red kidney beans powder [wt/wt]) for an additional 8 weeks. Introducing beans led to distinct microbiota β-diversity differences ($q<0.01$), and notable changes in relative abundance of cecal microbiota including higher relative abundance of *Prevotella*, S24-7, and short chain fatty acids, and lower *Dorea*, *Papillibacter*, *Parabacteroides*, *Mucispirillum*, along with a reduced Firmicutes/Bacteroidetes ratio ($p<0.05$). While bean varieties did not differently alter the microbiota composition and inferred function, WB increased *Lactobacillus* compared to HF→LF and HF, also reduced *rc4-4* compared to HF→LF. Conversely, DB increased *Akkermansia* compared to HFD-fed obese control group. While nest-building behavior did not show significant difference between groups, transitioning from HFD to LFD mitigated anxiety behaviors associated with obesity. Notably, WB significantly reduced the latency for the first entrance into the open arm compared to the HF group, reflecting enhanced anxiolytic-like effects. Overall, in C57Bl/6 male mice, beans positively influenced the gut microbiota microenvironment and exhibited promising evidence of anxiolytic effects potentially through the gut-brain-axis.

Keywords: Obesity; gut microbiota; dietary pulses; SCFA, weight-loss; intestinal health, Anxiety

1. Introduction

The gut microbiota has emerged as a potential contributing factor in the development of obesity and related metabolic disorders [1]. Obesity-associated dysbiosis, characterized by reduced phylogenetic diversity [2,3] and alterations in the composition of the gut microbiota [4–6], can contribute to various adverse effects on intestinal health including damage to the intestinal epithelial cells, increased intestinal epithelial permeability, disruption of mucus production, and consequently intestinal barrier dysfunction [7–9]. Furthermore, evidence supports a bidirectional communication between the intestinal tract and the central nervous system [10–12]. Therefore, dysbiosis may not solely be linked to intestinal diseases but could also be associated with neurological disorders through the microbiome-gut-brain axis [9,13,14], thereby potentially playing a role in mental health and mood-related disorders, including anxiety and depression [15,16].

Modifications in dietary patterns, particularly those aimed at reducing calorie intake, can result in weight loss and subsequently decreasing the risk of obesity-related complications [30] such as enhanced intestinal barrier function [17,18]. While behavioral weight loss interventions show overall improvements in mental health, concerns persist about the impact of dietary restrictions on disordered eating and psychological distress [19] and unfavorable psychological outcomes associated with weight loss, such as an increase in depressive symptoms [20,21], and lower psychological wellbeing [22]. Evidence suggests that prebiotics (such as inulin) have the potential to manipulate the gut microbiota, thereby facilitating weight loss or preventing obesity [23]. On the other hand, clinical evidence support the use of probiotics in improving mental health, such as reducing anxiety and alleviating stress responses [24–26]. The aforementioned factors have

prompted the investigation of innovative dietary approaches aimed at modulating the microbiota to address both intestinal and behavioral dysfunctions associated with obesity [27,28]

Dietary pulses, such as common beans, chickpeas, and lentils [29], are ecologically sustainable and affordable protein sources [30], enriched with microbial-accessible non-digestible carbohydrates (NDCs) and polyphenols with potential properties to alter the gut microbiome-metabolome [31]. NDCs, fermented by intestinal microbiota, result in the production of short-chain fatty acids (SCFAs) [32], crucial for maintaining colonocyte health, providing energy to intestinal epithelial cells, and preserving intestinal barrier integrity [7]. Diets lacking NDCs have been linked to degradation of intestinal mucus layer glycans by certain gut microbial species [33], leading to defective mucus strength, invasion of enteric pathogens, and a higher risk of metabolic diseases [34]. Polyphenols can enhance gut health by stimulating beneficial bacteria, leading to increased SCFA production. These SCFAs support mucus-secreting goblet cells, thereby boosting mucus production and thickness, and maintaining gut barrier integrity [35]. Recent evidence suggests a direct role of polyphenols on goblet cells and mucin secretion independent of gut microbiota [36], however the exact underlying mechanisms are likely not yet fully understood.

Previous research from our group utilizing pre-clinical mouse models demonstrated that consumption of diets supplemented with either dark-colored or light-colored beans improved intestinal health and demonstrated additional health benefits of dark-colored beans, including biomarkers of colon barrier integrity in lean mice [37], highlighting that the diverse profile of phenolic compounds in certain beans, such as red, black, and blue-violet varieties, may contribute to their beneficial effects [38]. However, no research has exclusively targeted the intestinal and mental health in high-fat-fed diet obese mice by incorporating common beans into a calorie-restriction diet. As described in **project 1**, the inclusion of white (WB) and dark red (DB) kidney

beans (15% wt/wt) in a low-fat diet (LFD) led to favorable changes in the fecal gut microbiota composition. Therefore, in this study we aimed to investigate whether, the observed changes induced by common beans still exist in cecum. Subsequently we aimed to determine the impacts of WB and DB supplementation with various phenolic contents on the biomarkers of intestinal and mental health in an established obesity mouse model.

2. Materials and Methods

2.1 Experimental Design

The current study represents a secondary analysis of the data previously collected for Project 1. The method of beans flour preparation was explained in detail in **Project 1 manuscript**. The bean flour incorporated into the LFD at a ratio of 15% (w/w) which is equal to 1 cup of pulses; a reasonable serving size that aligns with the minimum daily recommendation for enhancing the nutrient density of a healthy diet in most of the populations [39].

In terms of experimental design, briefly, five-weeks old wild-type C57BL/6 male mice were fed a low-fat (13.5 Kcal % fat) purified diet (referred to as LFD, TD. 190833) for a week to facilitate habituation to the new environment, and then animals were randomly assigned to two groups: one group continued to be fed with the LFD (n=8), and the other group was fed a high-fat (60 kcal % fat) diet (referred to as HFD, TD.190378) for 10 weeks to induce obesity (n=48). The diet induced obese (DIO) mice were then randomly assigned into four dietary groups for the interventional phase of the study : (1) continuing to be fed with the HFD (HF control), (2) switching from HFD to LFD (HF→LF), (3) switching from HFD to LFD supplemented with 15% (wt/wt) WB (HF→WB), and (4) switching from HFD to LFD supplemented with 15% (wt/wt) DB (HF→DB) for 8 weeks (n=12 mice/dietary group). Diet composition listed in detail in **Project 1**

manuscript. All the LFDs were isocaloric and their composition were matched in terms of macronutrient quantity and total fiber content**.**

At the end of the intervention period, all mice were euthanized by cervical dislocation and tissues including cecum and cecal contents were collected, weighed using an analytical scale, snap frozen in liquid nitrogen, and stored at −80°C until analysis. Colon was flushed with phosphate buffered saline (PBS) and then sections of proximal colon (≈ 1 cm) was placed in a histology cassette. The tissues were dipped in a 10% buffered formalin solution for 24 hours followed by 70% ethanol until histological analysis. The experimental procedure was approved by University of Ottawa Animal Care Committee (protocol#HS-2857).

2.2 Microbiota DNA Sequencing and Diversity Analysis

Genomic DNA was extracted from the collected cecal content using the QIAamp Fast DNA Stool Mini Kit (Qiagen, Cat. #51604, Germany), according to the manufacturer's instructions [40]. The V3-V4 regions of the 16S rRNA gene were amplified, and the libraries were quantified, normalized, and pooled as per the Illumina 16S Metagenomic Sequencing Library Preparation Guide [41]. The sequencing of the libraries was performed on the Illumina MiSeq platform (Illumina®, Miseq).

The microbial diversity analysis was performed using the QIIME2 bioinformatics pipeline (version 2022.2) [42]. The 300bp Casava 1.8 paired-end demultiplexed files were imported and subjected to quality filtering using DADA2 [43]. This process involved denoising, removal of chimeric sequences, correction of Illumina-sequenced amplicon errors, and generation of amplicon sequence variants (ASVs). A phylogenetic tree was constructed using the Greengenes 13_8 99% identity reference tree [44]. Core diversity analysis was conducted using the QIIME2 core-metric

method at a sampling depth of 10,000. Alpha (α)-diversity metrics, including Shannon, Observed, Pielou's evenness, and Faith's phylogenetic diversity (PD) metrics were generated. Statistical significance of differences in α -diversity between groups was assessed using the Kruskal–Wallis test, followed by Dunn's multiple comparison test. Additionally, dissimilarity matrices were computed to assess beta (β)-diversity distances based on Bray-Curtis matrix [45]. Principal coordinates analysis (PCoA) plots were used to visualize these dissimilarity matrices. PERMANOVA analysis was employed to identify differences in β-diversity between dietary groups, and p-values were adjusted using the Benjamini-Hochberg FDR correction. Taxa abundance comparison between groups was performed in GraphPad Prism (Version 9.5.1) software using the Mann-Whitney U test followed by the two-stage linear step-up method of Benjamini, Kreiger, and Yekutieli ($p<0.05$; FDR<10%). Additionally, to identify discriminating bacteria taxa based on both statistical significance and biological relevance [46], the microbiome taxonomic abundance data were analyzed using linear discriminant analysis with effect size (LEfSe) on the Galaxy Server (https://huttenhower.sph.harvard.edu/galaxy/ accessed on 12 Dec 2023), applying an LDA threshold of 2 and a p-value cut-off of 0.05.

2.3 Predicted Functions of the Metagenome

The microbial community's predictive functional profiling was conducted using Phylogenetic Investigation of Communities by Reconstruction of Unobserved States 2 (PICRUSt2) [47,48] , version 2.51. Briefly, the fragment insertion Qiime2 plugin [53] aligned Amplicon Sequence Variants (ASVs) to the HMMER sequence databases (www.hmmer.org). ASVs were placed optimally onto the reference phylogeny using the SATé-Enabled Phylogenetic Placement (SEPP) tool [49], and a new phylogenetic tree was constructed using the Genesis

applications for phylogenetic placement analysis (GAPPA) [50] Core hidden state prediction functions (hsp.py) were executed with the castor R-package [51] to predict gene family abundances for each ASV and Kyoto Encyclopedia of Genes and Genomes (KEGG) orthologs [52] (KO). Subsequently, the metagenome_pipeline.py command normalized the KO abundances based on 16S abundance. The resulting file (pred_metagenome_unstrat.tsv), containing mouse-specific KO abundances, underwent processing in RStudio (R = V4.2.2, R Studio: V2022.12.0+353) to determine the inferred function of the microbiota. A custom R code, similar to the categorize_by_function.py used in PICRUSt1 [53], aligned the KOs with a manually curated mapping file sourced from https://www.genome.jp/kegg-bin/get_htext?ko00001.keg (accessed on 15 December 2022) [52]. Finally, for outcomes representing inferred functional aspects and group comparisons, STAMP (Statistical Analysis of Taxonomic and Functional Profiles), version 2.1.3 [54], was employed. Welch's two-sided t-test with Benjamini-Hochberg multiple test correction ($q<0.05$) was applied.

2.4 Quantification of Cecal Short Chain Fatty Acids

The assessment of gut microbiota functionality involved the quantification of short-chain fatty acids (SCFAs), such as acetic acid, butyric acid, propionic acid, and valeric acid, along with branched-chain fatty acids (BCFAs), including iso-butyric and iso-valeric acids. The methodology employed in this study followed previously established procedures [55]. In brief, fecal samples were subjected to freeze-drying, and the dry weight was recorded. A 10% homogeneous cecal solution was prepared by diluting the samples in MilliQ water. Subsequent steps included centrifugation, pH measurement, acidification, filtration, and analysis using gas chromatography. Calibration was performed with a standard curve, allowing the identification of various SCFAs

based on retention times. The concentrations of these compounds were determined through comparison with analytical standards.

2.5 Histochemical Analysis

The excised colon tissue was prepared for histological analysis by flushing the colon lumen with phosphate buffered saline (PBS). Approximately 1 cm sections of the proximal colon were placed in a histology cassette. The tissues were then immersed in a 10% buffered formalin solution for 24 hours, followed by 70% ethanol until further analysis. The colon segments were embedded in paraffin, cut into thin sections measuring 0.4 μm, and stained with Hematoxylin and eosin (H&E) and Alcian blue (AB) dyes. The staining procedures were performed by the University of Ottawa Histology Core Facility (Roger-Guidon Hall, Ottawa, ON, Canada). Images of the stained sections were captured at magnifications of 5x (for mucus content analysis) and 10x (for goblet cells and crypt length analysis) using a Zeiss Axiocam 506 microscope camera. The images were scored blindly, meaning that the scorer was unaware of the specific dietary intervention associated with each slide.

To measure crypt length, the H&E-stained sections from the proximal region of the colon was used. In each colon section, 20 fully elongated crypts were selected, and the length of these crypts was measured from the base towards the uppermost enterocyte closest to the colonic lumen using ImageJ software (version:2.9.0/1.53t). Additionally, AB-stained sections from the proximal colon were utilized to quantify the goblet cell density per crypt and to evaluate the colon crypt mucus content. The number of goblet cells were counted in ~20 crypts per mouse in the proximal cross-sectioned regions. To analyze the mucus content from the captured images, the RGB color channels (red, blue, and green) were separated and the mucus present in the center of the lumen

was excluded from the analysis, then, the intensity of the AB-stained areas was quantified using the red channel area, and this value was divided by the total mucosal area and presented as mucus content percentage.

2.6 Assessments of well-being and mental health

The mice underwent behavioral evaluations using a nest building assessment and an elevated plus maze (EPM) test during week 15 of the study at the Animal Behaviour and Physiology Core, University of Ottawa, as described below.

2.6.1 Nest Building Behavior

Nest building is a habitual practice among animals, serving as a means of protection, heat preservation, and reproduction [56]. Better performance on these home cage behaviors may represent normal behavioral function or general well-being of animals [57]. Additionally, nest construction has been proposed as a means of evaluating mood and behavior disturbances linking to neurological disorders like depression and schizophrenia, as well as assessing movement-related disorders such as Parkinson's disease [58]. As a result, we assessed mice nesting behaviour to evaluate mental health and general well-being of animals. Two new pieces of pressed cotton nestlet squares were placed inside the front of the mice cages. Subsequently, nest pictures were captured using a digital camera at 2-hour and 24-hours and used to assign scores for nest quality features, including nestlet shredding, nest shape, and nest wall height adapted from previously established nest scoring methods [59,60], with total scores ranging from 0 to 4.5. The nests were evaluated by two observers who were blinded to time (2h or 24 h) and dietary intervention group, based on the scoring guide **(Supplemental Table 3-3(S1)).**

2.6.2 Anxiety Like Behaviors assessed by Elevated Plus Maze (EPM)

An EPM was utilized as a validated method [61] to assess anxiety-like behaviors and locomotor activity in mice. This test reflects the natural aversion and avoidance behavior of mice when placed in elevated and open areas. Additionally, it evaluates the locomotor activity including general activity performance and natural spontaneous exploratory behavior of mice in novel environments [61,62]. Following acclimatization for 1 hour in the behavior core facility, mice from different groups were randomly placed in an apparatus consisting of two unprotected open arms and two protected closed arms surrounded by walls, horizontally crossed in the centre of the maze. They were allowed to freely explore the maze for 10 minutes, and their movement was recorded by a high-resolution camera suspended above the maze center. The Ethovision XT 15 software (Noldus Information Technology) was employed to analyze activity by measuring parameters such as distance traveled, frequency of entries into the open and closed arms, and time spent in each arm. The ratio of time spent in the unprotected open arms to the time spent in the protected enclosed arms is interpreted as an indicator of anti-anxiety-like behavior in the literature [62].

2.7 Statistical Analysis

Statistical analyses were conducted using GraphPad Prism. The ROUT method, with a significance level (q) set at 1%, was employed to detect outliers in the dataset. D'Agostino-Pearson omnibus test (K2) was performed to evaluate the normality assumption, and both the Brown-Forsythe test and Bartlett's test were conducted to examine the homogeneity of variances for the parametric data. To evaluate the impact of the intervention on parametric data among the different dietary groups, a one-way analysis of variance (ANOVA) was conducted. Further post-hoc analyses, including the Student-Newman-Keuls (SNK) or Tukey's multiple comparison test, were

performed to examine specific pairwise differences between the dietary groups if the ANOVA results were statistically significant. For non-parametric data, two different approaches were utilized depending on the data distribution. In cases where the non-parametric data could be log-transformed to achieve normality, the data was transformed prior to analysis using One-way ANOVA. Alternatively, a Kruskal-Wallis test was conducted followed by Dunn's multiple comparisons test as a post-hoc analysis. The significance level for all statistical tests was set at $p < 0.05$. The detailed statistical results from the ANOVA, Kruskal-Wallis, and other relevant analyses, are provided in Appendix VIII for further reference.

3. Results

3.1. Comprehensive Analysis of the Intestinal Microbiota

In **Project 1** manuscript, we presented the findings of the mice fecal microbiota analysis. We chose fecal samples as our primary focus due to their frequent use in human studies, facilitating the translation of our results to the human gut microbiome. In brief, we demonstrated that bean consumption provided promising indications of improved composition and functionality within the fecal intestinal microbiota when compared to the control group. However, recognizing the potential diversity in microbiota composition among different segments of the intestinal tract [63], we extended our investigation to include cecal samples. We aimed to explore how dietary components were processed and metabolized by various microbial populations in different colon regions. To assess whether the observed beneficial changes in fecal microbiota composition and activity induced by bean consumption were consistent in the cecum, the region responsible for producing SCFAs, as opposed to feces where SCFAs are excreted, we initially employed PCoA β-diversity visualization of microbiota using the Bray Curtis matrix generated by

MicrobiomeAnalyst (available at microbiomeanalyst.ca), for a combination of feces and cecum samples. As shown in **Figure 3-1**, while the abundances of the two sample clusters in cecal and fecal sites exhibited overlapping areas, PERMANOVA analysis confirmed significant differences between the sites**.** These observations prompted us to further explore cecal microbiota analyses to validate the findings observed in fecal samples and investigate how dietary components are processed and metabolized by distinct microbial populations in these regions, contributing to the overall health and function of the gut.

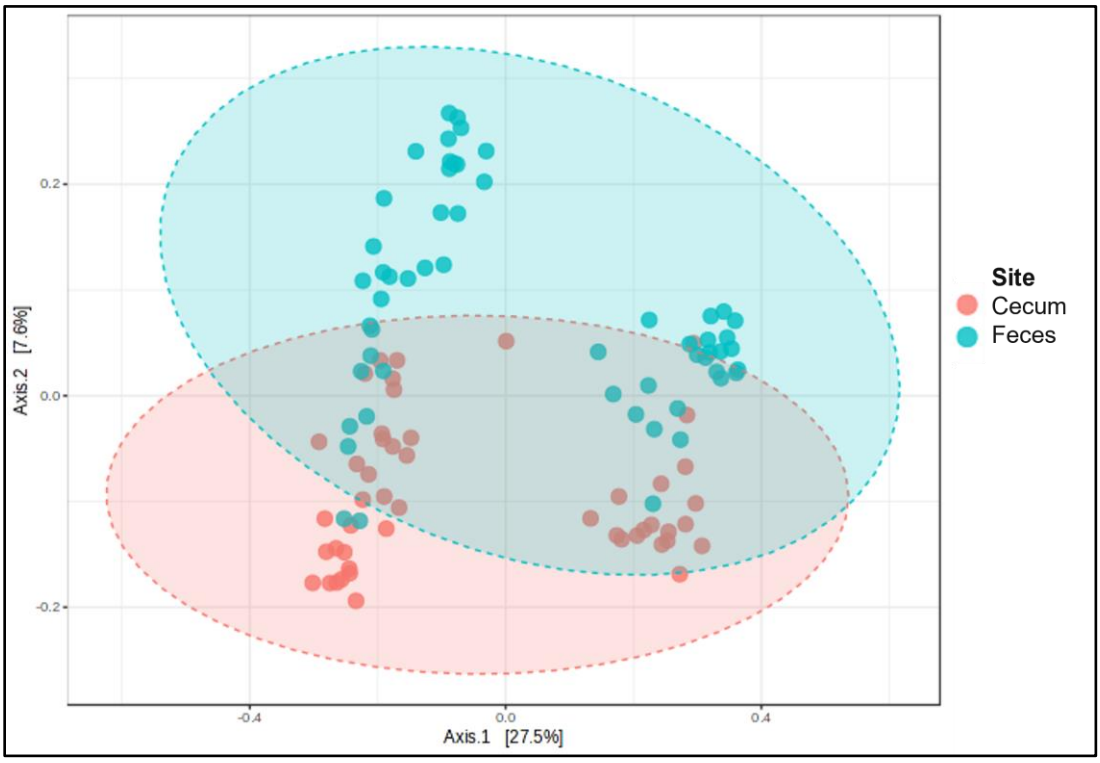

Figure 3-1. Cecal and Fecal Microbiota β -diversity. Bray-Curtis distance matrices were used to explain β-diversity across diet groups. Permutational multivariate analysis of variance (PERMANOVA) pairwise comparisons were used to test the differences between groups (F-value: 7.2239; R-squared: 0.066138; p-value: 0.001). Samples are colored and grouped by their corresponding diet group into ellipses. The multi-testing adjustment conducted based on Benjamini-Hochberg procedure (FDR<0.05).

3.2 Cecal Microbial Community Structure

3.2.1 Cecal Microbiota Diversity

The richness (number of unique species) and evenness (distribution of abundances across the species) [64] within the cecal microbiota samples were evaluated using α-diversity measures. Observed Features (**Figure 3-2B)**, and Faith's PD (**Figure 3-2C)** did not exhibit significant differences among groups. However, introducing beans reduced cecal bacterial community α-diversity indicated by Shannon diversity and Pileou's Evenness compared to other groups (**Figure 3-2A and Figure 3-2D**, respectively).

The PCoA visualization of β-diversity distance matrices, based on Bray-Curtis analysis, demonstrated that the microbial communities clustered according to their respective diets (**Figure 3-2E**). The PERMANOVA analysis revealed no statistically significant differences between bean supplemented groups. Conversely, notable differences were observed between all other dietary groups (**Figure 3-2F**).

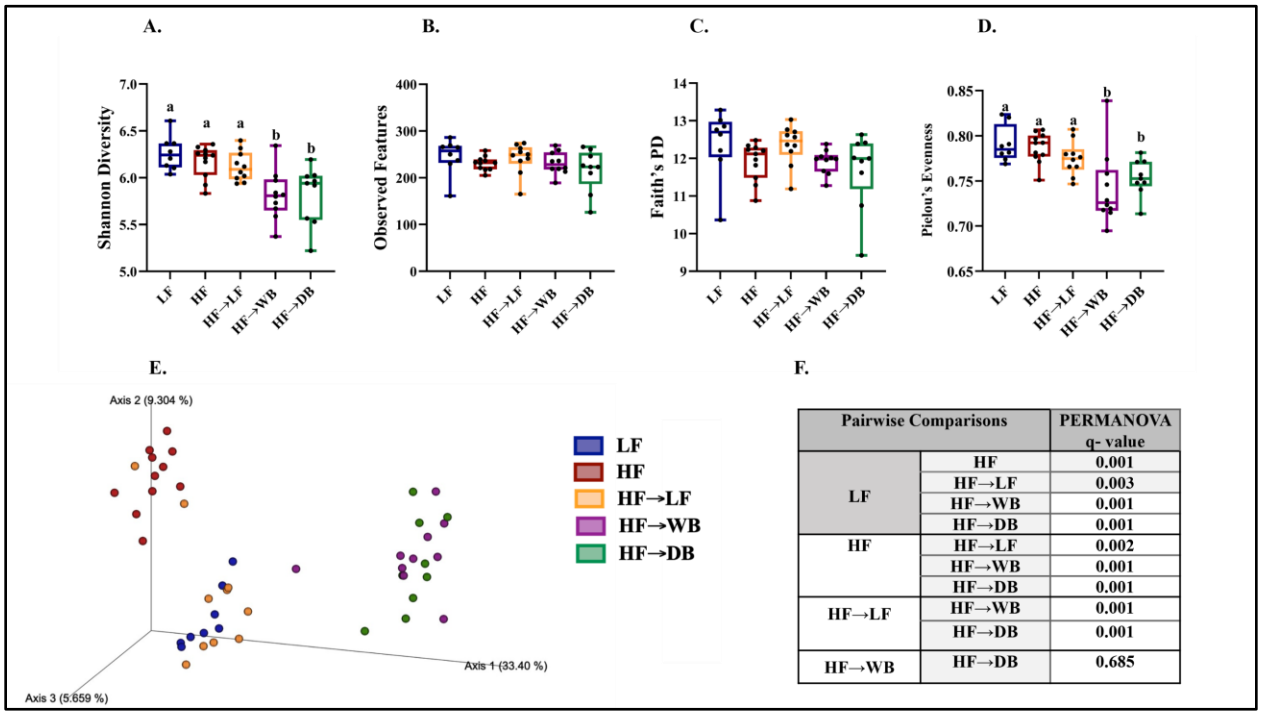

Pairwise Comparisons		PERMANOVA q- value
LF	HF	0.001
	HF→LF	0.003
	HF→WB	0.001
	HF→DB	0.001
HF	HF→LF	0.002
	HF→WB	0.001
	HF→DB	0.001
HF→LF	HF→WB	0.001
	HF→DB	0.001
HF→WB	HF→DB	0.685

Figure 3-2. Cecal Microbiota α-diversity Metrics. **A.** Shannon diversity**, B.** Observed features, **C-** Faith's phylogenetic diversity (PD)**, D.** Pielou's Evenness. **E. Microbiota β-diversity** across the diet groups at the ASVs level visualized by principal component analysis (PCoA) of Bray-Curtis distance matrices. The results are shown in a 3D plot, where the three axes, PC1, PC2, and PC3, indicate the distance between bacterial communities. The microbial communities of samples from each of the intervention groups, including HF, HF→LF, HF→WB, and HF→DB, were clustered together based on their respective diets. Each dot in the plot represented a mouse bacterial

community, and each color represented a different dietary group. The percentage of variation in the data set explained by each principal coordinate was shown in brackets. **F.** PERMANOVA pairwise comparisons q-values. Kruskal-Wallis test was used to analyze the α-diversity data. Adjusted P value (q-value<0.05) was computed following the Benjamini-Hochberg procedure. The plots that did not share a lowercase letter were significantly different. The differences in β-diversity data were analyzed by the permutational multivariate analysis of variance using distance matrices (PERMANOVA), p-value=0.001. (n=8-11/group). LF: Low-fat diet fed lean control group, HF: High-fat diet fed group, HF→LF: High-fat to low-fat diet transition group, HF→WB: High-Fat to low fat + white kidney beans diet transition group, HF→DB: High-fat to low-fat + dark-red kidney beans diet transition group.

3.2.2 Cecal Microbiota Composition

The taxonomic cecal microbial composition from each dietary group as depicted in **Figure 3-3** and detailed in **Table 3-1**, is outlined as follows;

i). Cecal Microbiota Composition in Lean and Obese Controls

The taxonomic analysis of cecal microbial composition revealed notable differences at both phylum and genus levels between lean (LF) and HF obese control groups. Consumption of a HFD for 18 weeks resulted in an increase in TM7 (*F16* (f)) and Deferribacteres (*Mucispirillum* (g)), as well as *Dorea* (g) and *Clostridiales* (o), both belonging to the Firmicutes phylum. Conversely, the relative abundance of *Papillibacter* (g) from the Firmicutes phylum was reduced, along with *Prevotella* (g) and *S24-7* (f), both from the Bacteroidetes phylum, known as carbohydrate-fermenting bacteria [65,66]. These findings align with the reduced carbohydrate content of the HFD fed to obese mice. However, despite these observed alterations, the ratio of Firmicutes/Bacteroidetes did not differ significantly between the LF and HF groups.

ii). Impact of Diet Change on Microbiota Composition Subsequent to Obesity Development

Similar alterations to the previously mentioned microbiota changes were noted in the HF control group when compared to obese mice transitioned to a low-fat diet (LFD), with the exception of *Prevotella* (g) and *Papillibacter* (g), which exhibited no significant changes

Additionally, certain bacterial members such as *Alistipes* (g) from the Bacteroidetes phylum increased, while *Clostridium* (g) from *Lachnospiraceae* (f) which belongs to the Firmicutes phylum, experienced further reductions upon diet change in HF→LF group compared to HF group. These results align to some extent with the β-diversity analysis, which shows more similarity between LF and HF→LF groups, indicating that the diet composition may play a more significant role in affecting microbiota composition than the BW change.

iii). Impact of Introducing Beans to the Low-fat diet on Microbiota Composition

Comparison with HF→LF group: The introduction of beans into the LFD in DIO mice, effectively modified the cecal microbiota composition compared to the HF and HF→LF and groups, including higher abundance of *Prevotella* (g) and *S24-7* (f) and *Clostridium* (g) (from *Lachnospiraceae* (f)). Conversely, beans supplementation resulted in lower abundance of *Dorea* (g), *Papillibacter* (g), *Sporobacter* (g), *Clostridium* (g) (from *Ruminococcaceae* (f)), *Clostridiales* (o), and other undefined members of *Ruminococcaceae* (f), all belonging to the Firmicutes phylum. Furthermore, there was a decrease in the abundance of *Parabacteroides* (g) from the Bacteroidetes phylum, and *Mucispirillum* (g) from the Deferribacteres phylum. The observed bacterial alterations overall contributed to a significantly reduced abundance of Firmicutes and Deferribacteres phyla, while promoting an increased abundance of the Bacteroidetes phylum in beans supplemented groups when compared to the HF and HF→LF groups. These changes ultimately led to a further reduction in the Firmicutes/Bacteroidetes ratio in both bean-supplemented diets, which, according to some studies but not all, has been considered a hallmark of obesity [67] and thereby could be potentially regarded as a favorable shift in gut microbiota composition.

Comparison with HF group: In addition to the alterations mentioned above, incorporation of beans to the LFD resulted in significant further increases in Proteobacteria (*Alphaproteobacteria* (c)) when compared to the obese mice cecal microbiota remained on HFD.

iv). Differential Effects of White and Dark-red Kidney Beans on Microbiota Composition

The diets supplemented with beans showed overall similarities in microbial structure at the genus and phyla levels. However, subtle differences were observed between the different varieties of beans and their effects on certain bacterial taxa compared to HF→LF and HF obese control groups.

Comparison with HF→LF group*:* In addition to the common observed microbial alterations induced by both bean diets, few bacterial genera from the Firmicutes phylum modified differently in HF→WB group, when compared to the HF→LF group. Specifically, consumption of WB significantly increased the abundance of *Lactobacillus (*g), while reducing the abundance of *rc4-4* (g), *Oscillospira (g),* and *Defluviitalea (g).* On the other hand, DB supplementation, showed a reduced Cyanobacteria in comparison with HF→LF group.

Comparison with HF group: In HF→WB group, there was an increase in Lactobacillus (g) from the Firmicutes phylum, which was not seen in DB supplemented diet group when compared to the HF group. Additionally, the HF→DB group exhibited increased abundance of Verrucomicrobia (*Akkermansia* (g)), indicating unique effects of this bean variety. In contrast, the HF→DB group revealed a significant reduction in certain bacterial genera, including *Papillibacter* (g) and *Clostridium* (g) from the Firmicutes phylum and *Bacteroides* (g) from the Bacteroidetes phylum, when compared to the HF diet fed obese controls.

Overall, these findings highlight the potential impact of different bean types on the gut microbiota and may offer valuable insights into their distinct role in promoting gut health.

Table 3-1. Relative abundance of the cecal microbiota in mice (phyla and genus).

Taxonomy	Relative abundance (%)				
	LF	HF	HF→LF	HF→WB	HF→DB
p-Firmicutes	49.47 ±2.48	52.74±1.71	48.25±2.20	32.44±1.90 [1, 2, 3]	32.44±1.90 [1, 2, 3]
f__Bacillaceae;g__	0.08±0.04	0.00±0.00	0.11±0.04 [1]	0.26±0.11	0.45±0.30
g__Lactobacillus	0.08±0.04	0.22±0.06	0.17±0.08	0.46±0.08 [1, 2]	0.25±0.09
o__Clostridiales;f__;g__	5.01±0.83	4.16±0.52	4.51±0.46	4.83±0.67	3.78±0.50
o__Clostridiales;f__;g__	5.56±0.68 [1]	10.03±0.79	6.53±1.80 [1]	1.73±0.39 [1, 2]	2.38±0.40 [1, 2]
f__Lachnospiraceae;g__	11.04±2.10	6.77±1.10	11.12±1.74	8.00±0.89	7.47±1.34
f__Lachnospiraceae; g__Clostridium	3.06±0.52	2.83±0.25	1.72±0.17 [1]	3.34±0.47 [2]	3.36±0.63 [2]
g__Defluviitalea	0.75±0.11	0.86±0.20	0.65±0.14	0.20±0.03 [2]	0.27±0.06
g__Dorea	0.47±0.06 [1]	0.74±0.06	0.48±0.05 [1]	0.25±0.04 [1, 2]	0.29±0.06 [1, 2]
g__rc4-4	0.62±0.16	0.30±0.06	0.45±0.13	0.12±0.02 [2]	0.25±0.05
f__Peptostreptococcaceae ;g__[Clostridium]	0.97±0.58	0.34±0.19	0.47±0.28	0.82±0.24	0.60±0.22
f__Ruminococcaceae;g__	5.28±0.68	7.03±0.30	4.90±0.40 [1]	4.07±0.45 [1]	4.15±0.53 [1]
f__Ruminococcaceae;g__	9.65±1.25	9.19±0.53	9.75±0.70	4.51±0.54 [1, 2]	4.68±0.44 [1, 2]
f__Ruminococcaceae; g__Clostridium	2.39±0.40	4.82±0.52	2.54±0.40 [1]	1.40±0.14 [1, 2]	1.25±0.15 [1, 2]
g__Oscillospira	1.18±0.21	0.96±0.24	1.38±0.13	0.98±0.13 [2]	1.18±0.22
g__Papillibacter	0.64±0.15 [1]	0.16±0.04	0.23±0.05	0.07±0.03 [2]	0.06±0.02 [1, 2]
g__Ruminococcus	0.21±0.041	0.11±0.02	0.21±0.04	0.19±0.05	0.12±0.02
g__Sporobacter	2.35±0.44	3.97±0.46	2.71±0.35	1.03±0.21 [1, 2]	1.47±0.30 [1,2]
p-Bacteroidetes	46.22 ±2.28	40.51±1.53	46.10±2.27	64.31±2.14 [1, 2, 3]	64.31±2.14 [1,2, 3]
o__Bacteroidales;f__;g__	0.80±0.37	0.21±0.03	0.31±0.06	0.30±0.05	0.21±0.05
g__Bacteroides	10.93±1.28	14.33±1.27	13.10±1.95	10.89±1.30	9.13±1.37 [1]
g__Parabacteroides	0.95±0.43	0.91±0.10	0.86±0.12	0.30±0.08 [1,2]	0.22±0.06 [1, 2]
g__Prevotella	0.16±0.04 [1]	0.05±0.03	0.13±0.04	10.23±1.31 [1, 2]	10.22±1.10 [1, 2]
g__Alistipes	16.06±0.91	15.45±0.70	18.12±0.81 [1]	21.17±2.15 [1]	20.04±0.94 [1]
f__S24-7;g__	17.32±2.20[1]	9.56±0.55	13.59±0.80 [1]	21.43±1.64 [1, 2]	24.86±1.32 [1, 2]
p-Deferribacteres	2.29±0.43 [1]	5.01±0.52	3.90±0.72	1.39±0.27[1, 2]	1.03±0.20 [1, 2, 3]
g__Mucispirillum	2.29±0.43 [1]	5.01±0.52	3.90±0.72	1.39±0.27 [1, 2]	1.03±0.20 [1, 2]
p-Proteobacteria	0.65±0.19	0.24±0.04	0.57±0.16	0.71±0.12 [1]	0.71±0.12 [1]
c__Alphaproteobacteria; g__	0.65±0.19	0.24±0.04	0.57±0.16	0.71±0.12 [1]	0.71±0.12 [1]
p-TM7	0.14±0.07 [1]	0.54±0.07	0.20±0.06 [1]	0.18±0.06 [1]	0.09±0.02 [1]
f__F16;g__	0.14±0.07 [1]	0.54±0.07	0.20±0.06 [1]	0.18±0.06 [1]	0.09±0.02 [1]
p-Verrucomicrobia	0.66±0.30	0.49±0.22	0.58±0.27	0.57±0.31	1.39±0.38 [1]
g__Akkermansia	0.66±0.30	0.49±0.21	0.58±0.27	0.57±0.31	1.39±0.38 [1]
p-Cyanobacteria	0.55±0.12	0.46±0.12	0.40±0.06	0.38±0.15	0.17±0.06 [1,2]
o__YS2;f__;g__	0.55±0.12	0.46±0.12	0.40±0.06	0.38±0.15	0.17±0.06

Relative abundance (mean±S.E.M.) of cecal bacterial taxa at the phylum level (rows highlighted in grey), or the corresponding order (o), family (f), or genus level (g) (white rows) with mean abundance greater than 0.2% in at least one group. The data analysed by Mann-Whitney test followed by a two-stage linear step-up procedure of Benjamini, Kreiger and Yekutieli to correct for multiple comparisons (corrected p-value<0.05; FDR<10%) (n=8-11 mice/group) to compare LF vs HF; HF vs HF→LF, HF→WB and HF→WD; HF→LF vs HF→WB and HF→WD; and HF→WB vs HF→WD. Significantly different values are indicated by [1, 2] superscript. [1] Significantly different from the HF group; [2] Significantly different from HF→LF. LF: Low-fat diet fed lean control group, HF: High-fat diet fed group,

HF→LF: High-fat to low-fat diet transition group, HF→WB: High-Fat to low fat + white kidney beans diet transition group, HF→DB: High-fat to low-fat + dark-red kidney beans diet transition group.

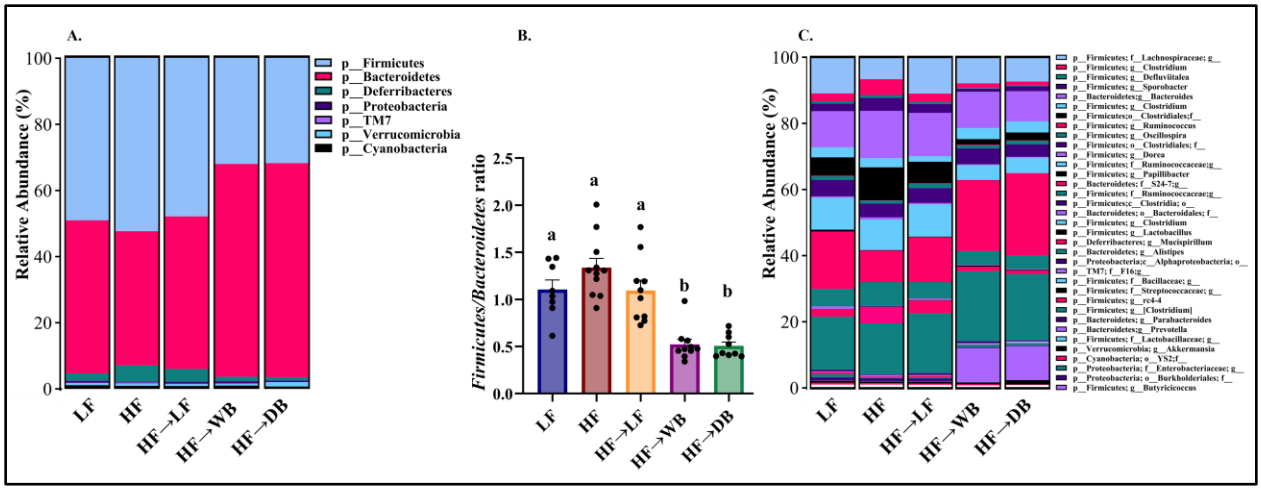

Figure 3-3. Taxonomic Structure of Cecal Microbiota. A- Taxonomic relative abundance of cecal microbiota at the phylum level (p), **B.** Firmicutes/Bacteroidetes ratio **C.** Taxonomic relative abundance of cecal microbiota at the genus level (g) (labels show microbiota taxa composition according to the phyla and genus where applicable, or the family (f)/order (o) for the unclassified genera), (n=8-11 mice/group). LF: Low-fat diet fed lean control group, HF: High-fat diet fed group, HF→LF: High-fat to low-fat diet transition group, HF→WB: High-Fat to low fat + white kidney beans diet transition group, HF→DB: High-fat to low-fat + dark-red kidney beans diet transition group.

The discriminant analysis of gut microbiota composition using the LEfSe method revealed results like those presented in **Table 3-1**. However, when comparing the microbiota of mice in the HF→LF group with the HF group, we identified fewer differentially abundant taxonomic classes compared to the distinctions observed between the LF and HF groups. This suggests that despite the diet switch in HF→LF, the microbiota composition has not fully returned to a normal state. Notably, our results indicated that introducing beans, along with a switch to a LFD in HFD fed obese mice, not only restored the microbiota composition to that observed in LF mice, but also induced a greater number of differentially abundant taxonomic classes. Moreover, despite observing a few more differences in microbial taxa abundance between the HF→DB and HF group

compared to the HF→WB and HF group, no significant differences were found between the WB and DB supplemented groups (**Figure 3-4B)**.

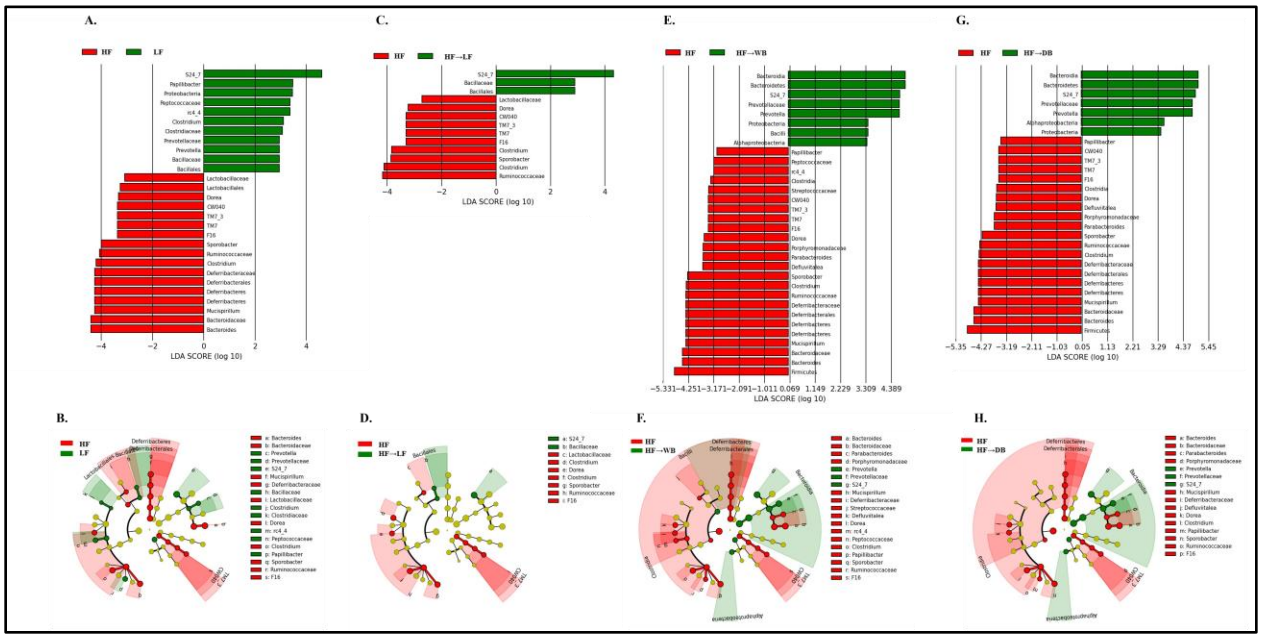

Figure 3-4. LEfSe Results on Cecal Microbial Taxonomy. Histogram of the LDA scores computed for features differentially abundant between; **A.** HF and LF, **C**. HF and HF→LF, **E**. HF and HF→WB, **G.** HF and HF→DB. **B**, **D, F, and H.** Taxonomic Cladogram (phylum to genus) from LEfSe, depicting taxonomic association between microbiome communities of the respective groups. Each node represents a specific taxonomic type. Red and green nodes denote the taxonomic types with more abundance within the respective groups. ($LDA > 2$, $p < 0.05$). (n=8-11 mice/group). LF: Low-fat diet fed lean control group, HF: High-fat diet fed group, HF→LF: High-fat to low-fat diet transition group, HF→WB: High-Fat to low fat + white kidney beans diet transition group, HF→DB: High-fat to low-fat + dark-red kidney beans diet transition group.

3.3 Cecal and Colon Health Parameters

The consumption of both bean-supplemented diets led to a significant increase in the total weight of the cecum, cecum content weight and moisture content when compared to the other groups **(Table 3-2)**. Similarly, consumption of beans led to a significant increase in colon length compared to the LF and HF control groups. On the other hand, colon weight remained unaffected by the dietary treatments. Furthermore, the proximal colon histomorphology, including crypt length measured in proximal colon cross-sections stained with H&E, as well as mucin-containing

goblet cell density and mucus content percentage quantified in the proximal sections stained with AB, showed no significant differences between groups.

Table 3-2. Cecal and Colon Parameters in Treatment groups.

	Groups				
	LF	**HF**	**HF→LF**	**HF→WB**	**HF→DB**
Total Cecum Weight (g)	0.24±0.01	0.25±0.01	0.26±0.01	0.35±0.01[a]	0.33±0.02[a]
Cecum Content (g)	0.17±0.01	0.18±0.01	0.18±0.01	0.26±0.01[a]	0.24±0.01 [a]
Cecum Content Moisture, %	70.49±0.96[b]	67.09±0.68[b]	70.18±0.96[b]	75.94±0.64[a]	75.41±0.74[a]
Colon Length (cm)	7.54±0.06 [b]	7.62±0.09[b]	8.07±0.16[ab]	8.26±0.17 [a]	8.52±0.13 [a]
Colon Weight (g)	0.15±0.00	0.18±0.01	0.18±0.01	0.19±0.01	0.18±0.01
Crypt Length (µm)	120.1±3.67	104.8±3.05	111.4±4.48	122.8±8.14	122.4±5.39
Mucus Content, %	30.87±2.36	26.50±1.61	35.22±4.13	30.94±2.15	32.89±3.19
Goblet Cell Count	10.82±1.1	9.74±0.46	11.13±0.78	12.54±0.90	12.77±1.09

Parametric data was analysed by One-way ANOVA (Total cecum weight followed by Tukey's post-hoc multiple comparisons test, and non-parametric data was either log-transformed (Cecum content and cecum content moisture, %) to normalize or analysed by Kruskal-Wallis (Colon length) followed by Dunn's multiple comparisons test. Significantly different values are indicated by [1, 2, 3] superscripts. Values with different superscripts are significantly different ($p< 0.05$). Values are displayed as means±S.E.M. (n=5-8 in LF and n=9-12 mice other groups). LF: Low-fat diet fed lean control group, HF: High-fat diet fed group, HF→LF: High-fat to low-fat diet transition group, HF→WB: High-Fat to low fat + white kidney beans diet transition group, HF→DB: High-fat to low-fat + dark-red kidney beans diet transition group.

3.4 Cecal Microbial Community Function

3.4.1 Functional Metagenome Prediction Analysis

To identify the differential predicted metagenomic functional pathways in the microbial populations KEGG pathways were compared among the dietary groups. Surprisingly, when comparing the HF obese and HF→LF groups, no distinct changes in KEGG pathways were detected. On the other hand, the mean proportion of 202 metagenomic pathways were found significantly different between the HF→WB and HF control mice microbial community **(Figure 3-5A)**. Further, the mean proportion of 197 metagenomic pathways were found significantly different between the HF→DB group and HF groups **(Figure 3-5B)**. As expected, in line with the microbiota composition results, no difference was observed in functional pathways of the microbial communities in bean-supplemented groups. The Venn diagram analysis revealed 97

shared pathways that exhibited an increase in both the HF→WB and HF→DB groups when compared to HF group. Additionally, there were 17 pathways that were uniquely increased in HF→WB group, and 6 pathways that were uniquely increased in HF→DB group when compared to the HF control group **(Figure 3-5C)**. On the contrary, there were 84 shared pathways that showed a reduction by both bean diets compared to the HF control group, while 4 pathways were uniquely reduced in HF→WB and 10 pathways were uniquely reduced in HF→DB group **(Figure 3-5D)**. To provide specific examples, flagellar assembly, bacterial chemotaxis, transcription factors, glucagon signaling pathway, NOD-like receptor signaling, and Plant pathogen interaction were overrepresented in HF when compared to the beans supplemented groups. Conversely, some other pathways such as thermogenesis, lysosome, apoptosis, adipocytokine signaling pathway, and PPAR signaling pathway were underrepresented in HF compared to the bean groups.

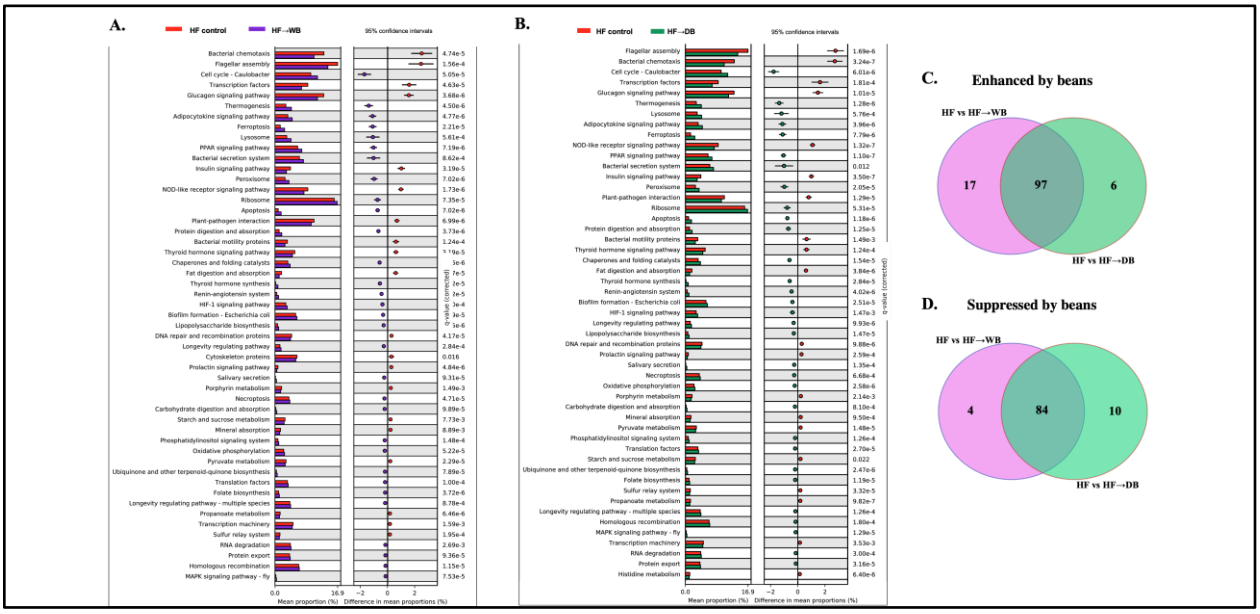

Figure 3-5. Predicted Functional Differences of the Microbial Communities. PICRUSt2 results indicating significantly altered bacterial Kyoto Encyclopedia of Genes and Genomes (KEGG) pathways at level 3 between; **A.** HF control vs HF →WB, **B.** HF control vs HF →DB. The PICRUSt2 data was analyzed in STAMP using Welch's two-sided t-test with Benjamini-Hochberg multiple test correction (q<0.05), (n=9-11 mouse/group). The illustration displayed the average percentage of predicted KEGG pathways on the left and the variation in average percentages on the right for each comparison. Venn diagrams displaying the total number of unique and common bacterial functional pathways that were; **C.** up-regulated or, **D.** down-regulated in beans-supplemented groups compared to the HF control group. (n=8-11 mice/group). LF: Low-fat diet fed lean control group, HF: High-fat diet fed group, HF→LF: High-fat to low-fat diet transition group, HF→WB: High-Fat to low fat + white kidney beans diet transition group, HF→DB: High-fat to low-fat + dark-red kidney beans diet transition group.

3.4.2 Cecal Short-Chain Fatty Acids and pH

SCFAs and branched chain fatty acids (BCFAs) were measured in the cecum content as indicators of microbial fermentation activity. The pH of cecal content reduced significantly in the HF→DB group compared to HF→LF and HF control, with no significant difference observed between bean-supplemented groups **(Figure 3-6A).** Total cecal SCFAs, as well as the individual levels of acetic, propionic, and butyric acids did not exhibit any significant difference between HF→LF and HF mice, whereas, both bean diets significantly augmented the levels of total SCFAs, as well as the aforementioned individual SCFAs, compared to the HF→LF and HF control groups. Although there was a noticeable trend of increased SCFA levels in the cecal content of mice consuming the DB supplemented diet, no significant differences were observed between the bean varieties. Conversely, valeric acid levels did not show any difference among groups **(Figure 5B-F)**. Similarly, total BCFAs and the individual levels of iso-butyric and iso-valeric levels did not differ between groups **(Figure 3-6G-H)**.

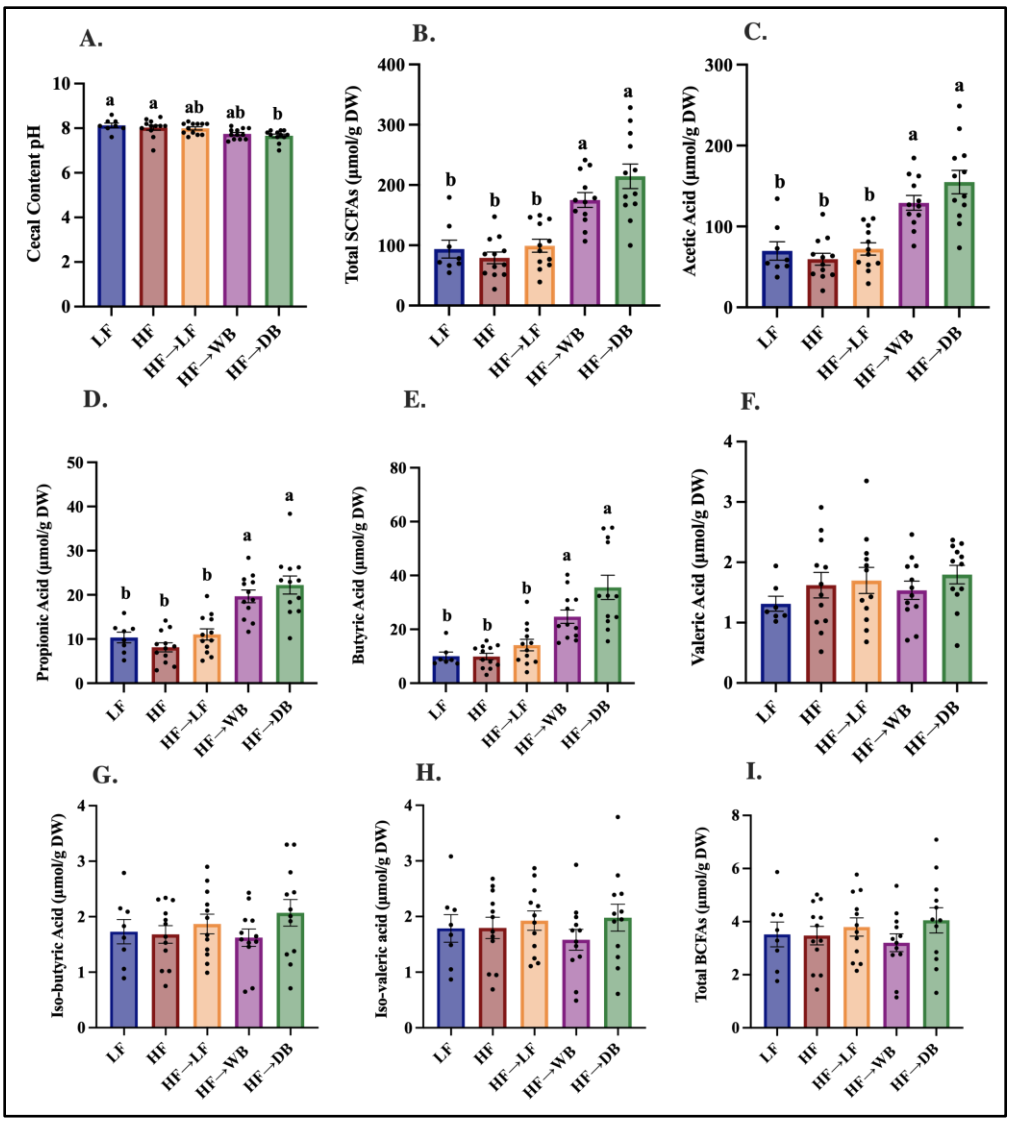

Figure 3-6. Analysis of Cecal Short-chain Fatty Acids (SCFAs). Cecal content pH. **B.** Total cecal SCFAs (µmol/g DW). **C.** Cecal Acetic acid. **D.** Cecal Propionic acid (µmol/g DW). **E.** Cecum Butyric acid (µmol/g DW). **F.** Cecal Valeric acid (µmol/g DW). **G.** Cecal Iso-butyric acid (µmol/g DW). **H.** Cecal Iso-valeric acid (µmol/g DW). **I.** Total cecal Branched chain fatty acids (BCFAs) **(**µmol/g DW). Values are means±S.E.M. Parametric data was analysed by One-way ANOVA (Total cecal SCFAs, acetic acid, and propionic acid) followed by Tukey's post-hoc multiple comparisons test, and non-parametric data was either log-transformed to normalize (Butyric acid) or analysed by Kruskal-Wallis (Cecal content pH) followed by Dunn's multiple comparisons test. Bars not sharing a lower-case letter differ significantly ($p<0.05$). (n=8-11 mice/group). LF: Low-fat diet fed lean control group, HF: High-fat diet fed group, HF→LF: High-fat to low-fat diet transition group, HF→WB: High-Fat to low fat + white kidney beans diet transition group, HF→DB: High-fat to low-fat + dark-red kidney beans diet transition group.

3.5 Mental Health Related Outcomes

3.5.1 Nest Quality

The nest scores given blindly by two observers were averaged and displayed on a scale of 0 to 4.5. The analysis of nesting scores revealed a significant improvement in nest quality over a 24-hour period within groups, while the nest scores did not differ between groups in any of the 2-hour or 24-hour evaluation sessions **(Figure 3-7A and 3-7B).**

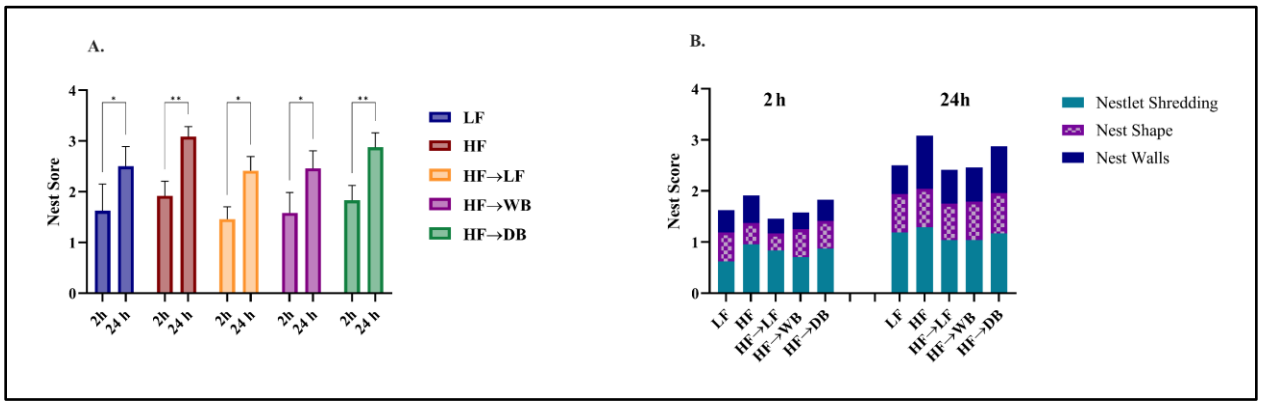

Figure 3-7. Assessment of Nest Quality. A. Nesting behavior in 2-hour vs 24-hour within the dietary groups. **B.** Changes of nesting score parameters in 2-hour vs 24-hour between groups. Data was analyzed by two-way ANOVA followed by Tukey's post-hoc test (n=8-12 mice/group). (P <0.05 and P<0.01 are displayed as * and **, respectively), (n=8 in LF and n=12 other groups). LF: Low-fat diet fed lean control group, HF: High-fat diet fed group, HF→LF: High-fat to low-fat diet transition group, HF→WB: High-Fat to low fat + white kidney beans diet transition group, HF→DB: High-fat to low-fat + dark-red kidney beans diet transition group.

3.5.2 Anxiety-like Behaviors

Since evidence has shown that experimental manipulations like exposure to stress, psychoactive pharmacological agents [68] as well as diet-induced obesity [69] have the potential to alter the open arm aversion and general performance of the mice, the EPM test was performed in mice from different dietary groups near the termination of the study at week 16. The percentage of time spent in the open arms of the maze was calculated as a percentage of the total test time using the following formula: open arm time % = open arm time (sec) / 600 (sec) * 100. The center point tracking of HF mice revealed decreased number of entries into the open arms when compared to the lean mice, while it was attenuated in all DIO mice transitioning to LFD **(Figure 3-8A).** The

latency of the first entry into the open arms increased in both LF and HF groups when compared with HF→WB **(Figure 3-8B)**, which is likely an indication of anxiolytic-like effects of WB supplementation. However, the percentage of time spent on the open arms did not differ between dietary groups **(Figure 3-8C)**. When anxiety levels were assessed by tracking the mice nose point, similar results were found in the number of entries into the open arms as in the center point tracking **(Figure 3-8D)**. The reduced number of entries into the open arms was accompanied by a significant increase in the percentage of time spent on the closed arms in HF mice compared to the lean mice **(Figure 3-8E)**. Additionally, we found a significant decrease in percentage of time spent in the open arms in HF and HF→LF when compared with the lean group **(Figure 3-8F)**. This is likely representative of anxiety-like behaviors, while no such difference was found in any of the HF→WB and HF→DB groups.

Overall, the EPM results suggested some evidence of increased anxiety-like behaviors in HFD fed obese mice, while switching the diet composition into an LF diet and, in particular, in combination with beans, could to some extent reverse this effect.

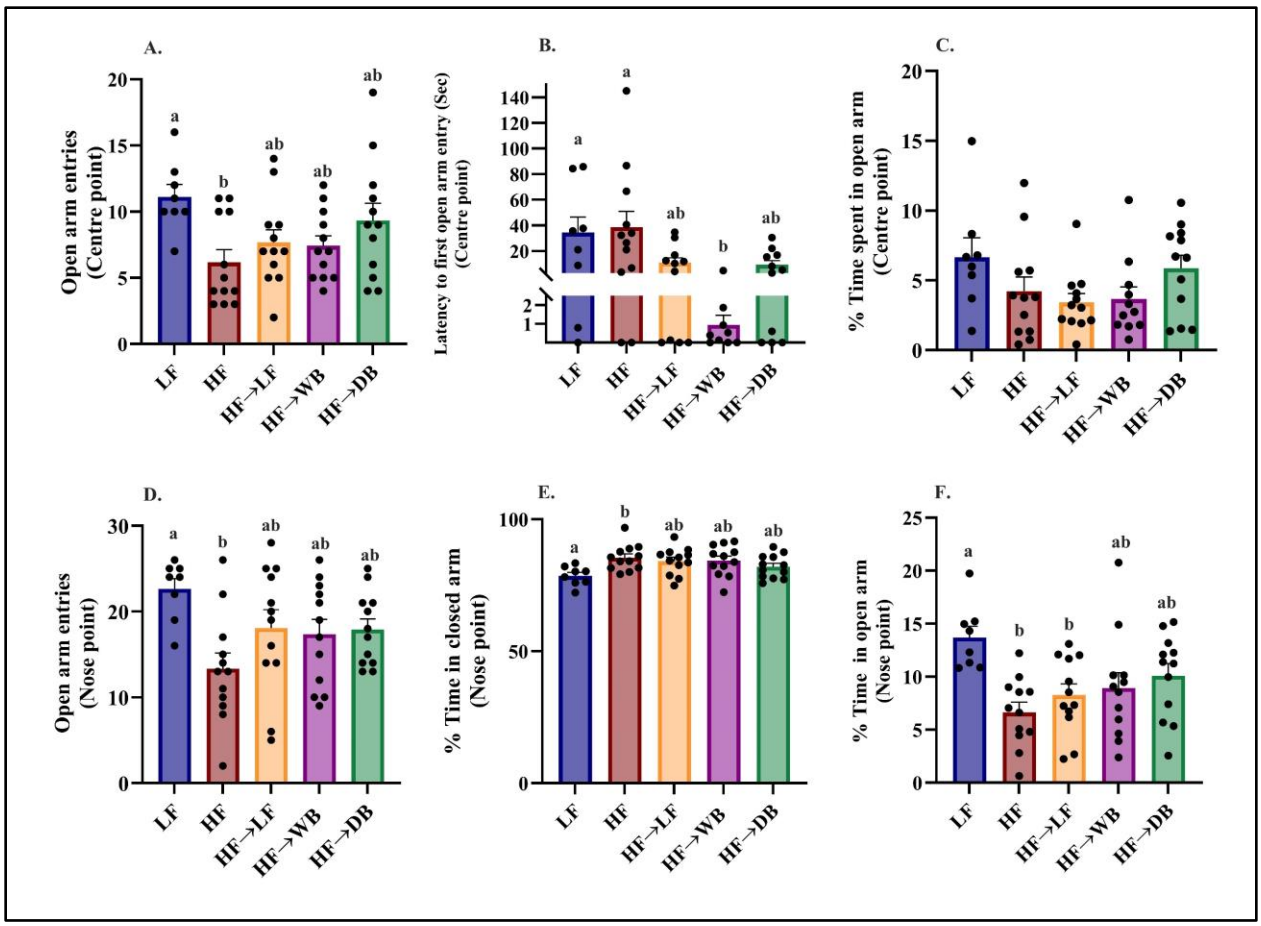

Figure 3-8. Anxiety Like Behavior Assessment. Mice centre point tracking: A. Total number of entries into the open arms of the elevated plus maze, **B.** Latency to enter to the open arms, **C.** Percent time spent in the open arms. **Mice nose point tracking: D.** Total number of entries into the open arms of the elevated plus maze, **E.** Percent time spent in the closed arms. **F.** Percent time spent in the open arms. Parametric data was analysed by One-way ANOVA followed by Tukey's multiple comparisons test (Total number of entries into the open arms (centre and nose points), Percent time spent in the closed arms and open arms (nose point)) and non-parametric data was either log-transformed to normalize or analysed by Kruskal-Wallis test (Latency to enter to the open arms) followed by Dunn's multiple comparisons test. (n=8-12 mice/groups). LF: Low-fat diet fed lean control group, HF: High-fat diet fed group, HF→LF: High-fat to low-fat diet transition group, HF→WB: High-Fat to low fat + white kidney beans diet transition group, HF→DB: High-fat to low-fat + dark-red kidney beans diet transition group.

4. Discussion

The consumption of modern Western diets with low amounts of dietary fibers malnourishes the gut microbiota, causing a disruption in gut microbiota composition and metabolic dysfunctions which can negatively affect host health [70,71]. To the best of our knowledge, the present study is the first to focus on the effects of two common bean varieties, with distinct quantities and profiles

of phenolic compounds [38], on colonic microenvironment, including the microbiota composition and function, as well as colon histological structure in an established obesity animal model. Additionally, in this study we explored the potential for bean supplemented diets to impact aspects of the gut-brain axis. Findings of this study revealed that white and dark bean supplemented diets increased the production of cecal SCFAs. Additionally, both bean varieties elicited shared beneficial alterations in microbiota composition and predicted metagenomic functional pathways, while they also demonstrated unique individual effects. Additionally, bean supplementation showed promising effects in mitigating anxiety-like behaviors.

The rise in cecal SCFAs in beans supplemented groups in this study (**Figure 3-6)** was consistent with a significant increase in SCFAs-producing bacteria, including *Prevotella* (g) and *S24-7* (f) **(Table 3-1)**. The *S24-7* is mainly a butyrate producer with anti-obesity effects [72] which has been shown to be involved in reinforcing intestinal epithelial cell health and enhancing energy metabolism [73]. Butyrate plays a protective role in intestinal barrier function and reducing inflammation [74]. In the current study, no significant differences were noted between groups supplemented with different types of beans with respect to the total SCFAs, as well as individual levels of acetate, propionate, and butyrate. However, compared to the HF control group, the abundance of *Akkermansia* from the Verrucomicrobia phylum, which is known to be inversely associated with obesity, diabetes, and inflammatory responses [75], increased by 2.8-fold only in the DB supplemented group. On the other hand, the abundance of *Bacteroides,* which has been reported to be positively correlated with BMI [76], decreased by 64% in response to DB supplementation when compared to HF obese controls. In contrast, the supplementation of WB did not show such effects. These distinct effects observed between DB and WB could potentially be attributed to the higher content of phenolic compounds in dark beans [38]. However, the cecal

microbiota composition of mice fed diet supplemented with WB powder showed significant differences in the abundance of some of the certain bacterial genera, including a higher abundance of *Lactobacillus* (known for its probiotic properties and its potential in alleviating obesity-associated dysfunctions [77]) compared to both HF and HF→LF groups. In contrast, lower abundances of rc4-4, *Oscillospira* (positively correlated with leanness and negatively correlated to intestinal inflammation [78]), *Defluviitalea,* and unclassified genera belonging to *Clostridiales* were observed compared to the *HF→LF* group. These differences may be related to the distinct phenolic profile in WB compared to DB. The abundance of *Dorea* (g) was significantly higher in the HF controls compared to all other groups. *Dorea* has been reported to be positively correlated with BMI and obesity-associated metabolic dysfunction (like waist circumference and diastolic blood pressure), as well as having pro-inflammatory properties in the intestine [72]. Conversely, a significant surge in *Alistipes* abundance in DIO mice, after the transition from an HFD to an LFD irrespective of bean incorporation, underscores its potential contribution to alleviating adiposity and mitigating metabolic syndrome, as suggested by available literature [79,80]. Although controversial [81], existing literature seems to support greater *Firmicutes*/*Bacteroidetes* ratio in the gut microbiota of obese animals and humans living with obesity [67,82]. In our study, no difference was found in Firmicutes/Bacteroidetes ratio between lean and obese control groups. However, the ratio of Firmicutes/Bacteroidetes significantly decreased by 39% and 38 % in WB and DB fed mice, respectively, when compared to the obese control group. Both bean diets similarly altered microbiota composition at the phylum level by profoundly reducing *Firmicutes* and increasing *Bacteroidetes* abundances. These results are consistent with other trials that have used common beans in obesity development or established obesity rodent models [83–86].

The inferred metagenomic properties of the gut microbiota, as predicted from the KEGG pathways, demonstrated distinct potential functional capabilities in the beans-supplemented groups compared to the other groups **(Figure 3-5)**. Both beans-enriched diets upregulated pathways such as protein digestion and absorption, carbohydrate digestion and absorption, and starch and sucrose metabolism. In contrast, they downregulated pathways related to fat digestion and absorption, insulin signaling pathway, and insulin resistance, when compared to both the HF and HF→LF groups. No difference in inferred metagenomic pathways was observed between the beans-containing diets, suggesting a similar functional profile of the gut microbiota, which was further confirmed by the similar concentrations of SCFAs as an actual functional outcome.

The increased cecal SCFAs levels in our study were accompanied by a significant rise in several parameters related to intestinal size, including total cecum weight, cecum content, and colon length in beans supplemented groups **(Table 3-2)**. However, our findings did not support enhancement of proximal colon histomorphology outcomes. One plausible explanation for this finding comes from existing evidence, which has shown that obesity, can independently lead to an increase in crypt length and goblet cells in the small intestine in DIO mice, suggesting higher adaptability in cellular differentiation and proliferation towards more functional cells at the crypt-villus axis, potentially influenced by the high-fat content of the diet in HF mice [87]. Therefore, administering beans alone may not sufficiently enhance histological outcomes in the proximal colon of established-obese mice, given the pre-existing impact of obesity on these parameters. Further investigation is warranted to understand the specific mechanisms underlying histological changes and how diet composition, obesity and microbiota-derived metabolites interact to influence these outcomes. Additionally, exploring the effects of different dosages or longer intervention durations may provide valuable insights into the observed effects.

To our knowledge, no study has assessed nesting behaviour as a measure of mental health in bean-fed mice. In present study, the dietary intervention showed no influence on nesting quality of the mice **(Figure 3-7)**. This could be partly due to the use of cotton squares as the nest-building material, which may only fulfill the basic nesting behavior needs of all mice and not provide enough material for mice to build more complex nests with higher quality [60]. As a result, it may be difficult to distinguish a specific dietary group of mice in the current study from others based on their nest-building quality scores. Unlike the nest-building behavior, HFD-fed mice exhibited increased anxiety-like behavior compared to the LF group in the EPM test **(Figure 3-8)**. This aligns with studies linking HFD and altered anxiety-related indices [88–90]. Transitioning from HFD to LFD could ameliorate the obesity associated anxiety effects in all the DIO mice compared to the obese control group. Additionally, the introduction of beans also showed a trend of increased time spent in the open arm (nose-point) compared to both HF and HF→LF groups, suggesting potential anxiolytic-like effects. While this trend was not statistically significant, it may be partly attributed to higher SCFAs production, supported by evidence linking butyrate to memory, cognition, and mood improvement, while propionate may have stress-reducing effects [91]. Moreover, the WB-supplemented group showed further anxiolytic-like effects, such as reducing the first visit latency to the open arms, possibly due to unique phenolic profile and interactions with the gut microbiota, reflecting the gut-brain axis responses.

Since the EPM test relatively exposes higher anxiety load to rodents compared to other anxiety assessment tests [92,93], it might explain subtle differences between bean-fed and other groups. On the other hand, the EPM test has been widely used to evaluate the anxiolytic or anxiogenic effects of pharmacological agents [94,95]. Therefore, it could be speculated that feeding mice with a diet incorporating beans may not provide a strong enough stimulus to mitigate

anxiety-related behaviors associated with DIO. Thus, it is advisable to utilize additional behavior tests such as Open Field test which is widely used to assess the exploratory and anxiety related behaviors [94]. One of our study strengths was the level of cooked common beans powder supplementation, which represents an achievable level of pulse intake in humans. Additionally, in this study, we established obesity in mice by feeding them a HFD analogous to western diets prior to incorporating beans into their diet. This enabled us to preclinically replicate the obesity-associated dysbiosis and metabolic dysfunction typically seen in humans. Therefore, the observed beneficial effects of beans on various aspects of intestinal health could be more translatable to humans living with obesity. However, it is important to note that this study exclusively focused on male mice, which may limit the generalizability of the findings to females.

Collectively, from the evidence presented and discussed herein we conclude that cooked beans regardless of the seed coat color, when combined into a low-fat diet, have the potential to improve colonic microbiota structure and function. Additionallyintroducing beans to the diet may exhibit anxiolytic-like effects in established obese models, thereby could be considered as an adjuvant therapeutic approach for treatment of obesity associated intestinal health dysfunction. However, dark red kidney beans despite having a higher content of phenolic compounds, exerted only modest extra benefits on some of the aspects of colonic microenvironment (such as higher abundance of *Akkermansia*). While the observed effects are promising, further research is needed to fully understand the specific mechanisms by which different bean varieties influence the colonic microbiota and the overall gut health and behaviour outcomes in the context of obesity.

Table 3-3(S1). Nest Building Scoring Guide

Criteria	Scoring details	Representative pictures
Nestlet Shredding	According to our novel developed scoring system, nests were assigned scores of **0, 0.5, 1, and 1.5** based on the percentage of shredding: **A. <50%, B. 50-75%, C.75-95%, and D. >95%,** respectively.	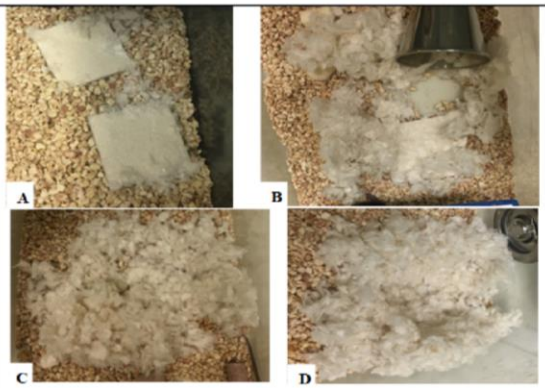
Nest Shape	**A.** a score of **0** for when nestlets were not manipulated by the mice at all or were scattered with no defined shape. **B.** Score of **0.5** for when nest cupped into a specific location, exhibiting a somewhat defined shape, but with materials still disconnected and edges sticking out. **C.** Score of **1** for a nest with a mostly rounded shape, but the nest was either very dispersed within the cage or had one edge sticking out. **D.** Score of **1.5** for a nest with a rounded shape, including at most one edge sticking out.	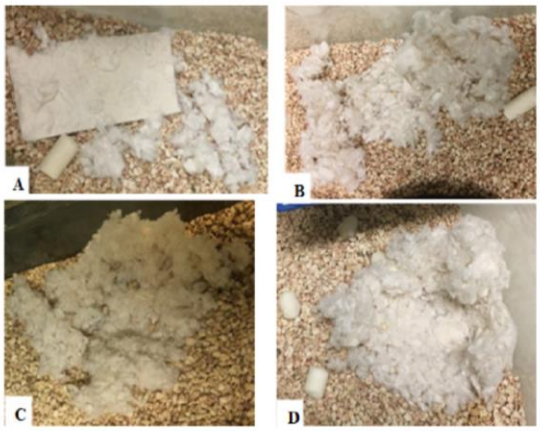
Nest Walls	The nest was imagined as a flattened sphere and scored only based on the presence or absence of identifiable walls. This approach was applied due to the remote scoring method employed, which relied on digital pictures with limited resolution. As a result, evaluating the closure of the walls surrounding the nest cavity was not possible. Thus, the nest walls were scored **0, 0.5, 1, and 1.5** for when the walls surrounding <25 %, 25-50%, 50-75% and >75% of the nest, respectively.	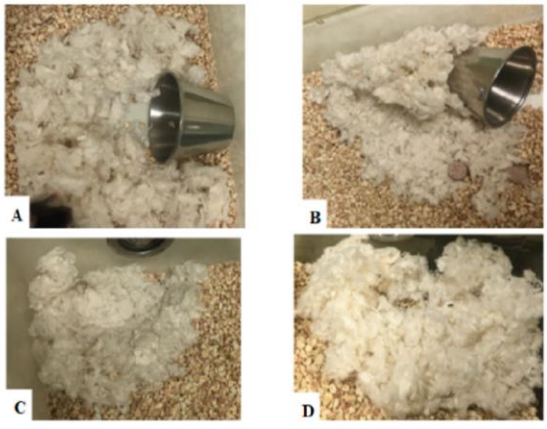

Author Contributions:
Conceptualization, S.M., É. D., and K.A.P.; Methodology, S.M., and L.K.; Formal analysis, S.M., and K.A.P.; Resources/Equipment, K.A.P.; Writing– Original Draft Preparation, S.M.; Writing – Review & Editing, S.M., and K.A.P.; Supervision, É. D., and K.A.P.; Project Administration, S.M.; Funding Acquisition, K.A.P.

Funding:
This research was supported by the following funding sources: NSERC Discovery, Ontario Research Fund, and the Nutrition and Mental Health Doctoral Scholarship from the School of Nutrition at the University of Ottawa.

Institutional Review Board Statement:
This study was conducted according to the National Institute of Health Guide for the Care and Use of Laboratory Animals and received approval from the Institutional Review Board at the University of Ottawa (Animal Care Committee, Protocol#HS-2857).

Data Availability Statement:
The data presented in this study are available on request from the corresponding author.

Acknowledgments:
The authors would like to express their gratitude to the department of Plant Agriculture, University of Guelph, Guelph, ON, for generously supplying the donation of kidney beans. Additionally, we would like to acknowledge the valuable assistance provided by the animal care and veterinary services (ACVS) team at the University of Ottawa in animal care aspect of this research. We gratefully acknowledge Histology/ Staining services provided by the Louise Pelletier Histology Core RRID: SCR_021737. Furthermore, we extend our thanks to Dr. Mahmoud Aly for providing comprehensive training on SCFA analysis and guiding the implementation of microbiota sequencing analysis.

Conflicts of Interest:
The authors declare no conflicts of interest.

5. References

1. Davis, C.D. The Gut Microbiome and Its Role in Obesity. *Nutr. Today* **2016**, *51*, 167–174, doi:10.1097/NT.0000000000000167.
2. Duan, M.; Wang, Y.; Zhang, Q.; Zou, R.; Guo, M.; Zheng, H. Characteristics of Gut Microbiota in People with Obesity. *PLOS ONE* **2021**, *16*, e0255446.
3. Turnbaugh, P.J.; Hamady, M.; Yatsunenko, T.; Cantarel, B.L.; Duncan, A.; Ley, R.E.; Sogin, M.L.; Jones, W.J.; Roe, B.A.; Affourtit, J.P.; et al. A Core Gut Microbiome in Obese and Lean Twins. *Nature* **2009**, *457*, 480–484, doi:10.1038/nature07540.
4. DeGruttola, A.K.; Low, D.; Mizoguchi, A.; Mizoguchi, E. Current Understanding of Dysbiosis in Disease in Human and Animal Models. *Inflamm. Bowel Dis.* **2016**, *22*, 1137–1150, doi:10.1097/MIB.0000000000000750.
5. Soto, M.; Herzog, C.; Pacheco, J.A.; Fujisaka, S.; Bullock, K.; Clish, C.B.; Kahn, C.R. Gut Microbiota Modulate Neurobehavior through Changes in Brain Insulin Sensitivity and Metabolism. *Mol. Psychiatry* **2018**, *23*, 2287–2301, doi:10.1038/s41380-018-0086-5.
6. Scheithauer, T.P.M.; Rampanelli, E.; Nieuwdorp, M.; Vallance, B.A.; Verchere, C.B.; van Raalte, D.H.; Herrema, H. Gut Microbiota as a Trigger for Metabolic Inflammation in Obesity and Type 2 Diabetes. *Front. Immunol.* **2020**, *11*, 571731, doi:10.3389/fimmu.2020.571731.
7. Usuda, H.; Okamoto, T.; Wada, K. Leaky Gut: Effect of Dietary Fiber and Fats on Microbiome and Intestinal Barrier. *Int. J. Mol. Sci.* **2021**, *22*, doi:10.3390/ijms22147613.
8. Cani, P.D.; Bibiloni, R.; Knauf, C.; Waget, A.; Neyrinck, A.M.; Delzenne, N.M.; Burcelin, R. Changes in Gut Microbiota Control Metabolic Endotoxemia-Induced Inflammation in High-Fat Diet–Induced Obesity and Diabetes in Mice. *Diabetes* **2008**, *57*, 1470–1481, doi:10.2337/db07-1403.
9. Agustí, A.; García-Pardo, M.P.; López-Almela, I.; Campillo, I.; Maes, M.; Romaní-Pérez, M.; Sanz, Y. Interplay Between the Gut-Brain Axis, Obesity and Cognitive Function. *Front. Neurosci.* **2018**, *12*, 155, doi:10.3389/fnins.2018.00155.
10. Borre, Y.E.; O'Keeffe, G.W.; Clarke, G.; Stanton, C.; Dinan, T.G.; Cryan, J.F. Microbiota and Neurodevelopmental Windows: Implications for Brain Disorders. *Trends Mol. Med.* **2014**, *20*, 509–518, doi:10.1016/j.molmed.2014.05.002.
11. Silva, Y.P.; Bernardi, A.; Frozza, R.L. The Role of Short-Chain Fatty Acids From Gut Microbiota in Gut-Brain Communication. *Front. Endocrinol.* **2020**, *11*, 25, doi:10.3389/fendo.2020.00025.
12. Cryan, J.F.; Dinan, T.G. Mind-Altering Microorganisms: The Impact of the Gut Microbiota on Brain and Behaviour. *Nat. Rev. Neurosci.* **2012**, *13*, 701–712, doi:10.1038/nrn3346.
13. Niccolai, E.; Boem, F.; Russo, E.; Amedei, A. The Gut¯Brain Axis in the Neuropsychological Disease Model of Obesity: A Classical Movie Revised by the Emerging Director "Microbiome." *Nutrients* **2019**, *11*, 156, doi:10.3390/nu11010156.
14. Cenit, M.C.; Sanz, Y.; Codoñer-Franch, P. Influence of Gut Microbiota on Neuropsychiatric Disorders. *World J. Gastroenterol.* **2017**, *23*, 5486–5498, doi:10.3748/wjg.v23.i30.5486.
15. Clapp, M.; Aurora, N.; Herrera, L.; Bhatia, M.; Wilen, E.; Wakefield, S. Gut Microbiota's Effect on Mental Health: The Gut-Brain Axis. *Clin. Pract.* **2017**, *7*, doi:10.4081/cp.2017.987.
16. Xiong, R.-G.; Li, J.; Cheng, J.; Zhou, D.-D.; Wu, S.-X.; Huang, S.-Y.; Saimaiti, A.; Yang, Z.-J.; Gan, R.-Y.; Li, H.-B. The Role of Gut Microbiota in Anxiety, Depression, and Other

Mental Disorders as Well as the Protective Effects of Dietary Components. *Nutrients* **2023**, *15*, doi:10.3390/nu15143258.
17. Ott, B.; Skurk, T.; Hastreiter, L.; Lagkouvardos, I.; Fischer, S.; Büttner, J.; Kellerer, T.; Clavel, T.; Rychlik, M.; Haller, D.; et al. Effect of Caloric Restriction on Gut Permeability, Inflammation Markers, and Fecal Microbiota in Obese Women. *Sci. Rep.* **2017**, *7*, 11955, doi:10.1038/s41598-017-12109-9.
18. Rosendo-Silva, D.; Viana, S.; Carvalho, E.; Reis, F.; Matafome, P. Are Gut Dysbiosis, Barrier Disruption, and Endotoxemia Related to Adipose Tissue Dysfunction in Metabolic Disorders? Overview of the Mechanisms Involved. *Intern. Emerg. Med.* **2023**, *18*, 1287–1302, doi:10.1007/s11739-023-03262-3.
19. Jones, R.A.; Lawlor, E.R.; Birch, J.M.; Patel, M.I.; Werneck, A.O.; Hoare, E.; Griffin, S.J.; van Sluijs, E.M.F.; Sharp, S.J.; Ahern, A.L. The Impact of Adult Behavioural Weight Management Interventions on Mental Health: A Systematic Review and Meta-Analysis. *Obes. Rev. Off. J. Int. Assoc. Study Obes.* **2021**, *22*, e13150, doi:10.1111/obr.13150.
20. Koster, A.; van Gool, C.H.; Kempen, G.I.J.M.; Penninx, B.W.J.H.; Lee, J.S.; Rubin, S.M.; Tylavsky, F.A.; Yaffe, K.; Newman, A.B.; Harris, T.B.; et al. Late-Life Depressed Mood and Weight Change Contribute to the Risk of Each Other. *Am. J. Geriatr. Psychiatry Off. J. Am. Assoc. Geriatr. Psychiatry* **2010**, *18*, 236–244, doi:10.1097/JGP.0b013e3181c65837.
21. Forman-Hoffman, V.L.; Yankey, J.W.; Hillis, S.L.; Wallace, R.B.; Wolinsky, F.D. Weight and Depressive Symptoms in Older Adults: Direction of Influence? *J. Gerontol. B. Psychol. Sci. Soc. Sci.* **2007**, *62*, S43-51, doi:10.1093/geronb/62.1.s43.
22. Jackson, S.E.; Steptoe, A.; Beeken, R.J.; Kivimaki, M.; Wardle, J. Psychological Changes Following Weight Loss in Overweight and Obese Adults: A Prospective Cohort Study. *PloS One* **2014**, *9*, e104552, doi:10.1371/journal.pone.0104552.
23. Megur, A.; Daliri, E.B.-M.; Baltriukienė, D.; Burokas, A. Prebiotics as a Tool for the Prevention and Treatment of Obesity and Diabetes: Classification and Ability to Modulate the Gut Microbiota. *Int. J. Mol. Sci.* **2022**, *23*, doi:10.3390/ijms23116097.
24. Liu, R.T.; Walsh, R.F.L.; Sheehan, A.E. Prebiotics and Probiotics for Depression and Anxiety: A Systematic Review and Meta-Analysis of Controlled Clinical Trials. *Neurosci. Biobehav. Rev.* **2019**, *102*, 13–23, doi:10.1016/j.neubiorev.2019.03.023.
25. Cryan, J.F.; O'Mahony, S.M. The Microbiome-Gut-Brain Axis: From Bowel to Behavior: From Bowel to Behavior. *Neurogastroenterol. Motil.* **2011**, *23*, 187–192, doi:10.1111/j.1365-2982.2010.01664.x.
26. Rao, A.V.; Bested, A.C.; Beaulne, T.M.; Katzman, M.A.; Iorio, C.; Berardi, J.M.; Logan, A.C. A Randomized, Double-Blind, Placebo-Controlled Pilot Study of a Probiotic in Emotional Symptoms of Chronic Fatigue Syndrome. *Gut Pathog.* **2009**, *1*, 6, doi:10.1186/1757-4749-1-6.
27. Guillemot-Legris, O.; Muccioli, G.G. Obesity-Induced Neuroinflammation: Beyond the Hypothalamus. *Trends Neurosci.* **2017**, *40*, 237–253, doi:10.1016/j.tins.2017.02.005.
28. Fong, W.; Li, Q.; Yu, J. Gut Microbiota Modulation: A Novel Strategy for Prevention and Treatment of Colorectal Cancer. *Oncogene* **2020**, *39*, 4925–4943, doi:10.1038/s41388-020-1341-1.
29. Tosh, S.M.; Yada, S. Dietary Fibres in Pulse Seeds and Fractions: Characterization, Functional Attributes, and Applications. *Food Res. Int.* **2010**, *43*, 450–460, doi:https://doi.org/10.1016/j.foodres.2009.09.005.

30. Ferreira, H.; Vasconcelos, M.; Gil, A.M.; Pinto, E. Benefits of Pulse Consumption on Metabolism and Health: A Systematic Review of Randomized Controlled Trials. *Crit. Rev. Food Sci. Nutr.* **2021**, *61*, 85–96, doi:10.1080/10408398.2020.1716680.
31. Kadyan, S.; Sharma, A.; Arjmandi, B.H.; Singh, P.; Nagpal, R. Prebiotic Potential of Dietary Beans and Pulses and Their Resistant Starch for Aging-Associated Gut and Metabolic Health. *Nutrients* **2022**, *14*, doi:10.3390/nu14091726.
32. Lazar, V.; Ditu, L.-M.; Pircalabioru, G.G.; Picu, A.; Petcu, L.; Cucu, N.; Chifiriuc, M.C. Gut Microbiota, Host Organism, and Diet Trialogue in Diabetes and Obesity. *Front. Nutr.* **2019**, *6*, 21, doi:10.3389/fnut.2019.00021.
33. Desai, M.S.; Seekatz, A.M.; Koropatkin, N.M.; Kamada, N.; Hickey, C.A.; Wolter, M.; Pudlo, N.A.; Kitamoto, S.; Terrapon, N.; Muller, A.; et al. A Dietary Fiber-Deprived Gut Microbiota Degrades the Colonic Mucus Barrier and Enhances Pathogen Susceptibility. *Cell* **2016**, *167*, 1339-1353.e21, doi:10.1016/j.cell.2016.10.043.
34. Schroeder, B.O. Fight Them or Feed Them: How the Intestinal Mucus Layer Manages the Gut Microbiota. *Gastroenterol. Rep.* **2019**, *7*, 3–12, doi:10.1093/gastro/goy052.
35. Rodríguez-Daza, M.C.; Pulido-Mateos, E.C.; Lupien-Meilleur, J.; Guyonnet, D.; Desjardins, Y.; Roy, D. Polyphenol-Mediated Gut Microbiota Modulation: Toward Prebiotics and Further. *Front. Nutr.* **2021**, *8*, 689456, doi:10.3389/fnut.2021.689456.
36. Forgie, A.J.; Ju, T.; Tollenaar, S.L.; Willing, B.P. Phytochemical-Induced Mucin Accumulation in the Gastrointestinal Lumen Is Independent of the Microbiota. *bioRxiv* **2022**, 2022.03.11.483917, doi:10.1101/2022.03.11.483917.
37. Monk, J.M.; Lepp, D.; Wu, W.; Pauls, K.P.; Robinson, L.E.; Power, K.A. Navy and Black Bean Supplementation Primes the Colonic Mucosal Microenvironment to Improve Gut Health. *J. Nutr. Biochem.* **2017**, *49*, 89–100, doi:https://doi.org/10.1016/j.jnutbio.2017.08.002.
38. Ombra, M.N.; d'Acierno, A.; Nazzaro, F.; Riccardi, R.; Spigno, P.; Zaccardelli, M.; Pane, C.; Maione, M.; Fratianni, F. Phenolic Composition and Antioxidant and Antiproliferative Activities of the Extracts of Twelve Common Bean (*Phaseolus Vulgaris* L.) Endemic Ecotypes of Southern Italy before and after Cooking. *Oxid. Med. Cell. Longev.* **2016**, *2016*, 1398298, doi:10.1155/2016/1398298.
39. Marinangeli, C.P.F.; Curran, J.; Barr, S.I.; Slavin, J.; Puri, S.; Swaminathan, S.; Tapsell, L.; Patterson, C.A. Enhancing Nutrition with Pulses: Defining a Recommended Serving Size for Adults. *Nutr. Rev.* **2017**, *75*, 990–1006, doi:10.1093/nutrit/nux058.
40. QIAGEN QIAamp ® Fast DNA Stool Mini Kit. *Sample Assay Tecnol.* **2014**, 4.
41. Illumina 16S Metagenomic Sequencing Library. *Illumina.com* **2013**, 1–28.
42. Bolyen, E.; Rideout, J.R.; Dillon, M.R.; Bokulich, N.A.; Abnet, C.C.; Al-Ghalith, G.A.; Alexander, H.; Alm, E.J.; Arumugam, M.; Asnicar, F.; et al. Reproducible, Interactive, Scalable and Extensible Microbiome Data Science Using QIIME 2. *Nat. Biotechnol.* **2019**, *37*, 852–857, doi:10.1038/s41587-019-0209-9.
43. Callahan, B.J.; McMurdie, P.J.; Rosen, M.J.; Han, A.W.; Johnson, A.J.A.; Holmes, S.P. DADA2: High-Resolution Sample Inference from Illumina Amplicon Data. *Nat. Methods* **2016**, *13*, 581–583, doi:10.1038/nmeth.3869.
44. McDonald, D.; Price, M.N.; Goodrich, J.; Nawrocki, E.P.; DeSantis, T.Z.; Probst, A.; Andersen, G.L.; Knight, R.; Hugenholtz, P. An Improved Greengenes Taxonomy with Explicit Ranks for Ecological and Evolutionary Analyses of Bacteria and Archaea. *ISME J.* **2012**, *6*, 610–618, doi:10.1038/ismej.2011.139.

45. Bray, J.R.; Curtis, J.T. An Ordination of the Upland Forest Communities of Southern Wisconsin. *Ecol. Monogr.* **1957**, *27*, 326–349, doi:10.2307/1942268.
46. Segata, N.; Izard, J.; Waldron, L.; Gevers, D.; Miropolsky, L.; Garrett, W.S.; Huttenhower, C. Metagenomic Biomarker Discovery and Explanation. *Genome Biol.* **2011**, *12*, R60, doi:10.1186/gb-2011-12-6-r60.
47. Douglas, G.M.; Maffei, V.J.; Zaneveld, J.R.; Yurgel, S.N.; Brown, J.R.; Taylor, C.M.; Huttenhower, C.; Langille, M.G.I. PICRUSt2 for Prediction of Metagenome Functions. *Nat. Biotechnol.* **2020**, *38*, 685–688, doi:10.1038/s41587-020-0548-6.
48. Langille, M.G.I.; Zaneveld, J.; Caporaso, J.G.; McDonald, D.; Knights, D.; Reyes, J.A.; Clemente, J.C.; Burkepile, D.E.; Vega Thurber, R.L.; Knight, R.; et al. Predictive Functional Profiling of Microbial Communities Using 16S rRNA Marker Gene Sequences. *Nat. Biotechnol.* **2013**, *31*, 814–821, doi:10.1038/nbt.2676.
49. MIRARAB, S.; NGUYEN, N.; WARNOW, T. SEPP: SATé-Enabled Phylogenetic Placement. In *Biocomputing 2012*; WORLD SCIENTIFIC, 2011; pp. 247–258 ISBN 978-981-4596-37-4.
50. Czech, L.; Stamatakis, A. Scalable Methods for Analyzing and Visualizing Phylogenetic Placement of Metagenomic Samples. *PloS One* **2019**, *14*, e0217050, doi:10.1371/journal.pone.0217050.
51. Louca, S.; Doebeli, M. Efficient Comparative Phylogenetics on Large Trees. *Bioinformatics* **2018**, *34*, 1053–1055, doi:10.1093/bioinformatics/btx701.
52. Kanehisa, M.; Goto, S. KEGG: Kyoto Encyclopedia of Genes and Genomes. *Nucleic Acids Res.* **2000**, *28*, 27–30, doi:10.1093/nar/28.1.27.
53. Douglas, G. PiCrust2 Categorize_by_function.Py · Issue #1 · Gavinmdouglas/Picrust2_manuscript Available online: https://github.com/gavinmdouglas/picrust2_manuscript/issues/1 (accessed on 17 June 2022).
54. Parks, D.H.; Tyson, G.W.; Hugenholtz, P.; Beiko, R.G. STAMP: Statistical Analysis of Taxonomic and Functional Profiles. *Bioinforma. Oxf. Engl.* **2014**, *30*, 3123–3124, doi:10.1093/bioinformatics/btu494.
55. Livingston, D.B.H.; Sweet, A.; Rodrigue, A.; Kishore, L.; Loftus, J.; Ghali, F.; Mahmoodianfard, S.; Celton, C.; Hosseinian, F.; Power, K.A. Dietary Flaxseed and Flaxseed Oil Differentially Modulate Aspects of the Microbiota Gut–Brain Axis Following an Acute Lipopolysaccharide Challenge in Male C57Bl/6 Mice. *Nutrients* **2023**, *15*, 3542, doi:10.3390/nu15163542.
56. Cathomas, F.; Hartmann, M.N.; Seifritz, E.; Pryce, C.R.; Kaiser, S. The Translational Study of Apathy-an Ecological Approach. *Front. Behav. Neurosci.* **2015**, *9*, 241, doi:10.3389/fnbeh.2015.00241.
57. Jirkof, P. Burrowing and Nest Building Behavior as Indicators of Well-Being in Mice. *J. Neurosci. Methods* **2014**, *234*, 139–146, doi:https://doi.org/10.1016/j.jneumeth.2014.02.001.
58. Kraeuter, A.-K.; Guest, P.C.; Sarnyai, Z. The Nest Building Test in Mice for Assessment of General Well-Being BT - Pre-Clinical Models: Techniques and Protocols. In; Guest, P.C., Ed.; Springer New York: New York, NY, 2019; pp. 87–91 ISBN 978-1-4939-8994-2.
59. Deacon, R.M.J. Assessing Nest Building in Mice. *Nat. Protoc.* **2006**, *1*, 1117–1119, doi:10.1038/nprot.2006.170.
60. Hess, S.E.; Rohr, S.; Dufour, B.D.; Gaskill, B.N.; Pajor, E.A.; Garner, J.P. Home Improvement: C57BL/6J Mice given More Naturalistic Nesting Materials Build Better Nests. *J. Am. Assoc. Lab. Anim. Sci.* **2008**, *47*, 25–31.

61. Komada, M.; Takao, K.; Miyakawa, T. Elevated plus Maze for Mice. *J. Vis. Exp. JoVE* **2008**, doi:10.3791/1088.
62. Brolese, G.; Lunardi, P.; Lopes, F.; Gonçalves, C.-A. Chapter 2 - Prenatal Alcohol Exposure and Neuroglial Changes in Neurochemistry and Behavior in Animal Models. In *Addictive Substances and Neurological Disease*; Watson, R.R., Zibadi, S.B.T.-A.S. and N.D., Eds.; Academic Press, 2017; pp. 11–22 ISBN 978-0-12-805373-7.
63. Lkhagva, E.; Chung, H.-J.; Hong, J.; Tang, W.H.W.; Lee, S.-I.; Hong, S.-T.; Lee, S. The Regional Diversity of Gut Microbiome along the GI Tract of Male C57BL/6 Mice. *BMC Microbiol.* **2021**, *21*, 44, doi:10.1186/s12866-021-02099-0.
64. Plassais, J.; Gbikpi-Benissan, G.; Figarol, M.; Scheperjans, F.; Gorochov, G.; Derkinderen, P.; Cervino, A.C.L. Gut Microbiome Alpha-Diversity Is Not a Marker of Parkinson's Disease and Multiple Sclerosis. *Brain Commun.* **2021**, *3*, fcab113, doi:10.1093/braincomms/fcab113.
65. Sawicka-Śmiarowska, E.; Moniuszko-Malinowska, A.; Kamiński, K.A. Which Microbes Like My Diet and What Does It Mean for My Heart? *Nutrients* **2021**, *13*, doi:10.3390/nu13114146.
66. Chen, T.; Long, W.; Zhang, C.; Liu, S.; Zhao, L.; Hamaker, B.R. Fiber-Utilizing Capacity Varies in Prevotella- versus Bacteroides-Dominated Gut Microbiota. *Sci. Rep.* **2017**, *7*, 2594, doi:10.1038/s41598-017-02995-4.
67. Magne, F.; Gotteland, M.; Gauthier, L.; Zazueta, A.; Pesoa, S.; Navarrete, P.; Balamurugan, R. The Firmicutes/Bacteroidetes Ratio: A Relevant Marker of Gut Dysbiosis in Obese Patients? *Nutrients* **2020**, *12*, doi:10.3390/nu12051474.
68. Schrader, A.J.; Taylor, R.M.; Lowery-Gionta, E.G.; Moore, N.L.T. Repeated Elevated plus Maze Trials as a Measure for Tracking Within-Subjects Behavioral Performance in Rats (Rattus Norvegicus). *PLOS ONE* **2018**, *13*, e0207804.
69. André, C.; Dinel, A.-L.; Ferreira, G.; Layé, S.; Castanon, N. Diet-Induced Obesity Progressively Alters Cognition, Anxiety-like Behavior and Lipopolysaccharide-Induced Depressive-like Behavior: Focus on Brain Indoleamine 2,3-Dioxygenase Activation. *Brain. Behav. Immun.* **2014**, *41*, 10–21, doi:10.1016/j.bbi.2014.03.012.
70. Janssen, A.W.F.; Kersten, S. The Role of the Gut Microbiota in Metabolic Health. *FASEB J.* **2015**, *29*, 3111–3123, doi:10.1096/fj.14-269514.
71. García-Montero, C.; Fraile-Martínez, O.; Gómez-Lahoz, A.M.; Pekarek, L.; Castellanos, A.J.; Noguerales-Fraguas, F.; Coca, S.; Guijarro, L.G.; García-Honduvilla, N.; Asúnsolo, A.; et al. Nutritional Components in Western Diet Versus Mediterranean Diet at the Gut Microbiota-Immune System Interplay. Implications for Health and Disease. *Nutrients* **2021**, *13*, 699, doi:10.3390/nu13020699.
72. Guo, S.; Zhao, H.; Ma, Z.; Zhang, S.; Li, M.; Zheng, Z.; Ren, X.; Ho, C.-T.; Bai, N. Anti-Obesity and Gut Microbiota Modulation Effect of Secoiridoid-Enriched Extract from Fraxinus Mandshurica Seeds on High-Fat Diet-Fed Mice. *Molecules* **2020**, *25*, doi:10.3390/molecules25174001.
73. Wei, G.; Ye, Y.; Yan, X.; Chao, X.; Yang, F.; Wang, M.; Zhang, W.; Yuan, C.; Zeng, Q. Effect of Banana Pulp Dietary Fibers on Metabolic Syndrome and Gut Microbiota Diversity in High-Fat Diet Mice. *J. Food Biochem.* **2020**, *44*, 1–15, doi:10.1111/jfbc.13362.
74. Liu, H.; Wang, J.; He, T.; Becker, S.; Zhang, G.; Li, D.; Ma, X. Butyrate: A Double-Edged Sword for Health? *Adv. Nutr. Bethesda Md* **2018**, *9*, 21–29, doi:10.1093/advances/nmx009.
75. Rodrigues, V.F.; Elias-Oliveira, J.; Pereira, Í.S.; Pereira, J.A.; Barbosa, S.C.; Machado, M.S.G.; Carlos, D. Akkermansia Muciniphila and Gut Immune System: A Good Friendship

That Attenuates Inflammatory Bowel Disease, Obesity, and Diabetes. *Front. Immunol.* **2022**, *13*, 934695, doi:10.3389/fimmu.2022.934695.
76. Tseng, C.-H.; Wu, C.-Y. The Gut Microbiome in Obesity. *J. Formos. Med. Assoc.* **2019**, *118*, S3–S9, doi:https://doi.org/10.1016/j.jfma.2018.07.009.
77. Wang, M.; Zhang, B.; Hu, J.; Nie, S.; Xiong, T.; Xie, M. Intervention of Five Strains of Lactobacillus on Obesity in Mice Induced by High-Fat Diet. *J. Funct. Foods* **2020**, *72*, 104078, doi:https://doi.org/10.1016/j.jff.2020.104078.
78. Gophna, U.; Konikoff, T.; Nielsen, H.B. Oscillospira and Related Bacteria - From Metagenomic Species to Metabolic Features. *Environ. Microbiol.* **2017**, *19*, 835–841, doi:10.1111/1462-2920.13658.
79. Wu, Z.; Du, Z.; Tian, Y.; Liu, M.; Zhu, K.; Zhao, Y.; Wang, H. Inulin Accelerates Weight Loss in Obese Mice by Regulating Gut Microbiota and Serum Metabolites. *Front. Nutr.* **2022**, *9*, 980382, doi:10.3389/fnut.2022.980382.
80. Louis, S.; Tappu, R.-M.; Damms-Machado, A.; Huson, D.H.; Bischoff, S.C. Characterization of the Gut Microbial Community of Obese Patients Following a Weight-Loss Intervention Using Whole Metagenome Shotgun Sequencing. *PloS One* **2016**, *11*, e0149564, doi:10.1371/journal.pone.0149564.
81. Walters, W.A.; Xu, Z.; Knight, R. Meta-Analysis of Human Gut Microbes Associated with Obesity and IBD. *FEBS Lett.* **2014**, *588*, 4223–4233, doi:10.1016/j.febslet.2014.09.039.
82. Schéle, E.; Grahnemo, L.; Anesten, F.; Hallén, A.; Bäckhed, F.; Jansson, J.O. Regulation of Body Fat Mass by the Gut Microbiota: Possible Mediation by the Brain. *Peptides* **2016**, *77*, 54–59, doi:10.1016/j.peptides.2015.03.027.
83. Lutsiv, T.; Weir, T.L.; McGinley, J.N.; Neil, E.S.; Wei, Y.; Thompson, H.J. Compositional Changes of the High-Fat Diet-Induced Gut Microbiota upon Consumption of Common Pulses. *Nutrients* **2021**, *13*, doi:10.3390/nu13113992.
84. Tan, Y.; Tam, C.C.; Meng, S.; Zhang, Y.; Alves, P.; Yokoyama, W. Cooked Black Turtle Beans Ameliorate Insulin Resistance and Restore Gut Microbiota in C57BL/6J Mice on High-Fat Diets. *Foods* **2021**, *10*, doi:10.3390/foods10081691.
85. Neil, E.S.; McGinley, J.N.; Fitzgerald, V.K.; Lauck, C.A.; Tabke, J.A.; Streeter-McDonald, M.R.; Yao, L.; Broeckling, C.D.; Weir, T.L.; Foster, M.T.; et al. White Kidney Bean (Phaseolus Vulgaris L.) Consumption Reduces Fat Accumulation in a Polygenic Mouse Model of Obesity. *Nutrients* **2019**, *11*, doi:10.3390/nu11112780.
86. McGinley, J.N.; Fitzgerald, V.K.; Neil, E.S.; Omerigic, H.M.; Heuberger, A.L.; Weir, T.L.; McGee, R.; Vandemark, G.; Thompson, H.J. Pulse Crop Effects on Gut Microbial Populations, Intestinal Function, and Adiposity in a Mouse Model of Diet-Induced Obesity. *Nutrients* **2020**, *12*, doi:10.3390/nu12030593.
87. Zhou, W.; Davis, E.A.; Dailey, M.J. Obesity, Independent of Diet, Drives Lasting Effects on Intestinal Epithelial Stem Cell Proliferation in Mice. *Exp. Biol. Med. Maywood NJ* **2018**, *243*, 826–835, doi:10.1177/1535370218777762.
88. Yang, J.L.; Liu, D.X.; Jiang, H.; Pan, F.; Ho, C.S.; Ho, R.C. The Effects of High-Fat-Diet Combined with Chronic Unpredictable Mild Stress on Depression-like Behavior and Leptin/LepRb in Male Rats. *Sci. Rep.* **2016**, *6*, 35239, doi:10.1038/srep35239.
89. Sharma, S.; Fulton, S. Diet-Induced Obesity Promotes Depressive-like Behaviour That Is Associated with Neural Adaptations in Brain Reward Circuitry. *Int. J. Obes. 2005* **2013**, *37*, 382–389, doi:10.1038/ijo.2012.48.

90. Sharma, S.; Fernandes, M.F.; Fulton, S. Adaptations in Brain Reward Circuitry Underlie Palatable Food Cravings and Anxiety Induced by High-Fat Diet Withdrawal. *Int. J. Obes. 2005* **2013**, *37*, 1183–1191, doi:10.1038/ijo.2012.197.
91. Chakrabarti, A.; Geurts, L.; Hoyles, L.; Iozzo, P.; Kraneveld, A.D.; La Fata, G.; Miani, M.; Patterson, E.; Pot, B.; Shortt, C.; et al. The Microbiota-Gut-Brain Axis: Pathways to Better Brain Health. Perspectives on What We Know, What We Need to Investigate and How to Put Knowledge into Practice. *Cell. Mol. Life Sci. CMLS* **2022**, *79*, 80, doi:10.1007/s00018-021-04060-w.
92. Chun, E.; Yoon, S.; Parveen, A.; Jin, M. Alleviation of Irritable Bowel Syndrome-Like Symptoms and Control of Gut and Brain Responses with Oral Administration of Dolichos Lablab L. in a Mouse Model. *Nutrients* **2018**, *10*, doi:10.3390/nu10101475.
93. Heinz, D.E.; Schöttle, V.A.; Nemcova, P.; Binder, F.P.; Ebert, T.; Domschke, K.; Wotjak, C.T. Exploratory Drive, Fear, and Anxiety Are Dissociable and Independent Components in Foraging Mice. *Transl. Psychiatry* **2021**, *11*, 318, doi:10.1038/s41398-021-01458-9.
94. Sarkar, D. A Review of Behavioral Tests to Evaluate Different Types of Anxiety and Anti-Anxiety Effects. *Clin. Psychopharmacol. Neurosci. Off. Sci. J. Korean Coll. Neuropsychopharmacol.* **2020**, *18*, 341–351, doi:10.9758/cpn.2020.18.3.341.
95. Walf, A.A.; Frye, C.A. The Use of the Elevated plus Maze as an Assay of Anxiety-Related Behavior in Rodents. *Nat. Protoc.* **2007**, *2*, 322–328, doi:10.1038/nprot.2007.44.

4 CHAPTER 4: Project 3 Manuscript

The Abundance of *Akkermansia* as a Potential Link to Obesity Susceptibility in High-Fat Diet-Fed Mice

Authors

Salma Mahmoodianfard[1], Lalit Kishore[2], Alexane Rodrigue[3], Giorgio Freije[3], Valérie Roumelis[4], Éric Doucet[1], Krista A. Power[2,5*]

Affiliations:

1. School of Human Kinetics, Faculty of Health Science, University of Ottawa, Ottawa K1N 6N5, Canada
2. School of Nutrition Sciences, Faculty of Health Science, University of Ottawa, Ottawa, Canada, K1N 6N5
3. Department of Biochemistry, Microbiology and Immunology, Faculty of Medicine, University of Ottawa, Ottawa, Canada, K1H 8L1
4. Department of Biology, Faculty of Science, University of Ottawa
5. Department of Biology, Faculty of Science, University of Ottawa

***Corresponding Author:**
Krista A. Power
School of Nutrition Sciences
University of Ottawa
Roger Guindon Hall; Room 3260
Phone: 613-562-5800 ext. 2200
Krista.Power@uottawa.ca

ABSTRACT

Obese mice fed a high-fat diet (HFD) serve as valuable pre-clinical models for human metabolic dysfunctions linked to obesity. Under isocaloric conditions, rodents exhibit diverse obesity phenotypes, underscoring the multifaceted etiology of obesity. This research aimed to investigate the intricate interplay between diet, inflammation, and gut microbiota involved in the development of phenotypes associated with susceptibility or resistance to obesity in C57BL/6 male mice. Over an 18-week period, mice were randomly assigned to either a low-fat diet (LFD) or HFD. Subsequently, the HFD-fed mice were further classified into diet-induced obesity resistant (DIO-R) or prone (DIO-P) groups based on their weight gain. Higher fat mass, daily food and energy intake, and adipocyte size were observed in DIO-P mice. Microbiota analysis revealed comparable diversity but distinct compositions, notably in *Akkermansia* abundance. Predicted functional pathways highlighted differences between DIO-R and DIO-P, correlating positively with *Akkermansia* abundance. Serum concentrations of Lipopolysaccharide-Binding Protein (LBP), Tumor Necrosis Factor-alpha (TNF-α), and Monocyte Chemoattractant Protein-1 (MCP-1), along with inflammatory adipokines like leptin and resistin, as well as insulin resistance, were elevated in DIO-P. Moreover, mRNA expressions of inflammatory markers in adipose tissue, including TNF-α, MCP-1, Toll-like receptor 4 (TLR4), G protein-coupled receptor (GPR)41, and GPR43, were upregulated in DIO-P mice compared to the DIO-R group. Overall, our findings underscore the potential role of gut microbiota in shaping obesity phenotypes with distinct inflammatory and metabolic profiles in C57Bl/6 male mice.

Key Words: Diet-induced obesity (DIO), Resistant to obesity, Gut microbiota, *Akkermansia*, Inflammation, Adipose tissue, Metabolic profile

1. Introduction

Obesity has emerged as a major global public health concern, leading to a rise in obesity-related chronic diseases [1]. As the prevalence of obesity continues to rise, the utilization of mice as models for diet-induced obesity (DIO) has become progressively widespread due to their high reliability in replicating human obesity, as compared to genetic models [2,3]. Mice fed a high-fat diet (HFD) develop an obesity syndrome that features metabolic complications like those observed in humans including hyperleptinemia, hyperinsulinemia, and impaired glucose tolerance, mirroring human obesity-associated metabolic dysfunctions [4,5]. This positions them as potentially valuable models in pre-clinical studies for advancing obesity research.

Obesity occurs when energy intake surpasses expenditure, resulting in the expansion of adipose tissue and fat droplet storage, with dietary fat playing a crucial role in this process [6,7]. However, emerging evidence suggests that the etiology of obesity extends beyond the conventional focus on caloric intake and expenditure [8,9]. This implies a more intricate interplay of factors influencing obesity development. Overall, it is estimated that between 40% to 70% of the variance in obesity propensity can be attributed to genetic factors, highlighting the gene-environment interaction as a key contributor to obesity development [10,11]. Surprisingly, under isocaloric conditions within a group of rodents with the same genetic background, the metabolic responses to an HFD can vary, resulting in distinct prone (DIO-P) or resistant (DIO-R) obesity phenotypes [5,9–11], suggesting the multifaceted nature of obesity.

Emerging evidence suggests a profound influence of gut microbiota dysbiosis observed in both humans and rodent models, adversely affecting adiposity and body weight regulation [12–16]. The dysbiosis is characterized by an imbalance in bacterial composition and an overall shift in bacterial diversity within the gut [17]. This is supported by evidence of germ-free mice

consuming a HFD that do not exhibit hyperphagia, weight or adiposity gain, or other metabolic disfunctions associated with HFD consumption seen in conventionally raised mice. Remarkably, these effects persisted even when the germ-free mice consumed more calories from a normal chow or high-fat Western-type diet compared to conventional mice [18]. Conversely, conventionalization of germ-free mice with microbiota from lean or obese donors results in the reproducing the donors phenotypes. [18,19]. The increased susceptibility to body weight gain has been hypothesized to be associated with an improved efficiency in extracting calories from specific consumed foods, a phenomenon potentially enhanced by the microbial changes associated with obesity [13,20].

Evidence from studies on comparison of gut microbial community in individuals with obesity and their lean counterparts reported a higher abundance of several bacteria species from Firmicutes phylum in individuals living with obesity. Conversely, normal-weight individuals exhibited a higher abundance of several taxa from the Bacteroidetes phylum [21,22]. These microbial changes resulted in an elevated Firmicutes/Bacteroidetes ratio in individuals with obesity [21,22], a ratio that, according to some studies but not all, has been considered as a hallmark of obesity [23]. Additionally, *Akkermansia muciniphila* has been shown to have an anti-obesity protective effect in mice and humans [24,25], as well as contributing to a healthier metabolic status and better clinical outcomes (such as enhanced insulin sensitivity) in adults living with overweight/obesity under calorie restriction [26]. Therefore, altered gut microbiota composition could be a potential mechanism involved in the association of obesity prone or resistance in experimental models.

On the other hand, HFD is also associated with a persistent but low-grade chronic inflammation [27–29], possibly attributable to a shift in the gut microbiota and the direct effects

of high amounts of free-fatty acids (FFAs) present in HFD on barrier structure of intestinal cells [29–31]. Gut microbiota dysbiosis triggered by HFDs activates the TLR4 pathways, increases intestinal permeability to endotoxins like bacterial lipopolysaccharides (LPS) and subsequent translocation of LPS to the circulation, defined as metabolic endotoxemia [30,32–34]. Both LPS and/or FFAs trigger the production of pro-inflammatory cytokines including IL-1β, IL-6, and tumor necrosis factor (TNF-α) in the gut. The subsequent release of LPS, cytokines and FFAs into the circulation resulting in further systemic and peripheral tissue inflammation [28,35,36] and predisposing to obesity [29]. As for the inflammatory markers, they have been linked to insulin resistance [37–39], one potential mechanism relies on the downregulation of these markers in DIO-R mice, which may affect their ability to handle excessive fat intake by effectively clearing metabolic by-products and maintaining metabolic homeostasis in contrast to DIO-P mice [6].

The mechanisms underlying the precise contribution of host-microbial metabolism and obesity-resistant phenotype require comprehensive exploration, as previous studies have only partially addressed this issue and presented conflicting findings with respect to the changes in metabolic profile and gut microbiota composition between DIO-P and DIO-R phenotypes [6,33,40–42]. Therefore, in this study we aimed to investigate the interplay between diet, inflammatory status and gut microbiota composition and function in development of phenotypes with susceptibility or resistance to obesity in C57BL/6 mice.

2. Methods

2.1 Experimental Design

The research procedures received approval from the uOttawa Animal Care Committee (ACC) under Protocol number HSe-2857-R3. Five-week-old male C57BL/6 mice (Charles River lab, Kingston, NY, USA), were individually housed in polycarbonate rodent cages filled with

corncob bedding and cotton nesting material, and they were housed in an environment with a 12-hour light/dark cycle. The temperature was maintained within a range of 22-26 °C, and the relative humidity was kept at 40%. During the first week, mice were acclimated to this controlled environment and had unrestricted access to a low-fat diet (LFD; 13% kcal from fat; Envigo/Teklad USA) and water. After one week, mice were randomly assigned to two groups; One group (n=8) were maintained on LFD, while the remaining mice (n=110) were transitioned to a HFD (60% kcal from fat; Envigo/Teklad USA) to establish obesity throughout the duration of the study. The composition of the experimental diets is presented in **Table 1.**

2.2 Defining DIO-P and DIO-R Phenotypes

At week 18, the mice with the highest growth rate on HFD, approximately the top 10% of the cohort, were considered for the DIO-P group (n=12; Body weight=50.48 ± 0.40 g). Conversely, those with the lowest growth rate, approximately the bottom 10% of the cohort, were considered for the DIO-R group (n=10; Body weight=37.90 ± 0.61 g). Subsequently, mice with intermediate body weight gain were excluded for the purpose of this study. Additionally, the group of mice on the LFD were served as the control group (n=8 mice).

Fasting blood was collected during week 17 of the study. At the end of the intervention, mice were euthanized via decapitation, and trunk blood was collected. Tissues including epididymal adipose tissue (EAT), perirenal adipose tissue (PAT), and intrascapular brown adipose tissue (BAT), were excised, and their weights were recorded. The EAT was snap frozen in liquid nitrogen and stored at –80 °C for later RNA and protein extraction analysis.

Table 4-1. Experimental diet composition

Nutrients g/Kg	TD.190833 Low Fat Diet (LFD)	TD.190378 High Fat Diet (HFD)
Casein	200	265
L-Cystine	3	4
Corn Starch	414.49	0
Maltodextrin	132	160
Sucrose	100	92.59
Soybean Oil	34	30
Lard	19	310
Cellulose	50	70
Mineral Mix, AIN-93G-MX (94046)	35	48
Calcium Phosphate, dibasic	0	3.4
Vitamin Mix, AIN-93-VX (94047)	10	14
Choline Bitartrate	2.5	3
TBHQ, antioxidant	0.01	0.01
Sum	1000	1000
Macronutrient Contribution of Diets g/kg		
Protein, g/kg	177	235
Carbohydrate, g/kg	616	269
Fat, g/kg	55	343
Fiber, g/kg	50	70
Macronutrient Contribution of total Kcal %		
Protein, % kcal	19.3	18.4
Carbohydrate, % kcal	67.2	21.1
Fat, % kcal	13.5	60.5
Expected Daily Intake, g	3	2
Expected Daily Fiber intake, g	0.15	0.14
kcal/g	**3.7**	**5.1**

2.3 *Assessment of Body Weight, Diet Intake, and Body Composition*

Body weight and diet intake were assessed 2-3 times per week throughout the study using a digital scale. Body composition components including lean and fat mass, were determined using the Echo-MRI™-700 body composition analyzer at week 6 and at the end of week 18.

2.4 Assessment of Fecal Microbial Community Structure and Function

2.4.1 Microbiota DNA Sequencing and Diversity Analysis

Fresh fecal pellets were collected at week 18 from each mouse and stored in cryogenic storage vials at -80°C until analysis. Genomic DNA extraction was carried out using the QIAamp Fast DNA Stool Mini Kit (Qiagen, Cat. #51604, Germany) following the manufacturer's instructions. The V3-V4 regions of the 16S rRNA gene were amplified, and subsequent library quantification, normalization, and pooling were performed according to the Illumina 16S Metagenomic Sequencing Library Preparation Guide [43]. Sequencing was conducted on the Illumina MiSeq platform (Illumina®, Miseq). The dual-index paired-end reads retrieved from MiSeq sequencing were analyzed using the QIIME2 bioinformatics platform (version 2022.2) [44]. The 300 bp Casava 1.8 paired-end demultiplexed files were imported and subjected to quality filtering using DADA2 [45], involving denoising, removal of chimeric sequences, correction of Illumina-sequenced amplicon errors, and generation of amplicon sequence variants (ASVs). A phylogenetic tree was constructed using the Greengenes 13_8 99% identity reference tree [46].

Microbial diversity was analyzed using MicrobiomeAnalyst 2.0 [47,48], a free available on-line software (available from https://www.microbiomeanalyst.ca/). Beta (β)-diversity dissimilarity distance was assessed utilizing Bray-Curtis metric, and then visualized using Principal Coordinate Analysis (PCoA). Alpha (α)-diversity metrics were computed using the methods of Shannon and Simpson. The Kruskal-Wallis test with Benajmini–Hochberg corrections in Qiime2 assessed the statistical significance of differences in α-diversity between groups. PERMANOVA analysis in Qiime2 identified differences in β-diversity between dietary groups, with p-values adjusted using the Benjamini-Hochberg FDR correction. Microbial structure was analyzed using QIIME2. Taxa relative abundance comparison between groups utilized the Mann-

Whitney U test followed by the two-stage linear step-up method of Benjamini, Kreiger, and Yekutieli ($p<0.05$; FDR<5%). In our investigation of discriminating bacterial taxa with both statistical significance and biological relevance, we employed Linear Discriminant Analysis Effect Size analysis (LEfSe) [49]. This analysis was executed on the Galaxy Server (https://huttenhower.sph.harvard.edu/galaxy/, accessed on 15 Nov 2023), utilizing an LDA threshold of 2 and a p-value cut-off of 0.05.

2.4.2 Quantitative Analysis of Fecal Short Chain Fatty Acids

The evaluation of gut microbiota function involved quantifying levels of fecal short-chain fatty acids (SCFAs) and branched-chain fatty acids (BCFAs), specifically acetic acid, butyric acid, propionic acid, valeric acid, iso-butyric acid, and iso-valeric acid, as previously outlined [50]. In brief, the methodology included freeze-drying of fecal samples, recording dry weight, diluting in MilliQ water to achieve a 10% homogeneous fecal solution, centrifugation, pH measurement, acidification, filtration, and gas chromatography analysis with a standard curve for calibration. This analytical approach identified various SCFAs based on retention times and determined their concentrations using analytical standards.

2.4.3 Predicted Functions of the Metagenome

The analysis of microbial community predictive functional profiling was conducted using Phylogenetic Investigation of Communities by Reconstruction of Unobserved States 2 (PICRUSt2) [51,52], version 2.51. Initially, the fragment insertion Qiime2 plugin [53] aligned ASVs to the HMMER sequence databases (www.hmmer.org), placing them optimally onto the reference phylogeny using the SATé-Enabled Phylogenetic Placement (SEPP) tool [54] and

constructing a new phylogenetic tree using the genesis applications for phylogenetic placement analysis (GAPPA) [55]. Core hidden state prediction functions (hsp.py) were performed using the castor R-package [56] to predict gene family abundances for each ASV and Kyoto Encyclopedia of Genes and Genomes (KEGG) orthologs [57] (KO). The metagenome_pipeline.py command was then employed to normalize the KO abundances based on 16S abundance, resulting in the file (pred_metagenome_unstrat.tsv) containing mouse-specific KO abundances. This file was processed in RStudio (R =V4.2.2, R Studio: V2022.12.0+353) to determine the inferred function of the microbiota. Using custom R code analogous to the categorize_by_function.py used in PICRUST1 [58], the KOs were aligned with a manually curated mapping file sourced from https://www.genome.jp/kegg-bin/get_htext?ko00001.keg (accessed on 17 June 2022) [57].

Finally, STAMP (Statistical Analysis of Taxonomic and Functional Profiles), version 2.1.3 [59], was applied for the outcomes representing inferred functional aspects and two-group comparisons using Welch's two-sided t-test with Benjamini-Hochberg multiple test correction ($q<0.05$).

2.5 Serum Metabolic, Inflammatory and Endotoxemia Biomarkers Analysis

Fasted blood was collected during week 17 of the study, after an 8 hour overnight fast. The concentrations of fasted blood glucose (FBG) were measured using a glucometer (Contour®Next blood glucose monitoring system, Bayer, model 7268). The serum concentrations of ghrelin, glucose-dependent insulinotropic polypeptide (GIP), glucagon-like peptide-1 (GLP-1), glucagon, insulin, leptin, plasminogen activator inhibitor-1 (PAI-1), and resistin were quantified using a multiplex magnetic bead-based fluorescence sandwich immunoassay kit (Bio-Plex Pro Mouse Diabetes 8-Plex Immunoassay, Bio-Rad, Cat. #171F7001M). The homeostatic model assessment

of insulin resistance (HOMA-IR) index was calculated using the fasting glucose and insulin levels using the following formula: [fasting serum insulin (μIU/L) × fasting serum glucose (mM)] / 22.5. Insulin concentrations were converted from pg/mL to μIU/L using a molar mass of 5808 Da and a conversion factor of 1 μIU/L = 6.00 pmol/L [60]. Adiponectin concentrations were determined separately using a single-plex assay (Bio-Plex Pro Mouse Diabetes Adiponectin Assay, Cat. #171F7002M). Serum inflammatory cytokines concentrations were measured in non-fasting blood collected at euthanasia, using the Bio-Plex Pro Mouse Cytokine 23-plex Assay (Cat. #M60009RDPD). All these assays were conducted as per the manufacturer's instructions. The prepared assay plates were read on a Luminex® analyzer (MAGPIX®) equipped with Milliplex Analyst software, version 5.1.0.0, developed by VigeneTech Inc. Serum levels of lipopolysaccharide-binding protein (LBP), serving as an indicator of systemic LPS exposure [61], were assessed with samples diluted 1000x. The mouse LBP enzyme-linked immunosorbent assay kit (HyCultBiotech, Cat# HK205-01) was utilized following the manufacturer's instructions. Absorbance readings were taken at 450 nm using a Multimode Microplate Reader (Tecan, Switzerland).

2.6 Assessment of Inflammation in Adipose Tissue

2.6.1 Transcriptional Profiling of Inflammatory Markers in Adipose Tissue

RNA extraction was carried out using the Total RNA Purification Plus Kit (Norgen Biotek, #48400). The purified RNA was then normalized to a concentration of 1 μg RNA/10 μL using UltraPure™ DNase/RNase-Free Distilled Water. Subsequently, the normalized RNA underwent reverse transcription to complementary DNA (cDNA) with the High-Capacity cDNA Reverse Transcription Kit (Applied Biosystems, Cat. #4368814) in the thermal cycler. Quantitative real-

time PCR (qRT-PCR) analyses were performed using SYBR Green master mix (Applied Biosystems™, Cat. #A25742) in a CFX96 real-time PCR detection system (Bio-rad, model C1000 Touch™). The Cq values for each sample were obtained from CFX Maestro Software. To compare the relative expression of the target genes between samples, the ΔΔCq method was applied, with gene expression levels normalized to the expression levels of the RPLP0 housekeeping reference gene. Primer sequences are displayed in Supplemental **Table 4-3(S2)**.

2.6.2 Exploring Inflammatory Protein Expression in Adipose Tissue

The EAT protein extraction procedure involved homogenizing up to 50 mg of EAT with ceramic beads and lysis buffer. The lysis buffer, comprising 1x RIPA buffer (Cell Signaling, Cat. #9806) supplemented with protease inhibitor cocktail (Cell Signaling #5871) and PMSF (Cell Signaling #8553), at final concentrations of 1/100 and 1/200, respectively, facilitated homogenization using a Bead Mill 24 Homogenizer. After centrifugation, the supernatant was carefully transferred to a new 1.5 mL capped tube, minimizing lipid transfer using a gauge needle attached to a 1 ml syringe, and this step was repeated three times. This method ensured the collection of the smallest amount of fat possible, maintaining protein purity and quality. The protein solution was diluted 1/20, and the total protein content was quantified using the BCA assay (Pierce™ BCA Protein Assay Kit, Cat. #23225) following the manufacturer's instructions. The EAT-extracted protein was normalized using 1x RIPA to 1 mg/ml. Subsequently, the cytokine protein expressions, including IL-1β, MCP-1, TNF-α, IL-6, and IL-10, were analyzed using the Milliplex Mouse High Sensitivity Cytokine T Cell Magnetic Bead Panel (Cat. # MHSTCMAG-70K). For this analysis, 25 μg of the normalized protein was utilized, following the manufacturer's

instructions. The prepared plate was read on a Luminex® analyzer (MAGPIX®) equipped with Milliplex Analyst software, version 5.1.0.0, developed by VigeneTech Inc.

2.7 Spontaneous Locomotor Activity Assessment

To evaluate the spontaneous locomotor activity, the BBK test was conducted through automated home-cage activity monitoring which counts the total number of beam breaks during the light-dark cycles during week 15 of the study at the Animal Behavior and Physiology Core, University of Ottawa. This test is considered as a functional parameter representing physical and mental status of experimental animals while moving in a familiar environment [62]. The system tracks the general motor activity and movements of animals within a photocell-equipped open field system. It consists of a photocell emitter projecting the animal cages invisible horizontal infrared beam lights from one side to the other. The broken beams, resulting from the mouse movements, are enumerated, and analyzed to measure exploratory locomotor activity [62]. In present study, following acclimatization for 1 hour in the assessment area, mice were placed individually in clean cages with enough bedding materials covering the floor of the cage and supply of water and food, but without nesting materials to avoid interference with their spontaneous behavior activity. Since evidence has reported a reduction in activity levels during the dark cycle accompanied by disruptions in the circadian feeding behavior in mice and rats with DIO [63], mice were monitored over a 22-hour period to track motor activity during light and dark phases of the circadian cycle. The Fusion 5.3 software by Omnitech Electronics Inc., paired with the Micromax analyzer from Accuscan, was used for data analysis. Parameters such as horizontal activity counts (total beam interruptions) and ambulatory activity counts (reflecting actual locomotion) were measured and

summed in 30-minute intervals. The area under the curve for total activity and for each light and dark cycle was calculated using GraphPad Prism 10.0.3.

2.8 Histology and Adipocyte Size Measurements

EAT samples were fixed in 10% formalin for 48 hours, followed by preservation in 70% ethanol until processing. The samples were then paraffin-embedded, sectioned at 4 μm thickness, and stained using Hematoxylin and eosin (H&E) at the University of Ottawa Histology Core Facility (Roger-Guidon Hall, Ottawa, ON, Canada). Subsequently, images were captured at 20x magnification using a Zeiss Axiocam 506 microscope camera. The images were analyzed with the Fiji (Image J2) software (version: 2.9.0/1.53t) using the Adiposoft plugin, and then the adipocyte diameter and area was determined by analyzing an average of 25 adipocytes per mouse.

2.9 Statistical Analysis

Statistical analyses were carried out using GraphPad Prism software (Version 10.0.3). The normality assumption was assessed using the D'Agostino-Pearson omnibus test (K2). Additionally, homogeneity of variances for parametric data was examined using the Brown-Forsythe and Bartlett's tests. The impact of the intervention on parametric data among the different study groups was evaluated through one-way analysis of variance (ANOVA). Post-hoc analyses, including the Student-Newman-Keuls (SNK) or Tukey's multiple comparison tests, were conducted to explore specific pairwise differences between the study groups in case the ANOVA results were statistically significant. For non-parametric data, two different approaches were employed based on the data distribution. If the non-parametric data could be log-transformed to achieve normality, a One-way ANOVA was performed after the data transformation. Alternatively, a Kruskal-Wallis

test was conducted, followed by Dunn's multiple comparisons test as a post-hoc analysis. Additionally, Spearman correlation analysis was employed to investigate associations between the differentiated KEGG pathways and *Akkermancia* relative Abundance. The significance level for all statistical tests was set at $p < 0.05$. The detailed statistical results from the ANOVA, Kruskal-Wallis, and other relevant analyses, are provided in Appendix VIII for further reference.

3. Results

3.1 High-Fat Diet Induce Distinct Obesity Resistance and Prone Phenotypes

Figure 1A, depicts the body weight growth chart of the treatment groups over the 18-week study period. Unpaired t test indicated that the initial body weights in both groups were comparable at baseline (p=0.4). As demonstrated in **Figure 4-1B**, the final body weight analysis revealed a significant percentage increase in body weight in the DIO-P group (128.2 ± 2.55 %) compared to the DIO-R and control groups (81.82 ± 3.71 % and 89.91 ± 3.47 %, respectively). Notably, there was no significant difference in final body weight between the DIO-R and control groups **(Figure 4-1B)**. Although there were minor individual variations in the results of the Echo-MRI body composition analysis among mice in different groups, an overall trend of increasing fat mass as a percentage of body weight, (fat mass (% BW)), and decreasing lean mass as a percentage of body weight (lean mass (% BW)) were observed from week 6 to week 18, as depicted in **Figure 4-1C and 4-1E**, respectively. Notably, in line with the body weight results, by the end of the intervention, DIO-P mice exhibited a significantly higher fat mass (g) compared to both DIO-R and control group, while lean mass was notably greater in both the DIO-P and control groups in comparison to the DIO-R group, with no significant difference observed among them.

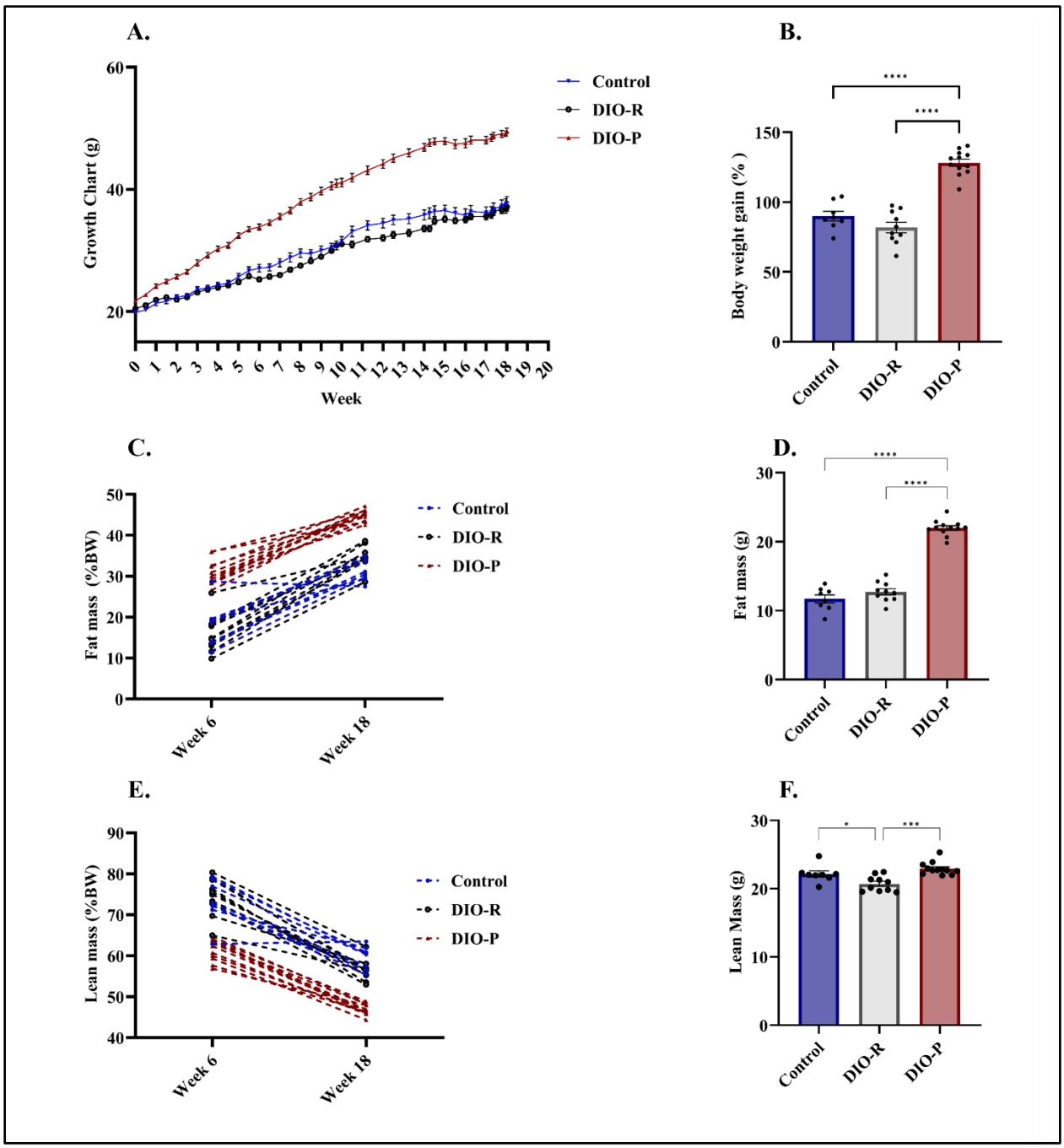

Figure 4-1. Body Weight and Body Composition. A. Body weight growth chart (g), **B.** Body weight gain percentage; Data was analysed by One-way ANOVA followed by Tukey's multiple comparisons test. **C.** Individual mice paired data illustrating fat mass as a percentage of body weight (% fat mass) from weeks 6 to 18, **D.** Final fat mass (g), **E.** Individual mice paired data illustrating lean mass as a percentage of body weight (% lean mass) from weeks 6 to 18, **F.** Final lean mass (g). Statistical significance was set at $p < 0.05$. Asterisks indicate level of statistical significance as: * $p<0.05$, **$p<0.01$, ***$p<0.001$, ****$p<0.0001$.DIO-R: Diet-induced obesity resistant group, DIO-P: Diet-induced obesity prone group.

3.2 Spontaneous Locomotor Activity

The home-cage activity was measured by the BBK test for over a 22-hour period (**Figure 4-2A)**. The two-way ANOVA analysis indicated a significant main effect of the light-dark cycle on ambulatory activity, demonstrating higher activity levels during the dark cycle compared to the light cycle, as anticipated **(Figure 4-2B)**. Additionally, a significant interaction effect between the intervention group and light-dark cycle was observed. Post-hoc analysis revealed significant lower AUC of dark cycle ambulatory activity in DIO-P mice when compared to both the DIO-R and control mice. Furthermore, DIO-R ambulatory activity was significantly lower than that in the control mice. Similarly, the AUC of total ambulatory activity revealed a significant decrease in DIO-P mice when compared to both the DIO-R and control mice. Additionally, DIO-R mice exhibited a significant decrease in the AUC of total ambulatory activity compared to the control mice **(Figure 4-2C)**. Overall, these findings provide evidence of reduced locomotor activity in DIO-P mice and, to a lesser extent, in DIO-R mice compared to the lean controls, emphasizing the impact of diet composition and obesity phenotype on home-cage activity patterns.

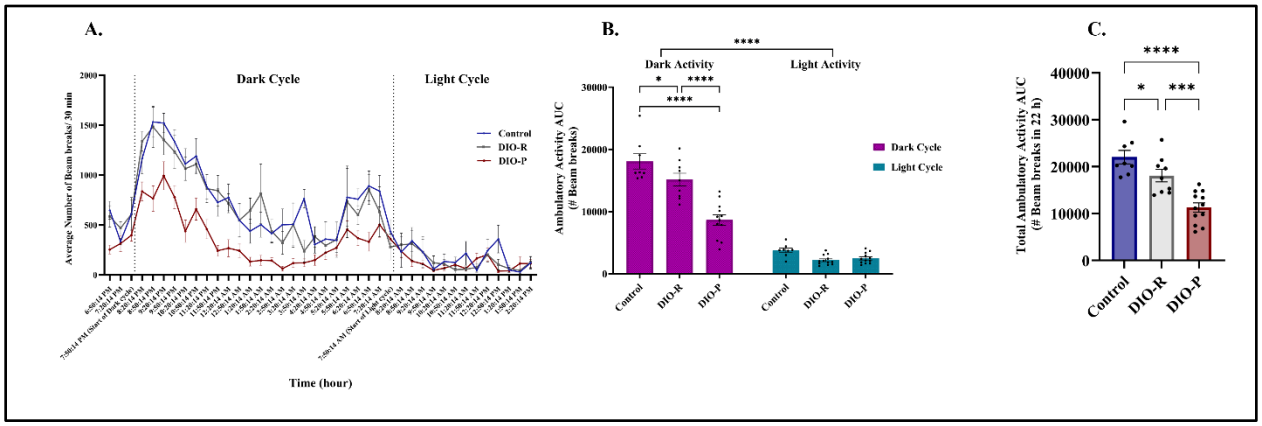

Figure 4-2. Spontaneous Locomotor Activity Measured in 30-min time bins. A. Infrared beam break counts resulted from mice ambulatory movements over the 22-h session. **B.** Area under the curve (AUC) analysis of ambulatory movements during the light and dark cycles, Data was analysed by two-way ANOVA followed by Tukey's multiple comparisons test, **C.)** AUC analysis of total ambulatory movements over the experiment session. Data was analysed by One-way ANOVA followed by Newman-Keuls multiple comparisons test. Asterisks indicate level of statistical significance as: * $p<0.05$, ***$p<0.001$, ****$p<0.0001$. Values are displayed as means±S.E.M.. DIO-R: Diet-induced obesity resistant group, DIO-P: Diet-induced obesity prone group.

3.2 Higher Food and Energy Consumption in Mice Prone to Obesity

The daily food intake (g/day/mouse) over the study duration and cumulative energy intake (Kcal) from baseline to week 18 are illustrated in **Figure 4-3A** and **Figure 4-3B**, respectively. Cumulative energy intake was calculated using the cumulative diet intake and converting the consumed amount from g/mouse into kcal/mouse according to the experimental diet composition presented in **Table 4-1**. Total energy intake was significantly higher in the DIO-P group compared to both the DIO-R group and the control group, with no significant differences observed between them.

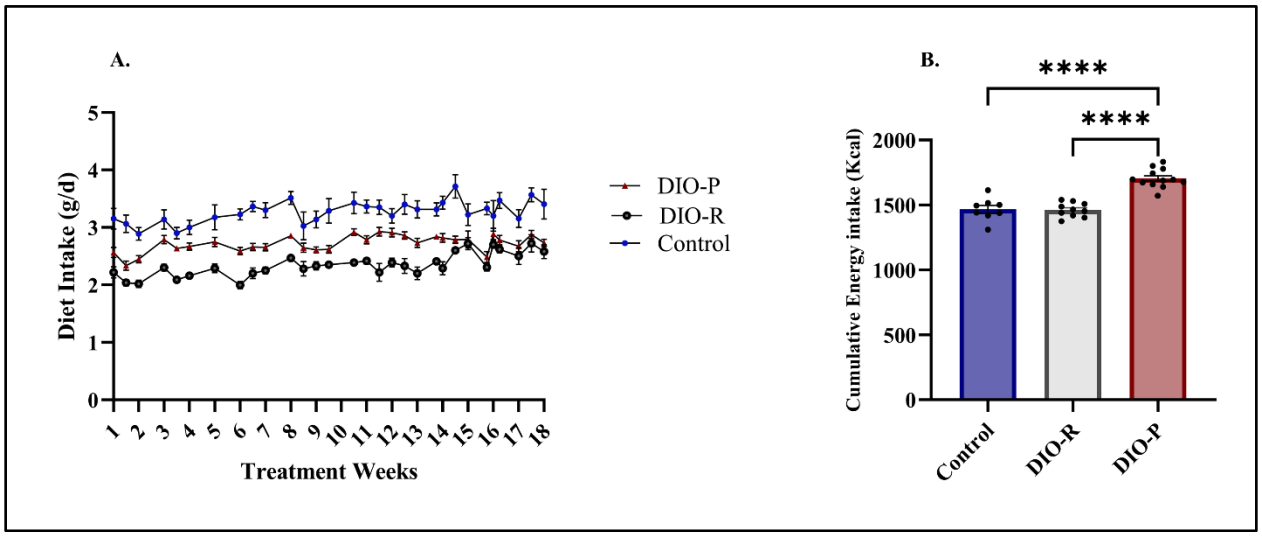

Figure 4-3. Diet and Energy Intake. A. Daily intake (g/day/mouse) throughout the study, **B.** Cumulative energy intake (kcal) from baseline to week 18, Data was analysed by One-way ANOVA followed by Newman-Keuls multiple comparisons test. Statistical significance was set at $p < 0.05$. Asterisks indicate level of statistical significance as: ****$p<0.0001$. Values are displayed as means±S.E.M. DIO-R: Diet-induced obesity resistant group, DIO-P: Diet-induced obesity prone group.

3.3 Fecal Microbial Community Structure

3.3.1 Comparable Intestinal Microbiota Diversity in Obesity-Prone and Obesity-Resistant Mice

The assessment of microbiota α- diversity, measured through both Simpson and Shannon indices **(Figure 4-4A and 4-4B)**, revealed significantly higher α- diversity in both DIO-P and DIO-R groups compared to the control group. Notably, no statistically significant differences were detected in α- diversity between the DIO-P and DIO-R groups, indicating a uniform impact of the HFD on microbial diversity, irrespective of the obesity phenotype.

The analysis of β-diversity using the Bray-Curtis dissimilarity index revealed a notable clustering pattern based on diet **(Figure 4-4C).** As such, both DIO-P and DIO-R clusters were overlapped with no significant differences among them, while forming a separate cluster significantly distinct from the control group.

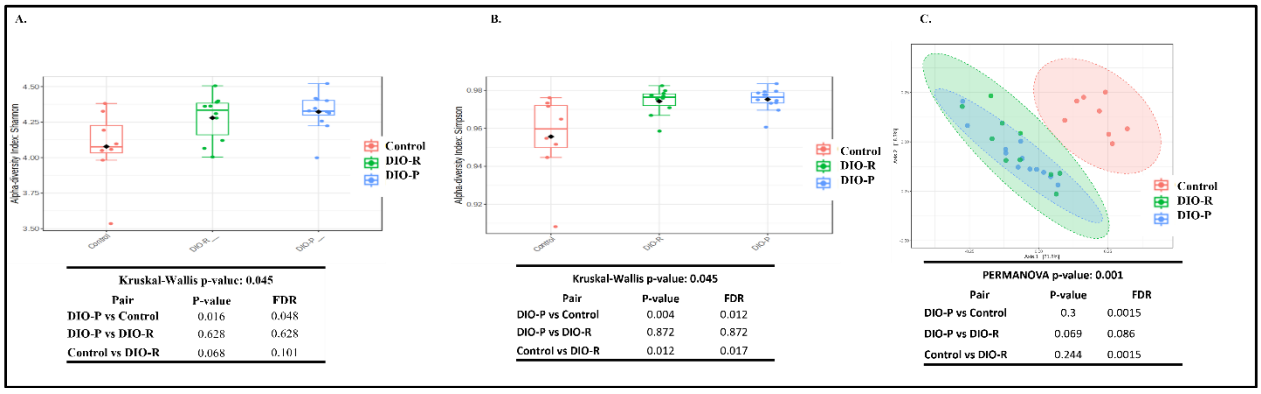

Figure 4-4. The Fecal Microbiota Diversity. α−diversity and pairwise comparison tables for A. Shannon index, **B.** Simpson index. **C.** β -diversity visualized by principal component analysis (PCoA) of Bray-Curtis distance matrices and PERMANOVA pairwise comparisons. The multi-testing adjustment conducted based on Benjamini-Hochberg procedure procedure (FDR<0.05). Values for each mouse are shown as a dot symbol. DIO-R: Diet-induced obesity resistant group, DIO-P: Diet-induced obesity prone group.

3.3.2 Different Microbiota Composition in Obesity-Prone and Obesity-Resistant Mice

At the end of the study, the analysis of microbiota composition at both phylum and genus levels yielded notable distinctions among the groups examined **(Figure 4-5A-G)**. In total, eight phyla were identified, with Firmicutes and Bacteroidetes standing out as the predominant phyla across all groups **(Figure 4-5A)**. At the phylum level, Kruskal-Wallis analysis did not indicate significant differences in the relative abundance of Firmicutes and Bacteroidetes or the Firmicutes/Bacteroidetes ratio.

However, the relative abundance of *F16*, the primary family member of the TM7 phylum, and *Ruminococcaceae* (f) from Firmicutes phylum, showed a significantly higher relative abundance in the DIO-P group compared to the control group. Conversely, *S24-7* (f) from Bacteroidetes and *Papillibacter* (g) from Firmicutes increased in control group compared to both the DIO-P and DIO-R groups. Additionally, *Akkermansia,* the principal genus member of the Verrucomicrobia phylum, as well as *Clostridium* (g) from Firmicutes exhibited a marked increase in the DIO-R group compared to both the DIO-P and control groups (**Figure 4-5B-G)**.

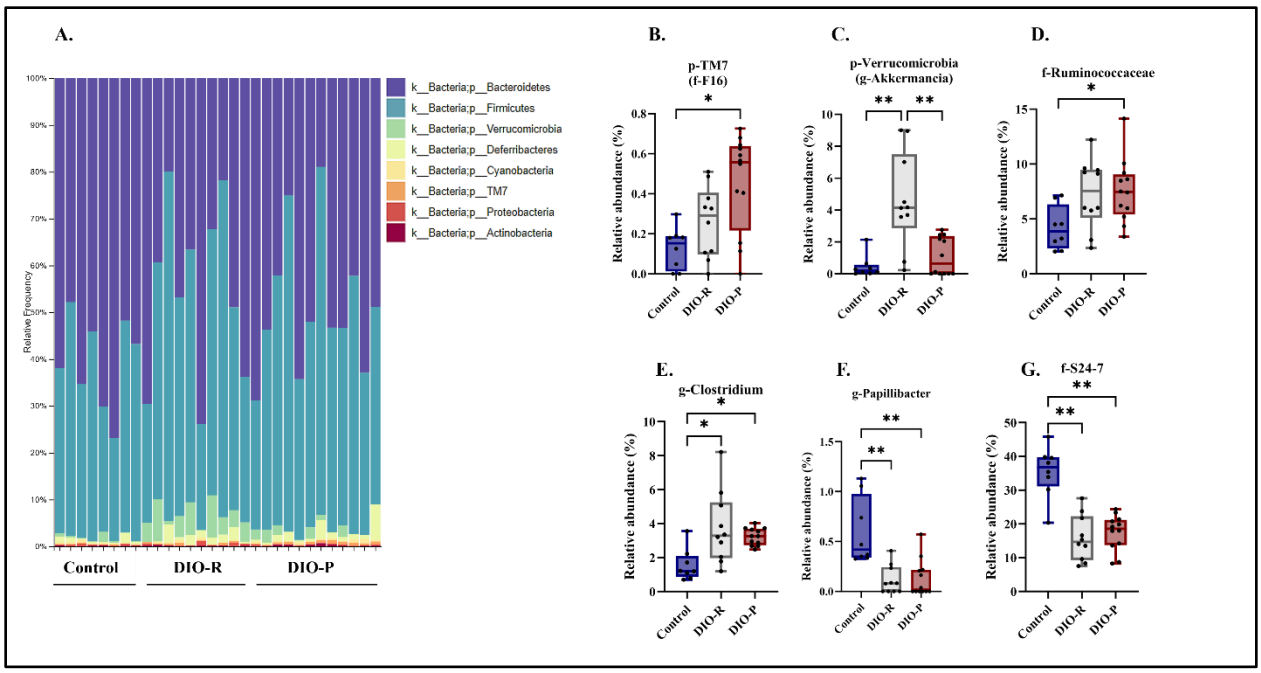

Figure 4-5. Fecal Microbial Community Structure. A. Taxonomic relative abundance of fecal microbiota at the phylum level (p), **B-G.** Relative abundance of key genus (g). The microbiota data was analyzed using Kruskal-Wallis test, followed by Dunn's multiple comparisons test. f; microbiota taxa composition at the family level for the unclassified genera. Statistical significance was set at $p < 0.05$. (n=8 Control, n=10 DIO-R, and n=12 DIO-P). DIO-R: Diet-induced obesity resistant group, DIO-P: Diet-induced obesity prone group.

Furthermore, the discriminant analysis of gut microbiota composition using the LEfSe method revealed consistent results, as presented earlier **(Figure 4-6A-F)**. When comparing the microbiota of DIO-P and DIO-R, we identified 10 differentially abundant taxonomic classes ($p<0.05$) with an LDA score higher than 2.0. Notably, the abundance of *Akkermansia* was statistically and biologically differentiated in the DIO-R group, emerging as a key genus in comparison to both the DIO-P and control groups.

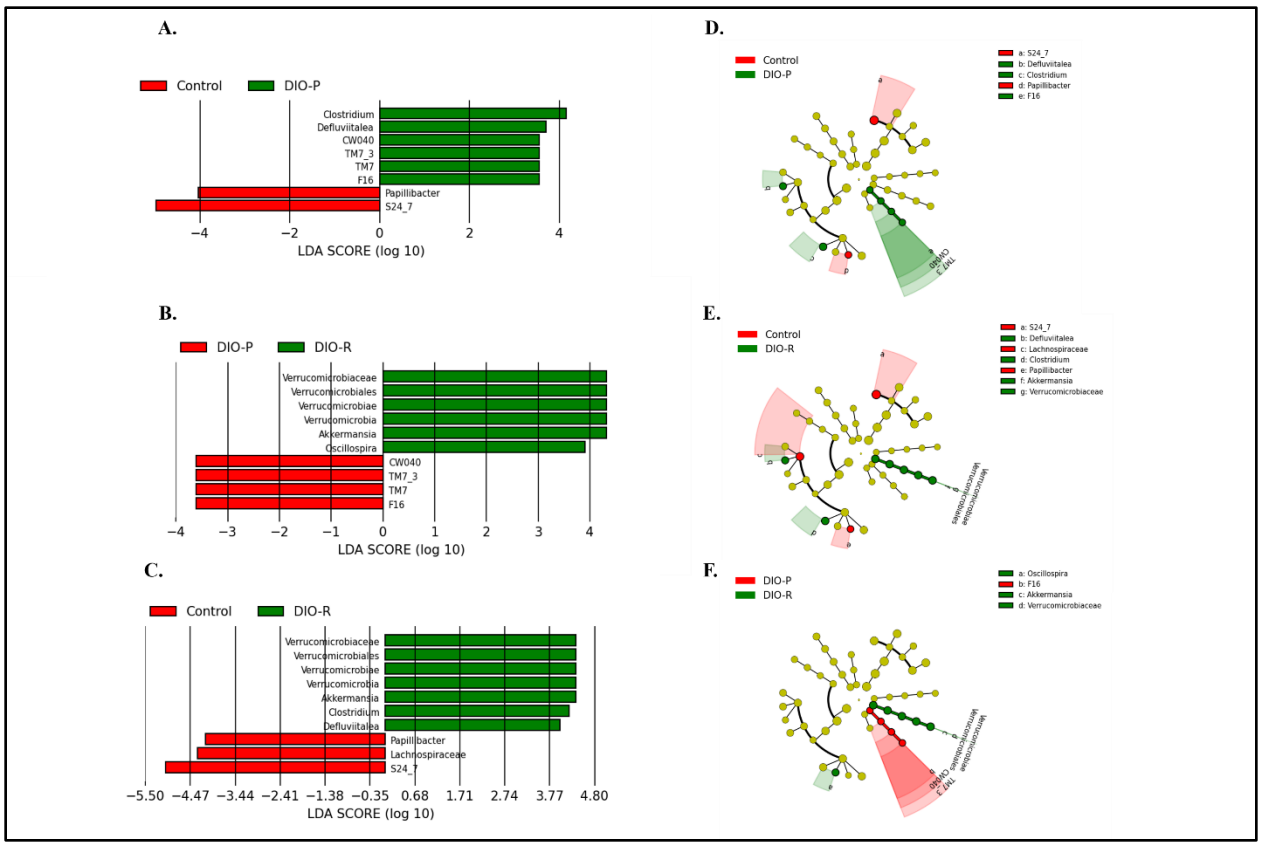

Figure 4-6. LEfSe Results on Fecal Microbial Taxonomy. A-C. Histogram of the Linear discriminant analysis (LDA) scores computed for features differentially abundant between; **A.** Control and DIO-P, **B.** DIO-P and DIO-R, and **C.** Control and DIO-R groups, **D-F.** Taxonomic Cladogram (phylum to genus) from LEfSe, depicting taxonomic association between microbiome communities from; **D.** Control and DIO-P, **E.** DIO-P and DIO-R, and **F.** Control and DIO-R groups. Each node represents a specific taxonomic type. Red and green nodes denote the taxonomic types with more abundance within the respective groups. ($LDA > 2$, $p < 0.05$). DIO-R: Diet-induced obesity resistant group, DIO-P: Diet-induced obesity prone group.

3.4 Microbial Community Function

3.4.1 Comparable Fecal SCFAs concentrations in Obesity-Prone and Obesity-Resistant Mice

Fecal concentrations of SCFAs, including acetate, propionate, butyrate, and Total SCFAs, did not exhibit significant differences among the study groups **(Figure 4-7A-D).** Given that the fiber source in both the low-fat and high-fat diets was cellulose, an insoluble and non-digestible fiber known for its poor fermentation by gastrointestinal bacteria [64], these findings were not unexpected.

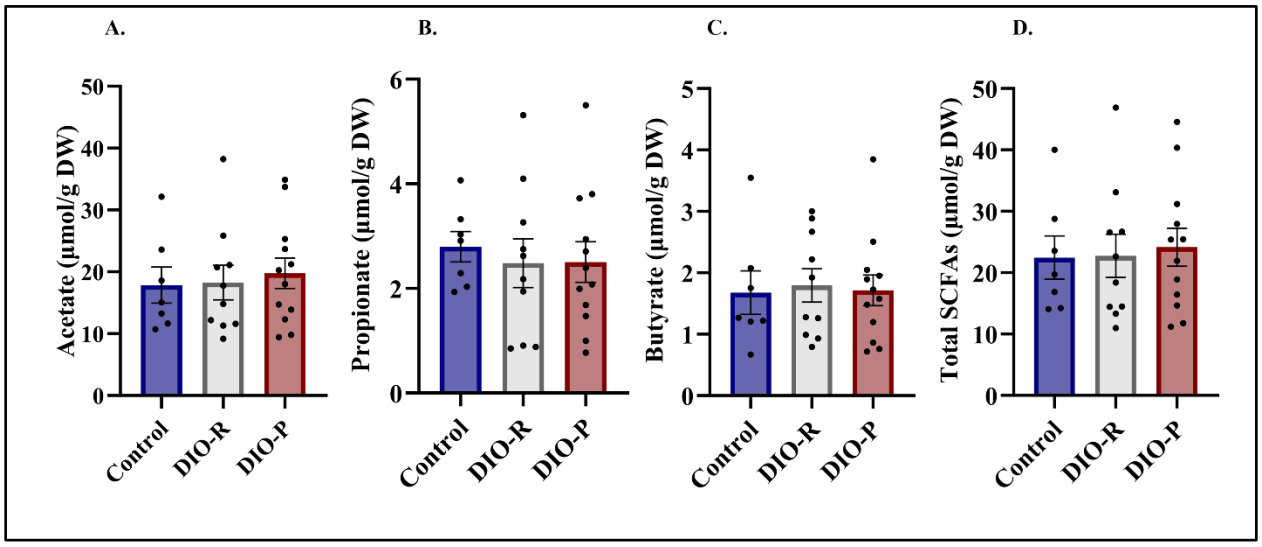

Figure 4-7. Short-chain Fatty Acid (SCFAs) Concentrations, (µmol/g DW). A. Acetic Acid**, B.** Propionic Acid, **C.** Butyric Acid**, D.** Total SCFAs**.** Data was analysed by One-way ANOVA followed by Tukey's multiple comparisons test. Values are displayed as means±S.E.M. DIO-R: Diet-induced obesity resistant group, DIO-P: Diet-induced obesity prone group.

3.4.2 Microbiota Predicted Function

The multiple groups comparison of predicted functional KEGG pathways in STAMP among control, DIO-R, and DIO-P groups, revealed 21 active features. Notably, post-hoc analysis identified four pathways specifically between the DIO-R and DIO-P groups that all were

significantly enriched in DIO-R mice. The regression analysis also revealed significant positive correlations between these pathways including biosynthesis of unsaturated fatty acids, steroid biosynthesis, carotenoid biosynthesis and sesquiterpenoid and triterpenoid biosynthesis and the relative abundance of *Akkermansia* **(Figure 4-8E-H).**

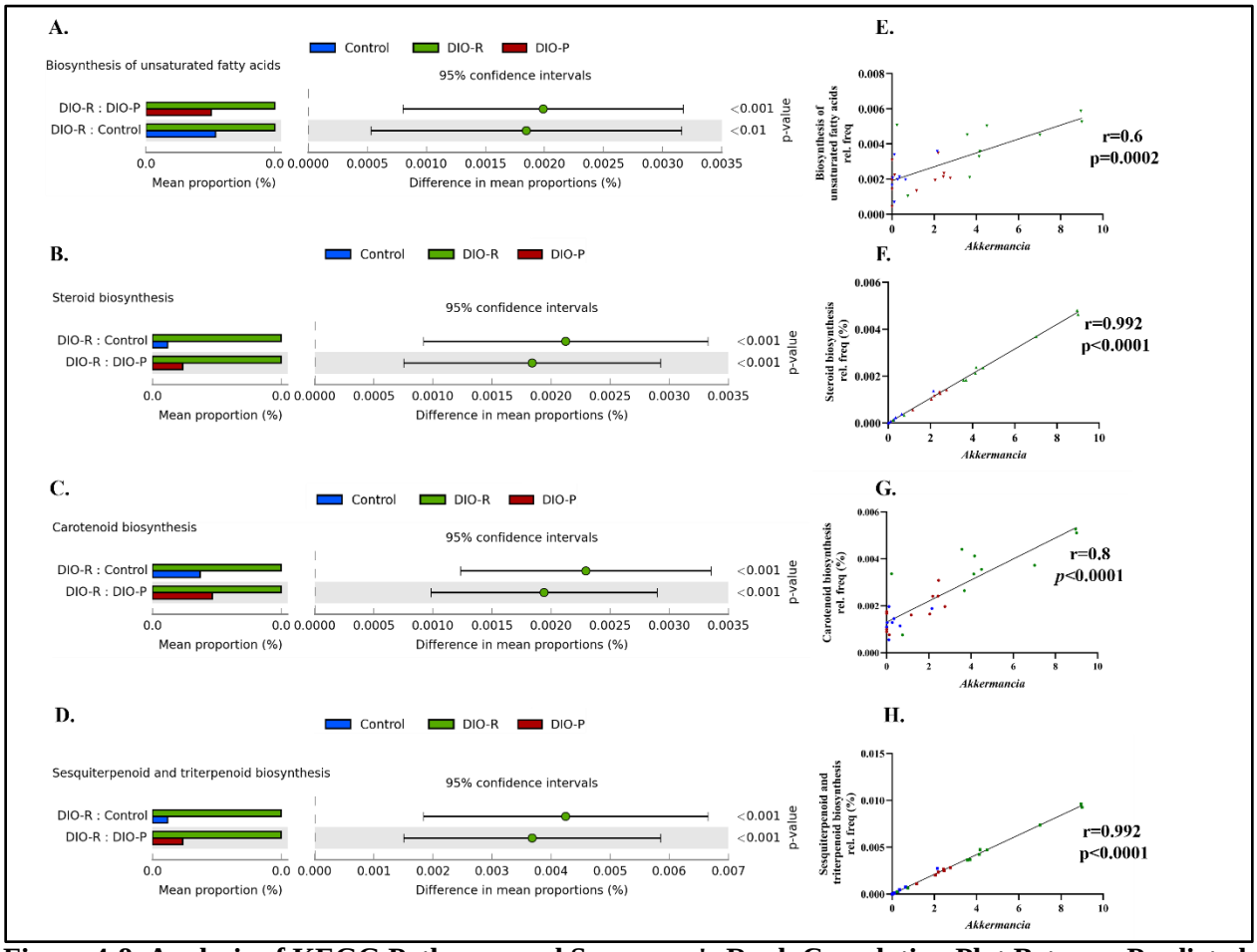

Figure 4-8. Analysis of KEGG Pathways and Spearman's Rank Correlation Plot Between Predicted Pathways and Microbiota. A-C. Multiple groups comparison of the differing functional pathways between DIO-R vs DIO-P and control groups. The PICRUSt2 data were analyzed in STAMP using ANOVA with Tukey-Kramer post-hoc test and Benjamini-Hochberg multiple test correction FDR (q<0.05). **D-F.** Simple linear regression between differentiated pathways and Akkermancia relative Abundance. Correlations with r > 0.4 and p < 0.05 are shown. DIO-R: Diet-induced obesity resistant group, DIO-P: Diet-induced obesity prone group.

3.5 Altered Endotoxemia and Systemic Inflammation Profiles in Obesity-Prone and Obesity-Resistant Mice

Serum LBP concentrations were measured as an indicator of LPS exposure, referring to endotoxemia [61]. The results revealed a significant increase in LBP concentrations in DIO-P group when compared to DIO-R, with no significant difference observed between DIO-R and control groups.

Serum cytokine levels could not be detected in all samples for some of the analytes measured by the 23-plex cytokine/chemokine assay kit. **Supplementary Table 4-4(S2)** depicts the number of samples with undetectable cytokine/chemokine concentrations and the median serum concentrations of the detectable ones within each of the control, DIO-R, and DIO-P groups. **Table 4-2** presents the mean±S.E.M. results for cytokines detected in 97%-100% of the samples. As can be seen, TNF- α and MCP-1 exhibited significant lower concentrations in DIO-R group when compared to both DIO-P and control groups. The levels of IL-6 did not demonstrate a significant difference between groups; however, it displayed a decreasing pattern in the DIO-R group compared to the DIO-P group (p=0.052). Additionally, keratinocyte-derived chemokine (KC or CXCL1), recognized for its role in adipose tissue inflammation and subsequent insulin resistance development [65], was decreased in both DIO-R and control groups compared to DIO-P group, with no significant difference observed between DIO-R and control groups. Conversely, no significant differences were observed in the levels of IL-1α, IL-5, MIP-1α, MIP-1β, IL-12P40, Eotoxin, IL-10, and IL-17A among the study groups.

Table 4-2. Cytokine and Chemokine Concentrations

Intervention group / **Biomarker**	**Control**	**DIO-R**	**DIO-P**	**p value**
LBP (ng/mL)	2524±200.3 [ab]	2164±255.5 [b]	3164±281.4[a]	p=0.02
TNF-α (pg/mL)	8.57±1.41 [a]	1.42±0.49 [b]	9.77±2.83 [a]	p=0.016
IL-6 (pg/mL)	6.89±2.40	3.81±1.42	6.80±1.47	p=0.052
MCP-1 (pg/mL)	243.30±36.52 [a]	117.40±19.95 [b]	328.70±57.66 [a]	p=0.006
IL-1α (pg/mL)	15.12±3.34	21.28±2.41	23.64±4.78	p=0.17
IL-5 (pg/mL)	10.59±1.80	9.801±1.47	24.00±6.10	p=0.18
MIP-1α (pg/mL)	3.26±0.28	2.35±0.25	3.11±0.48	p=0.16

MIP-1β (pg/mL)	6.52±1.46	2.35±0.64	7.09±2.04	p=14
IL-12P40 (pg/mL)	416.0±27.68	351.4±19.28	348.1±25.27	p=0.13
KC (CXCL1) (pg/mL)	246.9±30.06 [b]	172.5±11.45 [b]	309.2±30.81 [a]	p= 0.0012
G-CSF (pg/mL)	96.06±12.06	91.14±12.54	113.1±18.08	p=0.58
Eotoxin (pg/mL)	3261±371.6	3112±368.6	4534±659.8	p=0.12
IL-10 (pg/mL)	12.76±2.070	6.82±1.63	10.64±1.83	p=0.09
IL-17A (pg/mL)	8.25±1.86	4.66±1.65	4.05±1.65	p=0.14

Mean values are presented as Mean±S.E.M. Groups that do not share a lowercase letter are considered significantly different ($p<0.05$). Parametric data (including LBP, G-CSF and EOTOXIN) were analysed by One-way ANOVA followed by Newman-Keuls multiple comparisons test and non-parametric data were either was either log-transformed to normalize (including TNF- α, MCP-1, IL-5, KC, MIP-1β, IL-12P40, MIP-1α, and IL-10) followed by performing the ANOVA, or analysed by Kruskal-Wallis test (IL-6, IL-1α, and IL-17α) followed by Dunn's multiple comparisons test (n=8 Control, n=9 DIO-R, n=12 DIO-P). Statistical significance was set at $p < 0.05$. Values with different superscripts (a, b) are significantly different at $p < 0.05$. DIO-R: Diet-induced obesity resistant group, DIO-P: Diet-induced obesity prone group. LBP: Lipopolysaccharide-binding protein; TNF-α = tumor necrosis factor alpha; IL = interleukin; MCP-1=Monocyte Chemoattractant Protein-1; MIP=Macrophage inflammatory protein-1 alpha; KC= Keratinocyte-derived cytokine. G-CSF: Granulocyte Colony-Stimulating Factor.

3.6 Distinct Metabolic Profile in Obesity-Prone Mice and Obesity-Resistant Mice

Analysis of fasting serum markers **(Figure 4-9A-L)** revealed distinct metabolic profile among the experimental groups. Obesity-prone group exhibited a significantly elevated levels of pro-inflammatory adipokines of resistin and leptin compared to both DIO-R and control groups. Furthermore, FBG levels were significantly higher in DIO-P mice compared to DIO-R and control mice, suggesting altered glucose homeostasis in obesity-prone animals. The index of HOMA-IR revealed significantly higher values in DIO-P compared to DIO-R, indicating an impaired insulin sensitivity specifically in the obesity-prone group. Additionally, the adiponectin/leptin ratio, an indicator of functionality of adipose tissue and a useful estimator of obesity [66], was significantly lower in DIO-P mice compared to both DIO-R and control groups. However, fasting appetite-related hormones such as GLP-1 and ghrelin showed no significant differences among the groups, indicating that variations in appetite regulation might not be the primary drivers of the distinct phenotypes of obesity. Furthermore, no significant differences were observed in other factors related to inflammation and glucose homeostasis, including PAI-I, glucagon, and GIP. These

findings underscore the presence of a unique metabolic profile in obesity-prone mice characterized by dysregulated adipokines and impaired glucose homeostasis, highlighting potential factors contributing to their increased susceptibility to obesity.

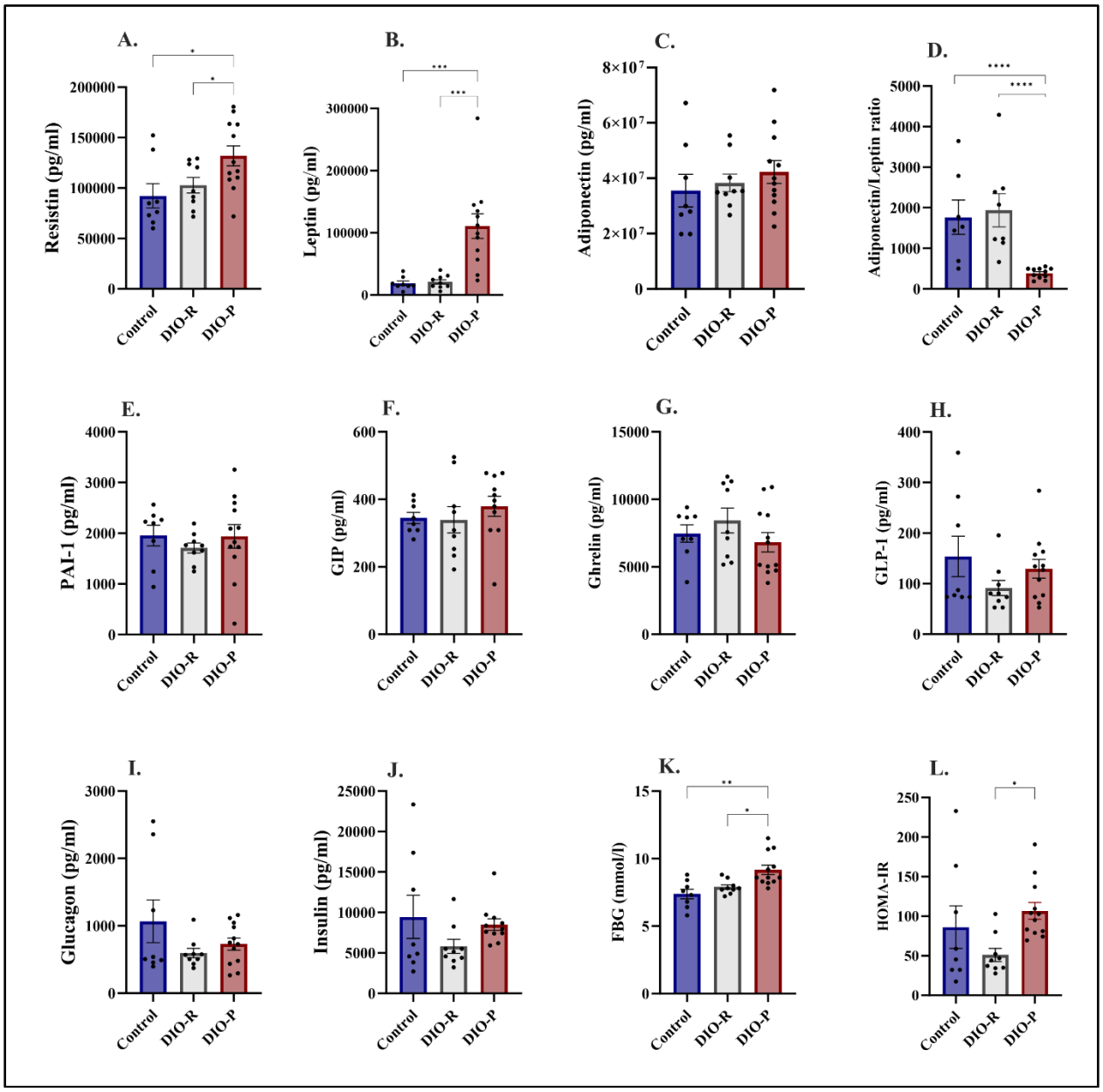

Figure 4-9. Serum Concentrations of Adipokines, Glucose and Insulin Homeostasis and Gut Peptides. **A.** Resistin, **B.** Leptin, **C.** Adiponectin, **D.** Adiponectin/Leptin ratio, **E.** PAI-1, **F.** GIP, **G.** Ghrelin, **H.** GLP-1, **I.** Glucagon, **J.** Insulin, **K.** FBG, **L.** HOMA-IR. Parametric data (including Resistin, PAI-I, Adiponectin, Ghrelin and, FBG) were analysed by One-way ANOVA, while non-parametric data were log-transformed to normalize (including GIP, and GLP-1, Glucagon, Insulin, HOMA-IR, Leptin and Adiponectin/Leptin) followed by performing the ANOVA and Newman-Keuls multiple comparisons test. Statistical significance was set at $p < 0.05$. Asterisks indicate level of statistical significance: * $p < 0.05$, **

p < 0.01, **** p < 0.0001. DIO-R: Diet-induced obesity resistant group, DIO-P: Diet-induced obesity prone group. PAI-1=Plasminogen activator inhibitor-1, FBG=Fasted-blood glucose, GIP=Glucose-dependent insulinotropic polypeptide HOMA-IR=Homeostatic Model Assessment of Insulin Resistance, GLP-1: Glucagon-like Peptide-1.Values are displayed as means±S.E.M.

3.7 Shifts in Adipose Tissue Depot Weights and Adipocyte Size in Obesity-Prone Mice

Figure 4-10A represents the weights of individual adipose depots in grams (g). Notably, both DIO-P and DIO-R groups exhibited significantly higher EAT weight compared to the control mice. Interestingly, there were no substantial differences in EAT weight between the DIO-P and DIO-R groups. PAT weight was significantly elevated in DIO-P mice compared to both DIO-R and control groups, while in the DIO-R group, it was significantly greater than that in the control group. Conversely, BAT weight reduced in the DIO-R group compared to the DIO-P group, with no significant difference observed compared to the control group. Analysis of H&E stained adipocyte images, **Figure 4-10B,** exhibited an increased average adipocyte size, quantified by adipocyte diameter and area, compared to the control mice. However, these changes were attenuated in DIO-R mice, suggesting an amelioration of the hypertrophic state in obesity resistant phenotype.

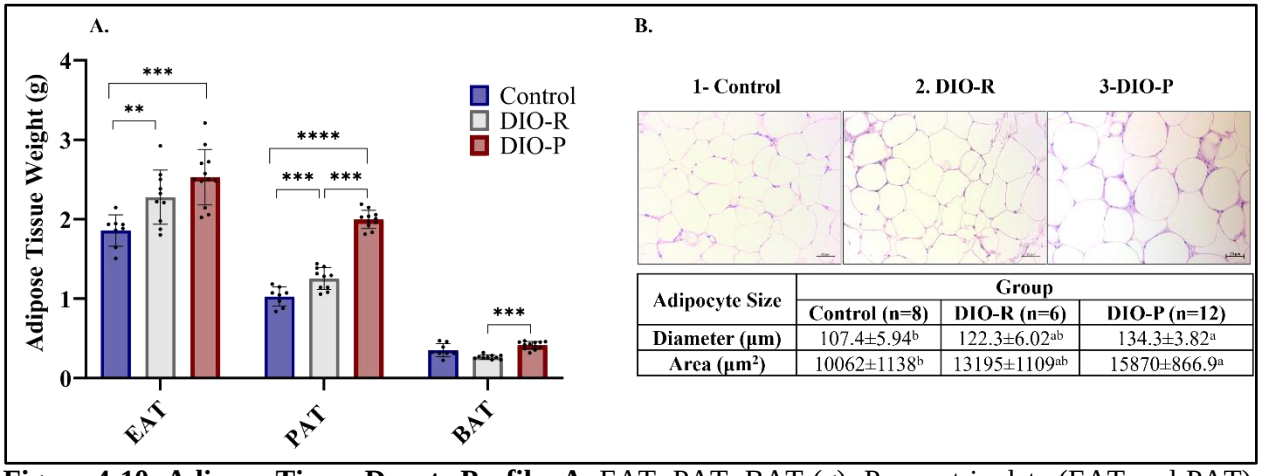

Adipocyte Size	Group		
	Control (n=8)	DIO-R (n=6)	DIO-P (n=12)
Diameter (µm)	107.4±5.94[b]	122.3±6.02[ab]	134.3±3.82[a]
Area (µm²)	10062±1138[b]	13195±1109[ab]	15870±866.9[a]

Figure 4-10. Adipose Tissue Depots Profile. A. EAT, PAT, BAT (g); Parametric data (EAT and PAT) were analyzed using One-way ANOVA followed by the Newman-Keuls multiple comparisons test. Non-parametric data were analyzed using Kruskal-Wallis test (BAT), followed by Dunn's multiple comparisons test. Asterisks indicate level of statistical significance as: * p<0.05, **p<0.01, ***p<0.001, ***p<0.0001. **B.** Representative H&E staining of EAT obtained from mice in; 1- Control, 2- DIO-R, 3- DIO-P groups

and the respective average measures of adipocyte diameter and adipocyte area. Data was analyzed using One-way ANOVA followed by the Newman-Keuls multiple comparisons test. Values with different superscripts (a, b) are significantly different. DIO-R: Diet-induced obesity resistant group, DIO-P: Diet-induced obesity prone group. EAT: epididymal adipose tissue. EAT: epididymal adipose tissue; PAT: perirenal adipose tissue; BAT: intrascapular brown adipose tissue. Values are shown as mean±SEM. Statistical significance was set at $p < 0.05$.

3.8 Obesity-Prone Mice Induced an Elevated Adipose Tissue Inflammation in Response to HFD

The EAT mRNA expression analysis revealed distinct patterns of gene expression of pro-inflammatory markers and G protein-coupled receptors (GPRs) among the study groups **(Figure 4-11A-F)**. In particular, the genes TNF-α, GPR41, and GPR43 showed significant upregulation in DIO-P group when compared to both the DIO-R and control groups. However, no significant differences were observed in the mRNA expression levels of these genes between the DIO-R and control groups. Additionally, the mRNA expression of MCP-1 exhibited a similar trend, with significant upregulation in the DIO-P group compared to both the DIO-R and Control groups. Furthermore, mRNA expression of MCP-1 was also significantly upregulated in the DIO-R group compared to the control group. Interestingly, Toll-like receptor (TLR)-4 mRNA expression was found to be significantly upregulated in the DIO-P group compared to the DIO-R group only, with no other significant differences observed between the DIO-R mice and control group. No significant difference was found in mRNA expression levels of IL-6 among the study groups.

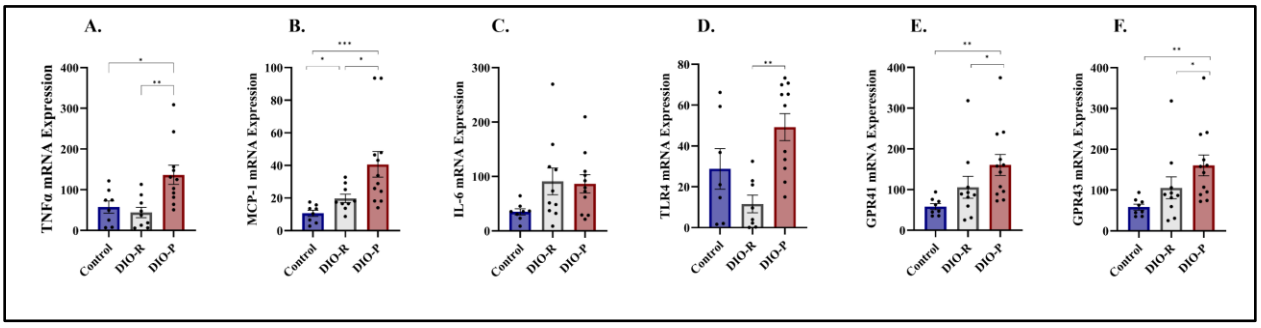

Figure 4-11. EAT mRNA Expression of Pro-Inflammatory Markers and SCFAs Receptors. A. TNF-α, **B.** MCP-1, **C.** IL-6, **D.** TLR4, **E.** GPR-41, **F.** GPR-43. Data was log-transformed to normalize then analysed by One-way ANOVA followed by Newman-Keuls multiple comparisons test. Asterisks indicate level of statistical significance: * $p < 0.05$, ** $p < 0.01$, *** $p < 0.001$. Data related to gene expression of each target gene was normalized to the expression levels of RPLP0 as the housekeeping gene. EAT: Epididymal adipose tissue. Values are displayed as means±S.E.M. TNF-α: Tumor Necrosis Factor-alpha,

IL-6: Interleukin-6, MCP-1: Monocyte Chemoattractant Protein-1, TLR-4: Toll-like receptor 4, GPR-41: G-protein coupled receptor 41, GPR-43: G-protein coupled receptor 43.

Following our mRNA measurements, we conducted an analysis of cytokines in the extracted protein from EAT **(Figure 4-12A-E)**. Consistent with our mRNA data, MCP-1 revealed upregulation in the DIO-P group compared to the other groups. Unexpectedly, TNF-α showed increased expression in the control group compared to DIO-P only, contrasting with the mRNA results. Conversely, we observed an increased IL-10 expression in the control group compared to both DIO-P and DIO-R. Notably, there were no significant differences in IL-1β as well as IL-6 expression among the groups, with the latter aligning with our mRNA findings.

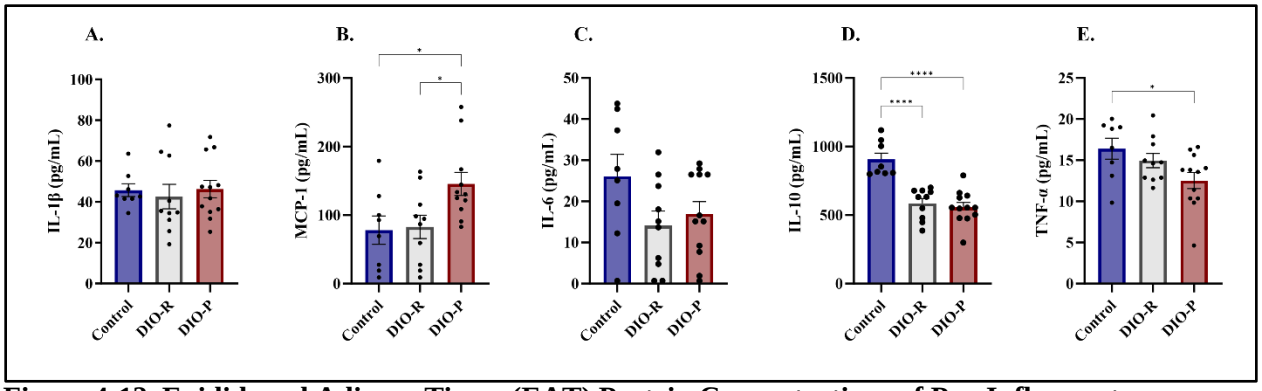

Figure 4-12. Epididymal Adipose Tissue (EAT) Protein Concentrations of Pro-Inflammatory Markers. A. IL-1 β, **B.** MCP-1, **C.** IL-6, **D.** IL-10, **E.** TNF-α. Data was log-transformed to normalize then analysed by One-way ANOVA followed by Newman-Keuls multiple comparisons test. Asterisks indicate level of statistical significance: * $p < 0.05$, ** $p < 0.01$, *** $p < 0.001$. EAT: Epididymal adipose tissue. Values are displayed as means±S.E.M.

4. Discussion

In this study, we aimed to explore the potential contributors underlying the observed variations in susceptibility or resistance to obesity in C57Bl/6 male mice, a well-established model to mimic human obesity and associated metabolic dysfunction. Stratifying the HFD-fed mice into the DIO-P and DIO-R phenotypes based on the body weight gain revealed marked differences in

food intake, gut microbiota, adipose tissue distribution and function, and systemic inflammatory and metabolic profiles.

To further explore the link between gut microbiota, inflammation, and endotoxemia, we conducted a comprehensive analysis of fecal microbial community structure and function. Previous research, has shown diverse results, including similar gut microbiota dysbiosis [40], an increase in the abundance of *Enterobacteriales* order [33], an elevated abundance of Firmicutes and Actinobacteria, coupled with a decreased abundance of Bacteroides and Proteobacteria in gut microbiota as well as a significant reduction in gut microbiota richness and diversity [42] in obesity prone compared to the obesity resistant rodents. In contrast to the observed microbial diversity similarities in this study, our examination of microbiota composition revealed distinct differences at the phylum and genus levels (**Figure 4-5)**. Specifically, we identified a higher abundance of *F16* from the TM7 phylum in DIO-P mice, which, despite inconsistent results in the literature [67,68], has evidence potentially associated with increased adiposity [69]. Conversely, *Akkermansia,* exhibited a marked increase as a key genus distinguishing DIO-R from DIO-P, aligning with findings from a recently published study [70]. This underscores its potential as a biomarker for the observed heterogeneity in obesity phenotype. It is noteworthy that the discrepancies in results across the literature could be attributed to differences in specimen origin (cecal vs. fecal), dietary fat content, background diet composition, and study duration among various research studies. This underscores the complexity of gut microbiota dynamics in the context of obesity and highlights the need for further investigation.

Akkermansia is recognized for its beneficial effects in alleviating obesity [71–73], supported by evidence from both preclinical and clinical studies that consistently reveal a decreased abundance of *Akkermansia muciniphila* species in obesity and associated metabolic

dysfunction [74,75]. Notably, administration of *Akkermansia muciniphila* has shown promise in preventing the harmful effects of HFD in mice [75,76]. This includes reversing colon mucosal barrier dysfunction observed in HFD-fed mice, demonstrated by an increase in mucus layer thickness and enhanced goblet cell density, thereby highlighting its role in promoting gut health [25,71]. In the current study, in line with other studies comparing obese groups to controls [77–79], serum concentrations of LBP were elevated in the obesity-prone group when compared to the resistant group, which suggests an enhanced gut integrity in DIO-R mice. This finding aligns with evidence associating gut microbiota dysbiosis with gut inflammation and increased gut permeability, supported by increase plasma LPS and reduced colonic tight junction protein expression such as Occludin and ZO-1 [42]. Overall, our findings suggest a pivotal role for higher *Akkermansia* relative abundance in attenuating the effects of HFD on endotoxemia and further inflammation state.

Exposure to pro-inflammatory stimuli, such as LPS, triggers a cascade of immune responses, leading to the secretion of pro-inflammatory cytokines that contribute to the chronic low-grade systemic inflammation observed in obesity [29,80–82]. Surprisingly, *Akkermansia* is reported to be inversely associated with low-grade systemic inflammation [75]. In our study, we found suppressed serum levels of MCP-1 and TNF-α in DIO-R compared to DIO-P **(Table 4-2)**. Notably, this reduction was evident even when contrasted with the control group, which had never been exposed to HFD. These findings align with reduced systemic pro-inflammatory markers observed in both humans and animal models undergoing weight-loss interventions [83–86]. Although our mice had *ad libitum* access to food, the reduced cumulative calorie intake could also be responsible for suppressing systemic inflammation in DIO-R mice in the present study .

Adipose tissue serves a dual role as an energy storage organ and a metabolically active endocrine organ with inflammation and immunity functions [87,88]. DIO-P mice exhibited a significant higher percentage of fat mass **(Figure 4-1)**, and subsequent elevated weights of adipose depots including PAT and BAT compared to DIO-R mice **(Figure 4-10)**. Unexpectedly, in line with the results reported in a previous study [6], HFD resulted in comparable fat accumulation in EAT in both the DIO-P and DIO-R, differing from that observed in control mice. However, the adipocyte size in EAT of DIO-P mice was visibly and statistically larger than that of the control group, indicating hypertrophy in the DIO-P group, an effect that was attenuated in DIO-R mice. The observed hypertrophy in EAT in DIO-P mice might be related to upregulation of TLR4 and the subsequent expression of proinflammatory cytokine genes such as TNF-α and MCP-1 when compared to the DIO-R mice **(Figure 4-11)**. These data align with reduced proinflammatory marker gene expression in adipose tissue when comparing obesity-resistant to obesity-prone phenotypes in mice [6], or HFD-fed mice switched to a low-fat chow diet in previously published reports [4]. It is important to note that these reports primarily examined gene expression, which may not accurately represent protein expression levels. In another study measuring adipose tissue protein levels of cytokines, a reduction was observed in TNF-α and IL-6 levels in HFD-fed mice switched to a low-fat chow diet, while MCP-1 showed no significant difference compared to the obese mice [89]. Our study stands out as the first to concurrently assessed both cytokine gene and protein concentrations in EAT, revealing consistent outcomes indicating the alleviation of inflammation and mitigation of adipose tissue dysfunction in HFD fed DIO-R mice.

Furthermore, like the findings of a previous study [90], DIO-P mice exhibited elevated glucose concentrations, insulin resistance, and higher serum levels of adipokines, including resistin and leptin, in comparison to DIO-R mice **(Figure 4-9)**. Notably, considering that resistin is known

for its potent proinflammatory properties and its association with EAT inflammation and insulin resistance [91,92], it closely corresponds with our observations. The hyperleptinemia observed in DIO-P mice aligns with the known correlation between leptin and adipose tissue mass [93]. Under obesogenic conditions, partial leptin deficiency protected the mice from obesity development and exerted beneficial effects on energy homeostasis [94], which could be involved in the resistance to obesity in our study. We also found a reduced Adiponectin/Leptin ratio, recognized as a predictive marker for metabolic syndrome [95]. These findings overall highlight the significant impact of adipose tissue on influencing the obesity phenotype and metabolic health.

In this study, differences in gut microbiota composition were noted, but no significant variations were observed in fecal SCFAs concentrations **(Figure 4-7)**. While evidence from human studies have revealed elevated SCFAs levels in obesity [96], SCFAs administration revealed protection against diet-induced obesity [97,98]. Despite comparable fecal SCFAs levels, DIO-P mice exhibited notably higher cumulative energy intake, raising questions about the complex interplay between gut microbiota activity, dietary factors, and SCFAs production. The discrepancy might be attributed, in part, to the low fermentability of cellulose [64], the primary fiber source in this study. On the other hand, DIO-P mice showed an upregulation of SCFAs receptors GPR 41 and 43 in EAT **(Figure 4-11)**, suggesting potential differences in SCFAs absorption and emphasizing the importance of studying SCFAs in serum as a reflection of their uptake.

The microbial predicted functional pathway analysis unveiled notable differences between the DIO-P and DIO-R groups including enriched pathways in DIO-R mice such as biosynthesis of unsaturated fatty acids and steroid biosynthesis. Interestingly, *Akkermansia* abundance exhibited a positive correlation with these pathways **(Figure 4-8)**. However, the information on

contributions of these microbial pathways in identifying the obesity phenotype is limited, underscoring the necessity for further research.

One of the strengths of this study lies in the comprehensive evaluation of inflammatory markers through both mRNA gene expression and protein concentrations in adipose tissue. While our study provides valuable insights with respect to the factors involved in development of various DIO phenotypes, it has some limitations. The exclusive focus on male mice restricts direct application to females. Additionally, the absence of baseline gut bacteria analysis limits our ability to fully understand whether the distinct obesity phenotypes were caused by variations in gut microbiota composition or if the observed phenotypes influenced the microbiota dynamics.

In summary, our study elucidates the complex interactions influencing the development of obesity-prone or obesity-resistant phenotypes in a DIO model of C57BL/6 male mice, while highlighting the crucial role of the gut microbiota in obesity pathogenesis. Our findings specifically emphasize the potential contributions of *Akkermansia* in mitigating obesity-associated inflammatory and metabolic dysfunctions, while offering prospects for innovative therapeutic interventions for obesity treatment.

Supplementary Materials

Table 4-3(S1). Forward and Reverse Primer Sequences Utilized for qRT-PCR

Target gene	Forward Primer (5'-3')	Reverse Primer (5'-3')
RPLP0	ACTGGTCTAGGACCCGAGAAG	TCCCACCTTGTCTCCAGTCT
TNF-α	CATCTTCTCAAAATTCGAGTGACAA	TGGGAGTAGACAAGGTACAACCC
IL-6	AACGATGATGCACTTGCAGA	GAGCATTGGAAATTGGGGTA
MCP-1	GCCTGCTGTTCACACAGTTGC	CAGGTGAGTGGGGCGTTA
TLR-4	AGAAAATGCCAGGATGATGC	CTGATCCATGCATTGGTAGGT
GPR-41	GTGACCATGGGGACAAGCTTC	CCCTGGCTGTAGGTTGCATT
GPR-43	GGCTTCTACAGCAGCATCTA	AAGCACACCAGGAAATTAAG

RPLP0: Ribosomal Protein Lateral Stalk Subunit P0, TNF-α: Tumor Necrosis Factor-alpha, IL-6: Interleukin-6, MCP-1: Monocyte Chemoattractant Protein-1, TLR-4: Toll-like Receptor 4, GPR-41: G Protein-Coupled Receptor 41, GPR-43: G Protein-Coupled Receptor 43.

Table 4-4(S2). Summary of Detectable and Undetectable Cytokine/Chemokine Concentrations in Serum Samples of Mice from the Control, DIO-R, and DIO-P Groups

Analyst	Undetctable *n* (%) [$]	Control (n=8)		DIO-R (n=10)			DIO-P (n=12)
		#	Median (IQR) [†]	#	Median (IQR)	#	Median (IQR)
IL-3	25 (83.3%)	8		8	3.985 (2.06, 5.91)	9	5.63 (0.01, 9.73)
IL-1B	12 (40%)	2	0.94 (0.35, 1.53)	6	3.19 (0.35, 14.91)	4	2.245 (0.65, 4.1)
TNF- α	0	0	10.62 (6.45, 10.62)	0	2.81 (0.37, 29.33)	0	8.53 (3.72, 24.53)
IL-9	19 (63%)	6	120.525 (0.47, 240.58)	6	5.585 (0.86, 273.53)	7	14.64 (0.29, 190.1)
IFN-γ	4 (13%)	0	0.12 (0.03, 2.56)	3	1.29 (0.02, 20.34)	1	3.22 (0.57, 13.42)
IL-2	2 (6%)	0	0.83 (0.28, 1.47)	1	0.21 (0.11, 5.60)	1	0.83 (0.0, 7)
IL-13	8 (26%)	1	3.32 (0.16, 3.32)	4	0.16 (0.16, 48.30)	3	15.26 (3.32, 80)
IL-6	0	0	4.865 (1.41, 11.34)	0	2.07 (1.34, 10.99)	0	5.4 (3.24, 9.28)
IL-4	25 (83%)	7	0.19 (0.19, 0.19)	9	11.79 (11.79, 11.79)	9	10.66 (4.07, 14.61)
MCP-1	0	0	256.81 (190.84, 317.57)	0	118.67 (99.41, 306.79)	0	287.19 (190.84, 374.05)
IL-5	0	0	10.4 (6.23, 14.93)	0	12.14 (7.88, 14.93)	0	16.82 (7.99, 36.41
IL-1α	0	0	13.63 (6.09, 22.74)	0	22.28 (16.83, 26.88)	0	19.68 (12.39, 30.22)
G-CSF	0	0	89.02 (69.29, 118.63)	0	91.21 (63.91, 169.16)	0	102.27 (73.11, 141.52)
RANTES	4 (26%)	3	12.94 (0.28, 16.84)	0	9.175 (4.34, 16.82)	1	16.04 (7.01, 34.74)
IL-10	1 (3%)	0	13.505 (7.62, 18.79)	0	6.77 (3.37, 14.45)	1	11.63 (4.01, 16.36
KC	0	0	256.85 (191.46, 269.47)	0	168.89 (145.78, 224.89)	0	253.07 (225.32, 409.43
IL-17A	1 (3%)	0	7.995 (3.39, 13.16)	0	4.675 (1.21, 9.21)	1	4.39 (1.95, 9.21
GM-CSF	19 (63%)	6	2.78 (2.78, 2.78)	7	2.78 (2.78, 94.95)	6	2.78 (2.78, 45.67
Eotoxin	0	0	3080.5 (2492.75, 4168.25)	0	348 (2415.75, 5191.00)	0	4978 (2628.00, 7061.75
MIP-1-β	0	0	7.015 (3.22, 9.23)	0	2.82 (1.39, 13.06)	0	5.285 (0.60, 11.02)
IL-12P40	0	0	402.05 (370.98, 445.12)	0	332.525 (319.54, 362.86)	0	340.805 (310.99, 395.21)
MIP-1 α	0	0	3.255 (2.58, 4.04)	0	2.425 (1.86, 3.10)	0	2.89 (1.96, 3.67)
IL-12P70	8 (26%)	3	8.37 (4.19, 33.34)	4	9.545 (0.72, 43.77)	1	8.37 (0.72, 24.49)

[$] Below than minimum detectable range. # Total number of undetectables in the respective groups. †25th and 75th percentile reported. IQR = interquartile range; IL = interleukin; TNF- α = tumor necrosis factor alpha; MCP-1=Monocyte Chemoattractant Protein-1; IFN-γ = interferon-γ; MIP=Macrophage

inflammatory protein-1 alpha; G-CSF=granulocyte-colony stimulating factor; KC= Keratinocyte-derived cytokine; GM-CSF = granulocyte-macrophage colony-stimulating

Author Contributions:

Conceptualization, S.M., É. D., and K.A.P.; Methodology, S.M., and L.K.; Investigation, S.M., L.K., G.F., V.R.; Formal analysis, S.M., and K.A.P.; Resources/Equipment, K.A.P.; Writing–Original Draft Preparation, S.M.; Writing – Review & Editing, S.M., and K.A.P.; Supervision, É. D., and K.A.P.; Project Administration, S.M.; Funding Acquisition, K.A.P.

Funding:

This research was supported by the following funding sources: NSERC Discovery, Ontario Research Fund, and the Nutrition and Mental Health Doctoral Scholarship from the School of Nutrition at the University of Ottawa.

Institutional Review Board Statement:

This study was conducted according to the National Institute of Health Guide for the Care and Use of Laboratory Animals and received approval from the Institutional Review Board at the University of Ottawa (Animal Care Committee, Protocol#HS-2857).

Data Availability Statement:

The data presented in this study are available on request from the corresponding author.

Acknowledgments:

The authors would like to acknowledge the valuable assistance provided by the University of Ottawa, animal care and veterinary services (ACVS) in animal care aspect of this research, and the Animal Behaviour and Physiology Core Facility team for supporting the behavior tests training and provision of essential equipment. We gratefully acknowledge Histology/ Staining services provided by the Louise Pelletier Histology Core RRID: SCR_021737.

Conflicts of Interest:

The authors declare no conflicts of interest.

5. References

1. World Health Organisation WHO | Obesity and Overweight. *Fact Sheet No 311* 2016.
2. de Moura e Dias, M.; dos Reis, S.A.; da Conceição, L.L.; Sediyama, C.M.N. de O.; Pereira, S.S.; de Oliveira, L.L.; Gouveia Peluzio, M. do C.; Martinez, J.A.; Milagro, F.I. Diet-Induced Obesity in Animal Models: Points to Consider and Influence on Metabolic Markers. *Diabetol. Metab. Syndr.* **2021**, *13*, doi:10.1186/s13098-021-00647-2.
3. Geiger, B.M.; Pothos, E.N. Chapter 1 - Translating Animal Models of Obesity and Diabetes to the Clinic. In *Translational Medicine in CNS Drug Development*; Nomikos, G.G., Feltner, D.E.B.T.-H. of B.N., Eds.; Elsevier, 2019; Vol. 29, pp. 1–16 ISBN 1569-7339.
4. Shi, H.; Akunuru, S.; Bierman, J.C.; Hodge, K.M.; Mitchell, M.C.; Foster, M.T.; Seeley, R.J.; Reizes, O. Diet-Induced Obese Mice Are Leptin Insufficient after Weight Reduction. *Obes. Silver Spring Md* **2009**, *17*, 1702–1709, doi:10.1038/oby.2009.106.
5. Gao, M.; Ma, Y.; Liu, D. High-Fat Diet-Induced Adiposity, Adipose Inflammation, Hepatic Steatosis and Hyperinsulinemia in Outbred CD-1 Mice. *PloS One* **2015**, *10*, e0119784, doi:10.1371/journal.pone.0119784.
6. Choi, J.-Y.; McGregor, R.A.; Kwon, E.-Y.; Kim, Y.J.; Han, Y.; Park, J.H.Y.; Lee, K.W.; Kim, S.-J.; Kim, J.; Yun, J.W.; et al. The Metabolic Response to a High-Fat Diet Reveals Obesity-Prone and -Resistant Phenotypes in Mice with Distinct mRNA-Seq Transcriptome Profiles. *Int. J. Obes.* **2016**, *40*, 1452–1460, doi:10.1038/ijo.2016.70.
7. Hill, J.O.; Melanson, E.L.; Wyatt, H.T. Dietary Fat Intake and Regulation of Energy Balance: Implications for Obesity. *J. Nutr.* **2000**, *130*, 284S-288S, doi:10.1093/jn/130.2.284S.
8. Wilborn, C.; Beckham, J.; Campbell, B.; Harvey, T.; Galbreath, M.; La Bounty, P.; Nassar, E.; Wismann, J.; Kreider, R. Obesity: Prevalence, Theories, Medical Consequences, Management, and Research Directions. *J. Int. Soc. Sports Nutr.* **2005**, *2*, 4–31, doi:10.1186/1550-2783-2-2-4.
9. Lin, X.; Li, H. Obesity: Epidemiology, Pathophysiology, and Therapeutics. *Front. Endocrinol.* **2021**, *12*, 706978, doi:10.3389/fendo.2021.706978.
10. Loos, R.J.F.; Yeo, G.S.H. The Genetics of Obesity: From Discovery to Biology. *Nat. Rev. Genet.* **2022**, *23*, 120–133, doi:10.1038/s41576-021-00414-z.
11. McPherson, R. Genetic Contributors to Obesity. *Can. J. Cardiol.* **2007**, *23 Suppl A*, 23A-27A, doi:10.1016/s0828-282x(07)71002-4.
12. Le Chatelier, E.; Nielsen, T.; Qin, J.; Prifti, E.; Hildebrand, F.; Falony, G.; Almeida, M.; Arumugam, M.; Batto, J.-M.; Kennedy, S.; et al. Richness of Human Gut Microbiome Correlates with Metabolic Markers. *Nature* **2013**, *500*, 541–546, doi:10.1038/nature12506.
13. Ley, R.E.; Bäckhed, F.; Turnbaugh, P.; Lozupone, C.A.; Knight, R.D.; Gordon, J.I. Obesity Alters Gut Microbial Ecology. *Proc. Natl. Acad. Sci. U. S. A.* **2005**, *102*, 11070–11075, doi:10.1073/pnas.0504978102.
14. Jumpertz, R.; Le, D.S.; Turnbaugh, P.J.; Trinidad, C.; Bogardus, C.; Gordon, J.I.; Krakoff, J. Energy-Balance Studies Reveal Associations between Gut Microbes, Caloric Load, and Nutrient Absorption in Humans. *Am. J. Clin. Nutr.* **2011**, *94*, 58–65, doi:10.3945/ajcn.110.010132.
15. Turnbaugh, P.J.; Bäckhed, F.; Fulton, L.; Gordon, J.I. Diet-Induced Obesity Is Linked to Marked but Reversible Alterations in the Mouse Distal Gut Microbiome. *Cell Host Microbe* **2008**, *3*, 213–223, doi:10.1016/j.chom.2008.02.015.
16. Shahi, S.K.; Ghimire, S.; Lehman, P.; Mangalam, A.K. Obesity Induced Gut Dysbiosis Contributes to Disease Severity in an Animal Model of Multiple Sclerosis. *Front. Immunol.* **2022**, *13*, 966417, doi:10.3389/fimmu.2022.966417.

17. DeGruttola, A.K.; Low, D.; Mizoguchi, A.; Mizoguchi, E. Current Understanding of Dysbiosis in Disease in Human and Animal Models. *Inflamm. Bowel Dis.* **2016**, *22*, 1137–1150, doi:10.1097/MIB.0000000000000750.
18. Bäckhed, F.; Manchester, J.K.; Semenkovich, C.F.; Gordon, J.I. Mechanisms Underlying the Resistance to Diet-Induced Obesity in Germ-Free Mice. *Proc. Natl. Acad. Sci. U. S. A.* **2007**, *104*, 979–984, doi:10.1073/pnas.0605374104.
19. Turnbaugh, P.J.; Ridaura, V.K.; Faith, J.J.; Rey, F.E.; Knight, R.; Gordon, J.I. The Effect of Diet on the Human Gut Microbiome: A Metagenomic Analysis in Humanized Gnotobiotic Mice. *Sci. Transl. Med.* **2009**, *1*, 6ra14, doi:10.1126/scitranslmed.3000322.
20. Turnbaugh, P.J.; Ley, R.E.; Mahowald, M. a; Magrini, V.; Mardis, E.R.; Gordon, J.I. An Obesity-Associated Gut Microbiome with Increased Capacity for Energy Harvest. *Nature* **2006**, *444*, 1027–1031, doi:10.1038/nature05414.
21. Kasai, C.; Sugimoto, K.; Moritani, I.; Tanaka, J.; Oya, Y.; Inoue, H.; Tameda, M.; Shiraki, K.; Ito, M.; Takei, Y.; et al. Comparison of the Gut Microbiota Composition between Obese and Non-Obese Individuals in a Japanese Population, as Analyzed by Terminal Restriction Fragment Length Polymorphism and next-Generation Sequencing. *BMC Gastroenterol.* **2015**, *15*, 100, doi:10.1186/s12876-015-0330-2.
22. Palmas, V.; Pisanu, S.; Madau, V.; Casula, E.; Deledda, A.; Cusano, R.; Uva, P.; Vascellari, S.; Loviselli, A.; Manzin, A.; et al. Gut Microbiota Markers Associated with Obesity and Overweight in Italian Adults. *Sci. Rep.* **2021**, *11*, 5532, doi:10.1038/s41598-021-84928-w.
23. Magne, F.; Gotteland, M.; Gauthier, L.; Zazueta, A.; Pesoa, S.; Navarrete, P.; Balamurugan, R. The Firmicutes/Bacteroidetes Ratio: A Relevant Marker of Gut Dysbiosis in Obese Patients? *Nutrients* **2020**, *12*, doi:10.3390/nu12051474.
24. Zhou, Q.; Zhang, Y.; Wang, X.; Yang, R.; Zhu, X.; Zhang, Y.; Chen, C.; Yuan, H.; Yang, Z.; Sun, L. Gut Bacteria Akkermansia Is Associated with Reduced Risk of Obesity: Evidence from the American Gut Project. *Nutr. Metab.* **2020**, *17*, 90, doi:10.1186/s12986-020-00516-1.
25. Everard, A.; Belzer, C.; Geurts, L.; Ouwerkerk, J.P.; Druart, C.; Bindels, L.B.; Guiot, Y.; Derrien, M.; Muccioli, G.G.; Delzenne, N.M.; et al. Cross-Talk between Akkermansia Muciniphila and Intestinal Epithelium Controls Diet-Induced Obesity. *Proc. Natl. Acad. Sci. U. S. A.* **2013**, *110*, 9066–9071, doi:10.1073/pnas.1219451110.
26. Dao, M.C.; Everard, A.; Aron-Wisnewsky, J.; Sokolovska, N.; Prifti, E.; Verger, E.O.; Kayser, B.D.; Levenez, F.; Chilloux, J.; Hoyles, L.; et al. Akkermansia Muciniphila and Improved Metabolic Health during a Dietary Intervention in Obesity: Relationship with Gut Microbiome Richness and Ecology. *Gut* **2016**, *65*, 426–436, doi:10.1136/gutjnl-2014-308778.
27. Murphy, E.A.; Velazquez, K.T.; Herbert, K.M. Influence of High-Fat Diet on Gut Microbiota: A Driving Force for Chronic Disease Risk. *Curr. Opin. Clin. Nutr. Metab. Care* **2015**, *18*, 515–520, doi:10.1097/MCO.0000000000000209.
28. Duan, Y.; Zeng, L.; Zheng, C.; Song, B.; Li, F.; Kong, X.; Xu, K. Inflammatory Links Between High Fat Diets and Diseases. *Front. Immunol.* **2018**, *9*, 2649, doi:10.3389/fimmu.2018.02649.
29. Bleau, C.; Karelis, A.D.; St-Pierre, D.H.; Lamontagne, L. Crosstalk between Intestinal Microbiota, Adipose Tissue and Skeletal Muscle as an Early Event in Systemic Low-Grade Inflammation and the Development of Obesity and Diabetes. *Diabetes Metab. Res. Rev.* **2015**, *31*, 545–561, doi:10.1002/dmrr.2617.

30. Kim, K.-A.; Gu, W.; Lee, I.-A.; Joh, E.-H.; Kim, D.-H. High Fat Diet-Induced Gut Microbiota Exacerbates Inflammation and Obesity in Mice via the TLR4 Signaling Pathway. *PloS One* **2012**, *7*, e47713, doi:10.1371/journal.pone.0047713.
31. Sanz, Y.; Moya-Pérez, A. Microbiota, Inflammation and Obesity. *Adv. Exp. Med. Biol.* **2014**, *817*, 291–317, doi:10.1007/978-1-4939-0897-4_14.
32. Khan, M.J.; Gerasimidis, K.; Edwards, C.A.; Shaikh, M.G. Role of Gut Microbiota in the Aetiology of Obesity: Proposed Mechanisms and Review of the Literature. *J. Obes.* **2016**, *2016*, 7353642, doi:10.1155/2016/7353642.
33. de La Serre, C.B.; Ellis, C.L.; Lee, J.; Hartman, A.L.; Rutledge, J.C.; Raybould, H.E. Propensity to High-Fat Diet-Induced Obesity in Rats Is Associated with Changes in the Gut Microbiota and Gut Inflammation. *Am. J. Physiol. Gastrointest. Liver Physiol.* **2010**, *299*, G440-448, doi:10.1152/ajpgi.00098.2010.
34. Cani, P.D.; Amar, J.; Iglesias, M.A.; Poggi, M.; Knauf, C.; Bastelica, D.; Neyrinck, A.M.; Fava, F.; Tuohy, K.M.; Chabo, C.; et al. Metabolic Endotoxemia Initiates Obesity and Insulin Resistance. *Diabetes* **2007**, *56*, 1761–1772, doi:10.2337/db06-1491.
35. Antonioli, L.; Caputi, V.; Fornai, M.; Pellegrini, C.; Gentile, D.; Giron, M.C.; Orso, G.; Bernardini, N.; Segnani, C.; Ippolito, C.; et al. Interplay between Colonic Inflammation and Tachykininergic Pathways in the Onset of Colonic Dysmotility in a Mouse Model of Diet-Induced Obesity. *Int. J. Obes. 2005* **2019**, *43*, 331–343, doi:10.1038/s41366-018-0166-2.
36. Fujiyama, Y.; Hokari, R.; Miura, S.; Watanabe, C.; Komoto, S.; Oyama, T.; Kurihara, C.; Nagata, H.; Hibi, T. Butter Feeding Enhances TNF-Alpha Production from Macrophages and Lymphocyte Adherence in Murine Small Intestinal Microvessels. *J. Gastroenterol. Hepatol.* **2007**, *22*, 1838–1845, doi:10.1111/j.1440-1746.2007.04905.x.
37. Ding, S.; Chi, M.M.; Scull, B.P.; Rigby, R.; Schwerbrock, N.M.J.; Magness, S.; Jobin, C.; Lund, P.K. High-Fat Diet: Bacteria Interactions Promote Intestinal Inflammation Which Precedes and Correlates with Obesity and Insulin Resistance in Mouse. *PloS One* **2010**, *5*, e12191, doi:10.1371/journal.pone.0012191.
38. Cani, P.D.; Amar, J.; Iglesias, M.A.; Poggi, M.; Knauf, C.; Bastelica, D.; Neyrinck, A.M.; Fava, F.; Tuohy, K.M.; Chabo, C.; et al. Metabolic Endotoxemia Initiates Obesity and Insulin Resistance. *Diabetes* **2007**, *56*, 1761–1772, doi:10.2337/db06-1491.
39. Cani, P.D.; Delzenne, N.M.; Amar, J.; Burcelin, R. Role of Gut Microflora in the Development of Obesity and Insulin Resistance Following High-Fat Diet Feeding. *Pathol. Biol. (Paris)* **2008**, *56*, 305–309, doi:10.1016/j.patbio.2007.09.008.
40. Wei, B.; Wang, S.; Wang, Y.; Ke, S.; Jin, W.; Chen, J.; Zhang, H.; Sun, J.; Henning, S.M.; Wang, J.; et al. Gut Microbiota-Mediated Xanthine Metabolism Is Associated with Resistance to High-Fat Diet-Induced Obesity. *J. Nutr. Biochem.* **2021**, *88*, 108533, doi:10.1016/j.jnutbio.2020.108533.
41. Belobrajdic, D.P.; King, R.A.; Christophersen, C.T.; Bird, A.R. Dietary Resistant Starch Dose-Dependently Reduces Adiposity in Obesity-Prone and Obesity-Resistant Male Rats. *Nutr. Metab.* **2012**, *9*, 93, doi:10.1186/1743-7075-9-93.
42. Zhang, P.; Yu, Y.; Qin, Y.; Zhou, Y.; Tang, R.; Wang, Q.; Li, X.; Wang, H.; Weston-Green, K.; Huang, X.-F.; et al. Alterations to the Microbiota–Colon–Brain Axis in High-Fat-Diet-Induced Obese Mice Compared to Diet-Resistant Mice. *J. Nutr. Biochem.* **2019**, *65*, 54–65, doi:10.1016/j.jnutbio.2018.08.016.
43. Illumina 16S Metagenomic Sequencing Library. *Illumina.com* **2013**, 1–28.

44. Bolyen, E.; Rideout, J.R.; Dillon, M.R.; Bokulich, N.A.; Abnet, C.C.; Al-Ghalith, G.A.; Alexander, H.; Alm, E.J.; Arumugam, M.; Asnicar, F.; et al. Reproducible, Interactive, Scalable and Extensible Microbiome Data Science Using QIIME 2. *Nat. Biotechnol.* **2019**, *37*, 852–857, doi:10.1038/s41587-019-0209-9.
45. Callahan, B.J.; McMurdie, P.J.; Rosen, M.J.; Han, A.W.; Johnson, A.J.A.; Holmes, S.P. DADA2: High-Resolution Sample Inference from Illumina Amplicon Data. *Nat. Methods* **2016**, *13*, 581–583, doi:10.1038/nmeth.3869.
46. McDonald, D.; Price, M.N.; Goodrich, J.; Nawrocki, E.P.; DeSantis, T.Z.; Probst, A.; Andersen, G.L.; Knight, R.; Hugenholtz, P. An Improved Greengenes Taxonomy with Explicit Ranks for Ecological and Evolutionary Analyses of Bacteria and Archaea. *ISME J.* **2012**, *6*, 610–618, doi:10.1038/ismej.2011.139.
47. Lu, Y.; Zhou, G.; Ewald, J.; Pang, Z.; Shiri, T.; Xia, J. MicrobiomeAnalyst 2.0: Comprehensive Statistical, Functional and Integrative Analysis of Microbiome Data. *Nucleic Acids Res.* **2023**, *51*, W310–W318, doi:10.1093/nar/gkad407.
48. Dhariwal, A.; Chong, J.; Habib, S.; King, I.L.; Agellon, L.B.; Xia, J. MicrobiomeAnalyst: A Web-Based Tool for Comprehensive Statistical, Visual and Meta-Analysis of Microbiome Data. *Nucleic Acids Res.* **2017**, *45*, W180–W188, doi:10.1093/nar/gkx295.
49. Segata, N.; Izard, J.; Waldron, L.; Gevers, D.; Miropolsky, L.; Garrett, W.S.; Huttenhower, C. Metagenomic Biomarker Discovery and Explanation. *Genome Biol.* **2011**, *12*, R60, doi:10.1186/gb-2011-12-6-r60.
50. Livingston, D.B.H.; Sweet, A.; Rodrigue, A.; Kishore, L.; Loftus, J.; Ghali, F.; Mahmoodianfard, S.; Celton, C.; Hosseinian, F.; Power, K.A. Dietary Flaxseed and Flaxseed Oil Differentially Modulate Aspects of the Microbiota Gut–Brain Axis Following an Acute Lipopolysaccharide Challenge in Male C57Bl/6 Mice. *Nutrients* **2023**, *15*, 3542, doi:10.3390/nu15163542.
51. Douglas, G.M.; Maffei, V.J.; Zaneveld, J.R.; Yurgel, S.N.; Brown, J.R.; Taylor, C.M.; Huttenhower, C.; Langille, M.G.I. PICRUSt2 for Prediction of Metagenome Functions. *Nat. Biotechnol.* **2020**, *38*, 685–688, doi:10.1038/s41587-020-0548-6.
52. Langille, M.G.I.; Zaneveld, J.; Caporaso, J.G.; McDonald, D.; Knights, D.; Reyes, J.A.; Clemente, J.C.; Burkepile, D.E.; Vega Thurber, R.L.; Knight, R.; et al. Predictive Functional Profiling of Microbial Communities Using 16S rRNA Marker Gene Sequences. *Nat. Biotechnol.* **2013**, *31*, 814–821, doi:10.1038/nbt.2676.
53. Janssen, S.; McDonald, D.; Gonzalez, A.; Navas-Molina, J.A.; Jiang, L.; Xu, Z.Z.; Winker, K.; Kado, D.M.; Orwoll, E.; Manary, M.; et al. Phylogenetic Placement of Exact Amplicon Sequences Improves Associations with Clinical Information. *mSystems* **2018**, *3*, e00021-18, doi:10.1128/mSystems.00021-18.
54. MIRARAB, S.; NGUYEN, N.; WARNOW, T. SEPP: SATé-Enabled Phylogenetic Placement. In *Biocomputing 2012*; WORLD SCIENTIFIC, 2011; pp. 247–258 ISBN 978-981-4596-37-4.
55. Czech, L.; Stamatakis, A. Scalable Methods for Analyzing and Visualizing Phylogenetic Placement of Metagenomic Samples. *PloS One* **2019**, *14*, e0217050, doi:10.1371/journal.pone.0217050.
56. Louca, S.; Doebeli, M. Efficient Comparative Phylogenetics on Large Trees. *Bioinformatics* **2018**, *34*, 1053–1055, doi:10.1093/bioinformatics/btx701.
57. Kanehisa, M.; Goto, S. KEGG: Kyoto Encyclopedia of Genes and Genomes. *Nucleic Acids Res.* **2000**, *28*, 27–30, doi:10.1093/nar/28.1.27.

58. Douglas, G. PiCrust2 Categorize_by_function.Py · Issue #1 · Gavinmdouglas/Picrust2_manuscript Available online: https://github.com/gavinmdouglas/picrust2_manuscript/issues/1 (accessed on 17 June 2022).
59. Parks, D.H.; Tyson, G.W.; Hugenholtz, P.; Beiko, R.G. STAMP: Statistical Analysis of Taxonomic and Functional Profiles. *Bioinforma. Oxf. Engl.* **2014**, *30*, 3123–3124, doi:10.1093/bioinformatics/btu494.
60. Chen, S.-Y.; Beretta, M.; Olzomer, E.M.; Shah, D.P.; Wong, D.Y.H.; Alexopoulos, S.J.; Aleksovska, I.; Salamoun, J.M.; Garcia, C.J.; Cochran, B.J.; et al. Targeting Negative Energy Balance with Calorie Restriction and Mitochondrial Uncoupling in Db/Db Mice. *Mol. Metab.* **2023**, *69*, 101684, doi:https://doi.org/10.1016/j.molmet.2023.101684.
61. Kit, E. Human LBP.
62. Crawley, J.N. *What's Wrong With My Mouse? : Behavioral Phenotyping of Transgenic and Knockout Mice*; Wiley-Liss: Hoboken, N.J., 2007; Vol. 2nd ed; ISBN 978-0-471-47192-9.
63. Blancas-Velazquez, A.; Mendoza, J.; Garcia, A.N.; la Fleur, S.E. Diet-Induced Obesity and Circadian Disruption of Feeding Behavior. *Front. Neurosci.* **2017**, *11*, 23, doi:10.3389/fnins.2017.00023.
64. Ashaolu, T.J.; Ashaolu, J.O.; Adeyeye, S. a. O. Fermentation of Prebiotics by Human Colonic Microbiota in Vitro and Short-Chain Fatty Acids Production: A Critical Review. *J. Appl. Microbiol.* **2021**, *130*, 677–687, doi:10.1111/jam.14843.
65. Neels, J.G.; Badeanlou, L.; Hester, K.D.; Samad, F. Keratinocyte-Derived Chemokine in Obesity: Expression, Regulation, and Role in Adipose Macrophage Infiltration and Glucose Homeostasis. *J. Biol. Chem.* **2009**, *284*, 20692–20698, doi:10.1074/jbc.M109.018556.
66. Frühbeck, G.; Catalán, V.; Rodríguez, A.; Ramírez, B.; Becerril, S.; Salvador, J.; Colina, I.; Gómez-Ambrosi, J. Adiponectin-Leptin Ratio Is a Functional Biomarker of Adipose Tissue Inflammation. *Nutrients* **2019**, *11*, 454, doi:10.3390/nu11020454.
67. de la Garza, A.L.; Martínez-Tamez, A.M.; Mellado-Negrete, A.; Arjonilla-Becerra, S.; Peña-Vázquez, G.I.; Marín-Obispo, L.M.; Hernández-Brenes, C. Characterization of the Cafeteria Diet as Simulation of the Human Western Diet and Its Impact on the Lipidomic Profile and Gut Microbiota in Obese Rats. *Nutrients* **2023**, *15*, doi:10.3390/nu15010086.
68. Hu, Y.; Xu, J.; Sheng, Y.; Liu, J.; Li, H.; Guo, M.; Xu, W.; Luo, Y.; Huang, K.; He, X. Pleurotus Ostreatus Ameliorates Obesity by Modulating the Gut Microbiota in Obese Mice Induced by High-Fat Diet. *Nutrients* **2022**, *14*, doi:10.3390/nu14091868.
69. Gomes, A.C.; Hoffmann, C.; Mota, J.F. Gut Microbiota Is Associated with Adiposity Markers and Probiotics May Impact Specific Genera. *Eur. J. Nutr.* **2020**, *59*, 1751–1762, doi:10.1007/s00394-019-02034-0.
70. Wen, Y.; Luo, Y.; Qiu, H.; Chen, B.; Huang, J.; Lv, S.; Wang, Y.; Li, J.; Tao, L.; Yang, B.; et al. Gut Microbiota Affects Obesity Susceptibility in Mice through Gut Metabolites. *Front. Microbiol.* **2024**, *15*, 1343511, doi:10.3389/fmicb.2024.1343511.
71. Dingemanse, C.; Belzer, C.; Van Hijum, S.A.F.T.; Günthel, M.; Salvatori, D.; Dunnen, J.T.D.; Kuijper, E.J.; Devilee, P.; De Vos, W.M.; Van Ommen, G.B.; et al. *Akkermansia Muciniphila* and *Helicobacter Typhlonius* Modulate Intestinal Tumor Development in Mice. *Carcinogenesis* **2015**, *36*, 1388–1396, doi:10.1093/carcin/bgv120.
72. Santacruz, A.; Collado, M.C.; García-Valdés, L.; Segura, M.T.; Martín-Lagos, J.A.; Anjos, T.; Martí-Romero, M.; Lopez, R.M.; Florido, J.; Campoy, C.; et al. Gut Microbiota Composition Is Associated with Body Weight, Weight Gain and Biochemical Parameters in Pregnant Women. *Br. J. Nutr.* **2010**, *104*, 83–92, doi:10.1017/S0007114510000176.

73. Karlsson, C.L.J.; Önnerfält, J.; Xu, J.; Molin, G.; Ahrné, S.; Thorngren-Jerneck, K. The Microbiota of the Gut in Preschool Children With Normal and Excessive Body Weight. *Obesity* **2012**, *20*, 2257–2261, doi:10.1038/oby.2012.110.
74. Xu, Y.; Wang, N.; Tan, H.-Y.; Li, S.; Zhang, C.; Feng, Y. Function of Akkermansia Muciniphila in Obesity: Interactions With Lipid Metabolism, Immune Response and Gut Systems. *Front. Microbiol.* **2020**, *11*, 219, doi:10.3389/fmicb.2020.00219.
75. Cani, P.D.; De Vos, W.M. Next-Generation Beneficial Microbes: The Case of Akkermansia Muciniphila. *Front. Microbiol.* **2017**, *8*, 1765, doi:10.3389/fmicb.2017.01765.
76. Derrien, M.; Belzer, C.; De Vos, W.M. Akkermansia Muciniphila and Its Role in Regulating Host Functions. *Microb. Pathog.* **2017**, *106*, 171–181, doi:10.1016/j.micpath.2016.02.005.
77. Dalby, M.J.; Aviello, G.; Ross, A.W.; Walker, A.W.; Barrett, P.; Morgan, P.J. Diet Induced Obesity Is Independent of Metabolic Endotoxemia and TLR4 Signalling, but Markedly Increases Hypothalamic Expression of the Acute Phase Protein, SerpinA3N. *Sci. Rep.* **2018**, *8*, 15648, doi:10.1038/s41598-018-33928-4.
78. Guerville, M.; Leroy, A.; Sinquin, A.; Laugerette, F.; Michalski, M.-C.; Boudry, G. Western-Diet Consumption Induces Alteration of Barrier Function Mechanisms in the Ileum That Correlates with Metabolic Endotoxemia in Rats. *Am. J. Physiol. Endocrinol. Metab.* **2017**, *313*, E107–E120, doi:10.1152/ajpendo.00372.2016.
79. Naito, E.; Yoshida, Y.; Makino, K.; Kounoshi, Y.; Kunihiro, S.; Takahashi, R.; Matsuzaki, T.; Miyazaki, K.; Ishikawa, F. Beneficial Effect of Oral Administration of Lactobacillus Casei Strain Shirota on Insulin Resistance in Diet-Induced Obesity Mice: Effect of LcS on Insulin Resistance. *J. Appl. Microbiol.* **2011**, *110*, 650–657, doi:10.1111/j.1365-2672.2010.04922.x.
80. Vetrani, C.; Di Nisio, A.; Paschou, S.A.; Barrea, L.; Muscogiuri, G.; Graziadio, C.; Savastano, S.; Colao, A.; Group, O.B.O.T.O.P.O.N.E.R.A.A.O. From Gut Microbiota through Low-Grade Inflammation to Obesity: Key Players and Potential Targets. *Nutrients* **2022**, *14*, doi:10.3390/nu14102103.
81. Hersoug, L.-G.; Møller, P.; Loft, S. Role of Microbiota-Derived Lipopolysaccharide in Adipose Tissue Inflammation, Adipocyte Size and Pyroptosis during Obesity. *Nutr. Res. Rev.* **2018**, *31*, 153–163, doi:10.1017/S0954422417000269.
82. Duan, Y.; Zeng, L.; Zheng, C.; Song, B.; Li, F.; Kong, X.; Xu, K. *Inflammatory Links Between High Fat Diets and Diseases*; 2018; Vol. 9; ISBN 1664-3224.
83. Sarin, H.V.; Lee, J.H.; Jauhiainen, M.; Joensuu, A.; Borodulin, K.; Männistö, S.; Jin, Z.; Terwilliger, J.D.; Isola, V.; Ahtiainen, J.P.; et al. Substantial Fat Mass Loss Reduces Low-Grade Inflammation and Induces Positive Alteration in Cardiometabolic Factors in Normal-Weight Individuals. *Sci. Rep.* **2019**, *9*, 3450, doi:10.1038/s41598-019-40107-6.
84. Bianchi, V.E. Weight Loss Is a Critical Factor to Reduce Inflammation. *Clin. Nutr. ESPEN* **2018**, *28*, 21–35, doi:https://doi.org/10.1016/j.clnesp.2018.08.007.
85. Wu, S.-C.; Rau, C.-S.; Lu, T.-H.; Tzeng, S.-L.; Wu, Y.-C.; Wu, C.-J.; Lin, C.-W.; Hsieh, C.-H. Effect of Weight-Reduction in Obese Mice Lacking Toll-Like Receptor 5 and C57BL/6 Mice Fed a Low-Fat Diet. *Mediators Inflamm.* **2015**, *2015*, 852126, doi:10.1155/2015/852126.
86. Dogan, S.; Ray, A.; Cleary, M.P. The Influence of Different Calorie Restriction Protocols on Serum Pro-Inflammatory Cytokines, Adipokines and IGF-I Levels in Female C57BL6 Mice: Short Term and Long Term Diet Effects. *Meta Gene* **2017**, *12*, 22–32, doi:10.1016/j.mgene.2016.12.013.

87. Coelho, M.; Oliveira, T.; Fernandes, R. Biochemistry of Adipose Tissue: An Endocrine Organ. *Arch. Med. Sci. AMS* **2013**, *9*, 191–200, doi:10.5114/aoms.2013.33181.
88. Khanna, D.; Khanna, S.; Khanna, P.; Kahar, P.; Patel, B.M. Obesity: A Chronic Low-Grade Inflammation and Its Markers. *Cureus* **2022**, *14*, e22711, doi:10.7759/cureus.22711.
89. Rodrigues, M.O.M.; Evangelista-Silva, P.H.; Neves, N.N.; Moreno, L.G.; Santos, C.S.; Rocha, K.L.S.; Ottone, V.O.; Batista-da-Silva, B.; Dias-Peixoto, M.F.; Magalhães, F.C.; et al. Caloric Restriction-Induced Weight Loss with a High-Fat Diet Does Not Fully Recover Visceral Adipose Tissue Inflammation in Previously Obese C57BL/6 Mice. *Appl. Physiol. Nutr. Metab. Physiol. Appl. Nutr. Metab.* **2020**, *45*, 1353–1359, doi:10.1139/apnm-2020-0220.
90. Choi, J.-Y.; McGregor, R.A.; Kwon, E.-Y.; Kim, Y.J.; Han, Y.; Park, J.H.Y.; Lee, K.W.; Kim, S.-J.; Kim, J.; Yun, J.W.; et al. The Metabolic Response to a High-Fat Diet Reveals Obesity-Prone and -Resistant Phenotypes in Mice with Distinct mRNA-Seq Transcriptome Profiles. *Int. J. Obes.* **2016**, *40*, 1452–1460, doi:10.1038/ijo.2016.70.
91. Bokarewa, M.; Nagaev, I.; Dahlberg, L.; Smith, U.; Tarkowski, A. Resistin, an Adipokine with Potent Proinflammatory Properties. *J. Immunol.* **2005**, *174*, 5789–5795, doi:10.4049/jimmunol.174.9.5789.
92. Qatanani, M.; Szwergold, N.R.; Greaves, D.R.; Ahima, R.S.; Lazar, M.A. Macrophage-Derived Human Resistin Exacerbates Adipose Tissue Inflammation and Insulin Resistance in Mice. *J. Clin. Invest.* **2009**, *119*, 531–539, doi:10.1172/JCI37273.
93. Martínez-Sánchez, N. There and Back Again: Leptin Actions in White Adipose Tissue. *Int. J. Mol. Sci.* **2020**, *21*, 6039, doi:10.3390/ijms21176039.
94. Zhao, S.; Li, N.; Zhu, Y.; Straub, L.; Zhang, Z.; Wang, M.-Y.; Zhu, Q.; Kusminski, C.M.; Elmquist, J.K.; Scherer, P.E. Partial Leptin Deficiency Confers Resistance to Diet-Induced Obesity in Mice. *Mol. Metab.* **2020**, *37*, 100995, doi:10.1016/j.molmet.2020.100995.
95. Vega, G.L.; Grundy, S.M. Metabolic Risk Susceptibility in Men Is Partially Related to Adiponectin/Leptin Ratio. *J. Obes.* **2013**, *2013*, 409679, doi:10.1155/2013/409679.
96. Kim, K.N.; Yao, Y.; Ju, S.Y. Short Chain Fatty Acids and Fecal Microbiota Abundance in Humans with Obesity: A Systematic Review and Meta-Analysis. *Nutrients* **2019**, *11*, 2512, doi:10.3390/nu11102512.
97. Weitkunat, K.; Stuhlmann, C.; Postel, A.; Rumberger, S.; Fankhänel, M.; Woting, A.; Petzke, K.J.; Gohlke, S.; Schulz, T.J.; Blaut, M.; et al. Short-Chain Fatty Acids and Inulin, but Not Guar Gum, Prevent Diet-Induced Obesity and Insulin Resistance through Differential Mechanisms in Mice. *Sci. Rep.* **2017**, *7*, 6109, doi:10.1038/s41598-017-06447-x.
98. Lu, Y.; Fan, C.; Li, P.; Lu, Y.; Chang, X.; Qi, K. Short Chain Fatty Acids Prevent High-Fat-Diet-Induced Obesity in Mice by Regulating G Protein-Coupled Receptors and Gut Microbiota. *Sci. Rep.* **2016**, *6*, 37589, doi:10.1038/srep37589.

5 CHAPTER 5: General Discussion and Conclusion

5.1 Integration of Findings

The overall goal of this thesis was to investigate the influence of dietary modifications on the gut microenvironment and their collective effects on inflammation, metabolic, and mental health outcomes, particularly in the context of obesity. In Project 1, detailed in chapter 2, and Project 2, detailed in chapter 3, I investigated the impact of incorporating white and dark red kidney beans into a low-fat diet on obesity-associated outcomes in mice previously subjected to high-fat diet-induced obesity. On the other hand, in Project 3, detailed in chapter 4, I focused on understanding the factors contributing to obesity resistance while under a HFD with a primary emphasis on the role of gut microbiota composition and function in shaping obesity-resistant phenotypes.

Since diets with reduced energy density align more with sustainable dietary management of obesity, in our study, mice were fed a LFD concurrent the beans consumption. This is contrary to most previous studies on animal models (discussed in chapter 1) that evaluated the effects of beans on gut microbiota structure and function while mice were being fed with an HFD. However, with respect to intestinal health, addition of cooked beans to the mice diet, despite its different composition, consistently attenuated obesity-associated dysbiosis and related intestinal health dysfunction. Also, this research holds translational significance for humans. The average pulse intake reported in Canada and United States by pulse consumers were 87 to 113 g/d, which is equivalent to more than one-half cup/day [154]. On the other hand, in Canada, high-pulse consumer adults take an average of 294 g (~325 kcal) of pulses per day, considering an average daily calorie intake of 2500 Kcal, which amounts to approximately 13% of the total calorie intake from pulses [224]. Therefore, the level of kidney bean supplementation used in current research

(15% w/w or ~ 12.7 % kcal), equivalent to approximately 1 cup of pulses, represents a realistic and achievable daily intake of beans in humans [180].

Transitioning obese mice from a HFD to a LFD supplemented with beans resulted in a significant attenuation of weight gain compared to the obese control group. However, the body weight of mice in the bean-fed group continued to increase when compared to the group HF→LF, without bean supplementation. This outcome may have been influenced by higher diet and energy intake in the bean-supplemented groups, aligning with findings of studies in healthy individuals where pulses demonstrated acute appetite-suppressing effects following pulse meals but did not necessarily lead to decreased food intake in subsequent meals [225]. The unique appearance, taste, and aroma of beans could have contributed to their higher palatability, potentially influencing overall food intake in our study. However, beans beneficially impacted body composition, particularly by enhancing lean mass compared to the bean-free diets. Moreover, they significantly reduced fat mass in comparison to the obese control, bringing it to a level with no significant differences from the HF→LF group, despite notable distinctions in body weight. Microbiota analysis of both fecal (distal colon) and cecal (proximal colon) samples in Projects 1 and 2, respectively, revealed that, in comparison to the lean group (LF), HFD led to minimal changes in the relative abundance of bacterial members at the phylum level in the HF group except for increased cecal abundances of TM7 and Deferribacteres in HF obese mice. Consequently, the ratio of Firmicutes/Bacteroidetes did not exhibit significant differences between the HF and LF controls at either sampling site. At the genus level, both fecal and cecal microbiota exhibited a shared pattern of reduced relative abundance in *Papillibacter* (g), *Prevotella* (g), and *S24-7* (f) in HF compared to the lean LF group. Additionally, both sampling sites showed an increased relative abundance of *Clostridiales* (o) in the obese HF group. These findings suggest a consistent

alteration of gut microbiota in response to HFD, resulting in gut dysbiosis, as evidenced by reports highlighting the association between an HFD and dysbiosis [226]. However, unique differences emerged between the two sampling sites. In fecal samples, the obese HF mice displayed a significant increase in the relative abundance of *Clostridium* (g) compared to the lean LF group. Conversely, the cecal microbiota of the HF group exhibited distinctive changes, including an increase in the relative abundance of *F16* (f), *Mucispirillum* (g), and *Dorea* (g) when compared to the lean LF group. These findings indicate site-specific variations in microbial responses to dietary challenges.

Incorporating beans, regardless of the seed coat color, into the diet induced distinct microbial changes in both cecal and fecal samples compared to the HF obese and HF→LF groups. Shared microbial changes included a lower relative abundance of *Dorea* in both fecal and cecal samples induced by beans and fecal Lactobacillus increased in both beans compared to the HF obese group. *Dorea* is known to have pro-inflammatory properties in the intestine and is associated with obesity and related dysfunctions [227]. Additionally, beans induced specific bacterial changes, such as a lower relative abundance of *Sporobacter* in the cecum and Parabacteroides and *Alistipes* in fecal samples. However, beans increased the relative abundance of cecal *Alistipes* compared to HF obese mice only. *Alistipes* has a dual role, as suggested by existing literature. Some studies support its role as a lean-associated genus that may contribute to alleviating adiposity and mitigating metabolic syndrome outcomes [228,229] and exerting protective roles in diseases such as colitis, autism spectrum disorder, and various liver and cardiovascular fibrotic disorders [230]. However, it also exhibits a pathogenic role in diseases such as anxiety, chronic fatigue syndrome, and depression, with implications depending on the specific circumstances of the studies [230]. This inconsistency in *Alistipes* role could be attributed to the diversity within the genus, encompassing

13 various species, each with distinct roles [230]. The species identified in my analysis, including *Alistipes massiliensis, Alistipes finegoldii*, and one uncategorized species, may contribute to the observed variations in relative abundances among fecal and cecal samples. These findings suggest a deeper exploration into the complex relationships between specific bacterial species and their influence on health outcomes. Concurrent with the aforementioned changes, there was an increase in the relative abundance of bacterial taxa such as fecal and cecal *Prevotella*, cecal *Mucispirillum* and S24-7 as well as fecal and Lactobacillus in both bean supplemented groups compared to the HF group. Both Prevotella, a well-known fiber fermenter, and S24-7 are recognized as butyrate producers, contributing to specific health benefits [227,231]. The *S24-7* has known to have anti-obesity effects [227] which has been shown to be involved in reinforcing intestinal epithelial cell health [232]. These findings emphasize the potential health implications of incorporating beans into the diet, influencing gut microbiota composition regardless of the sampling site. Additionally, unlike a previous study analyzing human gut microbiota [233] that found significant differences between cecal and fecal microbiota, my results highlight that although there are quantitative variations in the relative abundance of bacterial taxa between fecal and cecal samples in C57BL/6 mice, the overall composition remains qualitative similar. The question of whether these qualitative taxonomic similarities can reliably represent the proportions of bacterial taxa within the gut microbiota, especially from preferred sampling sites with easier access-like feces, remains a subject for further investigation.

Despite the overall similarities in microbial structure among diets enriched in various beans, subtle yet significant variations emerged when comparing their impact on specific bacterial taxa to the HF obese control group. Notably, the abundance of *Lactobacillus* which is a well-known probiotic with anti-obesity properties [234], increased in fecal samples with both types of

beans, but this increase was exclusive to the cecum in the HF→WB group. In contrast, *Papillibacter* exhibited a simultaneous reduction in both fecal and cecal samples in HF→DB compared to HF obese mice, whereas this effect was absent in HF→WB. A recent study [235] revealed that *Papillibacter cinnamivorans*, the same species found in the fecal and cecal analysis here, acted as a key mediator for the anti-obesogenic effects of a fungus-derived polysaccharide in HFD-induced obese mouse models, reducing the proinflammatory response and improving gut permeability. While these findings may seemingly contradict my results, the influence of background diet features and specific interactions between beans and other polysaccharide contents could contribute to this inconsistency. Moreover, *Papillibacter* is a relatively novel genus, and therefore, further research is needed to elucidate its intricate role in the gut microbiota and its response to dietary interventions. Moreover, HF→WB demonstrated a lower fecal relative abundance of *rc4-4*, a genus linked to obesity, while HF→DB exhibited a higher cecal relative abundance of *Akkermansia* compared to HF obese controls. These results highlight the diverse effects of bean varieties with varying phenolic content on gut microbiota composition.

The comparison of gut microbiota between obesity-prone and obesity-resistant subjects in Project 3 also highlighted *Akkermansia* as a key bacterium potentially involved in emerging phenotypes resistant to obesity. As discussed in chapter 4, it has shown for its anti-obesity effects and attenuating metabolic dysfunction in both preclinical and clinical studies [236,237]. Treatment with *Akkermansia muciniphila* has shown promise in preventing the harmful effects of HFD in mice [237,238]. This includes reversing colon mucosal barrier dysfunction observed in HFD-fed mice, demonstrated by an increase in mucus layer thickness and enhanced goblet cell density, thereby highlighting its role in promoting gut health [192,239]. *Akkermansia muciniphila* has been reported to be involved in communicating with host cells and subsequently stimulating mucus

production, primarily through the degradation and utilization of mucus glycans, as well as the expression of specific microbial protein compounds [240]. Therefore, the increased relative abundance of *Akkermansia* may have potentially contributed to enhanced barrier integrity, subsequently reducing systemic and local inflammation in obesity-resistant mice, even when consuming an HFD. Further investigation, including measurements of outcomes such as tight junction proteins or mucus content, is warranted to better understand the mechanisms underlying gut integrity and associated outcomes in obesity-resistant mouse models.

To examine the functionality of the above gut microbiota alterations such as microbiota fermentation activity induced by beans, the concentrations of fecal and cecal SCFAs, as an informative indicator, were measured in Projects 2 and 3, respectively. Across both sampling sites, total SCFAs, as well as the individual levels of acetic, propionic, and butyric acids, consistently increased in the beans-supplemented groups compared to the other dietary interventions. Interestingly, in the cecum, there was a slightly higher, although not statistically significant, total, and individual SCFAs concentration in HF→DB when compared to the HF→WB. In contrast, in fecal samples, there was a greater level of SCFAs in HF→WB, where only butyric acid reached significant levels compared to HF→DB. This finding was not expected as I hypothesized that if beans with darker seed coats would have additional benefits resulting from their higher phenolic content [241]. However, this could be attributed to the higher absorption of SCFAs mainly butyrate from microbial fermentation of dark beans into the circulation through moving towards the distal colon and reaching lower levels of butyrate in the fecal. This unexpected finding challenges our hypothesis that beans with darker seed coats would confer additional benefits due to higher phenolic content [241]. However, it may be attributed to the interaction between polyphenols, gut microbiota and modulated metabolites produced by bacterial fermentation, such as SCFAs [242].

This interaction potentially enhanced the absorption of butyrate produced from dark beans into the circulation as it moved towards the distal colon. This may consequently lead to lower levels of butyrate reaching the feces in HF→DB group. Notably, serum SCFAs levels were not identified in this research, and the actual mechanism remains to be clarified through further investigations.

Acetate, propionate, and butyrate are the most abundant ligands for G protein-coupled receptors of GPR41 and GPR43. In Project 2, despite increased production of SCFAs by the intestinal microbiota, incorporation of bean to the LFD, did not have any additional effects on the expression of these receptors in adipose tissue. It is important to note that mRNA measurements of these receptors in EAT may not correspond to the expression levels of the functional protein. Furthermore, it has been suggested that the expression levels of GPR41 and GPR43 are tissue-specific [243]. Considering the higher fecal SCFAs in bean-fed mice and the relatively low potency of SCFAs as the primary agonists of these receptors [243], it is plausible that the serum concentrations of SCFAs might not reach the levels necessary for the functional effects at the tissue level. It is essential to consider that the produced SCFAs in the colon are absorbed into colonocytes, serving as an energy source and undergoing immediate oxidation. A portion is transported to the liver through portal circulation, where further metabolism occurs. Only the SCFAs that pass the liver enter the peripheral circulation, resulting in low concentrations in blood serum or plasma [244]. In project 3, mRNA expression of GPR41 and GPR43 was downregulated in epididymal adipose tissue (EAT) of obesity-resistant mice compared to the prone group, despite no significant differences in fecal SCFA levels. This underscores the potential discrepancy between local SCFA concentrations and their systemic effects. Therefore, further studies are needed to investigate the ratio between production of SCFAs in the colon and the absorption into the circulation.

Among the SCFAs, butyrate specifically plays a role in reinforcing the colonic mucosal barrier by stimulating the synthesis and secretion of mucin into the lumen, promoting the expression of tight-junction proteins and acting as an anti-inflammatory metabolite [245]. In contrast, a western-style diet is known to induce changes in gut microbiota composition and reduce the rate of mucus growth, thereby increasing the mucus layer penetrability [246]. The increased SCFAs levels were accompanied by a significant rise in several parameters related to intestinal size, including total cecum weight, cecum content, and colon length. However, in project 2, the proximal colon histomorphology outcomes such as crypt length measurements, revealed that despite observing higher crypt length in proximal colon cross-sections in the beans-supplemented groups, no significant differences were found between the groups. It needs to be noted that the analysis was limited by the subset of measurable stained sections due to the slight discrepancies exhibited in the random region excised across the proximal colon for the histology analysis. As a result, the images of those stained sections were excluded from the final analysis, resulting in a reduced sample size, which may have contributed to the lack of reaching statistical significance.

Concomitant with the enhanced intestinal microbiota composition induced by beans, the predicted metagenomic functions of fecal and cecal microbiota exhibited distinct alterations, as compared to the obese control groups. Notably, the cecal predicted functions did not differ between the HF→LF and HF groups, despite observable variations in microbiota composition. However, when analyzing predicted functions in feces, 114 pathways were shared between HF→LF, HF→WB, and HF→DB in comparison to the HF control. These findings suggest that qualitative taxonomic similarities between fecal and cecal microbiota do not necessarily determine predicted functionality. Additionally, both bean varieties shared 175 fecal and 181 cecal pathways when

compared to HF, reflecting their similar gut microbial composition. However, each bean type presented unique shared pathways, representing their distinct gut microbial compositions mainly resulting from various phenolic compounds. While the exact specific bacterial taxa influencing these predicted functional pathways remain unknown, in Project 3, *Akkermansia* exhibited was significantly correlated with some distinct pathways. Though the exact role of these pathways is still unclear, they may play a partial role in the observed differential obesity phenotype in resistant versus prone mice.

In the context of the secondary outcomes of Project 2, focusing on the impacts of common beans on mental health and well-being through the gut-brain axis, it is crucial to acknowledge that the measurements conducted represent just an initial assessment in this field. The introduction of bean supplementation into LFD did not result in any alterations in nest-building behavior when compared to the HF controls. However, no significant differences were observed even between the lean mice in the LF group and the HF obese control group. It is noteworthy that the "Nest Building Scoring System" employed for rating nest-building behavior in Project 2 may lack the sensitivity needed to distinguish between lean and obese mice. On the contrary, the EPM not only demonstrated significantly enhanced anxiolytic effects in LF mice compared to HF obese mice but also exhibited mitigated anxiety-related outcomes in all groups transitioning from HFD to LFD. Notably, improvements in outcomes, such as the percentage of time spent in open arms in mice fed by diets incorporating both types of beans and lower latency to enter the open arm by white beans, were observed. The latter positive changes may be attributed to the higher fecal butyrate in the HF→WB group, linking to enhanced mood [247]. In Project 3, a notable decrease in ambulatory activity was observed in obesity-prone mice compared to both the lean and obesity-resistant groups, likely due to their higher body weight. However, the observed behavioral changes

in mice fed with beans could not be ascribed to their activity levels, measured by total and/or closed arm entries [248]. These entries reflected spontaneous motor activity and showed no variation among the groups (data not shown). This suggests that the reported differences in body weight between mice from different groups, as indicated in Project 1, did not influence animal movements during the EPM test. The interpretation of behavior outcomes in Project 2 could have been enhanced by conducting EPM tests at various time points, particularly after the establishment of obesity but before the introduction of beans (specifically at the end of week 10) for conducting pairwise comparisons. Alternatively, additional behavioral tests could have been considered.

5.1 Limitations and Future Research Directions

The current thesis while offering promising findings, was not without its limitations. The following limitations of this research are acknowledged alongside corresponding suggestions for future research directions.

One limitation of this thesis is its exclusive focus on male mice, which may restrict the generalizability of the findings to females. The decision to exclusively use male mice in this thesis was based on several considerations. Firstly, male mice are known to exhibit higher susceptibility to obesity [249,250], with studies demonstrating delayed development of obesity in female mice receiving a HFD compared to the weight-matched male mice [251]. Further, by exclusively selecting male mice, potential variations in metabolic outcomes [250] and behavioral responses attributed to hormonal fluctuations across estrous stages in female mice [252] were eliminated. Finally, according to the literature, some biological sex differences in gut microbiota composition were expected [253]. Therefore, due to the limitations of resources and financial constrains, it was not possible to include a large number of mice from both sex per group. Future research is encouraged to include female mice to broaden the scope and applicability of findings.

Another notable limitation pertains to the absence of pair-feeding food access implementation after transitioning from HFD to LFD in groups supplemented with/without beans. Therefore, implementing pair-feeding food restriction after transitioning from HFD to LFD could maintain consistent weight alterations among groups with/without beans supplementations, excluding the potential impact of increased body weight on other outcomes. Moreover, the DIO phase of this study coincided with the onset of the COVID-19 pandemic, affecting the study timeline. As a result, I could only assess body composition after obesity establishment and was unable to evaluate fasting serum markers prior to introducing beans. Measurement of serum metabolic outcomes after development of obesity for confirming the presence of obesity-associated metabolic dysfunctions is suggested.

In project 3, fecal microbiota was collected at baseline, prior to initiating feeding mice with an HFD; however, the microbiota composition was not assessed at that time. Since the DIO-R mice exhibited an increased abundance of *Akkermansia* at the study conclusion, future research aims to investigate whether this bacterial genus was higher at the beginning or is a consequence of resistance to obesity while consuming an HFD is recommended

Further, in this study, I did not investigate which specific microbial taxa were attributed to each observed predicted metagenomic function. Subsequent investigations could employ an interactive Multi-Omic Tool like BURRITO [254] for the simultaneous visualization of taxonomic and functional compositions of the microbiota, gaining a more profound understanding of the relationship between microbial taxonomy and functionality.

Another limitation arises from the lack of assessment of tight-junction (TJ) proteins mRNA expressions or concentrations in the proximal and distal colon. This limitation could be addressed in future studies by incorporating assessments of TJ proteins or utilizing alternative methods such

as the FITC (Fluorescein isothiocyanate–dextran) permeability assay [255]. These measures would contribute to a more comprehensive evaluation of gut integrity, offering valuable insights into the intestinal permeability associated with obesity and how it may be impacted by dietary interventions. Furthermore, this study did not measure other endotoxin transporters such as CD14, an LPS receptor [256], representing another limitation. Future directions could involve exploring additional endotoxin markers, supplementing the existing assessment of LBP.

Another limitation of this research is that protease inhibitors were not added during fasting blood collection. Consequently, the levels of GLP-1 and glucagon may not be reliable due to potential degradation of these markers in the absence of inhibitors.

Additionally, in current study the SCFAs were not measured in the bloodstream. Future studies could include measurements of serum SCFAs concentrations, providing insights into their absorption levels and their potential impact on metabolic health.

Lastly, regarding the assessment of mental health as secondary outcomes of project 2, the behavior assessments conducted in the study served as a preliminary exploration. Unfortunately, the COVID-19 pandemic necessitated a reduction in research activities, limiting me to measure behavior outcomes after the establishment of obesity but prior introducing beans. Also, at the end of the intervention, I anticipated that repeated handling and running various behavior tests could alter the animals physiological responses and potentially changing their behavioral responses in subsequent tests [257–259]. Therefore, I had to choose between conducting the open field and EPM tests as indicators of anxiety behavior. This decision also aimed to maintain the reliability of outcomes, particularly in light of the planned analysis of systemic and adipose tissue inflammatory markers. To deepen understanding, future studies may consider conducting thorough assessments of behavioral indicators associated with psychological well-being. It is recommended to distribute

these assessments among different sub-groups rather than subjecting the same group of mice to all tests. These assessments could include stress, memory, and mood disorders, utilizing validated tests to provide a more in-depth exploration. Additionally, in this study, the brain was excised, snap-frozen in liquid nitrogen, and stored at −80°C, but the dissection of specific brain regions did not occur. Future work will be conducted to explore neuroinflammation in brain regions such as the hypothalamus and hippocampus, with more relevance to mood disorders [132,260]. The evaluation of mRNA expression of pro-inflammatory markers in these regions is recommended. This investigation may highlight the impact of dietary intervention on neuroinflammatory changes in the CNS, which might not be immediately observable through behavioral modifications.

5.1 Conclusion

In conclusion, the incorporation of common beans into an LFD demonstrated a significant reduction in weight gain and induced favorable changes in body composition compared to the obese control group. Microbiota analysis underscored consistent alterations induced by HFD, leading to gut dysbiosis. The introduction of beans induced specific and shared changes in both fecal and cecal microbiota composition, accompanied by increased SCFA concentrations, highlighting the potential health benefits of bean consumption on intestinal health. The study further identified specific gut microbiota changes associated with WB and DB, potentially attributed to their distinct phenolic profiles. Additionally, the DB supplemented group exhibited a reduction in resistin, linked to inflammation, compared to the control group. However, with respect to other metabolic health related outcomes, after obesity establishment switching the diet from HFD to LFD exhibited most beneficial outcomes while introducing beans to mice diet at least within the supplemented range of 15% had either a modest effect or no additional effect. Further studies may benefit increasing the dosage of supplementation.

In the evaluation of mental health and well-being, the study did not reveal improvements in nest-building behavior, suggesting potential sensitivity limitations in the employed scoring system. However, the EPM test provided some evidence of anxiolytic effects by both types of beans, particularly in WB supplemented group. The research also elucidated the potential contributions of *Akkermansia* in generating resistance to obesity phenotypes and associated inflammatory and metabolic dysfunctions, even under an HFD with *ad libitum* food access. Overall, the findings of this thesis contribute to our understanding of factors involved in emerging diet-induced obesity phenotypes and emphasize the potential health implications of specific bean varieties, offering insights into both physiological and mental health outcomes in C57Bl/6 male mice.

6 CHAPTER 6- APPENDICES

6.1 APPENDIX A: Protocol for DNA extraction

DNA was extracted from the cecal content/fecal pellets using QIAamp® Fast DNA Stool kit (Qiagen, Cat. #51604, Germany) according to the manufacturer's instructions [261]. Briefly, 50 mg of the samples were placed in the 2 ml tough tubes (VWR® Reinforced Bead Mill Tubes, Cat.# 10158-556) containing five beads (VWR® 2.8 mm ceramic ceramic beads, Cat. #10158-554). The samples were lysed in 1 mL of InhibitEX Buffer to separate DNA-degrading substances and PCR inhibitors from DNA using the Bead Mill 24 (Fisherbrand™, Cat. #15-340-163) at 4 m/s for 2 minutes then the supernatant was collected in the 1.5 ml microcentrifuge tubes Fisherbrand™, Cat. # 05-408-129) and incubated in a water bath at 95°C for 6 minutes to remove impurities in InhibitEX buffer. The homogenated samples were vortexed for 15 sec then the supernatant (600 µl) were transferred in to a 2 ml microcentrifuge G-Tube® (VWR®,Cat. #21150-486) containing previously added 25 µl proteinase K and vortexed for another 15 sec, then Buffer AL (600 µl) were added, vortexed for 15 sec and incubated at 70°C for 10 minutes to digest and degrade proteins under denaturing conditions. Then, 600 µl of ethanol (96–100%) were added and vortexed for 30 seconds. Lysate was carefully applied to the QIAamp spin column using a pipette without touching the column membrane and centrifuged at 14, 000 rpm for 1min. The previous step was repeated until all the lysate was loaded on the column. The bounded DNA to the QIAamp membrane was washed using two wash buffers; first buffer AW1 (500 µl) was added, centrifuged at 14, 000 rpm for 1min and the QIAamp spin was placed in a new 2 ml collection tube and the filtrate was discarded. Second, Buffer AW2 (500 µl) was added centrifuged at 14, 000 rpm for 3 min and again the QIAamp spin was placed in a new collection tube and the filtrate was discarded and, centrifuged again for 3 min at the same speed. To elute DNA, the spin column was placed into a

new, labeled 1.5 ml microcentrifuge tube and Buffer ATE (30 µl) was directly pipetted onto the QIAamp membrane, incubated for 1 min at room temperature and centrifuged at full speed for 1 min. All centrifugation steps were carried out at room temperature (20–25°C). To determine the DNA purity in the eluate, DNA concentration was measured by absorbance at 260 nm and the ratio of absorbance at 260 nm to absorbance at 280 nm was calculated using the NanoDrop™ One (Thermo Scientific™, model ND-ONE-W).

6.2 APPENDIX B: Protocol for Microbiota DNA Sequencing and Diversity Analysis

The previously extracted DNA was quantified by PicoGreen assay using the protocol described by the manufacturer company [262] and the DNA was normalized to a concentration of 5 ng/µl using the diluted 1.0 M Tris HCl buffer at pH 8.5 (VWR®, Cat. #100220-254). The variable 3 (V3) and variable 4 (V4) regions of the 16S ribosomal RNA (rRNA) gene was amplified by PCR and then a second PCR using a Nextera XT DNA index kit was done to add multiplexing indices and Illumina sequencing adapters. The 16S libraries were pooled and sequenced using the Illumina Miseq platform (Illumina®, Miseq). Briefly, to the 12.5 µl of the normalized microbial genomic DNA, 5 µl of Amplicon PCR Reverse Primer (1 µM), 5 µl of Amplicon PCR Forward Primer (1 µM) and 2.5 µl of the 2x KAPA HiFi HotStart ReadyMix were added in a Hard-Shell® 96-Well, Low Profile 200 µl PCR Plate (Bio-Rad, Cat. # HSL-9601) (Table A1 shows forward and reverse primer sequences). The plate was sealed with a Microseal 'A' film (Bio-Rad, Cat. # MSA5001) and Amplicon PCR performed in a thermal cycler (Bio-rad, #1861096) using the following settings: 95°C for 3 minutes, 25 cycles of: — 95°C for 30 seconds — 55°C for 30 seconds — 72°C for 30 seconds, 72°C for 5 minutes and Hold at 4°C. The PCR product was confirmed by running samples on a 1.5% agarose gel. Prior to electrophoresis, 5 µl of the PCR product, along with a DNA ladder for size reference, was mixed with loading dye containing ethidium bromide. Subsequently, the gel was run, and the DNA bands were visualized under UV light. A photographic record of the gel was captured, and the corresponding image is available in **Figure 6-1**. Then the remaining PCR product was transferred into a Hard-Shell® 96-Well, high profile 300 µl PCR Plate (Bio-Rad, Cat. # HSS-9601). To purify the the 16S V3 and V4 amplicons, 20 µl AMPure XP beads were added to each of the plate ‘s well by a multichannel pipette and mixed. Then the plate was incubated at room at room temperature (RT) for 5 minutes followed by

a 2 min on a magnetic stand until the supernatant cleared. Next, the supernatant was removed and discarded and the supernatant without touching the beads pellets. While the plate was still on the magnetic stand, the beads were washed by adding 200 µl freshly prepared 80% ethanol to each well, incubated on the magnetic stand for 30 sec and, then ethanol was removed and discarded. The previous wash step was repeated followed by a 10 min of leaving the beads on the magnetic stand to air-dry. Then, the amplicon PCR plate was removed from the magnet and then 52.5 µl of 10 mM Tris pH 8.5 were added to each well, mixed by pipetting and incubated for 2 min at RT. Next, the plate was placed on the magnetic stand until the supernatant cleared and then 50 µl of the supernatant were transferred again into a new PCR plate and the plate was sealed with microseal "B"adhesive seal and stored at -20°C until the next day. Then, Index PCR was carried using the Nextera XT Index Kit (Set A-kits Cat no). Using the TruSeq Index Plate Fixture, the Index 1 primer tubes were arranged horizontally (aligned with columns 1 through 12) and Index 2 primer tubes were arranged vertically (aligned with rows A through H). Then, 5 µl of the supernatant from the previous step was transferred into a new low-profile PCR plate and the plate was placed in the Plate Fixture, 5 µl of Nextera XT index primer 1, and 5 µl of Nextera XT index primer 2 were added to their respective wells based on the plate layout. Next, 25 µl of 2x KAPA HiFi HotStart ReadyMix and then 10 µl of UltraPure™ DNase/RNase-Free Distilled Water (Invitrogen, Cat#10977015) were added to each well and mixed by pipetting. The plate was sealed with Microseal 'A' Sealing Film, centrifuged at 1,000 x g at RT for 1 minute followed by PCR on a thermal cycler using the following program: 95°C for 3 minutes, 8 cycles of:

— 95°C for 30 seconds, — 55°C for 30 seconds— 72°C for 30 seconds, 72°C for 5 minutes and hold at 4°C. The PCR product was confirmed by running samples on a 1.5 % agarose gel as described above. The PCR product was cleaned up using the AMPure XP beads followed by 2x

washes by 80% ethanol as described earlier. The plate was remained on the magnetic stand for 10 minutes to air dry, then the plate was removed, and 27.5 µl of 10 mM Tris pH 8.5 were added to resuspend the beads, centrifuged at 1800 rpm for 1 min and incubated for 2 min at RT. Next, the plate was placed on the magnetic stand until the supernatant cleared and then 20 µl of the supernatant were transferred into a new PCR plate and the plate was sealed with microseal "B"adhesive seal and stored at -20°C until the next day. The diluted DNA was quantified using the PicoGreen assay, normalised to 4 nM using 10 mM Tris pH 8.5 buffer and the pooled library was created by mixing 5 µl aliquots from each of the diluted DNA in a microcentrifuge tube. Then, 5 µl of the pooled library was denatured by adding 5 µl of 0.2 N NaOH, vortexed, centrifuged at 280 x g for 1min and incubate for 5min at RT to denature the DNA into single strands. Then, 990 µl of pre-chilled hybridization buffer (HT1) was added to the denatured DNA library to form a 20 pM denatured library in 1 mM NaOH and placed on ice until the final dilution. In the next step, 120 µl of 20 pM denatured library was diluted by 480 µl of HT1 resulting in 4 pM diluted denatured library, inverted several times, vortexed and placed on ice until the further usage. A PhiX library to the same concentration of amplicon library, 4 pM, was prepared to serve as an internal control by combining 2 µl of 10 nM PhiX and 3 µl of 10 mM Tris pH 8.5 resulting in 4 nM PhiX library followed by combining 5 µl of 4 nM PhiX library and 5 µl of 0.2 N NaOH, incubating for 5 min at RT to denature the diluted PhiX library, adding 10 µl of the denatured PhiX library to 990 µl of HT1, resulting in 20 pM denatured and diluted PhiX library and diluting 120 µl of it with 480 µl of HT1. A 15 % PhiX control solution was made by adding 90 µl of the denatured and diluted PhiX library to 510 µl of HT1 followed by combining 30 µl of control solution with 570 µl of previously prepared denatured and diluted amplicon library in a microcentrifuge tube. The combined solution was incubated at 96°C for 2 minutes on a heat block, inverted 1-2 times, placed

in an ice-water bath for 5 minutes and loaded onto the load sample reservoir on the previously thawed Miseq reagent kit v3 (600 cycle) cartridge (Illumina®, Cat. # MS-102-3003) and the Illumina Miseq (Illumina®, Miseq) was run for sequencing using the Illumina, MiSeq System Guide [263].

Table 6-1-*16S Amplicon PCR Primer Sequences*

Primer	Sequence 5'-to-3' direction
16S Amplicon PCR Reverse Primer	GTC TCG TGG GCT CGG AGA TGT GTA TAA GAG ACA GGA CTA CHV GGG TAT CTA ATC C
16S Amplicon PCR Forward Primer	TCG TCG GCA GCG TCA GAT GTG TAT AAG AGA CAG CCT ACG GGN GGC WGC AG

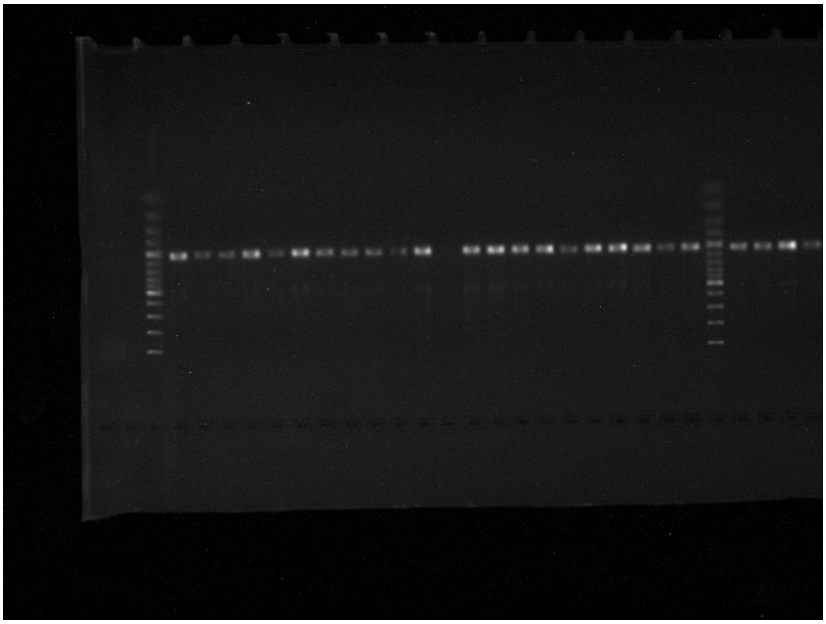

Figure 6-1-Gel electrophoresis image confirming the presence of PCR products following electrophoresis.

6.1 APPENDIX C: Protocol for Quantification of Cecal Short Chain Fatty Acids

Gut microbiota function was evaluated by measurements of SCFAs (acetic acid, butyric acid, propionic acid, and valeric acid) and branched chain fatty acids (BCFAs) concentrations (isobutyric and isovaleric acid) using gas chromatography (GC). In brief, 50-100 mg of the cecum content was freeze-dried for 24 hours (Labconco, FreeZone 12, bulk tray dryer) then the samples were diluted in MilliQ water to get 20% (dry w/v) homogenous cecal solution. The suspension was centrifuged at 14,000 g for 30 minutes (4°C) and the supernatant was collected (3 x times). The pH of the sample was measured using a benchtop pH meter (Orion™ Star™ A111 pH Benchtop Meter, Thermo Scientific, Canada). The samples were acidified by 10 µl of a solution containing 5.5mmol /L 2-ethylbutyric acid (Volatile acid standard mix (Sigma 46975-u, Canada), as an internal standard) in 100% formic acid. The sample was recentrifuged at 14,000 g for 30 minutes at 4°C and the supernatant was transferred into glass vials (Thermo Scientific™ 11mm Amber Glass Crimp/Snap Top Vials, Cat. #40116W) containing 200 µl glass inserts (Mandel, Cat. #SZ-220-91521-03). 1 µl of the sample was injected in triplicate into the GC equipped with a flame ionization detector which detects, identifies and quantitates the volatile organic compounds including SCFAs. The analysis of the components of the sample generates a chromatogram. Different SCFAs were identified by the times of retention. The area or height of each chromatographic peak shown in **Figure 6-22,** were used for determining the analyte concentration in comparison with the analytical standard solutions.

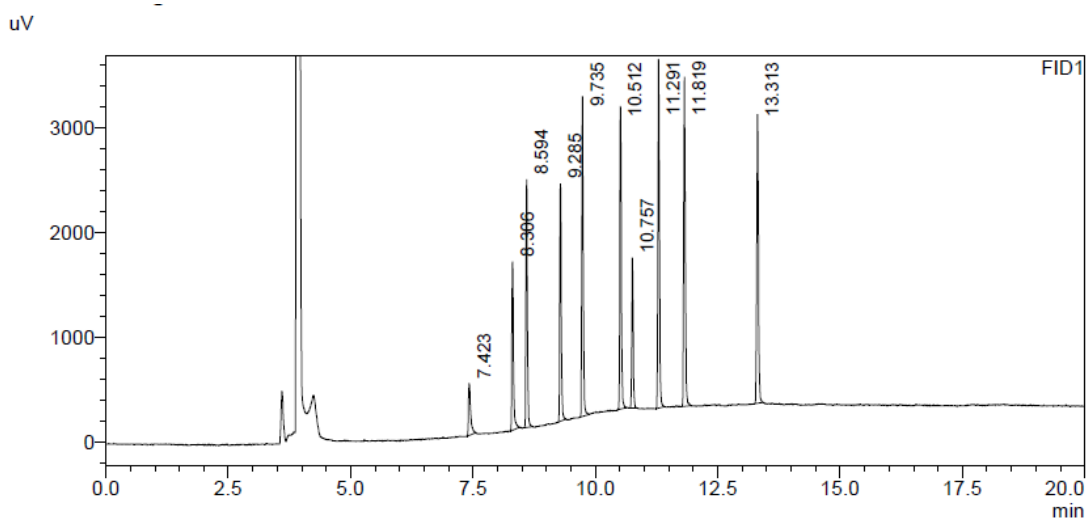

<Peak Table>

FID1

Peak#	Ret. Time	Area	Height	Conc.	Unit	Mark	Name
1	7.423	1500	496	0.689	mM		acetic acid
2	8.306	3603	1592	0.671	mM		proprionic acid
3	8.594	4905	2359	0.613	mM		isobutyric
4	9.285	4797	2260	0.630	mM		butyric
5	9.735	6271	3002	0.603	mM		isovaleric
6	10.512	6153	2882	0.612	mM		valeric
7	10.757	2973	1412	0.000	mM		ethyl butyric
8	11.291	7281	3321	0.603	mM		isocaproic
9	11.819	7124	3135	0.610	mM		hexanoic
10	13.313	6725	2744	0.606	mM		n-heptanoic
Total		51331	23204				

Figure 6-2-GC chromatogram depicting retention times and concentrations of Short-chain Fatty Acids.

6.4 APPENDIX D: Protocol for Adipose tissue mRNA Expression

6.4.1 Adipocytes RNA extraction

RNA was isolated from the previously excised adipose tissue and then purified using the Total RNA Purification Plus Kit (Norgen Biotek, #48400). Briefly, a small amount of the frozen adipose tissue (≈25 mg) was placed into a 2 ml tough tubes (VWR® Reinforced Bead Mill Tubes, Cat.# 10158-556) kept on ice containing five beads (VWR® 2.8 mm ceramic beads, Cat. #10158-554), 600 µL of Buffer RL and 6 µL of b-mercaptoethanol (aiding in RNase deactivation). Samples were lysed in the buffer using a Bead Mill 24 (Fisherbrand™, Cat. #15-340-163) at 4 m/s for 25 sec (repeated when the sample was not fully homogenized) and then the homogenate was collected in the 1.5 ml RNAse free microcentrifuge tubes. Fisherbrand™, Cat. # 05-408-129) and centrifuged for 2 minutes at 2000 RPM × 3 times. Following each time of the centrifugation, the supernatant was collected in a new microcentrifuge tube using a 1ml Tuberculin Syringe. The final lysate from the previous step was loaded onto a genomic DNA (gDNA) removal column and was centrifuged for 2 minutes at 8000 RPM. The sample was spined for an additional 1 minute at 14000 RPM if the entire lysate volume was not passed through the gDNA column. The flowthrough volume was retained and measured to calculate the require volume of Ethanol for the next step. To every 100 µL of flowthrough from the previous step, 60 µL of 96 – 100 % Ethanol was added and mixed by pipetting. Then up to 600 µL of the lysate with the ethanol was loaded onto the RNA Purification column and centrifuged for 1 minute at 6,000 RPM to isolate RNA and the flowthrough was discarded. This step was repeated until the entire lysate applied into the column. The isolated RNA was washed for 3 times by adding 400 mL of wash solution followed by centrifugation at 6,000 RPM for 1 minute × 3 times. The column was placed on a new collection tube and centrifuged for two more times at 14,000 RPM for 1 minute. The collection tube was

discarded, and the column was placed into a fully labeled microcentrifuge tube and then 50 mL of the Elution Solution A was added directly to the purified RNA in the column and centrifuged for 2 minutes at 2,000 RPM followed by another centrifugation for 1 minute at 14,000 RPM to elute the entire pure RNA from the column. All centrifugation steps were carried out at room temperature (20–25°C). To determine the RNA purity in the eluate, RNA concentration was measured by absorbance at 260 nm and the ratio of absorbance at 260 nm to absorbance at 280 nm was calculated using the NanoDrop™ One (Thermo Scientific™, model ND-ONE-W). The purified RNA was then aliquoted and stored at -80°C.

6.4.2 Complementary DNA (cDNA) synthesis

The Purified extracted RNA from all samples was normalized to a concentration of 1µg RNA/10µL using the UltraPure™ DNase/RNase-Free Distilled Water (Invitrogen, Cat. #10977015). The total normalized RNA (1 µg RNA) was reverse transcribed to complementary DNA (cDNA) using High-Capacity cDNA Reverse Transcription Kit (Applied Biosystems, Cat. #4368814). For each reaction 2 µL 10X RT Buffer, 0.8 µL 25X dNTP Mix (100 mM), 2 µL 10X RT Random Primers, 1 µL MultiScribeTM Revers and 4.2 µL Nuclease-free H2O was needed. The required volume of master mix was calculated and made accordingly. Then, 10 µL of the master mix was added to 0.2 mL PCR tubes (Eppendorf, Cat. #951010006) and mixed by 1 µg of RNA. The cDNA was synthesized in a thermal cycler (Bio-rad, Cat. #1861096) using the following settings: 10 minutes at 25°C, 120 minutes at 37°C, 5 minutes at 85°C and Hold at 4°C. The synthesized cDNA was diluted with 180 µL double distilled water and aliquoted for the further use.

6.4.3 Quantification of mRNA using RT-qPCR

Quantitative real-time reverse transcription polymerase chain reaction (qRT-PCR) analyses were performed in CFX96 Touch™ (Bio-rad, model C1000 Touch™) real-time PCR detection system. To each well of a Hard-Shell Low-Profile 96-Well Semi-Skirted PCR Plates (Bio-Rad, Cat. # HSL-9601), 6 µL of a master-mix created by mixing of 5 µL of SYBR Green (Applied Biosystems™, Cat. #A25742) as the detection reporter dye, 0.5 µL of both the forward and reverse primers (IDT™) appropriate for detection of the target genes, and 0.5 µL of nuclease free H2O was added. Next, 4 µL of cDNA from each sample in duplicates was added to each well and then the PCR plate was sealed using the Microseal 'B' PCR Plate Sealing Film (Bio-rad, #MSB1001). The plate was incubated on the CFX96 Touch™ Real-Time PCR Detection System for 2 minutes at 50°C, followed by 2 minutes at 95°C, then for 40 cycles of "15 sec at 95°C, 15 sec at 55-60 °C adjusted according to the primer melting point and finally 1 minute at 72°C". The Cq values for each of the samples were obtained from CFX Maestro Software. To compare relative expression of the target genes between samples, ΔΔCq method was applied while the gene expression levels were normalized to the expression levels of RPLP0 housekeeping reference genes. Primer sequences are displayed in Supplemental **Table S2**.

6.5 APPENDIX E: Protocol for Serum Metabolic and Inflammatory Biomarkers Analysis

The collected fasted serum at week 17, was analysed using a magnetic bead-based fluorescence sandwich immunoassay (Bio-Plex Pro Mouse Diabetes 8-Plex Immunoassay, Bio-Rad, Cat. #171F7001M), to detect multiple diabetes-related biomarkers including ghrelin, GIP, GLP-1, glucagon, insulin, leptin, PAI-1 and resistin using the manufactured instruction manual. Briefly, frozen serum samples were placed on ice and thawed in 15-20 min and then, were diluted fourfold (1:4) in a 96-well BCA plate by adding of 45 µL of the sample diluent followed by adding of 15 µL of serum and then the diluted samples were vortexed gently by pipetting. The BCA plate was placed on ice until being used. In order to prepare 8-points standard curve with a fourfold dilution between each point, nine 1.5 ml microcentrifuge tubes were labelled as S1-S8 plus blank and then 72 µL of standard diluent were added to each tube. To prepare the standards, the vial containing the lyophilized standard was gently tapped and reconstituted by adding 500 µL of the standard diluent, vortexed for 5 sec and placed on ice for exactly 30 min. Then, 128 µL of reconstituted standards were added to the S1 tube, vortexed and 50 µL of the S1 standard was added to S2 tube and then the serially dilution (1:4) was continued from tube S2 to S8. Wash buffer was prepared by 10 folds diluting of 10x Bio-Plex wash buffer stock (60 ml) in distilled water (540 ml). To make 1x coupled beads, 20x coupled magnetic beads were diluted in 5472 µL of assay buffer in a Falcon™ 15 mL Conical Centrifuge Tubes (Corning™, Cat#352095), vortexed at medium speed for 30 sec. Then, using a multichannel 50 µl of 1x beads were added in to each well of the assay plate. Then the assay plate was washed twice by adding 100 µL of 1x wash buffer into each well using a multichannel pipette followed by discarding the buffer from the wells by inverting the plate while the plate was placing on a magnetic stand. Next, 50 µl of the diluted serum samples were transferred into the assay plate. The plate was sealed and protected from the

light by aluminum foil and incubated for 1 hr on a plate shaker at 850 rpm at room temperature. After finishing the incubation time, the plate was unsealed and washed three times using the above-mentioned procedure. Ten minutes before ending the wash steps, the 20x detection antibodies stock was vortexed 20 sec at medium speed, followed by spinning for 30 sec and then, the 20x detection antibodies were diluted to 1x concentration by adding 150 µL of 20x detection antibody into 2,850 µL of detection antibody diluent. Next, 25 µl of detection antibody was added to each well using the multichannel pipette, then the assay plate was incubated on the plate shaker for 30 min at 850 rpm at room temperature. At the end of detection antibody incubation time, the plate was again unsealed and washed three times. Five minutes before ending the wash steps, the 100x Streptavidin-Phycoerythrin (SA-PE) stock was vortexed 5 sec at medium speed, followed by spinning for 30 sec. Then, the stock was diluted to 1x concentration by adding 60 µL of 100x SA-PE into 5,940 µL of assay buffer. Next, 50 µL of 1x SA-PE was added to each well using the multichannel pipette, then the assay plate was incubated on the plate shaker for 10 min on a plate shaker at 850 rpm at room temperature followed by washing the plate for three times. In the last step, the beads were resuspended by adding 125 µL of assay buffer to each well, sealed and placed on the plate shaker for 30 sec at room temperature at 850 rpm. Then, the plate was read on a Luminex® analyzer (MAGPIX®) with Milliplex Analyst software, version 5.1.0.0. by VigeneTech Inc.

The serum adiponectin concentrations were measured individually by Bio-Plex Pro Mouse Diabetes Adiponectin Assay, Cat. #171F7002M (as a single-plex assay), using the same protocol as the Mouse Diabetes 8-Plex Immunoassay, but in order to achieve the measurable concentrations within the standard curve due to high physiological levels of adiponectin in the serum, the samples

were diluted 1:1,600 in serum-based diluent in two diluting steps; 1: 10 µL sample + 390 µL serum-based diluent, 2: 10 µLfrom the first dilution + 390 µL serum-based diluent.

The analysis of serum inflammatory cytokines was conducted using Bio-Plex Pro Mouse Cytokine 23-plex Assay, Cat. #M60009RDPD as per the manufacturer's instructions, which was the same as the previously described Mouse Diabetes 8-Plex Immunoassay.

6.6 APPENDIX F: Protocol for Serum Lipopolysaccharide-Binding Protein Analysis

Mouse LBP enzyme- linked immunosorbent assay (ELISA) kits (HyCultBiotech, Cat# HK205-01) were used to measure lipopolysaccharide binding protein (LBP) levels in duplicates in mice serum as a biomarker of systemic lipopolysaccharide (LPS) exposure [264]. The assay was performed based on the sandwich principle using the manufactures instruction. Briefly, prior to running the assay, the reagents were brough from the fridge (4°C) to equilibrate into the room temperature (20 – 25°C). The required number of microwell strips were arranged in the supplied frame. To have 7-points on the standard curve with a fourfold dilution between each point, eight 1.5 ml microcentrifuge tubes were labelled as S2-S7 plus blank and then 225 µL of previously made wash/dilution buffer was added into each of the tubes. The vial containing the lyophilized standard was gently tapped and reconstituted by adding 598 µL (this volume was mentioned on the CoA; Certificate of Analysis in the standard vial) of the wash/dilution buffer and vortexed briefly (vial S1). Then, other standard solutions were made by mixing 225 µL of reconstituted standard from vial S1 into 225 µL of previously added wash/dilution buffer in S2 tube and then the serially dilution (1:2) was continued from tube S2 to S7. Serum samples were also brought from the freezer (-80°C) to the room temperature and mixed gently. Serum samples were diluted 1000x in two serial dilution steps: 1. 25 µL of sample was added into 225 µL of dilution buffer, 2. 10 µL pre-dilution sample in step 1, was added into 990 µL of dilution buffer. To prepare the wash/dilution buffers for two plates (running the assay in duplicates), 60 ml of 20x concentrated wash/dilution buffer was mixed with 540 ml distilled water (1:9) and 30 ml of 40x concentrated wash/dilution buffer B was mixed with 570 ml distilled water, then both solutions were combined into a conical flask and mixed properly. The tracer solution was made in two steps (for 1 x 96 tests); 1. One ml of distilled water was pipetted into the lyophilized biotinylated tracer vial, 2. One

ml reconstituted tracer was diluted with 11 ml wash/dilution buffer. The arranged tray was washed four times by adding 200 µL of wash buffer to each well strips, followed by inverting the tray after 20 sec and shaking it over the sink to empty the contents. Next, 100 µL of the prepared standards and diluted samples were added to the microwell strips in duplicates according to the pre-designed plate map without touching the side or bottom of the microtiter wells pre-coated with antibodies detecting mouse LBP, followed by incubating the covered tray for 1 hour at room temperature. Then, the tray was washed again four times using the above-mentioned procedure. In next step, 100 µL of diluted biotinylated tracer antibody was added followed by 1 hour incubation. In this step, biotinylated tracer antibody would bind to captured mouse LBP. Then the tray was washed four more times. Next, 100 µL of diluted streptavidin-peroxidase was added to each well with the same pipetting order of adding the standards and samples. The tray was covered and incubated for an hour at room temperature. In this step Streptavidin-peroxidase conjugate would bind to the biotinylated tracer antibody. Next, the tray was washed again four times and then, 100 µL of tetramethylbenzidine (TMB) substrate was added to each well, using the same sequence of pipetting as previous steps. In this step, Streptavidin-peroxidase conjugate would react with TMB. The tray was protected from direct light exposure by covering it in an aluminum foil followed by incubating for 30 minutes at room temperature. To stop the enzyme reaction, 100 µL of oxalic acid containing (2%) stop solution was added to each well with the same order and timing of adding TMB and the microwell strips contents were mixed by gently swirling the tray. Finally, the plate absorbance at 450 nm was measured within 30 min of adding the stop solution using a spectrophotometer plate reader (Spark® Multimode Microplate Reader). Serum LBP concentration was extrapolated using the corresponding concentrations of standards on standard curve.

6.7 APPENDIX G: Protocol for Adipose Tissue pro-Inflammatory Cytokines Expression

6.7.1 Epididymal Adipose Tissue Protein Extraction

Up to 50 mg of snap frozen Epididymal Adipose Tissue (EAT) was homogenized in a tube containing 5 ceramic beads and 1 ml of lysis buffer. The lysis buffer consisted of 1xRIPA buffer (Cell Signaling, Cat. #9806) supplemented with a protease inhibitor cocktail (Cell Signaling #5871) and PMSF (Cell Signaling #8553) at final concentrations of 1/100 and 1/200, respectively. Homogenization was performed at 6 m/s for 30 seconds or until tissue was completely lysed using a Bead Mill 24 Homogenizer (Fisherbrand™, Cat. #15-340-163). The samples were then centrifuged at 4°C, 11,000×g for 10 minutes, and the supernatant was transferred into a new 1.5 mL capped tube. To minimize lipid transfer from the top layer fat, a gauge needle attached to a 1 ml syringe was used during the supernatant transfer, and this step was repeated three times. This method ensured the collection of the smallest amount of fat possible, maintaining protein purity and quality. The protein solution was diluted 1/20, and the total protein content was quantified using the BCA assay (Pierce™ BCA Protein Assay Kit, Cat. #23225). A standard curve was generated using bovine serum albumin, and the absorbance at 562 nm was measured using a plate reader.

6.7.2 Epididymal Adipose Tissue Inflammatory Markers Analysis

The EAT extracted protein was normalized using 1x RIPA to 1mg/ml and then the cytokines protein expression including IL- 1β, MCP-1, TNF- α , IL-6 and IL-10 were measured measured by Milliplex Mouse High Sensitivity Cytokine T Cell Magnetic Bead Panel (Cat. # MHSTCMAG-70K) utilizing 25 µg of the normalized protein following the manufactures ‘instructions. Briefly, first, all the reagents were allowed to reach room temperature (20-25°C). Subsequently, 200 µL of Wash Buffer was added to each well, sealed, and shaken for 10 minutes

at room temperature. The Wash Buffer was decanted, and any residual liquid was removed by tapping the plate onto absorbent towels. Next, 50 µL of each standard or control was added to the appropriate wells, using the Serum Matrix for the 0 pg/mL standard (Background). Then, 25 µL of Assay Buffer was added to the sample wells, followed by 25 µL of the sample itself. The Mixing Bottle was vortexed, and 25 µL of the Mixed or Premixed Beads was added to each well, shaking the bead bottle intermittently during addition. The plate was sealed, wrapped with foil, and incubated with agitation on a plate shaker overnight (12 hrs) at 2-8°C. After incubation, the plate was washed, and Detection Antibodies were added. The plate was sealed, covered with foil, and incubated with agitation for 1 hour at room temperature. No aspiration was performed after incubation. Then, 25 µL of Streptavidin-Phycoerythrin was added to each well containing the Detection Antibodies. The plate was sealed, covered with foil, and incubated with agitation for an additional 30 minutes at room temperature. Following the second incubation, well contents were gently removed, and the plate was washed three times. Then, 150 µL of drive Fluid was added to all wells, and the beads were resuspended on a plate shaker for 5 minutes. Finally, the plate was run on a MAGPIX® with xPONENT® software. The Median Fluorescent Intensity (MFI) data were saved and analyzed using a 5-parameter logistic for calculating analyte concentrations in samples and controls and the samples dilution factor were considered accordingly. The resultant plate was then read by the Magpix Multiplex Reader (Luminex, Austin, TX, USA), and data were acquired using Luminex xPonent for Magpix (v4.2), then analyzed by Milliplex analyst (v5.1.0.0) (VigeneTech Inc., Carlisle, MA, USA) and presented as concentration (pg/mL). Once the samples were prepared and loaded onto the plate, the plate was read on a Luminex® analyzer (MAGPIX®) equipped with Milliplex Analyst software, version 5.1.0.0., developed by VigeneTech Inc.

6.8 APPENDIX H: Proximal Colon Histochemical Analysis

Sections of the proximal colon were placed in a histology cassette after flushing with phosphate buffered saline (PBS). The tissues were fixed in 10% buffered formalin and then processed for histological analysis. Paraffin-embedded colon segments were cut and stained with Hematoxylin and eosin (H&E) and Alcian blue (AB) dyes. Images were captured at different magnifications using a microscope camera and were blindly scored. Crypt length was measured from the base to the uppermost enterocyte using ImageJ software. Goblet cell counts and colon crypt mucus content were assessed in AB-stained sections. The mucus content was quantified by analyzing the intensity of the AB-stained areas and dividing it by the total outlined area. Representative images of colon cross-sections were taken to illustrate the analysis methods for crypt length, goblet cell counts, and mucus content.

For histological analyses, the excised colon lumen was flushed with phosphate buffered saline (PBS) and then sections of proximal colon (≈ 1 cm each) were placed in a histology cassette. The tissues were dipped in a 10% buffered formalin solution for 24 hours followed by 70% ethanol until histological analysis. The colon segments were paraffin-embedded, cut at 0.4 μm thickness and stained using Hematoxylin and eosin (H&E) and Alcian blue (AB) (University of Ottawa Histology Core Facility (Roger-Guidon Hall, Ottawa ON, Canada). Images were captured at 5x (mucus content analysis) and 10x (goblet cells and crypt length analysis) magnification using Zeiss, Axiocam 506 microscope camera and scored blindly. Proximal H&E-stained sections were used to measure crypt length. A total of 20 fully elongated crypts per colon section per mouse were used to measure the average crypt length from the base of the crypt towards the uppermost enterocyte nearest the colonic lumen end using the using ImageJ software. (**Figure 6-3 A**). AB-stained sections were used to measure the goblet cell counts per crypt and colon crypt mucus

content. The number of goblet cells also were counted in 20 crypts/mouse in the proximal cross sectioned regions (**Figure 6-3-B**). Briefly, the red, blue, and green colour channels (RGB) were split in the captured images area and the mucus in the centre of lumen were excluded, then the intensity of the AB-stained areas was quantified by the red channel and divided by the total outlined area (presented as mucus content %) (**Figure 6-3-C**).

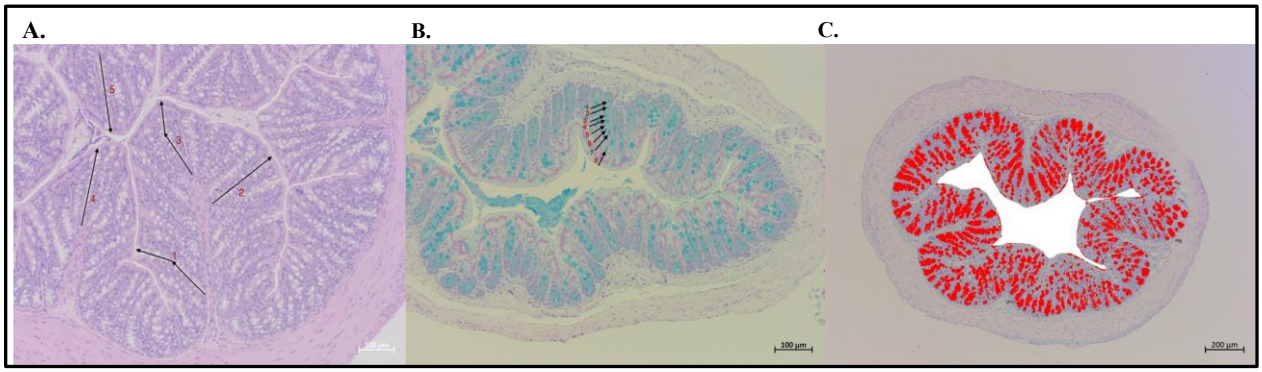

Figure 6-3-Representative images of colon cross-sections indicating the methods used to analyze epithelium. A. crypt length (µm) B. goblet cell counts; in this image 8 goblet cells were counted for this crypt C. mucus content.

6.9 APPENDIX I: Protocol for Mice Behavioural Assessment

Herein, the methods of the three established behavioral tests, including nest building, elevated EPM, and BBK tests, that were performed for the purpose of this thesis, are explained.

6.9.1 Development of the Nest Building Behavior Scoring System

Nest building is a habitual practice in numerous animal species protecting them against predators and plays a role in preserving heat and reproduction [265]. Behaviours associated to nest building (also referred as nesting) in mice and rats, are considered home cage behaviors likely translating activities of daily living (ADL) in humans. Better performance on such behaviors may represent normal behavioral function or general well-being of animals [266]. Nest construction is also proposed to be used as a means of evaluating the mood and behavior disturbances linking to psychiatric disorders like depression and schizophrenia, as well as, assessing the movement associated disorders like Parkinson disease [267]. As a result, I also assessed mice nesting behaviour before termination of the intervention to evaluate mental health and general well-being of animals. To do so, two new pieces of pressed cotton nestlet squares were placed at the front of the mice cages and then the nest pictures were captured by an iPhone camera in 2h and 24h for further analysis of mice nest building. A novel nesting score system ranging from 0-4.5 points **(Project 2 Manuscript, Table 3-3(S1): Nest Building Scoring Guide)** was developed focusing on nestlet shredding (0-1.5 points), nest shape (0-1.5 points), and nest wall height (0-1.5 points). The nests were then blindly scored by two observers according to both time intervals (2 hours or 24 hours) and the respective mice intervention group, utilizing the developed scoring guide. The details of each criterion are as follows:

1. **Nest Score Development -Nestlets Shredding**

To score the nestlet shredding, Deacon 2006 method [268] was used as the most widely used nesting score system. However, some modifications were made by considering additional parameters into this method in order to score the shredding degree of the nestlets more precisely. According to the novel developed scoring system for shredding criteria, nests scored 0, 0.5, 1 and 1.5 for <50%, 50-75%, 75-95% and >95% of shredding, respectively.

2. Nest Score Development - Nest Walls Construction

The nests were also scored according to the presence of walls surrounding the nest site. According to the Deacon 2006 method, the nest walls are scored either 4 or 5, with nest walls lower than 50 % or higher than 50% of mouse body height for its circumference, respectively. Thus, there is no distinct difference between a nest with somewhat identifiable walls (<50 % of mouse body height) or a completely flat nest. So, as a complementary to the Deacon 2006 method, Hess et al., 2008 [269] **(Figure 6-4)** scored the nest well based on the degree of walls construction around the nest cavity in an effort to shape a dome using a 'naturalistic nest score' system [269]. In this system, an imaginary sphere filling the nest hollow was considered and then the nest was scored based on walls height and the degree of enclosing the nest hollow (described as flat nest, cup-shaped, incomplete dome, or complete dome) [269].

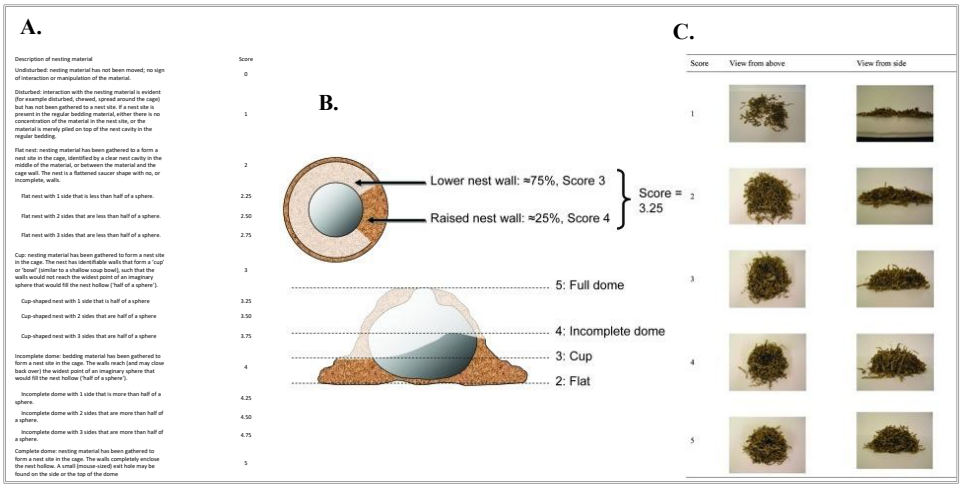

Figure 6-4- The Nest Score Ssytem Developed by Hess et al,. 2008 [270].

Figure above shows the naturalistic nest score system developed by Hess et al,. 2008 **A.** Nest building scoring parameters, **B.** Nest scoring diagram. The imaginary sphere filling the internal cavity, depicts different scoring wall heights, starting at a score of 2 for a flat nest, 3 for cupped shape nest, 4 for an incomplete dome and 5 for a full dome (a score of 0 for undisturbed nesting materials and a score of 1 for disturbed nesting material, when the interaction with the nesting material is evident but there is no distinguishable nesting site). **C.** Sample nests and their corresponding scores.

Similarly, to assess the nest walls I imagined the nest as a flattened sphere with the difference that the nest scored only based on the presence or absence of identifiable walls, because the nests were scored remotely using the digital pictures with not having enough resolution and thereby, making decision on the closure of the walls surrounding the nest cavity could be qualitative and estimation of the walls' height would not be accurate. In addition to that, Hess, and colleagues [269] also reported that providing the mice with shredded paper strips in the cage would help the mice to build nests with higher quality in terms of compared to the other materials such as compressed cotton squares that used in this study. It needs to be mentioned that the shredded

paper strips used by this group was made of 100% recycled biodegradable paper fibers that could not be a suitable option for project 2 of this thesis with controlled dietary amounts of fiber/g of the mice diet in the respective groups. Thus, overall, in this novel developed scoring system, the nest walls rated between 0, to 1.5 points in 0.5 increments for nest walls with <25 %, 25-50%, 50-75% and >75% 0-24% surrounding the nest, respectively.

3. Nest Score Development- Nest Shape

In the previously mentioned studies, the nest quality was quantified mainly either with the nestlets shredding degree [268] or height of the walls surrounding the nest to shape a dome [269], but the details on the structure of the nest was less highlighted. Thus, in addition to assessing the nestlet shredding and nest walls construction in scoring the nest building behavior, structure of the nest was also included in the scoring method. For this purpose, the nest shape was scored as follows; a score of 0 was allocated when nestlets were not manipulated by the mice at all or scattered with no defined shape, a score of 0.5 was allocated to nests cupped into a specific location with a somewhat defined shape while the materials were still disconnected with edges sticking out, a score of 1 was allocated to a nest with a mostly rounded shape but the nest was either very dispersed within the cage or one edge sticking out and finally a score of 1.5 was allocated to a nest with a rounded shape including at most one edge sticking out. To evaluate the nest shape, I assigned scores as follows:

A score of 0 was given when the nestlets were not manipulated by the mice at all or were scattered with no defined shape.

A score of 0.5 was assigned to nests that were cupped into a specific location, exhibiting a somewhat defined shape, but with materials still disconnected and edges sticking out.

A score of 1 was allocated to nests with a mostly rounded shape, but either the nest was dispersed within the cage or had one edge sticking out.

Finally, a score of 1.5 was designated for nests with a rounded shape, including at most one edge sticking out.

By considering the nest structure in this scoring system, I aimed to provide a more comprehensive assessment of nest-building behavior, in addition to evaluating nestlet shredding and nest wall construction.

6.9.2 Assessment of Anxiety Like Behaviors-Elevated Plus Maze

Elevated plus maze (EPM) is a widely used validated test for the anxiety-like behaviors assessment in mice. EPM apparatus is consisted of two unprotected open arms and two protected closed arms surrounded by walls, horizontally crossed in the centre of the maze. Mice can enter to all the areas on the maze and spontaneously move toward the open and enclosed arms [271]. This test reflects the natural aversion and avoidance behavior of mice when being placed in elevated and open areas. In addition, this test also evaluates the locomotor activity including general activity performance and natural spontaneous exploratory behavior of mice when being placed in novel environments using the indices of total travelled distance through the trial duration and the total frequency of entries in to the open and closed arms, respectively [271,272]. The ratio of time spent in the unprotected open arms to the time spent in the protected enclosed arms is translated as anti-anxiety behavior [272]. Since evidence has shown that experimental manipulations like exposure to stress, psychoactive pharmacological agents [273] as well as diet-induced obesity [274] have this potential to alter the open arm aversion and general performance of the mice, the EPM test

was performed in mice from different intervention groups at week 16 of this study. The test was performed individually at Animal Behaviour and Physiology Core, University of Ottawa nearly close to the termination of the study at week 16. Prior testing, the individually housed mice were transferred into a place near the testing room to be acclimatized for 1 hour. The maze had two main arms (measuring 6 cm wide, 75 cm long and raised 74 cm off of the floor) crossing perpendicularly and were open at the meeting area in the centre, one arm had open platforms while the other was enclosed by walls (20 cm high). The light intensity on the central platform was set on 100 lux. Individual mouse from different groups was randomly placed in the center of the maze and had freely access to explore the maze for 10 minutes. Mouse videotaped from a mounted camera above the maze and the researcher left the room while was watching the mouse behavior on a computer outside of the room. Ethovision XT 15 software (Noldus Information Technology) was used for the video tracking of the mouse under 100 lux illumination by a high-resolution camera suspended above the center of the maze, and analyzing the behavior, movement, and activity of the mouse. This software is enabled to detect the different segments of the mouse including center point, tail base, and nose point to accurately record the position of the animal, which helps the user to distinguish between when the subject only poking its nose or entering the entire body into one of the open arms of the maze. The number of entries into the each of the open or closed arms and the time spent in each arm were recorded. The maze was cleaned carefully in between each trial by ethanol and wiped out gently to eliminate all olfactory cues or any urine/feces left from the previous trial.

6.9.3 Assessment of Locomotor Activity- Beam Break Test

Beam break (BBK) is a behavior test that uses a photocell-equipped open field system tracking general motor activity and animal's movements through projecting infrared light beams from one side of the animals' cage to the other, when animals are individually placed in a new housing cage (referred as automated home-cage activity monitoring). Home cages with specially designed frames surrounding them, are made of materials that can transmit the beams without blocking them and, in turn the beams do not interfere with mice normal movement behavior. The system consists of a photocell emitter sending out horizontal infrared beam lights to the animal cages (invisible to the rodents) which are equipped with photocell receivers. When mouse moves around the cage, the emitted beams are broken by and recorded by the photocell analyzer and then the number of broken beams associating exploratory locomotor activity are enumerated by a computer-assisted analyzer [275]. For the purpose of this study (thesis), mice were randomly divided to three batches BBK test at Animal Behaviour and Physiology Core, University of Ottawa at week 16 To perform the test mice were habituated to the novel environment for an hour followed by placing them individually in pre-set up clean cages located inside the metal frames of the open field system. The cages were provided with enough bedding materials covering the floor of the cage and supply of water and food but, without any nesting materials which may affect the spontaneous behavior activity of mice. The test was performed across 22-hour period to track motor activity during the light and dark phase of circadian cycle. The software used was Fusion 5.3 developed by Omnitech Electronics Inc. for the Micromax analyzer from Accuscan. The obtained data during the trial was summed over 30-min intervals and parameters related to motor activity such as horizontal activity counts (total counts of beams interruption) and ambulatory

activity counts (reflecting actual locomotion). The area under the curve for the total and each of the light and dark cycles were calculated using the Graph Pad (Prism 9.4.1).

6.10 APPENDIX J: Detailed Statistical Analysis Results (ANOVA, Kruskal-Wallis, etc.)

Chapter 2-Project 1

Figure 2-1. A. Body weight (g) throughout the intervention phase (Week 10-18)

Two-way RM ANOVA	Matching: Stacked			
Assume sphericity?	No			
Alpha	0.05			
Source of Variation	% of total variation	P value	P value summary	Significant?
Time x Group	3.276	<0.0001	****	Yes
Time	11.80	<0.0001	****	Yes
Group	55.81	<0.0001	****	Yes
Subject	25.13	<0.0001	****	Yes

Figure 2-1. B. Final Body Weight

ANOVA summary	
F	34.92
P value	<0.0001
P value summary	****
Significant diff. among means (P < 0.05)?	Yes
R squared	0.7326

Figure 2-1. D. Cumulative energy intake (kcal) during the intervention phase

ANOVA summary	
F	17.81
P value	<0.0001
P value summary	****
Significant diff. among means (P < 0.05)?	Yes
R squared	0.5828

Figure 2-2. A. Body Composition, % Fat mass (Week 18)

ANOVA summary	
F	64.98
P value	<0.0001
P value summary	****
Significant diff. among means (P < 0.05)?	Yes
R squared	0.8360

Figure 2-2. B. Body Composition, Lean mass (g) (Week 18)

ANOVA summary	
F	7.586
P value	0.0003
P value summary	***
Significant diff. among means (P < 0.05)?	Yes
R squared	0.3409

Figure 2-3. A. Pielou's Evenness

Kruskal-Wallis test	
P value	<0.0001

Exact or approximate P value?	Approximate
P value summary	****
Do the medians vary signif. (P < 0.05)?	Yes
Number of groups	4
Kruskal-Wallis statistic	27.02

Figure 2-3. B. Shannon diversity

Kruskal-Wallis test	
P value	<0.0001
Exact or approximate P value?	Approximate
P value summary	****
Do the medians vary signif. (P < 0.05)?	Yes
Number of groups	4
Kruskal-Wallis statistic	27.92

Figure 2-4. B. Firmicutes/Bacteroidetes ratio

P value	<0.0001
Exact or approximate P value?	Approximate
P value summary	****
Do the medians vary signif. (P < 0.05)?	Yes
Number of groups	5
Kruskal-Wallis statistic	25.14

Figure 2-5. A. Short-chain fatty acid (SCFAs) B. Fecal pH

Acetic Acid

ANOVA summary	
F	15.92
P value	<0.0001
P value summary	****
Significant diff. among means (P < 0.05)?	Yes
R squared	0.5505

Propionic Acid

ANOVA summary	
F	10.68
P value	<0.0001
P value summary	****
Significant diff. among means (P < 0.05)?	Yes
R squared	0.4510

Butyric Acid

ANOVA summary	
F	21.50
P value	<0.0001
P value summary	****
Significant diff. among means (P < 0.05)?	Yes
R squared	0.6232

Total SCFAs

ANOVA summary	
F	16.95

P value	<0.0001
P value summary	****
Significant diff. among means (P < 0.05)?	Yes
R squared	0.5659

Figure 2-5. B. Fecal pH

ANOVA summary	
F	14.80
P value	<0.0001
P value summary	****
Significant diff. among means (P < 0.05)?	Yes
R squared	0.5023

Figure 2-7. D. Ratio of LBP levels to the relative abundance of Proteobacteria and Bacteroidetes.
LBP/ Bacteroidetes RA

Kruskal-Wallis test	
P value	0.0003
Exact or approximate P value?	Approximate
P value summary	***
Do the medians vary signif. (P < 0.05)?	Yes
Number of groups	4
Kruskal-Wallis statistic	18.57

LBP/ Proteobacteria RA

Kruskal-Wallis test	
P value	0.0137
Exact or approximate P value?	Approximate
P value summary	*
Do the medians vary signif. (P < 0.05)?	Yes
Number of groups	4
Kruskal-Wallis statistic	10.66

Figure 2-8. A. EAT weight (g), B. Adipocyte diameter, C. Adipocyte area

ANOVA summary	
F	10.11
P value	<0.0001
P value summary	****
Significant diff. among means (P < 0.05)?	Yes
R squared	0.4080

Figure 2 8. B. Adipocyte diameter

ANOVA summary	
F	4.367
P value	0.0092
P value summary	**
Significant diff. among means (P < 0.05)?	Yes
R squared	0.2377

Figure 2-8. C. Adipocyte area

ANOVA summary	
F	4.600
P value	0.0071
P value summary	**
Significant diff. among means (P < 0.05)?	Yes
R squared	0.2473

Figure 2-9. MCP-1

ANOVA summary	
F	6.643
P value	0.0009
P value summary	***
Significant diff. among means (P < 0.05)?	Yes
R squared	0.3271

Table 2-3

Resistin

ANOVA summary	
F	3.068
P value	0.0376
P value summary	*
Significant diff. among means (P < 0.05)?	Yes
R squared	0.1730

Leptin

ANOVA summary	
F	13.72
P value	<0.0001
P value summary	****
Significant diff. among means (P < 0.05)?	Yes
R squared	0.4833

Adpn/Lep

ANOVA summary	
F	11.60
P value	<0.0001
P value summary	****
Significant diff. among means (P < 0.05)?	Yes
R squared	0.4532

Insulin

Kruskal-Wallis test	
P value	0.0162
Exact or approximate P value?	Approximate
P value summary	*
Do the medians vary signif. (P < 0.05)?	Yes
Number of groups	4
Kruskal-Wallis statistic	10.30

HOMA-IR

ANOVA summary	

F	6.582
P value	0.0010
P value summary	***
Significant diff. among means (P < 0.05)?	Yes
R squared	0.3251

Figure 2-10 (S1)-A. Faith's phylogenetic diversity (PD)

Mann Whitney test	
P value	0.0201
Exact or approximate P value?	Exact
P value summary	*
Significantly different (P < 0.05)?	Yes
One- or two-tailed P value?	Two-tailed
Sum of ranks in column A,B	114 , 96
Mann-Whitney U	18

Chapter 3-Project 2

Figure 3-2. Cecal Microbiota α-diversity Metrics.
A. Shannon diversity

Kruskal-Wallis test	
P value	0.0003
Exact or approximate P value?	Approximate
P value summary	***
Do the medians vary signif. (P < 0.05)?	Yes
Number of groups	5
Kruskal-Wallis statistic	21.03

D. Pielou's Evenness.

Kruskal-Wallis test	
P value	0.0005
Exact or approximate P value?	Approximate
P value summary	***
Do the medians vary signif. (P < 0.05)?	Yes
Number of groups	5
Kruskal-Wallis statistic	20.17

Figure 3-3. B. Firmicutes/Bacteroidetes ratio

Kruskal-Wallis test	
P value	<0.0001
Exact or approximate P value?	Approximate
P value summary	****
Do the medians vary signif. (P < 0.05)?	Yes
Number of groups	5
Kruskal-Wallis statistic	32.81

Table 3-2. Cecal and Colon Parameters in Treatment groups.

Total Cecum Weight (g)

ANOVA summary	
F	15.08
P value	<0.0001
P value summary	****
Significant diff. among means (P < 0.05)?	Yes
R squared	0.5418

Cecum Content (g)

ANOVA summary	
F	13.24
P value	<0.0001
P value summary	****
Significant diff. among means (P < 0.05)?	Yes
R squared	0.5094

Cecum Content Moisture, %

ANOVA summary	
F	22.93
P value	<0.0001
P value summary	****
Significant diff. among means (P < 0.05)?	Yes
R squared	0.6518

Colon Length (cm)

Kruskal-Wallis test	
P value	<0.0001
Exact or approximate P value?	Approximate
P value summary	****
Do the medians vary signif. (P < 0.05)?	Yes
Number of groups	5
Kruskal-Wallis statistic	25.03

Figure 3-6. Analysis of Cecal Short-chain Fatty Acids (SCFAs).
Cecal content pH

Kruskal-Wallis test	
P value	0.0013
Exact or approximate P value?	Approximate
P value summary	**
Do the medians vary signif. (P < 0.05)?	Yes
Number of groups	5
Kruskal-Wallis statistic	17.93

B. Total cecal SCFAs (µmol/g DW)

ANOVA summary	
F	17.91
P value	<0.0001
P value summary	****
Significant diff. among means (P < 0.05)?	Yes
R squared	0.5842

C. Cecal Acetic acid

ANOVA summary	
F	17.24
P value	<0.0001
P value summary	****
Significant diff. among means (P < 0.05)?	Yes
R squared	0.5748

D. Cecal Propionic acid (µmol/g DW)

ANOVA summary	
F	18.33
P value	<0.0001
P value summary	****
Significant diff. among means (P < 0.05)?	Yes
R squared	0.5898

E. Cecum Butyric acid (µmol/g DW)

ANOVA summary	
F	17.55
P value	<0.0001
P value summary	****
Significant diff. among means (P < 0.05)?	Yes
R squared	0.5841

Figure 3-7. A. Nesting behavior in 2-hour vs 24-hour within the dietary groups.

Table Analyzed	2h vs 24h (Times in rows)			
Two-way RM ANOVA	Matching: Stacked			
Assume sphericity?	Yes			
Alpha	0.05			
Source of Variation	% of total variation	P value	P value summary	Significant?
Time x Column Factor	0.2277	0.9688	ns	No
Time	17.58	<0.0001	****	Yes
Column Factor	3.617	0.5190	ns	No
Subject	56.30	0.0004	***	Yes

Figure 3-8. Anxiety Like Behavior Assessment.
Mice centre point tracking:
A. Total number of entries into the open arms of the elevated plus maze

ANOVA summary	
F	3.099
P value	0.0233
P value summary	*
Significant diff. among means (P < 0.05)?	Yes
R squared	0.1955

B. Latency to enter to the open arms

Kruskal-Wallis test	
P value	0.0022
Exact or approximate P value?	Approximate
P value summary	**
Do the medians vary signif. (P < 0.05)?	Yes

Number of groups	5
Kruskal-Wallis statistic	16.69

Mice nose point tracking:

D. Total number of entries into the open arms of the elevated plus maze

ANOVA summary	
F	3.141
P value	0.0220
P value summary	*
Significant diff. among means (P < 0.05)?	Yes
R squared	0.1976

E. Percent time spent in the closed arms

ANOVA summary	
F	2.823
P value	0.0343
P value summary	*
Significant diff. among means (P < 0.05)?	Yes
R squared	0.1813

F. Percent time spent in the open arms

ANOVA summary	
F	4.277
P value	0.0046
P value summary	**
Significant diff. among means (P < 0.05)?	Yes
R squared	0.2512

Chapter 4-Project 3

Figure 4-1.

B. Body weight gain percentage

ANOVA summary	
F	65.65
P value	<0.0001
P value summary	****
Significant diff. among means (P < 0.05)?	Yes
R squared	0.8294

D. Final fat mass (g)

ANOVA summary	
F	177.5
P value	<0.0001
P value summary	****
Significant diff. among means (P < 0.05)?	Yes
R squared	0.9293

F. Final lean mass (g)

ANOVA summary	
F	11.84

P value	0.0002
P value summary	***
Significant diff. among means (P < 0.05)?	Yes
R squared	0.4672

Figure 4-2.

C. AUC analysis of total ambulatory movements over the experiment session.

ANOVA summary	
F	21.00
P value	<0.0001
P value summary	****
Significant diff. among means (P < 0.05)?	Yes
R squared	0.6177

Figure 4-3.

B. Cumulative energy intake (kcal) from baseline to week 18

ANOVA summary	
F	40.06
P value	<0.0001
P value summary	****
Significant diff. among means (P < 0.05)?	Yes
R squared	0.7480

Figure 4-5.

B-G. Relative abundance of key genus (g).

***F16* (f)**

Kruskal-Wallis test	
P value	0.0119
Exact or approximate P value?	Approximate
P value summary	*
Do the medians vary signif. (P < 0.05)?	Yes
Number of groups	3
Kruskal-Wallis statistic	8.857

***Akkermansia* (g)**

Kruskal-Wallis test	
P value	0.0011
Exact or approximate P value?	Approximate
P value summary	**
Do the medians vary signif. (P < 0.05)?	Yes
Number of groups	3
Kruskal-Wallis statistic	13.55

***Ruminococcaceae* (f)**

Kruskal-Wallis test	
P value	0.0280
Exact or approximate P value?	Approximate
P value summary	*

Do the medians vary signif. (P < 0.05)?	Yes
Number of groups	3
Kruskal-Wallis statistic	7.155

***Clostridium* (g)**

Kruskal-Wallis test	
P value	0.0053
Exact or approximate P value?	Approximate
P value summary	**
Do the medians vary signif. (P < 0.05)?	Yes
Number of groups	3
Kruskal-Wallis statistic	10.47

***Papillibacter* (g)**

Kruskal-Wallis test	
P value	0.0053
Exact or approximate P value?	Approximate
P value summary	**
Do the medians vary signif. (P < 0.05)?	Yes
Number of groups	3
Kruskal-Wallis statistic	10.47

***S24-7* (f)**

Kruskal-Wallis test	
P value	0.0006
Exact or approximate P value?	Approximate
P value summary	***
Do the medians vary signif. (P < 0.05)?	Yes
Number of groups	3
Kruskal-Wallis statistic	14.73

Table 4-2. Cytokine and Chemokine Concentrations

LBP

ANOVA summary	
F	4.160
P value	0.0271
P value summary	*
Significant diff. among means (P < 0.05)?	Yes
R squared	0.2424

TNF-α

ANOVA summary	
F	5.055
P value	0.0156
P value summary	*
Significant diff. among means (P < 0.05)?	Yes
R squared	0.3149

MCP-1

ANOVA summary	
F	6.400

P value	0.0057
P value summary	**
Significant diff. among means (P < 0.05)?	Yes
R squared	0.3386

KC (CXCL1)

ANOVA summary	
F	8.788
P value	0.0012
P value summary	**
Significant diff. among means (P < 0.05)?	Yes
R squared	0.4034

IL-10

ANOVA summary	
F	2.561
P value	0.0973
P value summary	ns
Significant diff. among means (P < 0.05)?	No
R squared	0.1701

Figure 4-9. Serum Concentrations of Adipokines, Glucose and Insulin Homeostasis and Gut Peptides.

A. Resistin

ANOVA summary	
F	4.479
P value	0.0213
P value summary	*
Significant diff. among means (P < 0.05)?	Yes
R squared	0.2562

B. Leptin

ANOVA summary	
F	23.91
P value	<0.0001
P value summary	****
Significant diff. among means (P < 0.05)?	Yes
R squared	0.6478

C. Adiponectin

ANOVA summary	
F	0.6017
P value	0.5553
P value summary	ns
Significant diff. among means (P < 0.05)?	No
R squared	0.04424

D. Adiponectin/Leptin ratio

ANOVA summary	
F	22.62
P value	<0.0001
P value summary	****
Significant diff. among means (P < 0.05)?	Yes
R squared	0.6629

K. FBG

ANOVA summary	
F	8.989
P value	0.0011
P value summary	**
Significant diff. among means (P < 0.05)?	Yes
R squared	0.4088

L. HOMA-IR

ANOVA summary	
F	5.295
P value	0.0118
P value summary	*
Significant diff. among means (P < 0.05)?	Yes
R squared	0.2894

Figure 4-10. Adipose Tissue Depots Profile.

A.

EAT

ANOVA summary	
F	11.00
P value	0.0003
P value summary	***
Significant diff. among means (P < 0.05)?	Yes
R squared	0.4490

PAT

ANOVA summary	
F	161.3
P value	<0.0001
P value summary	****
Significant diff. among means (P < 0.05)?	Yes
R squared	0.9254

BAT

Kruskal-Wallis test	
P value	0.0003
Exact or approximate P value?	Approximate
P value summary	***
Do the medians vary signif. (P < 0.05)?	Yes
Number of groups	3
Kruskal-Wallis statistic	16.34

B.

Adipocyte diameter

ANOVA summary	
F	8.012
P value	0.0023
P value summary	**
Significant diff. among means (P < 0.05)?	Yes
R squared	0.4106

Adipocyte area

ANOVA summary	
F	8.960
P value	0.0013
P value summary	**
Significant diff. among means (P < 0.05)?	Yes
R squared	0.4379

Figure 4-11. EAT mRNA Expression of Pro-Inflammatory Markers and SCFAs Receptors.

A. TNF-α

ANOVA summary	
F	6.850
P value	0.0042
P value summary	**
Significant diff. among means (P < 0.05)?	Yes
R squared	0.3540

B. MCP-1

ANOVA summary	
F	13.02
P value	0.0001
P value summary	***
Significant diff. among means (P < 0.05)?	Yes
R squared	0.5005

D. TLR4

ANOVA summary	
F	7.688
P value	0.0028
P value summary	**
Significant diff. among means (P < 0.05)?	Yes
R squared	0.4007

E. GPR-41

ANOVA summary	
F	6.952
P value	0.0037
P value summary	**
Significant diff. among means (P < 0.05)?	Yes
R squared	0.3399

F. GPR-43

ANOVA summary	
F	6.952
P value	0.0037
P value summary	**
Significant diff. among means (P < 0.05)?	Yes
R squared	0.3399

Figure 4-12. Epididymal Adipose Tissue (EAT) Protein Concentrations of Pro-Inflammatory Markers.

B. MCP-1

ANOVA summary	
F	4.562
P value	0.0200
P value summary	*
Significant diff. among means (P < 0.05)?	Yes
R squared	0.2598

D. IL-10

ANOVA summary	
F	23.28
P value	<0.0001
P value summary	****
Significant diff. among means (P < 0.05)?	Yes
R squared	0.6329

E. TNF-α

ANOVA summary	
F	3.650
P value	0.0395
P value summary	*
Significant diff. among means (P < 0.05)?	Yes
R squared	0.2128

7 CHAPTER 7: REFERENCES FOR CHAPTERS 1 (INTRODUCTION), 5 (DISCUSSION AND CONCLUSION) & 6 (APPENDICES)

1. World Health Organisation Obesity and Overweight Available online: https://www.who.int/news-room/fact-sheets/detail/obesity-and-overweight.
2. Tiwari, A.; Balasundaram, P. Public Health Considerations Regarding Obesity. [Updated 2022 Sep 3]. In *StatPearls*; StatPearls Publishing: Treasure Island (FL), 2022.
3. *World Health Organization. (2024, March). Obesity and Overweight. World Health Organization. Https://Www.Who.Int/News-Room/Fact-Sheets/Detail/Obesity-and-Overweight*;
4. Safaei, M.; Sundararajan, E.A.; Driss, M.; Boulila, W.; Shapi'i, A. A Systematic Literature Review on Obesity: Understanding the Causes & Consequences of Obesity and Reviewing Various Machine Learning Approaches Used to Predict Obesity. *Comput. Biol. Med.* **2021**, *136*, 104754, doi:10.1016/j.compbiomed.2021.104754.
5. *An Overview of Weight and Height Measurements on World Obesity Day." Statistics Canada, 4 Mar. 2024, Www.Statcan.Gc.ca/O1/En/plus/5742-Overview-Weight-and-Height-Measurements-World-Obesity-Day*;
6. World Health Organisation Mental Disorders Available online: https://www.who.int/news-room/fact-sheets/detail/mental-disorders.
7. Mansur, R.B.; Brietzke, E.; McIntyre, R.S. Is There a "Metabolic-Mood Syndrome"? A Review of the Relationship between Obesity and Mood Disorders. *Neurosci. Biobehav. Rev.* **2015**, *52*, 89–104, doi:https://doi.org/10.1016/j.neubiorev.2014.12.017.
8. Leyrolle, Q.; Cserjesi, R.; Demeure, R.; Neyrinck, A.M.; Amadieu, C.; Rodriguez, J.; Kärkkäinen, O.; Hanhineva, K.; Paquot, N.; Cnop, M.; et al. Microbiota and Metabolite Profiling as Markers of Mood Disorders: A Cross-Sectional Study in Obese Patients. *Nutrients* **2021**, *14*, doi:10.3390/nu14010147.
9. Racette, S.B.; Deusinger, S.S.; Deusinger, R.H. Obesity: Overview of Prevalence, Etiology, and Treatment. *Phys. Ther.* **2003**, *83*, 276–288, doi:10.1093/ptj/83.3.276.
10. Kadouh, H.C.; Acosta, A. Current Paradigms in the Etiology of Obesity. *Tech. Gastrointest. Endosc.* **2017**, *19*, 2–11, doi:10.1016/j.tgie.2016.12.001.
11. de Moura e Dias, M.; dos Reis, S.A.; da Conceição, L.L.; Sediyama, C.M.N. de O.; Pereira, S.S.; de Oliveira, L.L.; Gouveia Peluzio, M. do C.; Martinez, J.A.; Milagro, F.I. Diet-Induced Obesity in Animal Models: Points to Consider and Influence on Metabolic Markers. *Diabetol. Metab. Syndr.* **2021**, *13*, doi:10.1186/s13098-021-00647-2.
12. Geiger, B.M.; Pothos, E.N. Chapter 1 - Translating Animal Models of Obesity and Diabetes to the Clinic. In *Translational Medicine in CNS Drug Development*; Nomikos, G.G., Feltner, D.E.B.T.-H. of B.N., Eds.; Elsevier, 2019; Vol. 29, pp. 1–16 ISBN 1569-7339.
13. Hu, S.; Wang, L.; Yang, D.; Li, L.; Togo, J.; Wu, Y.; Liu, Q.; Li, B.; Li, M.; Wang, G.; et al. Dietary Fat, but Not Protein or Carbohydrate, Regulates Energy Intake and Causes Adiposity in Mice. *Cell Metab.* **2018**, *28*, 415-431.e4, doi:10.1016/j.cmet.2018.06.010.
14. Shi, H.; Akunuru, S.; Bierman, J.C.; Hodge, K.M.; Mitchell, M.C.; Foster, M.T.; Seeley, R.J.; Reizes, O. Diet-Induced Obese Mice Are Leptin Insufficient after Weight Reduction. *Obes. Silver Spring Md* **2009**, *17*, 1702–1709, doi:10.1038/oby.2009.106.
15. Gao, M.; Ma, Y.; Liu, D. High-Fat Diet-Induced Adiposity, Adipose Inflammation, Hepatic Steatosis and Hyperinsulinemia in Outbred CD-1 Mice. *PloS One* **2015**, *10*, e0119784, doi:10.1371/journal.pone.0119784.

16. Goren, H.J.; Kulkarni, R.N.; Kahn, C.R. Glucose Homeostasis and Tissue Transcript Content of Insulin Signaling Intermediates in Four Inbred Strains of Mice: C57BL/6, C57BLKS/6, DBA/2, and 129X1. *Endocrinology* **2004**, *145*, 3307–3323, doi:10.1210/en.2003-1400.
17. Berglund, E.D.; Li, C.Y.; Poffenberger, G.; Ayala, J.E.; Fueger, P.T.; Willis, S.E.; Jewell, M.M.; Powers, A.C.; Wasserman, D.H. Glucose Metabolism In Vivo in Four Commonly Used Inbred Mouse Strains. *Diabetes* **2008**, *57*, 1790–1799, doi:10.2337/db07-1615.
18. Boudina, S.; Sena, S.; Sloan, C.; Tebbi, A.; Han, Y.H.; O'Neill, B.T.; Cooksey, R.C.; Jones, D.; Holland, W.L.; McClain, D.A.; et al. Early Mitochondrial Adaptations in Skeletal Muscle to Diet-Induced Obesity Are Strain Dependent and Determine Oxidative Stress and Energy Expenditure But Not Insulin Sensitivity. *Endocrinology* **2012**, *153*, 2677–2688, doi:10.1210/en.2011-2147.
19. Della Vedova, M.C.; Muñoz, M.D.; Santillan, L.D.; Plateo-Pignatari, M.G.; Germanó, M.J.; Tosi, M.E.R.; Garcia, S.; Gomez, N.N.; Fornes, M.W.; Mejiba, S.E.G.; et al. A Mouse Model of Diet-Induced Obesity Resembling Most Features of Human Metabolic Syndrome. *Nutr. Metab. Insights* **2016**, *9*, NMI.S32907, doi:10.4137/NMI.S32907.
20. Wang, C.-Y.; Liao, J.K. A Mouse Model of Diet-Induced Obesity and Insulin Resistance. *Methods Mol. Biol. Clifton NJ* **2012**, *821*, 421–433, doi:10.1007/978-1-61779-430-8_27.
21. Zhang, L.-N.; Morgan, D.G.; Clapham, J.C.; Speakman, J.R. Factors Predicting Nongenetic Variability in Body Weight Gain Induced by a High-Fat Diet in Inbred C57BL/6J Mice. *Obesity* **2012**, *20*, 1179–1188, doi:https://doi.org/10.1038/oby.2011.151.
22. Heeren, F.A.N.; Darcey, V.L.; Deemer, S.E.; Menon, S.; Tobias, D.; Cardel, M.I. Breaking down Silos: The Multifaceted Nature of Obesity and the Future of Weight Management. *Philos. Trans. R. Soc. B Biol. Sci.* **2023**, *378*, 20220215, doi:10.1098/rstb.2022.0215.
23. Wei, B.; Wang, S.; Wang, Y.; Ke, S.; Jin, W.; Chen, J.; Zhang, H.; Sun, J.; Henning, S.M.; Wang, J.; et al. Gut Microbiota-Mediated Xanthine Metabolism Is Associated with Resistance to High-Fat Diet-Induced Obesity. *J. Nutr. Biochem.* **2021**, *88*, 108533, doi:10.1016/j.jnutbio.2020.108533.
24. de La Serre, C.B.; Ellis, C.L.; Lee, J.; Hartman, A.L.; Rutledge, J.C.; Raybould, H.E. Propensity to High-Fat Diet-Induced Obesity in Rats Is Associated with Changes in the Gut Microbiota and Gut Inflammation. *Am. J. Physiol. Gastrointest. Liver Physiol.* **2010**, *299*, G440-448, doi:10.1152/ajpgi.00098.2010.
25. Choi, J.-Y.; McGregor, R.A.; Kwon, E.-Y.; Kim, Y.J.; Han, Y.; Park, J.H.Y.; Lee, K.W.; Kim, S.-J.; Kim, J.; Yun, J.W.; et al. The Metabolic Response to a High-Fat Diet Reveals Obesity-Prone and -Resistant Phenotypes in Mice with Distinct mRNA-Seq Transcriptome Profiles. *Int. J. Obes.* **2016**, *40*, 1452–1460, doi:10.1038/ijo.2016.70.
26. Belobrajdic, D.P.; King, R.A.; Christophersen, C.T.; Bird, A.R. Dietary Resistant Starch Dose-Dependently Reduces Adiposity in Obesity-Prone and Obesity-Resistant Male Rats. *Nutr. Metab.* **2012**, *9*, 93, doi:10.1186/1743-7075-9-93.
27. Zhang, P.; Yu, Y.; Qin, Y.; Zhou, Y.; Tang, R.; Wang, Q.; Li, X.; Wang, H.; Weston-Green, K.; Huang, X.-F.; et al. Alterations to the Microbiota–Colon–Brain Axis in High-Fat-Diet-Induced Obese Mice Compared to Diet-Resistant Mice. *J. Nutr. Biochem.* **2019**, *65*, 54–65, doi:10.1016/j.jnutbio.2018.08.016.
28. Wen, Y.; Luo, Y.; Qiu, H.; Chen, B.; Huang, J.; Lv, S.; Wang, Y.; Li, J.; Tao, L.; Yang, B.; et al. Gut Microbiota Affects Obesity Susceptibility in Mice through Gut Metabolites. *Front. Microbiol.* **2024**, *15*, 1343511, doi:10.3389/fmicb.2024.1343511.

29. Portincasa, P.; Bonfrate, L.; Khalil, M.; Angelis, M.D.; Calabrese, F.M.; D'Amato, M.; Wang, D.Q.-H.; Di Ciaula, A. Intestinal Barrier and Permeability in Health, Obesity and NAFLD. *Biomedicines* **2021**, *10*, 83, doi:10.3390/biomedicines10010083.
30. Di Vincenzo, F.; Del Gaudio, A.; Petito, V.; Lopetuso, L.R.; Scaldaferri, F. Gut Microbiota, Intestinal Permeability, and Systemic Inflammation: A Narrative Review. *Intern. Emerg. Med.* **2024**, *19*, 275–293, doi:10.1007/s11739-023-03374-w.
31. Bona, M.D.; Torres, C.H.D.M.; Lima, S.C.V.C.; Morais, A.H.D.A.; Lima, A.Â.M.; Maciel, B.L.L. Intestinal Barrier Permeability in Obese Individuals with or without Metabolic Syndrome: A Systematic Review. *Nutrients* **2022**, *14*, 3649, doi:10.3390/nu14173649.
32. Ahmad, R.; Rah, B.; Bastola, D.; Dhawan, P.; Singh, A.B. Obesity-Induces Organ and Tissue Specific Tight Junction Restructuring and Barrier Deregulation by Claudin Switching. *Sci. Rep.* **2017**, *7*, 5125, doi:10.1038/s41598-017-04989-8.
33. Shi, C.; Li, H.; Qu, X.; Huang, L.; Kong, C.; Qin, H.; Sun, Z.; Yan, X. High Fat Diet Exacerbates Intestinal Barrier Dysfunction and Changes Gut Microbiota in Intestinal-Specific ACF7 Knockout Mice. *Biomed. Pharmacother.* **2019**, *110*, 537–545, doi:10.1016/j.biopha.2018.11.100.
34. Schroeder, B.O.; Birchenough, G.M.H.; Ståhlman, M.; Arike, L.; Johansson, M.E.V.; Hansson, G.C.; Bäckhed, F. Bifidobacteria or Fiber Protects against Diet-Induced Microbiota-Mediated Colonic Mucus Deterioration. *Cell Host Microbe* **2018**, *23*, 27-40.e7, doi:10.1016/j.chom.2017.11.004.
35. Shi, H.; Wang, Q.; Zheng, M.; Hao, S.; Lum, J.S.; Chen, X.; Huang, X.-F.; Yu, Y.; Zheng, K. Supplement of Microbiota-Accessible Carbohydrates Prevents Neuroinflammation and Cognitive Decline by Improving the Gut Microbiota-Brain Axis in Diet-Induced Obese Mice. *J. Neuroinflammation* **2020**, *17*, 77, doi:10.1186/s12974-020-01760-1.
36. Di Ciaula, A.; Baj, J.; Garruti, G.; Celano, G.; De Angelis, M.; Wang, H.H.; Di Palo, D.M.; Bonfrate, L.; Wang, D.Q.-H.; Portincasa, P. Liver Steatosis, Gut-Liver Axis, Microbiome and Environmental Factors. A Never-Ending Bidirectional Cross-Talk. *J. Clin. Med.* **2020**, *9*, 2648, doi:10.3390/jcm9082648.
37. Brescia, P.; Rescigno, M. The Gut Vascular Barrier: A New Player in the Gut–Liver–Brain Axis. *Trends Mol. Med.* **2021**, *27*, 844–855, doi:10.1016/j.molmed.2021.06.007.
38. Hou, K.; Wu, Z.-X.; Chen, X.-Y.; Wang, J.-Q.; Zhang, D.; Xiao, C.; Zhu, D.; Koya, J.B.; Wei, L.; Li, J.; et al. Microbiota in Health and Diseases. *Signal Transduct. Target. Ther.* **2022**, *7*, 135, doi:10.1038/s41392-022-00974-4.
39. Cresci, G.A.M.; Izzo, K. Gut Microbiome. In *Adult Short Bowel Syndrome*; Elsevier, 2019; pp. 45–54 ISBN 978-0-12-814330-8.
40. Magne, F.; Gotteland, M.; Gauthier, L.; Zazueta, A.; Pesoa, S.; Navarrete, P.; Balamurugan, R. The Firmicutes/Bacteroidetes Ratio: A Relevant Marker of Gut Dysbiosis in Obese Patients? *Nutrients* **2020**, *12*, doi:10.3390/nu12051474.
41. Adak, A.; Khan, M.R. An Insight into Gut Microbiota and Its Functionalities. *Cell. Mol. Life Sci.* **2019**, *76*, 473–493, doi:10.1007/s00018-018-2943-4.
42. Martinez-Guryn, K.; Leone, V.; Chang, E.B. Regional Diversity of the Gastrointestinal Microbiome. *Cell Host Microbe* **2019**, *26*, 314–324, doi:10.1016/j.chom.2019.08.011.
43. Sekirov, I.; Russell, S.L.; Antunes, L.C.M.; Finlay, B.B. Gut Microbiota in Health and Disease. *Physiol. Rev.* **2010**, *90*, 859–904, doi:10.1152/physrev.00045.2009.
44. Rinninella, E.; Raoul, P.; Cintoni, M.; Franceschi, F.; Miggiano, G.; Gasbarrini, A.; Mele, M. What Is the Healthy Gut Microbiota Composition? A Changing Ecosystem across Age,

Environment, Diet, and Diseases. *Microorganisms* **2019**, *7*, 14, doi:10.3390/microorganisms7010014.
45. den Besten, G.; van Eunen, K.; Groen, A.K.; Venema, K.; Reijngoud, D.-J.; Bakker, B.M. The Role of Short-Chain Fatty Acids in the Interplay between Diet, Gut Microbiota, and Host Energy Metabolism. *J. Lipid Res.* **2013**, *54*, 2325–2340, doi:10.1194/jlr.R036012.
46. Usuda, H.; Okamoto, T.; Wada, K. Leaky Gut: Effect of Dietary Fiber and Fats on Microbiome and Intestinal Barrier. *Int. J. Mol. Sci.* **2021**, *22*, doi:10.3390/ijms22147613.
47. Hugenholtz, F.; de Vos, W.M. Mouse Models for Human Intestinal Microbiota Research: A Critical Evaluation. *Cell. Mol. Life Sci. CMLS* **2018**, *75*, 149–160, doi:10.1007/s00018-017-2693-8.
48. Carding, S.; Verbeke, K.; Vipond, D.T.; Corfe, B.M.; Owen, L.J. Dysbiosis of the Gut Microbiota in Disease. *Microb. Ecol. Health Dis.* **2015**, *26*, doi:10.3402/mehd.v26.26191.
49. Corfe, B.M.; Harden, C.J.; Bull, M.; Garaiova, I. The Multifactorial Interplay of Diet, the Microbiome and Appetite Control: Current Knowledge and Future Challenges. *Proc. Nutr. Soc.* **2015**, *74*, 235–244, doi:10.1017/S0029665114001670.
50. Kim, K.N.; Yao, Y.; Ju, S.Y. Short Chain Fatty Acids and Fecal Microbiota Abundance in Humans with Obesity: A Systematic Review and Meta-Analysis. *Nutrients* **2019**, *11*, 2512, doi:10.3390/nu11102512.
51. Fernandes, J.; Su, W.; Rahat-Rozenbloom, S.; Wolever, T.M.S.; Comelli, E.M. Adiposity, Gut Microbiota and Faecal Short Chain Fatty Acids Are Linked in Adult Humans. *Nutr. Diabetes* **2014**, *4*, e121–e121, doi:10.1038/nutd.2014.23.
52. Rahat-Rozenbloom, S.; Fernandes, J.; Gloor, G.B.; Wolever, T.M.S. Evidence for Greater Production of Colonic Short-Chain Fatty Acids in Overweight than Lean Humans. *Int. J. Obes. 2005* **2014**, *38*, 1525–1531, doi:10.1038/ijo.2014.46.
53. De La Cuesta-Zuluaga, J.; Mueller, N.; Álvarez-Quintero, R.; Velásquez-Mejía, E.; Sierra, J.; Corrales-Agudelo, V.; Carmona, J.; Abad, J.; Escobar, J. Higher Fecal Short-Chain Fatty Acid Levels Are Associated with Gut Microbiome Dysbiosis, Obesity, Hypertension and Cardiometabolic Disease Risk Factors. *Nutrients* **2018**, *11*, 51, doi:10.3390/nu11010051.
54. Barczyńska, R.; Litwin, M.; Sliżewska, K.; Szalecki, M.; Berdowska, A.; Bandurska, K.; Libudzisz, Z.; Kapuśniak, J. Bacterial Microbiota and Fatty Acids in the Faeces of Overweight and Obese Children. *Pol. J. Microbiol.* **2018**, *67*, 339–345, doi:10.21307/pjm-2018-041.
55. Murugesan, S.; Ulloa-Martínez, M.; Martínez-Rojano, H.; Galván-Rodríguez, F.M.; Miranda-Brito, C.; Romano, M.C.; Piña-Escobedo, A.; Pizano-Zárate, M.L.; Hoyo-Vadillo, C.; García-Mena, J. Study of the Diversity and Short-Chain Fatty Acids Production by the Bacterial Community in Overweight and Obese Mexican Children. *Eur. J. Clin. Microbiol. Infect. Dis.* **2015**, *34*, 1337–1346, doi:10.1007/s10096-015-2355-4.
56. Turnbaugh, P.J.; Ley, R.E.; Mahowald, M. a; Magrini, V.; Mardis, E.R.; Gordon, J.I. An Obesity-Associated Gut Microbiome with Increased Capacity for Energy Harvest. *Nature* **2006**, *444*, 1027–1031, doi:10.1038/nature05414.
57. Canfora, E.E.; Jocken, J.W.; Blaak, E.E. Short-Chain Fatty Acids in Control of Body Weight and Insulin Sensitivity. *Nat. Rev. Endocrinol.* **2015**, *11*, 577–591, doi:10.1038/nrendo.2015.128.
58. Lu, Y.; Fan, C.; Li, P.; Lu, Y.; Chang, X.; Qi, K. Short Chain Fatty Acids Prevent High-Fat-Diet-Induced Obesity in Mice by Regulating G Protein-Coupled Receptors and Gut Microbiota. *Sci. Rep.* **2016**, *6*, 37589, doi:10.1038/srep37589.

59. Canfora, E.E.; van der Beek, C.M.; Jocken, J.W.E.; Goossens, G.H.; Holst, J.J.; Olde Damink, S.W.M.; Lenaerts, K.; Dejong, C.H.C.; Blaak, E.E. Colonic Infusions of Short-Chain Fatty Acid Mixtures Promote Energy Metabolism in Overweight/Obese Men: A Randomized Crossover Trial. *Sci. Rep.* **2017**, *7*, 2360, doi:10.1038/s41598-017-02546-x.
60. Henagan, T.M.; Stefanska, B.; Fang, Z.; Navard, A.M.; Ye, J.; Lenard, N.R.; Devarshi, P.P. Sodium Butyrate Epigenetically Modulates High-Fat Diet-Induced Skeletal Muscle Mitochondrial Adaptation, Obesity and Insulin Resistance through Nucleosome Positioning. *Br. J. Pharmacol.* **2015**, *172*, 2782–2798, doi:10.1111/bph.13058.
61. Sanna, S.; Van Zuydam, N.R.; Mahajan, A.; Kurilshikov, A.; Vich Vila, A.; Võsa, U.; Mujagic, Z.; Masclee, A.A.M.; Jonkers, D.M.A.E.; Oosting, M.; et al. Causal Relationships among the Gut Microbiome, Short-Chain Fatty Acids and Metabolic Diseases. *Nat. Genet.* **2019**, *51*, 600–605, doi:10.1038/s41588-019-0350-x.
62. Vinolo, M.A.R.; Rodrigues, H.G.; Nachbar, R.T.; Curi, R. Regulation of Inflammation by Short Chain Fatty Acids. *Nutrients* **2011**, *3*, 858–876, doi:10.3390/nu3100858.
63. Nogal, A.; Valdes, A.M.; Menni, C. The Role of Short-Chain Fatty Acids in the Interplay between Gut Microbiota and Diet in Cardio-Metabolic Health. *Gut Microbes* **2021**, *13*, 1897212, doi:10.1080/19490976.2021.1897212.
64. Ecklu-Mensah, G.; Choo-Kang, C.; Maseng, M.G.; Donato, S.; Bovet, P.; Viswanathan, B.; Bedu-Addo, K.; Plange-Rhule, J.; Oti Boateng, P.; Forrester, T.E.; et al. Gut Microbiota and Fecal Short Chain Fatty Acids Differ with Adiposity and Country of Origin: The METS-Microbiome Study. *Nat. Commun.* **2023**, *14*, 5160, doi:10.1038/s41467-023-40874-x.
65. Ley, R.E.; Bäckhed, F.; Turnbaugh, P.; Lozupone, C.A.; Knight, R.D.; Gordon, J.I. Obesity Alters Gut Microbial Ecology. *Proc. Natl. Acad. Sci. U. S. A.* **2005**, *102*, 11070–11075, doi:10.1073/pnas.0504978102.
66. Liu, B.-N.; Liu, X.-T.; Liang, Z.-H.; Wang, J.-H. Gut Microbiota in Obesity. *World J. Gastroenterol.* **2021**, *27*, 3837–3850, doi:10.3748/wjg.v27.i25.3837.
67. Bäckhed, F.; Ding, H.; Wang, T.; Hooper, L.V.; Koh, G.Y.; Nagy, A.; Semenkovich, C.F.; Gordon, J.I. The Gut Microbiota as an Environmental Factor That Regulates Fat Storage. *Proc. Natl. Acad. Sci. U. S. A.* **2004**, *101*, 15718–15723, doi:10.1073/pnas.0407076101.
68. Bäckhed, F.; Ding, H.; Wang, T.; Hooper, L. V; Koh, G.Y.; Semenkovich, C.F.; Gordon, J.I.; Nagy, A.; Hoopert, L. V The Gut Microbiota as an Environmental Factor That Regulates Fat Storage. *Proc. Natl. Acad. Sci. U. S. A.* **2014**, *101*, 15718–15723.
69. Ridaura, V.K.; Faith, J.J.; Rey, F.E.; Cheng, J.; Duncan, A.E.; Kau, A.L.; Griffin, N.W.; Lombard, V.; Henrissat, B.; Bain, J.R.; et al. Gut Microbiota from Twins Discordant for Obesity Modulate Metabolism in Mice. *Science* **2013**, *341*, 1241214, doi:10.1126/science.1241214.
70. Xiao, H.; Kang, S. The Role of the Gut Microbiome in Energy Balance With a Focus on the Gut-Adipose Tissue Axis. *Front. Genet.* **2020**, *11*, 297, doi:10.3389/fgene.2020.00297.
71. Turnbaugh, P.J.; Ley, R.E.; Mahowald, M. a; Magrini, V.; Mardis, E.R.; Gordon, J.I. An Obesity-Associated Gut Microbiome with Increased Capacity for Energy Harvest. *Nature* **2006**, *444*, 1027–1031, doi:10.1038/nature05414.
72. Ley, R.E.; Turnbaugh, P.J.; Klein, S.; Gordon, J.I. Microbial Ecology: Human Gut Microbes Associated with Obesity. *Nature* **2006**, *444*, 1022–1023, doi:10.1038/4441022a.
73. Kho, Z.Y.; Lal, S.K. The Human Gut Microbiome – A Potential Controller of Wellness and Disease. *Front. Microbiol.* **2018**, *9*, 1835, doi:10.3389/fmicb.2018.01835.
74. Koliada, A.; Syzenko, G.; Moseiko, V.; Budovska, L.; Puchkov, K.; Perederiy, V.; Gavalko, Y.; Dorofeyev, A.; Romanenko, M.; Tkach, S.; et al. Association between Body Mass

Index and Firmicutes/Bacteroidetes Ratio in an Adult Ukrainian Population. *BMC Microbiol.* **2017**, *17*, 120, doi:10.1186/s12866-017-1027-1.
75. Zhang, H.; DiBaise, J.K.; Zuccolo, A.; Kudrna, D.; Braidotti, M.; Yu, Y.; Parameswaran, P.; Crowell, M.D.; Wing, R.; Rittmann, B.E.; et al. Human Gut Microbiota in Obesity and after Gastric Bypass. *Proc. Natl. Acad. Sci. U. S. A.* **2009**, *106*, 2365–2370, doi:10.1073/pnas.0812600106.
76. Chao, A.M.; Quigley, K.M.; Wadden, T.A. Dietary Interventions for Obesity: Clinical and Mechanistic Findings. *J. Clin. Invest.* **2021**, *131*, e140065, 140065, doi:10.1172/JCI140065.
77. Yannakoulia, M.; Poulimeneas, D.; Mamalaki, E.; Anastasiou, C.A. Dietary Modifications for Weight Loss and Weight Loss Maintenance. *Metabolism* **2019**, *92*, 153–162, doi:10.1016/j.metabol.2019.01.001.
78. Hernández-Calderón, P.; Wiedemann, L.; Benítez-Páez, A. *The Microbiota Composition Drives Personalized Nutrition: Gut Microbes as Predictive Biomarkers for the Success of Weight Loss Diets*; 2022; Vol. 9; ISBN 2296-861X.
79. Tagliabue, A.; Elli, M. The Role of Gut Microbiota in Human Obesity: Recent Findings and Future Perspectives. *Nutr. Metab. Cardiovasc. Dis.* **2013**, *23*, 160–168, doi:10.1016/j.numecd.2012.09.002.
80. Festi, D.; Schiumerini, R.; Eusebi, L.H.; Marasco, G.; Taddia, M.; Colecchia, A. Gut Microbiota and Metabolic Syndrome. *World J. Gastroenterol.* **2014**, *20*, 16079–16094, doi:10.3748/wjg.v20.i43.16079.
81. Wu, G.D.; Chen, J.; Hoffmann, C.; Bittinger, K.; Chen, Y.; Sue, A.; Bewtra, M.; Knights, D.; Walters, W. a; Knight, R.; et al. NIH Public Access. *Link. Long-Term Diet. Patterns Gut Microb. Enterotypes Gary Sci.* **2012**, *334*, 105–108, doi:10.1126/science.1208344.Linking.
82. Koutoukidis, D.A.; Jebb, S.A.; Zimmerman, M.; Otunla, A.; Henry, J.A.; Ferrey, A.; Schofield, E.; Kinton, J.; Aveyard, P.; Marchesi, J.R. The Association of Weight Loss with Changes in the Gut Microbiota Diversity, Composition, and Intestinal Permeability: A Systematic Review and Meta-Analysis. *Gut Microbes* **2022**, *14*, 2020068, doi:10.1080/19490976.2021.2020068.
83. Jie, Z.; Yu, X.; Liu, Y.; Sun, L.; Chen, P.; Ding, Q.; Gao, Y.; Zhang, X.; Yu, M.; Liu, Y.; et al. The Baseline Gut Microbiota Directs Dieting-Induced Weight Loss Trajectories. *Gastroenterology* **2021**, *160*, 2029-2042.e16, doi:10.1053/j.gastro.2021.01.029.
84. Walker, A.W.; Ince, J.; Duncan, S.H.; Webster, L.M.; Holtrop, G.; Ze, X.; Brown, D.; Stares, M.D.; Scott, P.; Bergerat, A.; et al. Dominant and Diet-Responsive Groups of Bacteria within the Human Colonic Microbiota. *ISME J.* **2011**, *5*, 220–230, doi:10.1038/ismej.2010.118.
85. Remely, M.; Hippe, B.; Zanner, J.; Aumueller, E.; Brath, H.; Haslberger, A.G. Gut Microbiota of Obese, Type 2 Diabetic Individuals Is Enriched in Faecalibacterium Prausnitzii, Akkermansia Muciniphila and Peptostreptococcus Anaerobius after Weight Loss. *Endocr. Metab. Immune Disord. Drug Targets* **2016**, *16*, 99–106, doi:10.2174/1871530316666160831093813.
86. Duncan, S.H.; Lobley, G.E.; Holtrop, G.; Ince, J.; Johnstone, A.M.; Louis, P.; Flint, H.J. Human Colonic Microbiota Associated with Diet, Obesity and Weight Loss. *Int. J. Obes. 2005* **2008**, *32*, 1720–1724, doi:10.1038/ijo.2008.155.
87. Sowah, S.A.; Milanese, A.; Schübel, R.; Wirbel, J.; Kartal, E.; Johnson, T.S.; Hirche, F.; Grafetstätter, M.; Nonnenmacher, T.; Kirsten, R.; et al. Calorie Restriction Improves Metabolic State Independently of Gut Microbiome Composition: A Randomized Dietary Intervention Trial. *Genome Med.* **2022**, *14*, 30, doi:10.1186/s13073-022-01030-0.

88. Koutoukidis, D.A.; Jebb, S.A.; Zimmerman, M.; Otunla, A.; Henry, J.A.; Ferrey, A.; Schofield, E.; Kinton, J.; Aveyard, P.; Marchesi, J.R. The Association of Weight Loss with Changes in the Gut Microbiota Diversity, Composition, and Intestinal Permeability: A Systematic Review and Meta-Analysis. *Gut Microbes* **2022**, *14*, 2020068, doi:10.1080/19490976.2021.2020068.
89. Stone, W.L.; Basit, H.; Burns, B. Pathology, Inflammation. In *StatPearls*; StatPearls Publishing: Treasure Island (FL), 2024.
90. Khanna, D.; Khanna, S.; Khanna, P.; Kahar, P.; Patel, B.M. Obesity: A Chronic Low-Grade Inflammation and Its Markers. *Cureus* **2022**, *14*, e22711, doi:10.7759/cureus.22711.
91. Castro, A.M.; Macedo-de La Concha, L.E.; Pantoja-Meléndez, C.A. Low-Grade Inflammation and Its Relation to Obesity and Chronic Degenerative Diseases. *Rev. Médica Hosp. Gen. México* **2017**, *80*, 101–105, doi:10.1016/j.hgmx.2016.06.011.
92. Hersoug, L.-G.; Møller, P.; Loft, S. Role of Microbiota-Derived Lipopolysaccharide in Adipose Tissue Inflammation, Adipocyte Size and Pyroptosis during Obesity. *Nutr. Res. Rev.* **2018**, *31*, 153–163, doi:10.1017/S0954422417000269.
93. Da Cruz Nascimento, S.S.; Carvalho De Queiroz, J.L.; Fernandes De Medeiros, A.; De França Nunes, A.C.; Piuvezam, G.; Lima Maciel, B.L.; Souza Passos, T.; Morais, A.H.D.A. Anti-Inflammatory Agents as Modulators of the Inflammation in Adipose Tissue: A Systematic Review. *PLOS ONE* **2022**, *17*, e0273942, doi:10.1371/journal.pone.0273942.
94. Gonzalez-Quintela, A.; Alonso, M.; Campos, J.; Vizcaino, L.; Loidi, L.; Gude, F. Determinants of Serum Concentrations of Lipopolysaccharide-Binding Protein (LBP) in the Adult Population: The Role of Obesity. *PLoS ONE* **2013**, *8*, e54600, doi:10.1371/journal.pone.0054600.
95. Farhana, A.; Khan, Y.S. Biochemistry, Lipopolysaccharide. In *StatPearls*; StatPearls Publishing: Treasure Island (FL), 2024.
96. Dai, Y.-J.; Liu, W.-B.; Abasubong, K.P.; Zhang, D.-D.; Li, X.-F.; Xiao, K.; Wang, X.; Jiang, G.-Z. The Mechanism of Lipopolysaccharide Escaping the Intestinal Barrier in Megalobrama Amblycephala Fed a High-Fat Diet. *Front. Nutr.* **2022**, *9*, 853409, doi:10.3389/fnut.2022.853409.
97. Ciesielska, A.; Matyjek, M.; Kwiatkowska, K. TLR4 and CD14 Trafficking and Its Influence on LPS-Induced pro-Inflammatory Signaling. *Cell. Mol. Life Sci. CMLS* **2021**, *78*, 1233–1261, doi:10.1007/s00018-020-03656-y.
98. Gutsmann, T.; Müller, M.; Carroll, S.F.; MacKenzie, R.C.; Wiese, A.; Seydel, U. Dual Role of Lipopolysaccharide (LPS)-Binding Protein in Neutralization of LPS and Enhancement of LPS-Induced Activation of Mononuclear Cells. *Infect. Immun.* **2001**, *69*, 6942–6950, doi:10.1128/IAI.69.11.6942-6950.2001.
99. Tsukamoto, H.; Takeuchi, S.; Kubota, K.; Kobayashi, Y.; Kozakai, S.; Ukai, I.; Shichiku, A.; Okubo, M.; Numasaki, M.; Kanemitsu, Y.; et al. Lipopolysaccharide (LPS)-Binding Protein Stimulates CD14-Dependent Toll-like Receptor 4 Internalization and LPS-Induced TBK1–IKKϵ–IRF3 Axis Activation. *J. Biol. Chem.* **2018**, *293*, 10186–10201, doi:10.1074/jbc.M117.796631.
100. Vetrani, C.; Di Nisio, A.; Paschou, S.A.; Barrea, L.; Muscogiuri, G.; Graziadio, C.; Savastano, S.; Colao, A.; Group, O.B.O.T.O.P.O.N.E.R.A.A.O. From Gut Microbiota through Low-Grade Inflammation to Obesity: Key Players and Potential Targets. *Nutrients* **2022**, *14*, doi:10.3390/nu14102103.
101. Kadyan, S.; Sharma, A.; Arjmandi, B.H.; Singh, P.; Nagpal, R. Prebiotic Potential of Dietary Beans and Pulses and Their Resistant Starch for Aging-Associated Gut and Metabolic Health. *Nutrients* **2022**, *14*, doi:10.3390/nu14091726.

102. Ilyés, T.; Silaghi, C.N.; Crăciun, A.M. Diet-Related Changes of Short-Chain Fatty Acids in Blood and Feces in Obesity and Metabolic Syndrome. *Biology* **2022**, *11*, 1556, doi:10.3390/biology11111556.
103. Duca, F.A.; Lam, T.K.T. Gut Microbiota, Nutrient Sensing and Energy Balance. *Diabetes Obes. Metab.* **2014**, *16*, 68–76, doi:10.1111/dom.12340.
104. Kökten, T.; Hansmannel, F.; Ndiaye, N.C.; Heba, A.-C.; Quilliot, D.; Dreumont, N.; Arnone, D.; Peyrin-Biroulet, L. Calorie Restriction as a New Treatment of Inflammatory Diseases. *Adv. Nutr. Bethesda Md* **2021**, *12*, 1558–1570, doi:10.1093/advances/nmaa179.
105. Fontana, L.; Meyer, T.E.; Klein, S.; Holloszy, J.O. Long-Term Calorie Restriction Is Highly Effective in Reducing the Risk for Atherosclerosis in Humans. *Proc. Natl. Acad. Sci.* **2004**, *101*, 6659–6663, doi:10.1073/pnas.0308291101.
106. Montefusco, L.; D'Addio, F.; Loretelli, C.; Ben Nasr, M.; Garziano, M.; Rossi, A.; Pastore, I.; Plebani, L.; Lunati, M.E.; Bolla, A.M.; et al. Anti-Inflammatory Effects of Diet and Caloric Restriction in Metabolic Syndrome. *J. Endocrinol. Invest.* **2021**, *44*, 2407–2415, doi:10.1007/s40618-021-01547-y.
107. Hoevenaars, F.P.M.; Keijer, J.; Herreman, L.; Palm, I.; Hegeman, M.A.; Swarts, H.J.M.; van Schothorst, E.M. Adipose Tissue Metabolism and Inflammation Are Differently Affected by Weight Loss in Obese Mice Due to Either a High-Fat Diet Restriction or Change to a Low-Fat Diet. *Genes Nutr.* **2014**, *9*, 391, doi:10.1007/s12263-014-0391-9.
108. Singh, S.; Anshita, D.; Ravichandiran, V. MCP-1: Function, Regulation, and Involvement in Disease. *Int. Immunopharmacol.* **2021**, *101*, 107598, doi:10.1016/j.intimp.2021.107598.
109. Wang, Q.; Perrard, X.D.; Perrard, J.L.; Mansoori, A.; Raya, J.L.; Hoogeveen, R.; Smith, C.W.; Ballantyne, C.M.; Wu, H. Differential Effect of Weight Loss with Low-Fat Diet or High-Fat Diet Restriction on Inflammation in the Liver and Adipose Tissue of Mice with Diet-Induced Obesity. *Atherosclerosis* **2011**, *219*, 100–108, doi:10.1016/j.atherosclerosis.2011.07.025.
110. Patra, D.; Banerjee, D.; Ramprasad, P.; Roy, S.; Pal, D.; Dasgupta, S. Recent Insights of Obesity-Induced Gut and Adipose Tissue Dysbiosis in Type 2 Diabetes. *Front. Mol. Biosci.* **2023**, *10*, 1224982, doi:10.3389/fmolb.2023.1224982.
111. Gallai, B.; Esposito, M.; Roccella, M.; Marotta, R.; Lavano, F.; Lavano, S.M.; Mazzotta, G.; Bove, D.; Sorrentino, M.; Precenzano, F.; et al. Anxiety and Depression Levels in Prepubertal Obese Children: A Case-Control Study. *Neuropsychiatr. Dis. Treat.* **2014**, 1897, doi:10.2147/NDT.S69795.
112. Luppino, F.S.; De Wit, L.M.; Bouvy, P.F.; Stijnen, T.; Cuijpers, P.; Penninx, B.W.J.H.; Zitman, F.G. Overweight, Obesity, and Depression: A Systematic Review and Meta-Analysis of Longitudinal Studies. *Arch. Gen. Psychiatry* **2010**, *67*, 220, doi:10.1001/archgenpsychiatry.2010.2.
113. Zhao, G.; Ford, E.S.; Dhingra, S.; Li, C.; Strine, T.W.; Mokdad, A.H. Depression and Anxiety among US Adults: Associations with Body Mass Index. *Int. J. Obes.* **2009**, *33*, 257–266, doi:10.1038/ijo.2008.268.
114. Gariepy, G.; Nitka, D.; Schmitz, N. The Association between Obesity and Anxiety Disorders in the Population: A Systematic Review and Meta-Analysis. *Int. J. Obes.* **2010**, *34*, 407–419, doi:10.1038/ijo.2009.252.
115. Rutsch, A.; Kantsjö, J.B.; Ronchi, F. The Gut-Brain Axis: How Microbiota and Host Inflammasome Influence Brain Physiology and Pathology. *Front. Immunol.* **2020**, *11*, 604179, doi:10.3389/fimmu.2020.604179.

116. Appleton, J. The Gut-Brain Axis: Influence of Microbiota on Mood and Mental Health. *Integr. Med. Encinitas Calif* **2018**, *17*, 28–32.
117. Hu, Q.; Hou, S.; Xiong, B.; Wen, Y.; Wang, J.; Zeng, J.; Ma, X.; Wang, F. Therapeutic Effects of Baicalin on Diseases Related to Gut–Brain Axis Dysfunctions. *Molecules* **2023**, *28*, 6501, doi:10.3390/molecules28186501.
118. Han, Y.; Wang, B.; Gao, H.; He, C.; Hua, R.; Liang, C.; Zhang, S.; Wang, Y.; Xin, S.; Xu, J. Vagus Nerve and Underlying Impact on the Gut Microbiota-Brain Axis in Behavior and Neurodegenerative Diseases. *J. Inflamm. Res.* **2022**, *15*, 6213–6230, doi:10.2147/JIR.S384949.
119. Mayer, E.A.; Savidge, T.; Shulman, R.J. Brain-Gut Microbiome Interactions and Functional Bowel Disorders. *Gastroenterology* **2014**, *146*, 1500–1512, doi:10.1053/j.gastro.2014.02.037.
120. Agirman, G.; Yu, K.B.; Hsiao, E.Y. Signaling Inflammation across the Gut-Brain Axis. *Science* **2021**, *374*, 1087–1092, doi:10.1126/science.abi6087.
121. Rusch, J.A.; Layden, B.T.; Dugas, L.R. Signalling Cognition: The Gut Microbiota and Hypothalamic-Pituitary-Adrenal Axis. *Front. Endocrinol.* **2023**, *14*, 1130689, doi:10.3389/fendo.2023.1130689.
122. O'Mahony, S.M.; Marchesi, J.R.; Scully, P.; Codling, C.; Ceolho, A.-M.; Quigley, E.M.M.; Cryan, J.F.; Dinan, T.G. Early Life Stress Alters Behavior, Immunity, and Microbiota in Rats: Implications for Irritable Bowel Syndrome and Psychiatric Illnesses. *Biol. Psychiatry* **2009**, *65*, 263–267, doi:10.1016/j.biopsych.2008.06.026.
123. Vanuytsel, T.; Van Wanrooy, S.; Vanheel, H.; Vanormelingen, C.; Verschueren, S.; Houben, E.; Salim Rasoel, S.; Tóth, J.; Holvoet, L.; Farré, R.; et al. Psychological Stress and Corticotropin-Releasing Hormone Increase Intestinal Permeability in Humans by a Mast Cell-Dependent Mechanism. *Gut* **2014**, *63*, 1293–1299, doi:10.1136/gutjnl-2013-305690.
124. Koblinsky, N.D.; Power, K.A.; Middleton, L.; Ferland, G.; Anderson, N.D. The Role of the Gut Microbiome in Diet and Exercise Effects on Cognition: A Review of the Intervention Literature. *J. Gerontol. A. Biol. Sci. Med. Sci.* **2023**, *78*, 195–205, doi:10.1093/gerona/glac166.
125. Kalyan, M.; Tousif, A.H.; Sonali, S.; Vichitra, C.; Sunanda, T.; Praveenraj, S.S.; Ray, B.; Gorantla, V.R.; Rungratanawanich, W.; Mahalakshmi, A.M.; et al. Role of Endogenous Lipopolysaccharides in Neurological Disorders. *Cells* **2022**, *11*, 4038, doi:10.3390/cells11244038.
126. Bonaz, B.; Bazin, T.; Pellissier, S. The Vagus Nerve at the Interface of the Microbiota-Gut-Brain Axis. *Front. Neurosci.* **2018**, *12*, 49, doi:10.3389/fnins.2018.00049.
127. Jiang, H.; Zhang, X.; Yu, Z.; Zhang, Z.; Deng, M.; Zhao, J.; Ruan, B. Altered Gut Microbiota Profile in Patients with Generalized Anxiety Disorder. *J. Psychiatr. Res.* **2018**, *104*, 130–136, doi:10.1016/j.jpsychires.2018.07.007.
128. Ericsson, A.C.; Hart, M.L.; Kwan, J.; Lanoue, L.; Bower, L.R.; Araiza, R.; Kent Lloyd, K.C.; Franklin, C.L. Supplier-Origin Mouse Microbiomes Significantly Influence Locomotor and Anxiety-Related Behavior, Body Morphology, and Metabolism. *Commun. Biol.* **2021**, *4*, 716, doi:10.1038/s42003-021-02249-0.
129. Xiong, R.-G.; Li, J.; Cheng, J.; Zhou, D.-D.; Wu, S.-X.; Huang, S.-Y.; Saimaiti, A.; Yang, Z.-J.; Gan, R.-Y.; Li, H.-B. The Role of Gut Microbiota in Anxiety, Depression, and Other Mental Disorders as Well as the Protective Effects of Dietary Components. *Nutrients* **2023**, *15*, doi:10.3390/nu15143258.
130. Wu, J.; Chai, T.; Zhang, H.; Huang, Y.; Perry, S.W.; Li, Y.; Duan, J.; Tan, X.; Hu, X.; Liu, Y.; et al. Changes in Gut Viral and Bacterial Species Correlate with Altered 1,2-Diacylglyceride

Levels and Structure in the Prefrontal Cortex in a Depression-like Non-Human Primate Model. *Transl. Psychiatry* **2022**, *12*, 74, doi:10.1038/s41398-022-01836-x.
131. Lin, P.; Ding, B.; Feng, C.; Yin, S.; Zhang, T.; Qi, X.; Lv, H.; Guo, X.; Dong, K.; Zhu, Y.; et al. Prevotella and Klebsiella Proportions in Fecal Microbial Communities Are Potential Characteristic Parameters for Patients with Major Depressive Disorder. *J. Affect. Disord.* **2017**, *207*, 300–304, doi:10.1016/j.jad.2016.09.051.
132. Guillemot-Legris, O.; Muccioli, G.G. Obesity-Induced Neuroinflammation: Beyond the Hypothalamus. *Trends Neurosci.* **2017**, *40*, 237–253, doi:10.1016/j.tins.2017.02.005.
133. Salas-Venegas, V.; Flores-Torres, R.P.; Rodríguez-Cortés, Y.M.; Rodríguez-Retana, D.; Ramírez-Carreto, R.J.; Concepción-Carrillo, L.E.; Pérez-Flores, L.J.; Alarcón-Aguilar, A.; López-Díazguerrero, N.E.; Gómez-González, B.; et al. The Obese Brain: Mechanisms of Systemic and Local Inflammation, and Interventions to Reverse the Cognitive Deficit. *Front. Integr. Neurosci.* **2022**, *16*, 798995, doi:10.3389/fnint.2022.798995.
134. Tucsek, Z.; Toth, P.; Sosnowska, D.; Gautam, T.; Mitschelen, M.; Koller, A.; Szalai, G.; Sonntag, W.E.; Ungvari, Z.; Csiszar, A. Obesity in Aging Exacerbates Blood-Brain Barrier Disruption, Neuroinflammation, and Oxidative Stress in the Mouse Hippocampus: Effects on Expression of Genes Involved in Beta-Amyloid Generation and Alzheimer's Disease. *J. Gerontol. A. Biol. Sci. Med. Sci.* **2014**, *69*, 1212–1226, doi:10.1093/gerona/glt177.
135. Li, Y.; Cheng, Y.; Zhou, Y.; Du, H.; Zhang, C.; Zhao, Z.; Chen, Y.; Zhou, Z.; Mei, J.; Wu, W.; et al. High Fat Diet-Induced Obesity Leads to Depressive and Anxiety-like Behaviors in Mice via AMPK/mTOR-Mediated Autophagy. *Exp. Neurol.* **2022**, *348*, 113949, doi:10.1016/j.expneurol.2021.113949.
136. Conlon, M.A.; Bird, A.R. The Impact of Diet and Lifestyle on Gut Microbiota and Human Health. *Nutrients* **2014**, *7*, 17–44, doi:10.3390/nu7010017.
137. Martin, C.K.; Bhapkar, M.; Pittas, A.G.; Pieper, C.F.; Das, S.K.; Williamson, D.A.; Scott, T.; Redman, L.M.; Stein, R.; Gilhooly, C.H.; et al. Effect of Calorie Restriction on Mood, Quality of Life, Sleep, and Sexual Function in Healthy Nonobese Adults: The CALERIE 2 Randomized Clinical Trial. *JAMA Intern. Med.* **2016**, *176*, 743, doi:10.1001/jamainternmed.2016.1189.
138. Hussin, N.M.; Shahar, S.; Teng, N.I.M.F.; Ngah, W.Z.W.; Das, S.K. Efficacy of Fasting and Calorie Restriction (FCR) on Mood and Depression among Ageing Men. *J. Nutr. Health Aging* **2013**, *17*, 674–680, doi:10.1007/s12603-013-0344-9.
139. Perez-Cornago, A.; Ramírez, M.J.; Zulet, M.Á.; Martinez, J.A. Effect of Dietary Restriction on Peripheral Monoamines and Anxiety Symptoms in Obese Subjects with Metabolic Syndrome. *Psychoneuroendocrinology* **2014**, *47*, 98–106, doi:10.1016/j.psyneuen.2014.05.003.
140. Castro, A.; Gomez-Arbelaez, D.; Crujeiras, A.; Granero, R.; Aguera, Z.; Jimenez-Murcia, S.; Sajoux, I.; Lopez-Jaramillo, P.; Fernandez-Aranda, F.; Casanueva, F. Effect of A Very Low-Calorie Ketogenic Diet on Food and Alcohol Cravings, Physical and Sexual Activity, Sleep Disturbances, and Quality of Life in Obese Patients. *Nutrients* **2018**, *10*, 1348, doi:10.3390/nu10101348.
141. Lin, S.; Cienfuegos, S.; Ezpeleta, M.; Pavlou, V.; Chakos, K.; McStay, M.; Runchey, M.-C.; Alexandria, S.J.; Varady, K.A. Effect of Time-Restricted Eating versus Daily Calorie Restriction on Mood and Quality of Life in Adults with Obesity. *Nutrients* **2023**, *15*, 4313, doi:10.3390/nu15204313.
142. Jones, R.A.; Lawlor, E.R.; Birch, J.M.; Patel, M.I.; Werneck, A.O.; Hoare, E.; Griffin, S.J.; van Sluijs, E.M.F.; Sharp, S.J.; Ahern, A.L. The Impact of Adult Behavioural Weight Management

Interventions on Mental Health: A Systematic Review and Meta-Analysis. *Obes. Rev. Off. J. Int. Assoc. Study Obes.* **2021**, *22*, e13150, doi:10.1111/obr.13150.
143. Everard, A.; Cani, P.D. Diabetes, Obesity and Gut Microbiota. *Best Pract. Res. Clin. Gastroenterol.* **2013**, *27*, 73–83, doi:10.1016/j.bpg.2013.03.007.
144. Ferreira, H.; Vasconcelos, M.; Gil, A.M.; Pinto, E. Benefits of Pulse Consumption on Metabolism and Health: A Systematic Review of Randomized Controlled Trials. *Crit. Rev. Food Sci. Nutr.* **2021**, *61*, 85–96, doi:10.1080/10408398.2020.1716680.
145. McGinley, J.N.; Fitzgerald, V.K.; Neil, E.S.; Omerigic, H.M.; Heuberger, A.L.; Weir, T.L.; McGee, R.; Vandemark, G.; Thompson, H.J. Pulse Crop Effects on Gut Microbial Populations, Intestinal Function, and Adiposity in a Mouse Model of Diet-Induced Obesity. *Nutrients* **2020**, *12*, doi:10.3390/nu12030593.
146. McCrory, M.A.; Hamaker, B.R.; Lovejoy, J.C.; Eichelsdoerfer, P.E. Pulse Consumption, Satiety, and Weight Management. *Adv. Nutr. Bethesda Md* **2010**, *1*, 17–30, doi:10.3945/an.110.1006.
147. Weir, T.L.; McGinley, J.N.; Neil, E.S.; Thompson, H.J. Effect of Pulse Consumption on Obesity and the Metagenome. In Proceedings of the First International Electronic Conference on Nutrients, Microbiota and Chronic Disease; MDPI, October 30 2020; p. 23.
148. Didinger, C.; Thompson, H.J. The Role of Pulses in Improving Human Health: A Review. *Legume Sci.* **2022**, *4*, e147, doi:10.1002/leg3.147.
149. Kim, S.J.; de Souza, R.J.; Choo, V.L.; Ha, V.; Cozma, A.I.; Chiavaroli, L.; Mirrahimi, A.; Blanco Mejia, S.; Di Buono, M.; Bernstein, A.M.; et al. Effects of Dietary Pulse Consumption on Body Weight: A Systematic Review and Meta-Analysis of Randomized Controlled Trials. *Am. J. Clin. Nutr.* **2016**, *103*, 1213–1223, doi:10.3945/ajcn.115.124677.
150. Marinangeli, C.P.F.; Harding, S.V.; Zafron, M.; Rideout, T.C. A Systematic Review of the Effect of Dietary Pulses on Microbial Populations Inhabiting the Human Gut. *Benef. Microbes* **2020**, *11*, 457–468, doi:10.3920/BM2020.0028.
151. Prokopidis, K.; Giannos, P.; Ispoglou, T.; Witard, O.C.; Isanejad, M. Dietary Fiber Intake Is Associated with Cognitive Function in Older Adults: Data from the National Health and Nutrition Examination Survey. *Am. J. Med.* **2022**, *135*, e257–e262, doi:10.1016/j.amjmed.2022.03.022.
152. Health Canada *Canada's Dietary Guidelines for Health Professionals and Policy Makers*; 2019; ISBN 6139572991.
153. *U.S. Department of Health and Human Services and U.S. Department of Agriculture [(Accessed on 2 September 2020)];2015–2020 Dietary Guidelines for Americans. (8th Ed.). 2015 Dec; Available Online: Http://Health.Gov/Dietaryguidelines/2015/Guidelines/*;
154. Marinangeli, C.P.F.; Curran, J.; Barr, S.I.; Slavin, J.; Puri, S.; Swaminathan, S.; Tapsell, L.; Patterson, C.A. Enhancing Nutrition with Pulses: Defining a Recommended Serving Size for Adults. *Nutr. Rev.* **2017**, *75*, 990–1006, doi:10.1093/nutrit/nux058.
155. Kadyan, S.; Sharma, A.; Arjmandi, B.H.; Singh, P.; Nagpal, R. Prebiotic Potential of Dietary Beans and Pulses and Their Resistant Starch for Aging-Associated Gut and Metabolic Health. *Nutrients* **2022**, *14*, doi:10.3390/nu14091726.
156. Tosh, S.M.; Yada, S. Dietary Fibres in Pulse Seeds and Fractions: Characterization, Functional Attributes, and Applications. *Food Res. Int.* **2010**, *43*, 450–460, doi:https://doi.org/10.1016/j.foodres.2009.09.005.

157. Williams, B.; Grant, L.; Gidley, M.; Mikkelsen, D. Gut Fermentation of Dietary Fibres: Physico-Chemistry of Plant Cell Walls and Implications for Health. *Int. J. Mol. Sci.* **2017**, *18*, 2203, doi:10.3390/ijms18102203.
158. Mullins, A.P.; Arjmandi, B.H. Health Benefits of Plant-Based Nutrition: Focus on Beans in Cardiometabolic Diseases. *Nutrients* **2021**, *13*, 519, doi:10.3390/nu13020519.
159. Brummer, Y.; Kaviani, M.; Tosh, S.M. Structural and Functional Characteristics of Dietary Fibre in Beans, Lentils, Peas and Chickpeas. *Food Res. Int.* **2015**, *67*, 117–125, doi:10.1016/j.foodres.2014.11.009.
160. Campos-Vega, R.; Reynoso-Camacho, R.; Pedraza-Aboytes, G.; Acosta-Gallegos, J.A.; Guzman-Maldonado, S.H.; Paredes-Lopez, O.; Oomah, B.D.; Loarca-Piña, G. Chemical Composition and In Vitro Polysaccharide Fermentation of Different Beans (Phaseolus Vulgaris L.). *J. Food Sci.* **2009**, *74*, T59–T65, doi:10.1111/j.1750-3841.2009.01292.x.
161. Chen, Y.; McGee, R.; Vandemark, G.; Brick, M.; Thompson, H.J. Dietary Fiber Analysis of Four Pulses Using AOAC 2011.25: Implications for Human Health. *Nutrients* **2016**, *8*, doi:10.3390/nu8120829.
162. Leong, S.Y.; Duque, S.M.; Abduh, S.B.M.; Oey, I. Carbohydrates. In *Innovative Thermal and Non-Thermal Processing, Bioaccessibility and Bioavailability of Nutrients and Bioactive Compounds*; Elsevier, 2019; pp. 171–206 ISBN 978-0-12-814174-8.
163. Quagliani, D.; Felt-Gunderson, P. Closing America's Fiber Intake Gap: Communication Strategies From a Food and Fiber Summit. *Am. J. Lifestyle Med.* **2017**, *11*, 80–85, doi:10.1177/1559827615588079.
164. *Health Canada. (2019, January 22). Fibre. Government of Canada. Https://Www.Canada.ca/En/Health-Canada/Services/Nutrients/Fibre.Html*;
165. Ganesan, K.; Xu, B. Polyphenol-Rich Dry Common Beans (Phaseolus Vulgaris L.) and Their Health Benefits. *Int. J. Mol. Sci.* **2017**, *18*, 2331, doi:10.3390/ijms18112331.
166. Jamar, G.; Estadella, D.; Pisani, L.P. Contribution of Anthocyanin-Rich Foods in Obesity Control through Gut Microbiota Interactions. *BioFactors Oxf. Engl.* **2017**, *43*, 507–516, doi:10.1002/biof.1365.
167. Shabbir, U.; Tyagi, A.; Elahi, F.; Aloo, S.O.; Oh, D.-H. The Potential Role of Polyphenols in Oxidative Stress and Inflammation Induced by Gut Microbiota in Alzheimer's Disease. *Antioxidants* **2021**, *10*, 1370, doi:10.3390/antiox10091370.
168. Alves-Santos, A.M.; Sugizaki, C.S.A.; Lima, G.C.; Naves, M.M.V. Prebiotic Effect of Dietary Polyphenols: A Systematic Review. *J. Funct. Foods* **2020**, *74*, 104169, doi:10.1016/j.jff.2020.104169.
169. Zhang, Y.; Yu, W.; Zhang, L.; Wang, M.; Chang, W. The Interaction of Polyphenols and the Gut Microbiota in Neurodegenerative Diseases. *Nutrients* **2022**, *14*, 5373, doi:10.3390/nu14245373.
170. Papanikolaou, Y.; Fulgoni, V.L. Bean Consumption Is Associated with Greater Nutrient Intake, Reduced Systolic Blood Pressure, Lower Body Weight, and a Smaller Waist Circumference in Adults: Results from the National Health and Nutrition Examination Survey 1999-2002. *J. Am. Coll. Nutr.* **2008**, *27*, 569–576, doi:10.1080/07315724.2008.10719740.
171. Sichieri, R. Dietary Patterns and Their Associations with Obesity in the Brazilian City of Rio de Janeiro. *Obes. Res.* **2002**, *10*, 42–48, doi:10.1038/oby.2002.6.
172. Thompson, H.; McGinley, J.; Neil, E.; Brick, M. Beneficial Effects of Common Bean on Adiposity and Lipid Metabolism. *Nutrients* **2017**, *9*, 998, doi:10.3390/nu9090998.

173. McCrory, M.A.; Hamaker, B.R.; Lovejoy, J.C.; Eichelsdoerfer, P.E. Pulse Consumption, Satiety, and Weight Management. *Adv. Nutr. Bethesda Md* **2010**, *1*, 17–30, doi:10.3945/an.110.1006.
174. Viguiliouk, E.; Blanco Mejia, S.; Kendall, C.W.C.; Sievenpiper, J.L. Can Pulses Play a Role in Improving Cardiometabolic Health? Evidence from Systematic Reviews and Meta-analyses. *Ann. N. Y. Acad. Sci.* **2017**, *1392*, 43–57, doi:10.1111/nyas.13312.
175. Pusztai, A.; Grant, G.; Buchan, W.C.; Bardocz, S.; de Carvalho, A.F.F.U.; Ewen, S.W.B. Lipid Accumulation in Obese Zucker Rats Is Reduced by Inclusion of Raw Kidney Bean (Phaseolus Vulgaris) in the Diet. *Br. J. Nutr.* **1998**, *79*, 213–221, doi:DOI: 10.1079/BJN19980033.
176. Crujeiras, A.B.; Parra, D.; Abete, I.; Martínez, J.A. A Hypocaloric Diet Enriched in Legumes Specifically Mitigates Lipid Peroxidation in Obese Subjects. *Free Radic. Res.* **2007**, *41*, 498–506, doi:10.1080/10715760601131935.
177. Abete, I.; Parra, D.; Martinez, J.A. Legume-, Fish-, or High-Protein-Based Hypocaloric Diets: Effects on Weight Loss and Mitochondrial Oxidation in Obese Men. *J. Med. Food* **2009**, *12*, 100+.
178. Hermsdorff, H.H.M.; Zulet, M.Á.; Abete, I.; Martínez, J.A. A Legume-Based Hypocaloric Diet Reduces Proinflammatory Status and Improves Metabolic Features in Overweight/Obese Subjects. *Eur. J. Nutr.* **2011**, *50*, 61–69, doi:10.1007/s00394-010-0115-x.
179. Li, J.; Mao, Q.-Q. Legume Intake and Risk of Prostate Cancer: A Meta-Analysis of Prospective Cohort Studies. *Oncotarget* **2017**, *8*, 44776–44784, doi:10.18632/oncotarget.16794.
180. John, H.S.; Doucet, É.; Power, K.A. Dietary Pulses as a Means to Improve the Gut Microbiome, Inflammation, and Appetite Control in Obesity. *Obes. Rev. Off. J. Int. Assoc. Study Obes.* **2023**, *24*, e13598, doi:10.1111/obr.13598.
181. Fernando, W.; Hill, J.; Zello, G.; Tyler, R.; Dahl, W.; Van Kessel, A. Diets Supplemented with Chickpea or Its Main Oligosaccharide Component Raffinose Modify Faecal Microbial Composition in Healthy Adults. *Benef. Microbes* **2010**, *1*, 197–207, doi:10.3920/BM2009.0027.
182. Finley, J.W.; Burrell, J.B.; Reeves, P.G. Pinto Bean Consumption Changes SCFA Profiles in Fecal Fermentations, Bacterial Populations of the Lower Bowel, and Lipid Profiles in Blood of Humans. *J. Nutr.* **2007**, *137*, 2391–2398, doi:10.1093/jn/137.11.2391.
183. Sheflin, A.M.; Borresen, E.C.; Kirkwood, J.S.; Boot, C.M.; Whitney, A.K.; Lu, S.; Brown, R.J.; Broeckling, C.D.; Ryan, E.P.; Weir, T.L. Dietary Supplementation with Rice Bran or Navy Bean Alters Gut Bacterial Metabolism in Colorectal Cancer Survivors. *Mol. Nutr. Food Res.* **2017**, *61*, 1500905, doi:10.1002/mnfr.201500905.
184. Monk, J.M.; Wu, W.; Lepp, D.; Pauls, K.P.; Robinson, L.E.; Power, K.A. Navy Bean Supplementation in Established High-Fat Diet-Induced Obesity Attenuates the Severity of the Obese Inflammatory Phenotype. *Nutrients* **2021**, *13*, doi:10.3390/nu13030757.
185. Tan, Y.; Tam, C.C.; Meng, S.; Zhang, Y.; Alves, P.; Yokoyama, W. Cooked Black Turtle Beans Ameliorate Insulin Resistance and Restore Gut Microbiota in C57BL/6J Mice on High-Fat Diets. *Foods* **2021**, *10*, doi:10.3390/foods10081691.
186. Hou, D.; Zhao, Q.; Yousaf, L.; Xue, Y.; Shen, Q. Whole Mung Bean (Vigna Radiata L.) Supplementation Prevents High-Fat Diet-Induced Obesity and Disorders in a Lipid Profile and Modulates Gut Microbiota in Mice. *Eur. J. Nutr.* **2020**, *59*, 3617–3634, doi:10.1007/s00394-020-02196-2.
187. Neil, E.S.; McGinley, J.N.; Fitzgerald, V.K.; Lauck, C.A.; Tabke, J.A.; Streeter-McDonald, M.R.; Yao, L.; Broeckling, C.D.; Weir, T.L.; Foster, M.T.; et al. White Kidney Bean

(Phaseolus Vulgaris L.) Consumption Reduces Fat Accumulation in a Polygenic Mouse Model of Obesity. *Nutrients* **2019**, *11*, doi:10.3390/nu11112780.
188. Lutsiv, T.; Weir, T.L.; McGinley, J.N.; Neil, E.S.; Wei, Y.; Thompson, H.J. Compositional Changes of the High-Fat Diet-Induced Gut Microbiota upon Consumption of Common Pulses. *Nutrients* **2021**, *13*, doi:10.3390/nu13113992.
189. Monk, J.M.; Wu, W.; Lepp, D.; Wellings, H.R.; Hutchinson, A.L.; Liddle, D.M.; Graf, D.; Pauls, K.P.; Robinson, L.E.; Power, K.A. Navy Bean Supplemented High-Fat Diet Improves Intestinal Health, Epithelial Barrier Integrity and Critical Aspects of the Obese Inflammatory Phenotype. *J Nutr Biochem* **2019**, *70*, 91–104, doi:10.1016/j.jnutbio.2019.04.009.
190. Sánchez-Tapia, M.; Hernández-Velázquez, I.; Pichardo-Ontiveros, E.; Granados-Portillo, O.; Gálvez, A.; R Tovar, A.; Torres, N. Consumption of Cooked Black Beans Stimulates a Cluster of Some Clostridia Class Bacteria Decreasing Inflammatory Response and Improving Insulin Sensitivity. *Nutrients* **2020**, *12*, doi:10.3390/nu12041182.
191. Lutsiv, T.; McGinley, J.N.; Neil-McDonald, E.S.; Weir, T.L.; Foster, M.T.; Thompson, H.J. Relandscaping the Gut Microbiota with a Whole Food: Dose-Response Effects to Common Bean. *Foods Basel Switz.* **2022**, *11*, 1153, doi:10.3390/foods11081153.
192. Dingemanse, C.; Belzer, C.; Van Hijum, S.A.F.T.; Günthel, M.; Salvatori, D.; Dunnen, J.T.D.; Kuijper, E.J.; Devilee, P.; De Vos, W.M.; Van Ommen, G.B.; et al. *Akkermansia Muciniphila* and *Helicobacter Typhlonius* Modulate Intestinal Tumor Development in Mice. *Carcinogenesis* **2015**, *36*, 1388–1396, doi:10.1093/carcin/bgv120.
193. Santacruz, A.; Collado, M.C.; García-Valdés, L.; Segura, M.T.; Martín-Lagos, J.A.; Anjos, T.; Martí-Romero, M.; Lopez, R.M.; Florido, J.; Campoy, C.; et al. Gut Microbiota Composition Is Associated with Body Weight, Weight Gain and Biochemical Parameters in Pregnant Women. *Br. J. Nutr.* **2010**, *104*, 83–92, doi:10.1017/S0007114510000176.
194. Karlsson, C.L.J.; Önnerfält, J.; Xu, J.; Molin, G.; Ahrné, S.; Thorngren-Jerneck, K. The Microbiota of the Gut in Preschool Children With Normal and Excessive Body Weight. *Obesity* **2012**, *20*, 2257–2261, doi:10.1038/oby.2012.110.
195. Monk, J.M.; Zhang, C.P.; Wu, W.; Zarepoor, L.; Lu, J.T.; Liu, R.; Pauls, K.P.; Wood, G.A.; Tsao, R.; Robinson, L.E.; et al. White and Dark Kidney Beans Reduce Colonic Mucosal Damage and Inflammation in Response to Dextran Sodium Sulfate. *J. Nutr. Biochem.* **2015**, *26*, 752–760, doi:10.1016/j.jnutbio.2015.02.003.
196. Monk, J.M.; Lepp, D.; Wu, W.; Pauls, K.P.; Robinson, L.E.; Power, K.A. Navy and Black Bean Supplementation Primes the Colonic Mucosal Microenvironment to Improve Gut Health. *J. Nutr. Biochem.* **2017**, *49*, 89–100, doi:https://doi.org/10.1016/j.jnutbio.2017.08.002.
197. Monk, J.M.; Lepp, D.; Zhang, C.P.; Wu, W.; Zarepoor, L.; Lu, J.T.; Pauls, K.P.; Tsao, R.; Wood, G.A.; Robinson, L.E.; et al. Diets Enriched with Cranberry Beans Alter the Microbiota and Mitigate Colitis Severity and Associated Inflammation. *J. Nutr. Biochem.* **2016**, *28*, 129–139, doi:10.1016/j.jnutbio.2015.10.014.
198. Kawai, T.; Autieri, M.V.; Scalia, R. Adipose Tissue Inflammation and Metabolic Dysfunction in Obesity. *Am. J. Physiol.-Cell Physiol.* **2021**, *320*, C375–C391, doi:10.1152/ajpcell.00379.2020.
199. Fischer, A.; Schick, F. Towards Detection of Inflammation in Adipose Tissue: Microscopic Field Simulations to Estimate Water Signal Properties. *Z. Für Med. Phys.* **2021**, *31*, 394–402, doi:10.1016/j.zemedi.2021.03.002.

200. Mollard, R.C.; Luhovyy, B.L.; Panahi, S.; Nunez, M.; Hanley, A.; Anderson, G.H. Regular Consumption of Pulses for 8 Weeks Reduces Metabolic Syndrome Risk Factors in Overweight and Obese Adults. *Br. J. Nutr.* **2012**, *108*, S111–S122, doi:10.1017/S0007114512000712.
201. Safaeiyan, A.; Pourghassem-Gargari, B.; Zarrin, R.; Fereidooni, J.; Alizadeh, M. Randomized Controlled Trial on the Effects of Legumes on Cardiovascular Risk Factors in Women with Abdominal Obesity. *ARYA Atheroscler.* **2015**, *11*, 117–125.
202. Hartman, T.J.; Albert, P.S.; Zhang, Z.; Bagshaw, D.; Kris-Etherton, P.M.; Ulbrecht, J.; Miller, C.K.; Bobe, G.; Colburn, N.H.; Lanza, E. Consumption of a Legume-Enriched, Low-Glycemic Index Diet Is Associated with Biomarkers of Insulin Resistance and Inflammation among Men at Risk for Colorectal Cancer. *J. Nutr.* **2010**, *140*, 60–67, doi:10.3945/jn.109.114249.
203. Saraf-Bank, S.; Esmaillzadeh, A.; Faghihimani, E.; Azadbakht, L. Effect of Non-Soy Legume Consumption on Inflammation and Serum Adiponectin Levels among First-Degree Relatives of Patients with Diabetes: A Randomized, Crossover Study. *Nutrition* **2015**, *31*, 459–465, doi:10.1016/j.nut.2014.09.015.
204. Abeysekara, S.; Chilibeck, P.D.; Vatanparast, H.; Zello, G.A. A Pulse-Based Diet Is Effective for Reducing Total and LDL-Cholesterol in Older Adults. *Br. J. Nutr.* **2012**, *108*, S103–S110, doi:10.1017/S0007114512000748.
205. Ombra, M.N.; d'Acierno, A.; Nazzaro, F.; Riccardi, R.; Spigno, P.; Zaccardelli, M.; Pane, C.; Maione, M.; Fratianni, F. Phenolic Composition and Antioxidant and Antiproliferative Activities of the Extracts of Twelve Common Bean (*Phaseolus Vulgaris* L.) Endemic Ecotypes of Southern Italy before and after Cooking. *Oxid. Med. Cell. Longev.* **2016**, *2016*, 1398298, doi:10.1155/2016/1398298.
206. Zhang, C.; Monk, J.M.; Lu, J.T.; Zarepoor, L.; Wu, W.; Liu, R.; Pauls, K.P.; Wood, G.A.; Robinson, L.; Tsao, R.; et al. Cooked Navy and Black Bean Diets Improve Biomarkers of Colon Health and Reduce Inflammation during Colitis. *Br. J. Nutr.* **2014**, *111*, 1549–1563, doi:DOI: 10.1017/S0007114513004352.
207. Barber, T.M.; Valsamakis, G.; Mastorakos, G.; Hanson, P.; Kyrou, I.; Randeva, H.S.; Weickert, M.O. Dietary Influences on the Microbiota–Gut–Brain Axis. *Int. J. Mol. Sci.* **2021**, *22*, 3502, doi:10.3390/ijms22073502.
208. Paone, P.; Cani, P.D. Mucus Barrier, Mucins and Gut Microbiota: The Expected Slimy Partners? *Gut* **2020**, *69*, 2232–2243, doi:10.1136/gutjnl-2020-322260.
209. Akhtar, M.; Chen, Y.; Ma, Z.; Zhang, X.; Shi, D.; Khan, J.A.; Liu, H. Gut Microbiota-Derived Short Chain Fatty Acids Are Potential Mediators in Gut Inflammation. *Anim. Nutr.* **2022**, *8*, 350–360, doi:10.1016/j.aninu.2021.11.005.
210. Liu, H.; Wang, J.; He, T.; Becker, S.; Zhang, G.; Li, D.; Ma, X. Butyrate: A Double-Edged Sword for Health? *Adv. Nutr. Bethesda Md* **2018**, *9*, 21–29, doi:10.1093/advances/nmx009.
211. Li, M.; Van Esch, B.C.A.M.; Wagenaar, G.T.M.; Garssen, J.; Folkerts, G.; Henricks, P.A.J. Pro- and Anti-Inflammatory Effects of Short Chain Fatty Acids on Immune and Endothelial Cells. *Eur. J. Pharmacol.* **2018**, *831*, 52–59, doi:10.1016/j.ejphar.2018.05.003.
212. Cory, H.; Passarelli, S.; Szeto, J.; Tamez, M.; Mattei, J. The Role of Polyphenols in Human Health and Food Systems: A Mini-Review. *Front. Nutr.* **2018**, *5*, 87, doi:10.3389/fnut.2018.00087.
213. Catalkaya, G.; Venema, K.; Lucini, L.; Rocchetti, G.; Delmas, D.; Daglia, M.; De Filippis, A.; Xiao, H.; Quiles, J.L.; Xiao, J.; et al. Interaction of Dietary Polyphenols and Gut Microbiota: Microbial Metabolism of Polyphenols, Influence on the Gut Microbiota, and Implications on Host Health. *Food Front.* **2020**, *1*, 109–133, doi:10.1002/fft2.25.

214. Wang, X.; Qi, Y.; Zheng, H. Dietary Polyphenol, Gut Microbiota, and Health Benefits. *Antioxid. Basel Switz.* **2022**, *11*, doi:10.3390/antiox11061212.
215. Lassale, C.; Batty, G.D.; Baghdadli, A.; Jacka, F.; Sánchez-Villegas, A.; Kivimäki, M.; Akbaraly, T. Healthy Dietary Indices and Risk of Depressive Outcomes: A Systematic Review and Meta-Analysis of Observational Studies. *Mol. Psychiatry* **2019**, *24*, 965–986, doi:10.1038/s41380-018-0237-8.
216. Li, Y.; Dai, Q.; Tedders, S.H.; Arroyo, C.; Zhang, J. Legume Consumption and Severe Depressed Mood, the Modifying Roles of Gender and Menopausal Status. *Public Health Nutr.* **2010**, *13*, 1198–1206, doi:10.1017/S1368980009992059.
217. Saghafian, F.; Hajishafiee, M.; Rouhani, P.; Saneei, P. Dietary Fiber Intake, Depression, and Anxiety: A Systematic Review and Meta-Analysis of Epidemiologic Studies. *Nutr. Neurosci.* **2023**, *26*, 108–126, doi:10.1080/1028415X.2021.2020403.
218. Saghafian, F.; Sharif, N.; Saneei, P.; Keshteli, A.H.; Hosseinzadeh-Attar, M.J.; Afshar, H.; Esmaillzadeh, A.; Adibi, P. Consumption of Dietary Fiber in Relation to Psychological Disorders in Adults. *Front. Psychiatry* **2021**, *12*, 587468, doi:10.3389/fpsyt.2021.587468.
219. Leyrolle, Q.; Cserjesi, R.; D.G.H. Mulders, M.; Zamariola, G.; Hiel, S.; Gianfrancesco, M.A.; Portheault, D.; Amadieu, C.; Bindels, L.B.; Leclercq, S.; et al. Prebiotic Effect on Mood in Obese Patients Is Determined by the Initial Gut Microbiota Composition: A Randomized, Controlled Trial. *Brain. Behav. Immun.* **2021**, *94*, 289–298, doi:10.1016/j.bbi.2021.01.014.
220. Gamage, E.; Orr, R.; Travica, N.; Lane, M.M.; Dissanayaka, T.; Kim, J.H.; Grosso, G.; Godos, J.; Marx, W. Polyphenols as Novel Interventions for Depression: Exploring the Efficacy, Mechanisms of Action, and Implications for Future Research. *Neurosci. Biobehav. Rev.* **2023**, *151*, 105225, doi:10.1016/j.neubiorev.2023.105225.
221. Ibero-Baraibar, I.; Perez-Cornago, A.; Ramirez, M.J.; Martínez, J.A.; Zulet, M.A. An Increase in Plasma Homovanillic Acid with Cocoa Extract Consumption Is Associated with the Alleviation of Depressive Symptoms in Overweight or Obese Adults on an Energy Restricted Diet in a Randomized Controlled Trial. *J. Nutr.* **2016**, *146*, 897S-904S, doi:10.3945/jn.115.222828.
222. Esmaily, H.; Sahebkar, A.; Iranshahi, M.; Ganjali, S.; Mohammadi, A.; Ferns, G.; Ghayour-Mobarhan, M. An Investigation of the Effects of Curcumin on Anxiety and Depression in Obese Individuals: A Randomized Controlled Trial. *Chin. J. Integr. Med.* **2015**, *21*, 332–338, doi:10.1007/s11655-015-2160-z.
223. Lai, J.S.; Hiles, S.; Bisquera, A.; Hure, A.J.; McEvoy, M.; Attia, J. A Systematic Review and Meta-Analysis of Dietary Patterns and Depression in Community-Dwelling Adults. *Am. J. Clin. Nutr.* **2014**, *99*, 181–197, doi:10.3945/ajcn.113.069880.
224. Mudryj, A.N.; Yu, N.; Hartman, T.J.; Mitchell, D.C.; Lawrence, F.R.; Aukema, H.M. Pulse Consumption in Canadian Adults Influences Nutrient Intakes. *Br J Nutr* **2012**, *108 Suppl*, S27-36, doi:10.1017/S0007114512000724.
225. Li, S.S.; Kendall, C.W.C.; De Souza, R.J.; Jayalath, V.H.; Cozma, A.I.; Ha, V.; Mirrahimi, A.; Chiavaroli, L.; Augustin, L.S.A.; Blanco Mejia, S.; et al. Dietary Pulses, Satiety and Food Intake: A Systematic Review and Meta-Analysis of Acute Feeding Trials. *Obesity* **2014**, *22*, 1773–1780, doi:10.1002/oby.20782.
226. Murphy, E.A.; Velazquez, K.T.; Herbert, K.M. Influence of High-Fat Diet on Gut Microbiota: A Driving Force for Chronic Disease Risk. *Curr. Opin. Clin. Nutr. Metab. Care* **2015**, *18*, 515–520, doi:10.1097/MCO.0000000000000209.
227. Guo, S.; Zhao, H.; Ma, Z.; Zhang, S.; Li, M.; Zheng, Z.; Ren, X.; Ho, C.-T.; Bai, N. Anti-Obesity and Gut Microbiota Modulation Effect of Secoiridoid-Enriched Extract from Fraxinus

Mandshurica Seeds on High-Fat Diet-Fed Mice. *Molecules* **2020**, *25*, doi:10.3390/molecules25174001.
228. Wu, Z.; Du, Z.; Tian, Y.; Liu, M.; Zhu, K.; Zhao, Y.; Wang, H. Inulin Accelerates Weight Loss in Obese Mice by Regulating Gut Microbiota and Serum Metabolites. *Front. Nutr.* **2022**, *9*, 980382, doi:10.3389/fnut.2022.980382.
229. Louis, S.; Tappu, R.-M.; Damms-Machado, A.; Huson, D.H.; Bischoff, S.C. Characterization of the Gut Microbial Community of Obese Patients Following a Weight-Loss Intervention Using Whole Metagenome Shotgun Sequencing. *PloS One* **2016**, *11*, e0149564, doi:10.1371/journal.pone.0149564.
230. Parker, B.J.; Wearsch, P.A.; Veloo, A.C.M.; Rodriguez-Palacios, A. The Genus Alistipes: Gut Bacteria With Emerging Implications to Inflammation, Cancer, and Mental Health. *Front. Immunol.* **2020**, *11*, 906, doi:10.3389/fimmu.2020.00906.
231. Chen, T.; Long, W.; Zhang, C.; Liu, S.; Zhao, L.; Hamaker, B.R. Fiber-Utilizing Capacity Varies in Prevotella- versus Bacteroides-Dominated Gut Microbiota. *Sci. Rep.* **2017**, *7*, 2594, doi:10.1038/s41598-017-02995-4.
232. Wei, G.; Ye, Y.; Yan, X.; Chao, X.; Yang, F.; Wang, M.; Zhang, W.; Yuan, C.; Zeng, Q. Effect of Banana Pulp Dietary Fibers on Metabolic Syndrome and Gut Microbiota Diversity in High-Fat Diet Mice. *J. Food Biochem.* **2020**, *44*, 1–15, doi:10.1111/jfbc.13362.
233. Marteau, P.; Pochart, P.; Doré, J.; Béra-Maillet, C.; Bernalier, A.; Corthier, G. Comparative Study of Bacterial Groups within the Human Cecal and Fecal Microbiota. *Appl. Environ. Microbiol.* **2001**, *67*, 4939–4942, doi:10.1128/AEM.67.10.4939-4942.2001.
234. Wang, M.; Zhang, B.; Hu, J.; Nie, S.; Xiong, T.; Xie, M. Intervention of Five Strains of Lactobacillus on Obesity in Mice Induced by High-Fat Diet. *J. Funct. Foods* **2020**, *72*, 104078, doi:https://doi.org/10.1016/j.jff.2020.104078.
235. Zong, X.; Zhang, H.; Zhu, L.; Deehan, E.C.; Fu, J.; Wang, Y.; Jin, M. Auricularia Auricula Polysaccharides Attenuate Obesity in Mice through Gut Commensal Papillibacter Cinnamivorans. *J. Adv. Res.* **2023**, *52*, 203–218, doi:10.1016/j.jare.2023.08.003.
236. Xu, Y.; Wang, N.; Tan, H.-Y.; Li, S.; Zhang, C.; Feng, Y. Function of Akkermansia Muciniphila in Obesity: Interactions With Lipid Metabolism, Immune Response and Gut Systems. *Front. Microbiol.* **2020**, *11*, 219, doi:10.3389/fmicb.2020.00219.
237. Cani, P.D.; De Vos, W.M. Next-Generation Beneficial Microbes: The Case of Akkermansia Muciniphila. *Front. Microbiol.* **2017**, *8*, 1765, doi:10.3389/fmicb.2017.01765.
238. Derrien, M.; Belzer, C.; De Vos, W.M. Akkermansia Muciniphila and Its Role in Regulating Host Functions. *Microb. Pathog.* **2017**, *106*, 171–181, doi:10.1016/j.micpath.2016.02.005.
239. Everard, A.; Belzer, C.; Geurts, L.; Ouwerkerk, J.P.; Druart, C.; Bindels, L.B.; Guiot, Y.; Derrien, M.; Muccioli, G.G.; Delzenne, N.M.; et al. Cross-Talk between Akkermansia Muciniphila and Intestinal Epithelium Controls Diet-Induced Obesity. *Proc. Natl. Acad. Sci. U. S. A.* **2013**, *110*, 9066–9071, doi:10.1073/pnas.1219451110.
240. Paone, P.; Cani, P.D. Mucus Barrier, Mucins and Gut Microbiota: The Expected Slimy Partners? *Gut* **2020**, *69*, 2232–2243, doi:10.1136/gutjnl-2020-322260.
241. Ombra, M.N.; d'Acierno, A.; Nazzaro, F.; Riccardi, R.; Spigno, P.; Zaccardelli, M.; Pane, C.; Maione, M.; Fratianni, F. Phenolic Composition and Antioxidant and Antiproliferative Activities of the Extracts of Twelve Common Bean (*Phaseolus Vulgaris* L.) Endemic Ecotypes of Southern Italy before and after Cooking. *Oxid. Med. Cell. Longev.* **2016**, *2016*, 1398298, doi:10.1155/2016/1398298.

242. Zhang, W.; Qi, S.; Xue, X.; Al Naggar, Y.; Wu, L.; Wang, K. Understanding the Gastrointestinal Protective Effects of Polyphenols Using Foodomics-Based Approaches. *Front. Immunol.* **2021**, *12*, 671150, doi:10.3389/fimmu.2021.671150.
243. Ang, Z.; Ding, J.L. GPR41 and GPR43 in Obesity and Inflammation - Protective or Causative? *Front. Immunol.* **2016**, *7*, 28, doi:10.3389/fimmu.2016.00028.
244. Lange, O.; Proczko-Stepaniak, M.; Mika, A. Short-Chain Fatty Acids—A Product of the Microbiome and Its Participation in Two-Way Communication on the Microbiome-Host Mammal Line. *Curr. Obes. Rep.* **2023**, *12*, 108–126, doi:10.1007/s13679-023-00503-6.
245. Ibrahim, K.S.; Bourwis, N.; Dolan, S.; Lang, S.; Spencer, J.; Craft, J.A. Characterisation of Gut Microbiota of Obesity and Type 2 Diabetes in a Rodent Model. *Biosci. Microbiota Food Health* **2021**, *40*, 65–74, doi:10.12938/bmfh.2019-031.
246. Schroeder, B.O. Fight Them or Feed Them: How the Intestinal Mucus Layer Manages the Gut Microbiota. *Gastroenterol. Rep.* **2019**, *7*, 3–12, doi:10.1093/gastro/goy052.
247. Chakrabarti, A.; Geurts, L.; Hoyles, L.; Iozzo, P.; Kraneveld, A.D.; La Fata, G.; Miani, M.; Patterson, E.; Pot, B.; Shortt, C.; et al. The Microbiota-Gut-Brain Axis: Pathways to Better Brain Health. Perspectives on What We Know, What We Need to Investigate and How to Put Knowledge into Practice. *Cell. Mol. Life Sci. CMLS* **2022**, *79*, 80, doi:10.1007/s00018-021-04060-w.
248. Walf, A.A.; Frye, C.A. The Use of the Elevated plus Maze as an Assay of Anxiety-Related Behavior in Rodents. *Nat. Protoc.* **2007**, *2*, 322–328, doi:10.1038/nprot.2007.44.
249. Hong, J.; Stubbins, R.E.; Smith, R.R.; Harvey, A.E.; Núñez, N.P. Differential Susceptibility to Obesity between Male, Female and Ovariectomized Female Mice. *Nutr. J.* **2009**, *8*, 11, doi:10.1186/1475-2891-8-11.
250. Casimiro, I.; Stull, N.D.; Tersey, S.A.; Mirmira, R.G. Phenotypic Sexual Dimorphism in Response to Dietary Fat Manipulation in C57BL/6J Mice. *J. Diabetes Complications* **2021**, *35*, 107795, doi:10.1016/j.jdiacomp.2020.107795.
251. Nickelson, K.J.; Stromsdorfer, K.L.; Pickering, R.T.; Liu, T.-W.; Ortinau, L.C.; Keating, A.F.; Perfield, J.W. A Comparison of Inflammatory and Oxidative Stress Markers in Adipose Tissue from Weight-Matched Obese Male and Female Mice. *Exp. Diabetes Res.* **2012**, *2012*, 859395, doi:10.1155/2012/859395.
252. Lovick, T.A.; Zangrossi, H. Effect of Estrous Cycle on Behavior of Females in Rodent Tests of Anxiety. *Front. Psychiatry* **2021**, *12*, 711065, doi:10.3389/fpsyt.2021.711065.
253. Org, E.; Mehrabian, M.; Parks, B.W.; Shipkova, P.; Liu, X.; Drake, T.A.; Lusis, A.J. Sex Differences and Hormonal Effects on Gut Microbiota Composition in Mice. *Gut Microbes* **2016**, *7*, 313–322, doi:10.1080/19490976.2016.1203502.
254. McNally, C.P.; Eng, A.; Noecker, C.; Gagne-Maynard, W.C.; Borenstein, E. BURRITO: An Interactive Multi-Omic Tool for Visualizing Taxa–Function Relationships in Microbiome Data. *Front. Microbiol.* **2018**, *9*, 365, doi:10.3389/fmicb.2018.00365.
255. González-González, M.; Díaz-Zepeda, C.; Eyzaguirre-Velásquez, J.; González-Arancibia, C.; Bravo, J.A.; Julio-Pieper, M. Investigating Gut Permeability in Animal Models of Disease. *Front. Physiol.* **2019**, *9*, 1962, doi:10.3389/fphys.2018.01962.
256. Ebong, S.J.; Goyert, S.M.; Nemzek, J.A.; Kim, J.; Bolgos, G.L.; Remick, D.G. Critical Role of CD14 for Production of Proinflammatory Cytokines and Cytokine Inhibitors during Sepsis with Failure To Alter Morbidity or Mortality. *Infect. Immun.* **2001**, *69*, 2099–2106, doi:10.1128/IAI.69.4.2099-2106.2001.

257. Balcombe, J.P.; Barnard, N.D.; Sandusky, C. Laboratory Routines Cause Animal Stress. *Contemp. Top. Lab. Anim. Sci.* **2004**, *43*, 42–51.
258. Novak, J.; Jaric, I.; Rosso, M.; Rufener, R.; Touma, C.; Würbel, H. Handling Method Affects Measures of Anxiety, but Not Chronic Stress in Mice. *Sci. Rep.* **2022**, *12*, 20938, doi:10.1038/s41598-022-25090-9.
259. Rasmussen, S.; Miller, M.M.; Filipski, S.B.; Tolwani, R.J. Cage Change Influences Serum Corticosterone and Anxiety-like Behaviors in the Mouse. *J. Am. Assoc. Lab. Anim. Sci. JAALAS* **2011**, *50*, 479–483.
260. Campbell, S.; Macqueen, G. The Role of the Hippocampus in the Pathophysiology of Major Depression. *J. Psychiatry Neurosci. JPN* **2004**, *29*, 417–426.
261. QIAGEN QIAamp ® Fast DNA Stool Mini Kit. *Sample Assay Tecnol.* **2014**, 4.
262. ThermoFisher Quant-i(TM) PicoGreen (R) dsDNA Reagent and Kits. **2008**, 1–7.
263. Illumina MiSeq System Guide Document # 15027617 V05 M. **2019**, 1–226.
264. Dalby, M.J.; Aviello, G.; Ross, A.W.; Walker, A.W.; Barrett, P.; Morgan, P.J. Diet Induced Obesity Is Independent of Metabolic Endotoxemia and TLR4 Signalling, but Markedly Increases Hypothalamic Expression of the Acute Phase Protein, SerpinA3N. *Sci. Rep.* **2018**, *8*, 15648, doi:10.1038/s41598-018-33928-4.
265. Cathomas, F.; Hartmann, M.N.; Seifritz, E.; Pryce, C.R.; Kaiser, S. The Translational Study of Apathy-an Ecological Approach. *Front. Behav. Neurosci.* **2015**, *9*, 241, doi:10.3389/fnbeh.2015.00241.
266. Jirkof, P. Burrowing and Nest Building Behavior as Indicators of Well-Being in Mice. *J. Neurosci. Methods* **2014**, *234*, 139–146, doi:https://doi.org/10.1016/j.jneumeth.2014.02.001.
267. Kraeuter, A.-K.; Guest, P.C.; Sarnyai, Z. The Nest Building Test in Mice for Assessment of General Well-Being BT - Pre-Clinical Models: Techniques and Protocols. In; Guest, P.C., Ed.; Springer New York: New York, NY, 2019; pp. 87–91 ISBN 978-1-4939-8994-2.
268. Deacon, R.M.J. Assessing Nest Building in Mice. *Nat. Protoc.* **2006**, *1*, 1117–1119, doi:10.1038/nprot.2006.170.
269. Hess, S.E.; Rohr, S.; Dufour, B.D.; Gaskill, B.N.; Pajor, E.A.; Garner, J.P. Home Improvement: C57BL/6J Mice given More Naturalistic Nesting Materials Build Better Nests. *J. Am. Assoc. Lab. Anim. Sci.* **2008**, *47*, 25–31.
270. Hess, S.E.; Rohr, S.; Dufour, B.D.; Gaskill, B.N.; Pajor, E.A.; Garner, J.P. Home Improvement: C57BL/6J Mice given More Naturalistic Nesting Materials Build Better Nests. *J. Am. Assoc. Lab. Anim. Sci.* **2008**, *47*, 25–31.
271. Komada, M.; Takao, K.; Miyakawa, T. Elevated plus Maze for Mice. *J. Vis. Exp. JoVE* **2008**, doi:10.3791/1088.
272. Brolese, G.; Lunardi, P.; Lopes, F.; Gonçalves, C.-A. Chapter 2 - Prenatal Alcohol Exposure and Neuroglial Changes in Neurochemistry and Behavior in Animal Models. In *Addictive Substances and Neurological Disease*; Watson, R.R., Zibadi, S.B.T.-A.S. and N.D., Eds.; Academic Press, 2017; pp. 11–22 ISBN 978-0-12-805373-7.
273. Schrader, A.J.; Taylor, R.M.; Lowery-Gionta, E.G.; Moore, N.L.T. Repeated Elevated plus Maze Trials as a Measure for Tracking Within-Subjects Behavioral Performance in Rats (Rattus Norvegicus). *PLOS ONE* **2018**, *13*, e0207804.
274. André, C.; Dinel, A.-L.; Ferreira, G.; Layé, S.; Castanon, N. Diet-Induced Obesity Progressively Alters Cognition, Anxiety-like Behavior and Lipopolysaccharide-Induced Depressive-like Behavior: Focus on Brain Indoleamine 2,3-Dioxygenase Activation. *Brain. Behav. Immun.* **2014**, *41*, 10–21, doi:10.1016/j.bbi.2014.03.012.

275. Crawley, J.N. *What's Wrong With My Mouse? : Behavioral Phenotyping of Transgenic and Knockout Mice*; Wiley-Liss: Hoboken, N.J., 2007; Vol. 2nd ed; ISBN 9780471471929.